A desire for knowledge, an interminable thirst

Leads a dogged search, where truth comes first

The journey yields a need for yet more understanding

A cyclic path that is tortuous and winding

Each circular path reveals a logic to our existence

Each roundabout navigated feeds our persistence.

ANON

SOME ASPECTS OF THE NIOSOMAL DELIVERY OF DOXORUBICIN

A thesis presented by

Ijeoma Uchegbu B.Pharm., M.Phil., MPSN

in partial fulfilment of the requirements for the degree of

Doctor of Philosophy

of the University of London

March 1994

School of Pharmacy,
University of London,
29-39 Brunswick Square,
London WC1N 1AX.

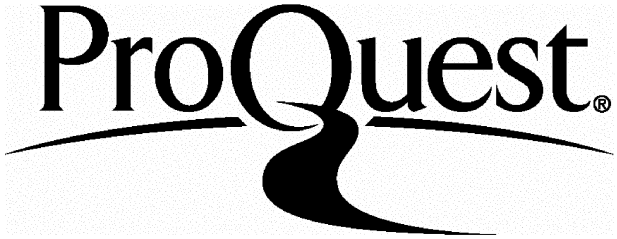

CONTENTS

TITLE	PAGE NUMBER
ACKNOWLEDGEMENTS	6
ABSTRACT	7
CHAPTER ONE	8
INTRODUCTION	8
1.2: Mechanism of Action of Doxorubicin	11
1.3: Doxorubicin Metabolism	19
1.4:Doxorubicin Toxicity	21
1.5: Doxorubicin Delivery Systems	27
1.6: Niosomal Drug Delivery Systems	33
1.7: The Intraperitoneal Administration of Doxorubicin Vesicular Systems	40
1.8: Doxorubicin Resistance	41
1.9: Vesicle to Micelle Phase Transitions	46
1.10: Outline of Work	47
CHAPTER TWO	49
THE PHYSICOCHEMICAL PROPERTIES OF DOXORUBICIN NIOSOMES AND SOME VESICLE TO MICELLE TRANSITIONS	49
2.1: The Need for an Optimum size, encapsulation efficiency and Latency	50
2.2: $C_{16}G_2$ - Solulan C24 vesicle to micelle transitions	53
2.3: Materials	54
Methods	54
2.4: The Physicochemical Properties of $C_{16}G_3$, $C_{16}G_2$ and Span surfactant Niosomes	54

2.5: Vesicle to Micelle Transitions for the
$C_{16}G_2$-Solulan C24 system 61
Results and Discussion 63
2.6: The Physicochemical Properties of
$C_{16}G_3$, $C_{16}G_2$ and Span Surfactant Niosomes 63
2.7: Vesicle to Micelle transitions in the
$C_{16}G_2$-Solulan C24 system 103
CHAPTER THREE 121
THE EVALUATION OF DOXORUBICIN NIOSOMES AGAINST A RESISTANT OVARIAN CANCER CELL LINE 121
3.1: Drug Delivery initiatives and Multidrug Resistance 122
3.2: Materials 123
3.3: Methods 123
3.4: Results and Discussion 126
CHAPTER FOUR 133
THE INTRAPERITONEAL ADMINISTRATION OF DOXORUBICIN $C_{16}G_2$ NIOSOMES 133
4.1: The Intraperitoneal Administration of Doxorubicin Niosomes 134
4.2: Materials 134
4.3: Methods 134
4.4: Results and Discussion 140
CHAPTER FIVE 158
NIOSOMAL DISTRIBUTION, METABOLISM AND TUMORICIDAL ACTIVITY IN MICE 158

5.1: Doxorubicin Distribution, Metabolism and Tumoricidal Activity in Mice 159
5.2: Materials 161
Methods 161
5.3: Metabolism and Distribution of Doxorubicin Span 60 Niosomes 161
5.4: The *In Vitro* Release of Span 60 Niosome Associated Doxorubicin Metabolites 165
5.5: The Evaluation of the Tumoricidal Activity of Doxorubicin Niosomes 166
Results and Discussion 168
5.6: Metabolism and Distribution of Doxorubicin Span 60 Niosomes 168
5.7: The Evaluation of the Tumoricidal Activity of Doxorubicin Niosomes 195
CHAPTER SIX 206
CONCLUSIONS AND FUTURE WORK 206
REFERENCES 211
PUBLICATIONS 257

ACKNOWLEDGEMENTS

The following people are gratefully acknowledged. First and foremost Professor Alexander T. Florence for patiently leading me through this veritable minefield of postgraduate study in the kindest possible way. His excellent supervision will always be remembered. Dr John Turton is also thanked for teaching me the practical aspects of *in vivo* study. I would also like to acknowledge the input of Dr John Double. His help with the tumour bearing mouse model was an invaluable asset to every part of this study. The input of Dr Lloyd Kelland is much appreciated. Mr Dave McCarthy is thanked for his very good work in the processing of tissue samples for histology and his work in producing the scanning electron micrographs of vesicle dispersion samples. The technical support of Adrain Rogers at the start of this project is acknowledged. Dr Joke Bouwstra and Dr Moody are thanked for their help, specifically in the production of freeze fracture and cryo-transmission electron micrographs of various vesicle dispersions. Miss Barbara Grant is also thanked, especially for her kindness to me during my stay in CDDR.

L'Oreal France is gratefully acknowledged for financial support.

I would also like to thank all my colleagues in the CDDR basement laboratories, most notably Ron, Ana, Maria, Nasir, Sophia and Praful for making the often long and tiring days spent down there seem somewhat shorter. A big thank you to you all. And of course there are the three little girls who had to put up with me during this period. It's over now it's over girls!

ABSTRACT

Vesicular drug delivery systems prepared from two types of non-ionic surfactants, cholesterol and other additives were studied and characterized with regard to their physicochemical and biological properties. Sorbitan ester (Span) niosomes containing doxorubicin showed an inverse correlation between mean vesicle size and surfactant hydrophilic lipophilic balance (HLB) number ($r = -0.92$). The remote loading method (exploiting transmembrane proton gradients) was used to increase the encapsulation efficiency of doxorubicin niosomes. Encapsulation efficiency of Span surfactant niosomes increased with increasing mean niosome size, except with Span 80 niosomes which gave lower than expected values. Span 60 niosomes in female NMRI mice bearing the MAC 15A tumour were fairly stable in vivo, with 90% of plasma doxorubicin being niosome associated (determined by a gel filtration technique) 4h after dosing and 50% niosome associated 24h after dosing. Plasma area under the time level curve (AUC) was increased 6 fold by encapsulation of the drug. Doxorubicin levels in all tissues, except the heart, were also increased. The AUC tumour to heart ratio was increased from 0.27 to 0.36. Hexadecyl-diglycerol ether ($C_{16}G_2$) niosomes containing doxorubicin, when compared to the free drug, doubled the area under the plasma level time curve (plasma AUC), following intraperitoneal injection, but resulted in an inflammatory response in the lung of male AKR mice. This response was however not seen when empty niosomes were administered intraperitoneally, doxorubicin niosomes were administered intravenously or with doxorubicin solution, by any route. In vivo $C_{16}G_2$ niosomes were equiactive with doxorubicin solution, against a subcutaneously implanted MAC 13A tumour whereas Span 60 niosomes doubled the activity of doxorubicin against a subcutaneously implanted MAC 15A tumour. In vitro doxorubicin niosomes reduced the IC_{50}, slightly against a resistant variant of a human ovarian cancer cell line.

Large (12-60μm) disc shaped structures formed from $C_{16}G_2$ were found to be an intermediate structure in the Solulan C24-mediated $C_{16}G_2$ vesicle to micelle transition and were termed discomes. These structures were able to encapsulate and retain 45% of an aqueous marker (5-(6)-carboxyfluorescein) after 24h at room temperature.

From the above, there appears to be a future for niosomal drug delivery systems in the field of drug targeting.

CHAPTER ONE

INTRODUCTION

1.1 Data presented in this thesis will detail efforts at drug targeting by the encapsulation of the chemotherapeutic anthracycline antibiotic doxorubicin (DOX) (Figure 1.1) in non-ionic surfactant vesicles (niosomes). Niosomes, initially based on surfactants synthesised by L'Oreal (Vanleberghe *et al.*,1972) have been studied in our laboratories as alternatives to liposomes for some time (Azmin *et al.*, 1985; Baillie *et al.*, 1985; Baillie *et al.*, 1986; Rogerson *et al.*, 1987; Hunter *et al.*, 1988; Kerr *et al.*, 1988; Rogerson *et al.*, 1988; Rogerson *et al.*, 1989; Florence and Baillie, 1989; Florence *et al.*, 1990; Florence, 1993; Yoshioka and Florence, 1994; Yoshioka *et al.*, 1994). These and similar vesicles have also been studied in the laboratories of others (Handjani-Vila *et al.*, 1979; Vanleberghe *et al.*, 1978; Okahata *et al.*, 1981; Kiwada *et al.* 1985; Echegoyen *et al.*, 1988; Kiwada *et al.*, 1988; Moser *et al.*, 1989; Chandraprakesh *et al.*, 1990; Handjani-Vila *et al.*, 1990; Lesieur *et al.*, 1990; Moser *et al.*, 1990; Schenk *et al.*, 1990; Tanaka *et al.*, 1990; Özer *et al.*, 1991; Hofland *et al.*, 1992; Seras *et al.*, 1992; Parthasarathi *et al.*, 1994). This brief introduction to the topic deals with the general pharmacology of doxorubicin to emphasise the need for drug targeting and also presents a review of other DOX drug delivery systems and the previously established properties of niosomal drug delivery systems.

Conventional drug delivery systems can be inefficient and imprecise. Optimization of therapy requires that the drug molecule enjoys an exclusive interaction with the tissue of interest, rather than the systemic exposure to which the organism is usually subjected e.g. after intravenous injection of a drug in solution. Novel drug delivery systems have been used to achieve this selectivity with varying degrees of success (Juliano, 1991; Leyland-Jones, 1993). In no other area is the need for an exclusive

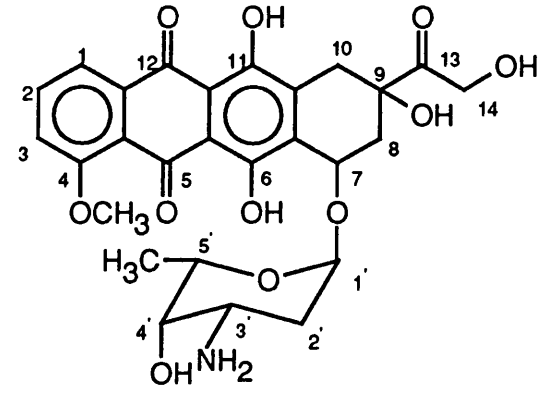

I

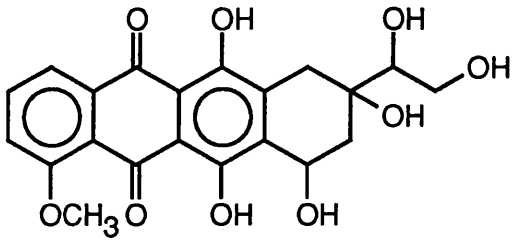

IV

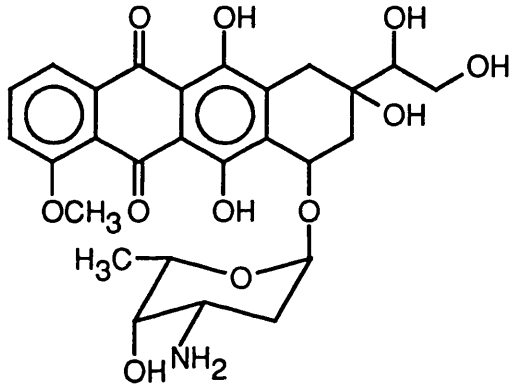

II

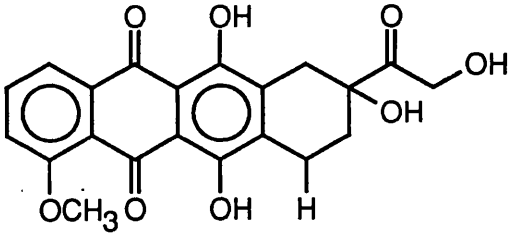

V

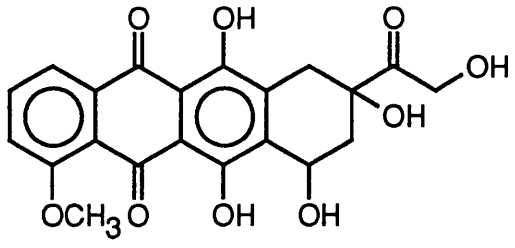

III

Figure 1.1: DOX and DOX metabolites. I = DOX, II = doxorubicinol (DXOL), III = doxorubicinone (DXONE), IV = doxorubicinolone (DXOLONE), V = 7-deoxydoxorubicinone (DEOXONE)

pharmacodynamic relationship greater than in the field of cancer chemotherapy (Gupta, 1990). The indiscriminate pharmacological actions of antineoplastic agents means that their clinical use is associated with severe systemic toxicity (Calaberesi and Chabner, 1990), leading to poor host compliance and, in some cases therapeutic failure.

DOX was first identified in 1969 (Arcamone, 1969), a product of the fungus *Streptomyces peucetius* var *caesius*. It is a potent antineoplastic agent, used either as the sole agent or in combination chemotherapy (Calaberesi and Chabner, 1990). This drug is effective against solid tumours, namely carcinomas of the ovaries, breast, small cell carcinoma of the lung, non-Hodgkins lymphoma, a wide range of sarcomas, bladder carcinomas, neuroblastoma and is also active against acute leukaemia (Calaberesi and Chabner, 1990).

1.2 MECHANISM OF ACTION OF DOXORUBICIN

The cell life cycle is divided into a number of phases, namely the G_0 phase in which the cell is performing its normal function and is not usually engaged in activities necessary for cell division; the G_1 phase in which cellular organelles are manufactured; an S phase in which there is DNA replication; a G_2 phase in which there is a brief period of protein synthesis and finally the G_m phase in which there is actual cell division (Martini, 1992). At low concentrations ($< 0.15\ \mu g.mL^{-1}$), DOX is most active in the period covering the late S phase through to the G_2 and G_m phases of the cell cycle (Minderman *et al.*, 1993). These are the cell cycle phases where DNA cell

content is highest. At higher concentrations, however, DOX is most active in the S phase, the cell cycle phase of highest DNA synthetic activity (Calaberesi and Chabner, 1990).

A number of mechanisms have been said to account for the cytotoxicity of DOX - intercalation of deoxyribonucleic acid (DNA); inhibition of the enzyme necessary for DNA replication - topoisomerase II; the generation of free radicals and an action on the cell membrane. DOX also induces apoptosis (programmed cell death) by a mechanism which is unrelated to the activity of DOX against DNA, killing the cells in the G_2 phase (Skladanowski and Knopa, 1993). Although DOX has been shown to exert all these effects, the principal mechanism responsible for its cytotoxicity *in vivo*, remains unclear.

1.2:1 INTERCALATION OF DNA AND INHIBITION OF DNA TOPOISOMERASE II

DOX in the presence of copper ions (Cu^{3+}), forms a ternary complex with DNA (Yourtee *et al.*, 1992). This complexation amplifies the mutagenicity of DOX. DOX intercalates between cytosine and guanine base pairs in the DNA molecule (Wang *et al.*, 1987), with the aglycone portion of the molecule orientated at right angles to the long dimension of the DNA base pairs. The O14 hydroxy group (Figure 1.1) is hydrogen bonded to a water molecule which is in turn hydrogen bonded to a nearby phosphate group. Substituents on the cyclohexane ring A are hydrogen bonded to the base pairs above and below the intercalation site while the O9 hydroxy group forms 2 hydrogen bonds with an adjacent guanine base. The DOX molecule in order to

accommodate this interaction is present in an altered conformation about ring A. The DNA-DOX complex is a distorted form of DNA with slight unwinding of the DNA helix.

Within the complex described above, the sugar molecule sits with its functional hydroxy and amino groups facing outwards for possible interaction with polymerases. Mammalian DNA topoisomerase II is responsible for the catalysis of a number of topological isomerization reactions via a transient intermediate involving protein linked double strand breaks. DNA topoisomerase II reversibly cuts double stranded DNA and becomes covalently linked to the break site via phosphotyrosyl bonds. The enzyme then allows passage of an intact DNA double strand through the cut and then closes the break. The net result is a topological modification of the DNA molecule. The DNA-topoisomerase II intermediate is called the cleavable complex. In vivo this action of topoisomerase II serves mainly to separate daughter chromosomes at the end of DNA synthesis (Darnell *et al.*, 1990). DOX stabilises the topoisomerase II cleavable complex (Tewey *et al.*, 1984), by an interaction with topoisomerase II at position C10 (Jensen *et al.*, 1993). A combination of the intercalation of DNA and stabilisation of the cleavable complex inhibits DNA strand passing activity and results in DNA strand breaks (Tewey *et al.*, 1984) and the inhibition of RNA synthesis (Calaberesi and Chabner, 1990). The fact that the cleavage of DNA by DOX is not quantitatively correlated with the drug's cytotoxicity (Belvedere *et al.*, 1989) suggests that this may not be the only mode of action of this drug *in vivo*. However the strong binding of DOX to DNA (Frezard and Garnier-Suillerot, 1991; Mustonan and Kinnunen, 1993), which allows the drug to traverse vesicular membranes in response

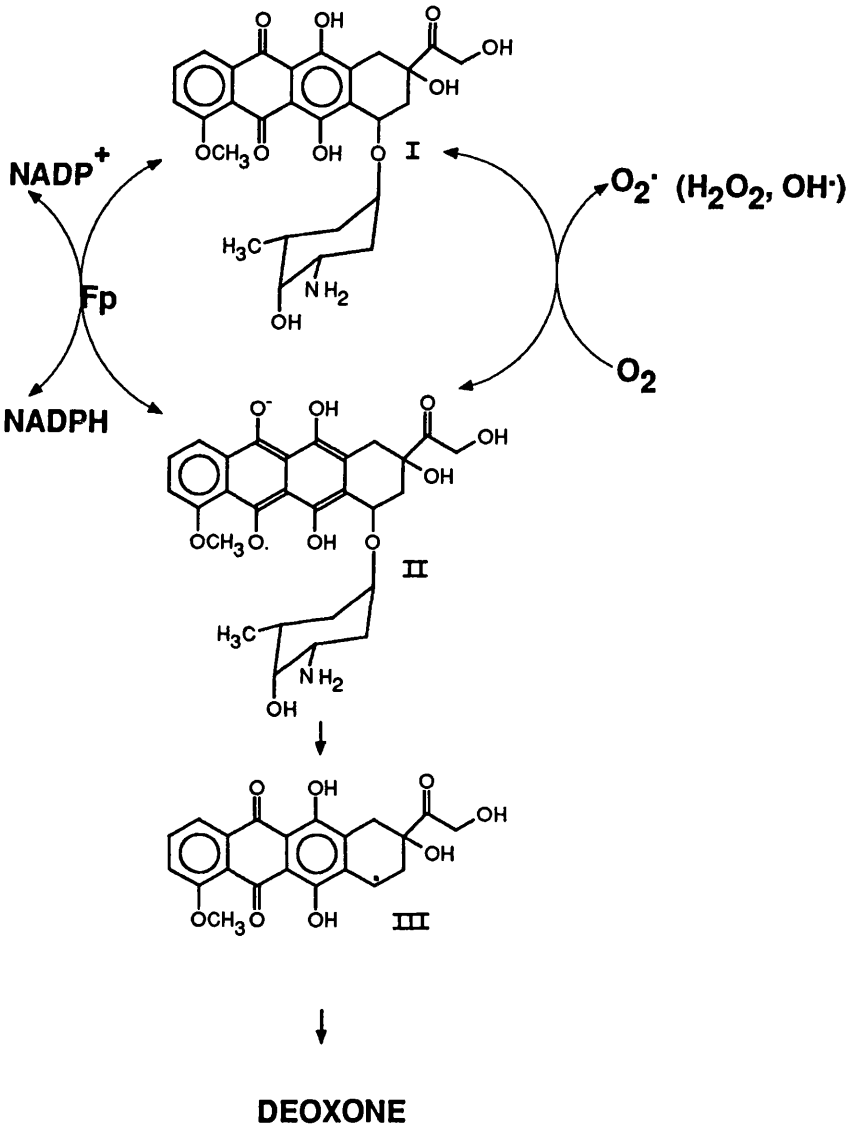

Figure 1.2: The generation of free radicals by redox cycling of DOX. I = DOX, II = DOX semiquinone, III = C7-free radical. Fp = cytochrome P450 reductase.

to a driving force provided by intravesicular DNA (Frezard and Garnier-Suillerot, 1991) implies that the interaction of DOX with DNA is a major mechanism of action, probably by way of the interaction of DOX with topoisomerase II, a conclusion drawn in an excellent review on the subject by Cummings and others (1991).

1.2:2 THE GENERATION OF FREE RADICALS

DOX can generate free radicals either by a process known as redox cycling (Figure 1.2) or by the formation of a DOX-iron complex (Figure 1.3) (Keizer *et al.*, 1990). DOX in the presence of oxygen is oxidised enzymatically to the semiquinone free radical (Figure 1.2). The semiquinone free radical on reduction back to the parent compound produces a superoxide free radical (Bachur *et al.* 1977; Goodman and Hochstein 1977), which could in turn lead to the formation of the toxic free radical $OH^{\bullet}$. This reaction demonstrates an absolute requirement for NADPH (Bachur *et al.*, 1977; Goodman and Hochstein, 1977) and is catalysed by NADPH-cytochrome P450 reductase (Gutiérrez *et al.*, 1983; Goodman and Hochstein, 1977; Doroshow, 1983) in the endoplasmic and sarcoplasmic reticulum; a requirement for NADH and is catalysed by NADH dehydrogenase in the cardiac mitochondria (Doroshow, 1983; Davies *et al.*, 1983) or a requirement for xanthine and is catalysed by xanthine oxidase in the cytoplasm (Doroshow, 1983). The reaction has also been identified in the nucleus (Bachur *et al.*, 1982) and is termed redox cycling, due to the fact that there is no net metabolite formation during this process although there is the production of oxygen free radicals, toxic hydroxyl free radicals and hydrogen peroxide. Following the depletion of oxygen (under anaerobic conditions), the semiquinone free radical is converted to the aglycone metabolite 7-deoxydoxorubicinone (DEOXONE - Figure

1.2) (Gutiérrez *et al.*, 1983), hence the presence of DEOXONE *in vivo* (Takanashi and Bachur 1976) is indicative of the generation of potentially toxic DOX and oxygen free radicals (Bachur *et al.*, 1977; Goodman and Hochstein, 1977; Gutiérrez *et al.*, 1983). Theoretically these free radicals, once produced can then attack endogenous macromolecules, and cause cell membrane lipid peroxidation, although it has been stated that for reasons of non-site-specific production, an action of oxygen free radicals originating from redox cycling on endogenous macromolecules is unlikely (Cummings *et al.*, 1991). Nonetheless, evidence exists that the production of reactive short lived DOX metabolites, (most probably free radicals) by enzymatic redox cycling does increase the cytotoxicity of the drug (Bartoszek and Wolf, 1992) and that specifically these reactive intermediates do alkylate nucleic acids (Sinha and Gregory, 1981).

DOX binds iron (Fe^{3+}) between the C12-carbonyl and the C11-hydroxyl groups (Muindi *et al.*, 1985). This stable adduct in the presence of thiols generates free radicals (Figure 1.3) (Gutteridge, 1982; Muindi *et al.*, 1985)) which destroy deoxyribose (Gutteridge, 1982; Gutteridge and Toeg, 1982) and DNA (Eliot *et al.*, 1984; Muindi *et al.*, 1985) *in vitro*, as well as cause the peroxidation of lipids (Gutteridge, 1982). Although no evidence of this reaction has been found *in vivo* (Cummings *et al.*, 1991), the potential of the DOX iron complex to generate toxic free radicals is considered relevant to the drugs cardiotoxic propensity, especially as DOX is able to extract iron from ferritin stores *in vivo* (Muindi *et al.*, 1985; Keizer *et al.*, 1990; Dupou-Cézanne *et al.*, 1993).

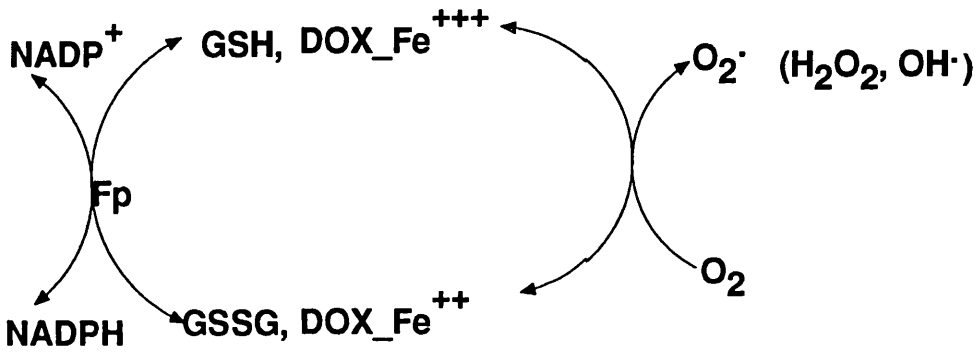

Figure 1.3: The generation of free radicals by the complexation of DOX with Fe^{3+}. DOX_Fe^{+++} = DOX ferric conjugate, DOX_Fe^{++} = DOX ferrous conjugate, Fp = cytochrome P450 reductase, GSH = reduced glutathione, GSSG = oxidised glutathione

1.2:3 DOX AND THE CELL MEMBRANE

DOX demonstrates activity at the site of the cell membrane. In an elegant study Tritton and Yee (1982), demonstrated that the drug can be cytotoxic even when located exclusively outside the cell. This was achieved by the covalent linkage of the drug to polymer beads. However, considering the affinity of DOX for DNA (Frezard and Garnier Suillerot, 1991; Mustonen and Kinnunen 1993), it is not clear how related this *in vitro* study is to the *in vivo* situation. The case for a cell membrane mediated mode of action, despite being by no means proven, cannot be entirely discounted, especially since DOX complexes with cardiolipin and other anionic and neutral membrane phospholipids *in vitro* (de Wolf *et al.*, 1991a; de Wolf *et al.*, 1991b; Burke and Tritton, 1985; Martí *et al.*, 1992). In a separate study, where the potential for an association of DOX with DNA was excluded, DOX was shown to alter the ultrastructure of erythrocyte plasma membranes, possibly by membrane insertion of the DOX molecule (Arancia and Donelli, 1991). These cells were chosen primarily because they lack a nucleus and hence DNA. Further evidence in support of a cell membrane mode of action is the lipid peroxidation of biomembranes by DOX free radicals generated by the DOX iron complex (Keizer *et al.*, 1990). In consideration of the foregoing it can be said that the exact mechanism of DOX cell-membrane mediated cytotoxicity is still unclear.

1.2:4 CONCLUSIONS ON THE MECHANISM OF ACTION OF DOXORUBICIN

In summary, it is broadly agreed that the main locus of action of DOX is intracellular, possibly at a DNA site. The action of free radicals on DNA is thought to be a minor one and the action of DOX at the cell membrane is not considered to be responsible

for its main activity. The consequences of DOX activity on such a fundamental and universal property of cells such as DNA function means that on drug administration, the effects of DOX will be widespread. By employing the drug targeting ability of novel drug delivery systems, it is hoped that the resulting systemic side effects will be reduced.

1.3 DOXORUBICIN METABOLISM

The impact of drug delivery systems on subsequent drug metabolism has not attracted much interest, despite the fact that alterations in metabolic profile on shifting from one delivery system to another are apparent (Azmin *et al.*, 1985; Rogerson *et al.*, 1988; Kerr *et al.*, 1988; Magnusson *et al.*, 1984). This alteration could affect the ultimate goal of the therapeutic strategy, leading to either increased formation of toxic metabolites or a greater inactivation of the drug by a deactivating pathway. The latter was, in fact, the case with a microencapsulated formulation of digoxin (Magnusson *et al.*, 1984). Although the desired goal of the drug delivery system, i.e. decreased gastric hydrolytic degradation was achieved, this was accompanied by increased inactivation of the drug by a reductive metabolic pathway.

The metabolism of DOX is complex (Powis, 1987) and the most commonly identified metabolites are given in Figure 1.1. DOX metabolism involves principally carbonyl reduction at the C13 side chain by the ubiquitous aldoketose reductase enzymes, reductive glycosidic cleavage taking place principally in the liver (Loveless *et al.*, 1978), hydrolytic glycosidic cleavage, and various other minor pathways such as O-

demethylation, O-sulfation and O-β-glucoronidation (Takanashi and Bachur, 1976; Powis, 1987). DOX metabolism in humans is not minor (Takanashi and Bachur, 1976) and of the metabolic pathways listed above, carbonyl reduction is the major enzymatic conversion encountered in humans giving rise to doxorubicinol (DXOL) (Takanashi and Bachur, 1976). This compound is cytotoxic and is implicated in the cardiotoxic reaction of DOX (Olson *et al.*, 1988). The next major metabolite is the inactive compound DEOXONE, the product of reductive glycosidic cleavage, which is also believed to undergo enterohepatic circulation (Mross *et al.*, 1988). The enzymatic production of DEOXONE (Figure 1.2) is accompanied by the generation of toxic free radicals (Keizer *et al.*, 1990). Although no metabolites were found in human tumours (Cummings and McArdle, 1986) after the administration of DOX solution, DEOXONE has been found in rat mammary tumours (Sp 107) *in vivo* (Cummings *et al.*, 1992a) after the administration of DOX albumin microspheres and DOX solution. It is interesting that the presence of this metabolite could not be correlated with either lipid peroxidation or drug-DNA adduct formation, indicating that the formation of this metabolite is not associated with these events in rat SP 107 tumours and is considered in this particular tumour model to be a deactivating transformation. It is known that the administration of DOX in albumin microspheres resulted in increased levels of DEOXONE in rat tumours (Cummings *et al.*, 1992a). The administration of DOX niosomes prepared from a C16 alkyl glycerol ether surfactant - $C_{16}G_3$ (Figure 1.6) increased the level of liver reductive glycosidase activity (Kerr *et al.*, 1988; Rogerson *et al.*, 1988), giving increased DEOXONE levels with the niosomal formulation over the free drug. An increased level of 7-hydroxymethotrexate was found with the administration of $C_{16}G_3$ methotrexate

niosomes (Azmin *et al.*, 1985).

Bearing these facts in mind we examined the metabolism of DOX subsequent to the administration of DOX in sorbitan monostearate (Span 60 - Figure 1.7) niosomes as it is possible that any alterations in the DOX metabolic profile, on the administration of DOX niosomes could have profound implications on the overall tolerance and/or activity of the preparation.

1.4 DOXORUBICIN TOXICITY

The main aim of drug delivery should be to improve the therapeutic index of the drug of interest. Any reductions in toxicity enhance the possibility of achieving this purpose. In order to fully appreciate the potential of niosomal drug delivery in alleviating any toxic responses to DOX chemotherapy, it is appropriate to identify the main biological sites of toxicity encountered with conventional DOX delivery systems and the main toxic manifestations experienced. The work carried out, at improving the clinical tolerance to DOX prior to the work described here, also will be mentioned.

A number of toxic reactions to DOX chemotherapy have been identified, namely cardiotoxicity and myelosuppression (Calabersi and Chabner, 1990), nephrotoxicity (Bertani *et al.*, 1986), ocular adverse reactions (Curran and Luce, 1989), ulcer formation after drug extravasation especially at the injection site (Powis, 1987) and other toxic skin reactions, namely palmar and plantar erythema and skin hyperpigmentation (Jones and Crawford, 1989; Kumar and Kochupillai, 1990; Konoha,

1992). A few other reversible and less worrying side effects are gastrointestinal tract disturbances, and alopecia (Calaberesi and Chabner, 1990).

Of all the above reactions, cardiotoxicity and myelosuppression offer significant threats to clinical use of the compound (Calaberesi and Chabner, 1990).

1.4:1 MYELOSUPRESSION

DOX induced myelosuppression is dose related and is characterised by leucopenia, thrombocytopenia and anaemia (Calaberesi and Chabner, 1990). Leucopenia and thrombocytopenia reach their lowest point approximately 16 days after the DOX dose returning to normal thereafter (Speth *et al.*, 1988). A relationship exists between the degree of systemic exposure to unencapsulated DOX (area under the serum level time curve - AUC) and the severity of myelosupression encountered in small cell lung cancer patients; the former being dependant on the presence or absence of hepatic impairment (Piscitelli *et al.*, 1993). The impact of the long circulation times of most vesicular preparations on the incidence of myelosupression has not been established and while liposomal DOX formulations do not appear to alleviate the bone marrow supression encountered with DOX solution (Cowens *et al.*, 1993; Hengge *et al.*, 1993), the effect of niosomal DOX on this toxic side effect has not been reported. It is hoped that future studies within the niosomal drug delivery programme will explore this area.

1.4:2 CARDIOTOXICITY

DOX cardiotoxicity can be either acute or chronic (Olson and Mushlin, 1990). The

former is less dangerous than the latter (Calaberesi and Chabner, 1990) and is usually characterised by electrocardiographic (ECG) changes, a decreased ejection fraction and, in rare cases, frank congestive cardiac failure. Chronic DOX cardiac toxicity, characterised by negative inotropy and negative chronotropy (Neri *et al.*, 1989) is directly correlated to cumulative life time dose and has a mortality in excess of 50%. Doses as low as 250 $mg.m^{-2}$ can trigger this response, although below a cumulative dose of 400 $mg.m^{-2}$, the risk of DOX induced cardiotoxicity is less than 3% (Doroshow, 1991). A lifetime cumulative dose upper limit is thus set at 400 - 500 $mg.m^{-2}$, for this reason. This fact notwithstanding extreme caution is recommended with the use of DOX; especially as sub-clinical signs of chronic DOX toxicity have been detected, characterised by impaired diastolic filling, at doses of 150-520 $mg.m^{-2}$ (Cittadini *et al.*, 1991). Recently a more insidious form of DOX cardiotoxicity has been recognised. Cancer survivors treated with the drug in childhood and with apparently normal cardiac function at the time of receiving treatment, have been shown to develop a DOX type cardiomyopathy in adulthood (Goorin *et al.*, 1990; Steinherz and Steinherz, 1991). In these individuals, cardiac musculature was found to be underdeveloped, and not commensurate to somatic growth. The need for cardiac follow up in cancer survivors treated with anthracyclines is emphasised by these reports.

Ultrastructural damage to cardiac tissue in the chronic phase of DOX cardiotoxicity is defined by a vacuolisation of the sarcoplasmic reticulum, swelling and disruption of the mitochondria and a disorganisation and eventual decrease in the number of myofibrils (Olson and Mushlin, 1990). The mechanism of DOX cardiotoxicity is still

uncertain, although a number of possibilities have been examined. An inhibition of muscle gene expression has been implicated in this myofibrillar loss (Ito *et al.*, 1990), indicating a possible role for anti-DNA activity in the origin of DOX cardiotoxicity. DOX (Combs *et al.*, 1985; Olson and Mushlin, 1990; Dodd *et al.*, 1993) and DOX aglycones (Sokolove and Shinaberry 1988) interfere with calcium homeostasis, causing calcium cytoplasmic overload and destroying the mechanisms of excitation contraction coupling. It has been widely thought that the ability of DOX to generate free radicals *in vitro* is directly responsible for its cardiotoxicity (Goodman and Hochstein, 1977; Myers *et al.*, 1977; Doroshow, 1983; Davies *et al.*, 1983; Keizer *et al.*, 1990; Doroshow, 1991). Free radicals generated by redox cycling (Bachur *et al.*, 1977; Goodman and Hochstein, 1977) or from DOX-iron complexes (Muindi et al, 1985) can lead to the peroxidation of membrane lipids (Goodman and Hochstein, 1977; Gutteridge, 1984) and cardiomyopathy (Cummings *et al.*, 1987; Fu *et al.*, 1990; Keizer *et al.*, 1990; Olson and Mushlin, 1990). One confounding aspect to this hypothesis is that free radical scavengers are unable to attenuate the histological lesions seen in chronic DOX dosing (Olson and Mushlin, 1990), even though tocopherol administration prior to DOX injection is associated with decreased lipid peroxidation and a decrease in the number of histological lesions seen after a single injection of the drug (Myers *et al.*, 1977). It may well be that the mechanisms of acute and chronic DOX cardiotoxicity are fundamentally different. Also, low concentrations ($0.5\ \mu g.ml^{-1}$) of DOX in the presence of an iron overload *in vitro* are not associated with increased lipid peroxidation (Hershko *et al.*, 1993).

The alteration in mitochondrial energy metabolism by DOX (Fu *et al.*, 1990) and

DOX aglycones (Sokolove, 1991) is also considered to be a contributory factor in DOX cardiotoxicity.

DOX metabolites have been strongly implicated in the toxic cardiac reaction to the drug. DXOL, a metabolite synthesized in cardiac muscle, is more cardiotoxic than the parent drug (Olson *et al.*, 1988: Mushlin *et al.*, 1993; de Jong *et al.*, 1993), disrupting calcium homeostasis to a greater extent than the parent drug (Boucek *et al.*, 1987; Olson *et al.*, 1988). Considering this fact in conjunction with the fact that toxic free radicals are produced by the bioreduction of DOX and also taking due cognisance of the action of DOX aglycones on calcium homeostasis (Sokolove and Shinaberry, 1988) and mitochondrial energy function (Sokolove, 1991), it is not untenable to suppose that the action of DOX on the heart may be potentiated by metabolite formation within the heart (Olson and Mushlin, 1990; Mushlin *et al.*, 1993)). Alternatively DXOL and the aglycones when synthesised elsewhere in the body may by their action on heart muscle amplify the cardiotoxic reaction observed with the clinical use of this agent.

The contribution of DOX metabolites to DOX cardiotoxicity is especially important with drug delivery systems that alter the metabolite profile of the drug, as this could well bring about fundamental changes to the degree of patient tolerance to the formulation - in either direction.

Various anthracycline analogues have been developed in an effort to abolish the problem of cardiotoxicity while still retaining the excellent therapeutic response to

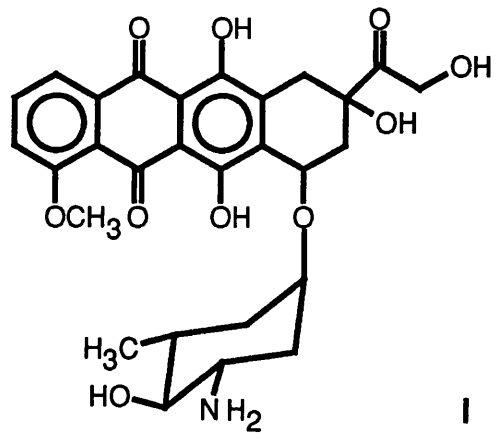

I

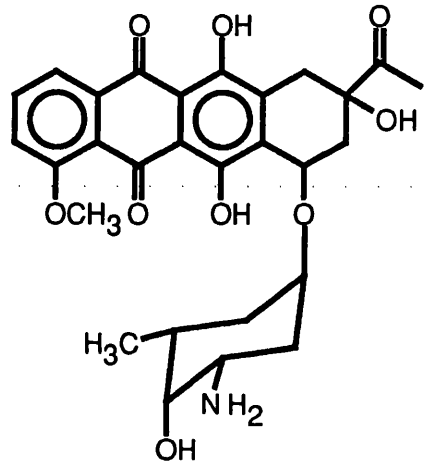

II

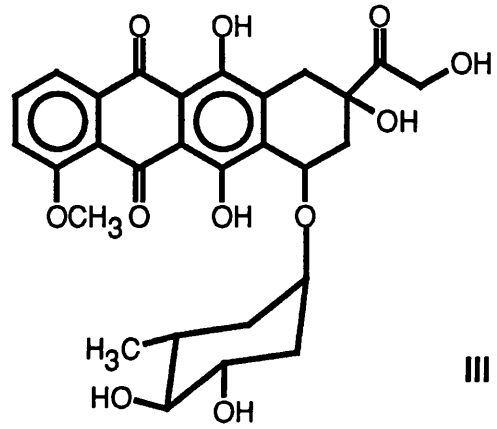

III

Figure 1.4: DOX analogues synthesized to overcome anthracycline cardiotoxicity. I = Epirubicin, II = Idarubicin, III = hydroxyrubicin. Epirubicin and idarubicin have been used clinically

these agents. Epirubicin (Figure 1.4), a C4′ stereoisomer of DOX gives a lower incidence of cardiotoxicity in clinical use than DOX (Neri *et al.*, 1989; Lahtinen *et al.*, 1991), and the clinical use of Idarubicin (Figure 1.4), in which the C4 methoxy group is replaced by a hydroxy group and which also lacks the C14 hydroxy group, is still associated with concern for its cardiotoxic effects (Chan-Lam *et al.*, 1992). Hydroxyrubicin (Figure 1.4), in which the basic C3′ amino group is replaced by a hydroxy group, is less cardiotoxic in mice than the parent drug (Priebe *et al.*, 1993).

Notwithstanding any slight improvements in therapeutic index by these chemical modifications, anthracycline cardiotoxicity in conventional drug delivery systems is still a problem (Doroshow, 1991). DOX is a broad spectrum anticancer agent, consequently the dose-limiting and irreversible nature of this adverse effect has led to the development of various drug delivery systems in an effort to circumvent this obvious limitation.

1.5 DOXORUBICIN DELIVERY SYSTEMS

DOX conjugates, emulsions, suspensions and particulate delivery systems have been studied in an effort to develop marketable DOX formulations that would offer all the benefits and fewer of the disadvantages of conventional drug delivery systems.

Micellar DOX polyethylene glycol-polyaspartic acid (Figure 1.5) (Yokoyama *et al.*, 1990) and DOX hydroxypropylmethacrylamide conjugates (Yeung *et al.*, 1991) gave therapeutic responses comparable to that obtainable with the free drug in murine

neoplasms. The use of the DOX polyethylene glycol-polyaspartic acid conjugate resulted in less body weight loss than controls and the use of the DOX hydroxypropylmethacrylamide conjugate resulted in a lower degree of cardiotoxicity. DOX dextran conjugates, on the other hand, have undergone phase I clinical trials (Danhauser-Riedl *et al.*, 1993), with resulting significant toxicity to the bone marrow and accompanying hepatotoxicity.

DOX hydrochloride emulsions containing polyoxyethylene (60) hydrogenated castor oil as the emulsifying agent showed that the amount of emulsifying agent used had a direct bearing on the distribution of the drug *in vivo* (Lin *et al.*, 1992). A stable lipiodol (a poppy seed fatty acid ethyl ester) suspension given by intrarterial injection resulted in demonstrable anti-cancer activity and prolonged drug levels in hepatic tumour patients, when compared to the administration of an emulsion formulation (Katagiri *et al.*, 1989)

Other particulate formulations that have been used are large (10μm) DOX albumin microspheres (Wilmott *et al.*, 1984). These were found to accumulate in the lung by capture in the lung capillary bed - a form of passive targeting, that may be exploited in lung carcinomas. These albumin microspheres also show improved therapeutic activity over the drug in solution (Wilmott and Cummings, 1987). Submicron albumin magnetic "microspheres" (0.75μm) injected via the tail vein extravasated in the tail and decreased DOX delivery to the heart (Gupta and Hung, 1989;

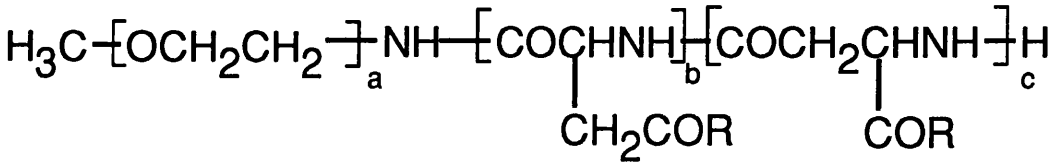

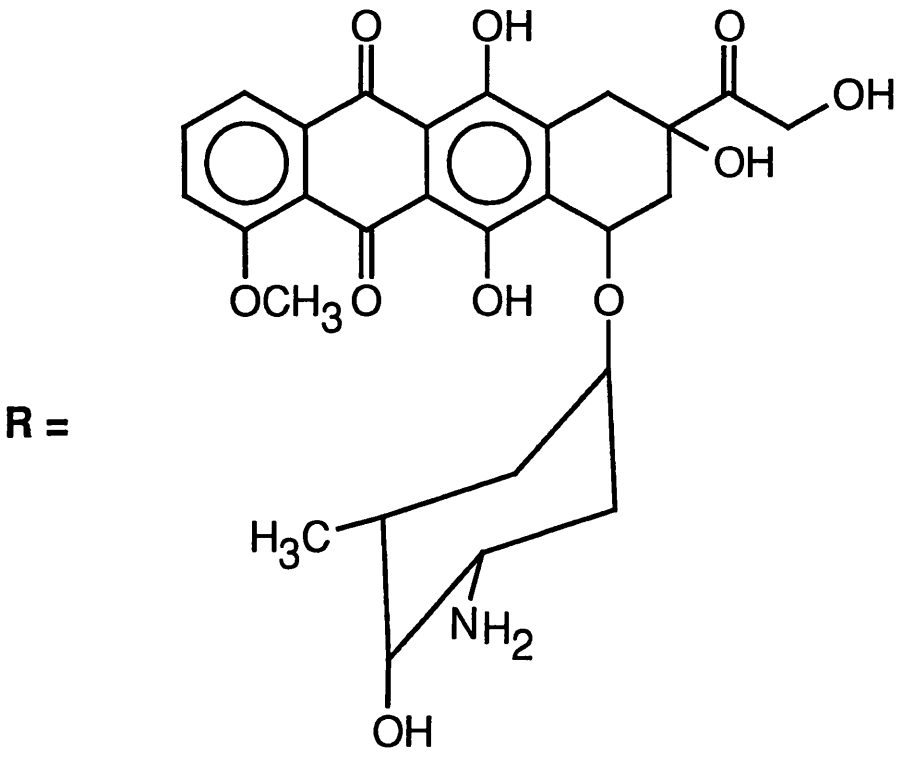

Figure 1.5: DOX polyethylene glycol-polyaspartic acid micelle forming conjugate, molecular weight ≈ 5,000. a, b and c refer to a variable number of subunits.

Gupta *et al.*, 1989) in response to an applied magnetic field. Clinical trials have been undertaken with DOX polyisohexylcyanoacrylate nanoparticles (Kattan *et al.*, 1992) and this formulation was not associated with any reported cardiotoxicity, although it must be stated that the dose did not exceed a cumulative level of 180 $mg.m^{-2}$.

Phospholipid vesicles (liposomes) loaded with DOX have received a considerable amount of attention in recent times and certain conventional liposomes, containing either phosphatidylcholine, phophatidlylglycerol or cardiolipin have entered clinical trials, with good patient tolerance and tumoricidal data being achieved (Rahman *et al.*, 1990; Owen *et al.*, 1992; Cowens *et al.*, 1993). Most scientific efforts have been focused on diverting vesicles away from their traditional *in vivo* target, (more correctly described as an anatomical sink for intravenously administered vesicles) namely the liver - as identified in the early days of liposome research (Gregoriadis and Ryman, 1971). This anatomical sink is now recognized to be the reticuloendothelial system (RES) (Hwang, 1987). Parallel efforts have centred on achieving ever longer blood residence times for these vesicles, as the longer blood residence time is deemed to directly influence tumour localization. However the effect of these long blood residence times on drug resistance after a durable sub-therapeutic blood level or the effect of long circulating vesicles on bone marrow localisation have not been fully addressed $_{to}$ date. The coating of liposomes with hydrophilic polymers exemplified by work with ganglioside G_{M1} (Unezaki *et al.*, 1993) and polyethylene glycol (Papahadjopoulos *et al.*, 1991; Huang *et al.*, 1992; Vaage *et al.*, 1992; Gabizon *et al.*, 1993; Williams *et al.*, 1993) has achieved extended blood residence times and, where

evaluated, improved tumoricidal activity. The use of high phase transition temperature phospholipid liposomes also achieved extended blood residence times (Gabizon *et al.*, 1989; Papahadjopoulos and Gabizon, 1990; Gabizon, 1992). The altered pharmacokinetics of hydrophilic coated liposomes has resulted in a broadly accepted hypothesis (Lasic *et al.*, 1991), which proposes that the confinement of these vesicles to the vascular space is due to the steric hinderance to opsonization by plasma molecular opsonins. This non-opsonization prevents recognition of the particles by the phagocytic apparatus of the reticuloendothelial system. However it is proposed, in some quarters, that ganglioside G_{M1} may act by some other as yet undefined mechanism (Mori *et al.*, 1991; Parr *et al.*, 1993). These extended circulation times, experienced with certain DOX phospholipid vesicles are advantageously associated with decreased DOX cardiac levels (Gabizon *et al.*, 1989; Gabizon, 1992; Unezaki *et al.*, 1993) and liposome DOX delivery does result in decreased cardiotoxicity (Herman *et al.*, 1983; Balazsovits *et al.*, 1989). The long residence time of DOX vesicles in the blood when compared to the drug in solution allows the tumour tissue a longer time to equilibrate with the drug and evidence has been presented of the extravasation of DOX liposomes containing ganglioside G_{M1} (Huang *et al.*, 1992). Also an increase in the level of DOX in malignant pleural and ascitic effusions was found in patients treated with liposomal DOX (Gabizon *et al.*, 1994). A depot of antineoplastic agent in such close proximity to the tumour cells gives these drug delivery systems great therapeutic potential.

Liposomal non-ionic surfactant vesicle formulations, specifically containing hydrogenated castor oil 60 (HCO60) have been prepared and could be adequately

targeted to the liver. Liposomes prepared with above 60% w/w levels of this non-ionic surfactant increased the accumulation of the liposomal marker in the liver (Kato *et al.*, 1993).

Thermosensitive liposomes which release their contents in response to a temperature stimulus accumulated in tumour tissue in response to local hyperthermia (Maruyama *et al.*, 1993). The use of this strategy on deep seated tumours may pose a problem however. Another fast growing area of research is the use of immunoliposomes. Surface antibodies have been used, with moderate success, to target vesicles to certain experimental neoplasms (Ohta *et al.*, 1993; Ahmad *et al.*, 1993).

While it is clear from the foregoing that liposomal DOX delivery has achieved an improvement in therapeutic response and a decrease in cardiotoxicity (Rahman *et al.*, 1985), efforts at ameliorating myelosupression have been less successful (Treat, 1989; Balley *et al.*, 1990; Rahman *et al.*, 1990; Owen *et al.*, 1992; Cowens *et al.*, 1993; Hengge *et al.*, 1993); an indication that this area of DOX toxicity is still an area requiring further study. A recent study in which conventional DOX liposomes were compared to DOX loaded microspheres suggests that in addition to DOX microspheres offering improved cytotoxicity, they also decrease DOX myelosuppressive effects compared to liposomal DOX (Codde *et al.*, 1993).

Although the data on DOX liposomes are extensive, the fact remains that phospholipids, the main ingredients of liposome manufacture have some disadvantages, as they are not yet produced at the relatively low cost demanded by pharmaceutical

excipients and also require stringent storage conditions (Florence *et al.*, 1990) to avoid degradation e.g. hydrolytic degradation (Kemps and Crommelin, 1988).

1.6 NIOSOMAL DRUG DELIVERY SYSTEMS

Niosomes are non-ionic surfactant vesicles prepared in a manner analogous to liposomes, except that the vesicle membrane is constructed from non-ionic surfactants (Handjani-Vila *et al.*, 1979; Baillie *et al.*, 1985; Rogerson *et al.*, 1988). These niosomes offer an alternative to liposomes in the field of drug delivery and have the potential applicability of liposomes as outlined above. An understanding of alternative drug delivery systems is desirable as this leads to the elucidation of unifying factors that could aid in the subsequent prediction of vesicle behaviour in vivo. Niosome surfaces differ somewhat from liposome surfaces as the latter are made up of charged or zwitterionic lipids and hence possess a defined potential for electrostatic association. It is not clear how these differences would affect the *in vivo* disposition of these particles, and indeed if any differences will be expressed which are solely attributable to the nature of the vesicle surface.

The various non-ionic surfactant molecular structures that form vesicles on hydration have been reviewed by Özer and others (1991) and Florence (1993). Israelachvili (1985, 1992) derived the critical packing parameter (CPP)

$$CPP = v/l_c a_0 \qquad 1.1$$

where v = hydrocarbon chain volume, l_c = hydrocarbon critical chain length,

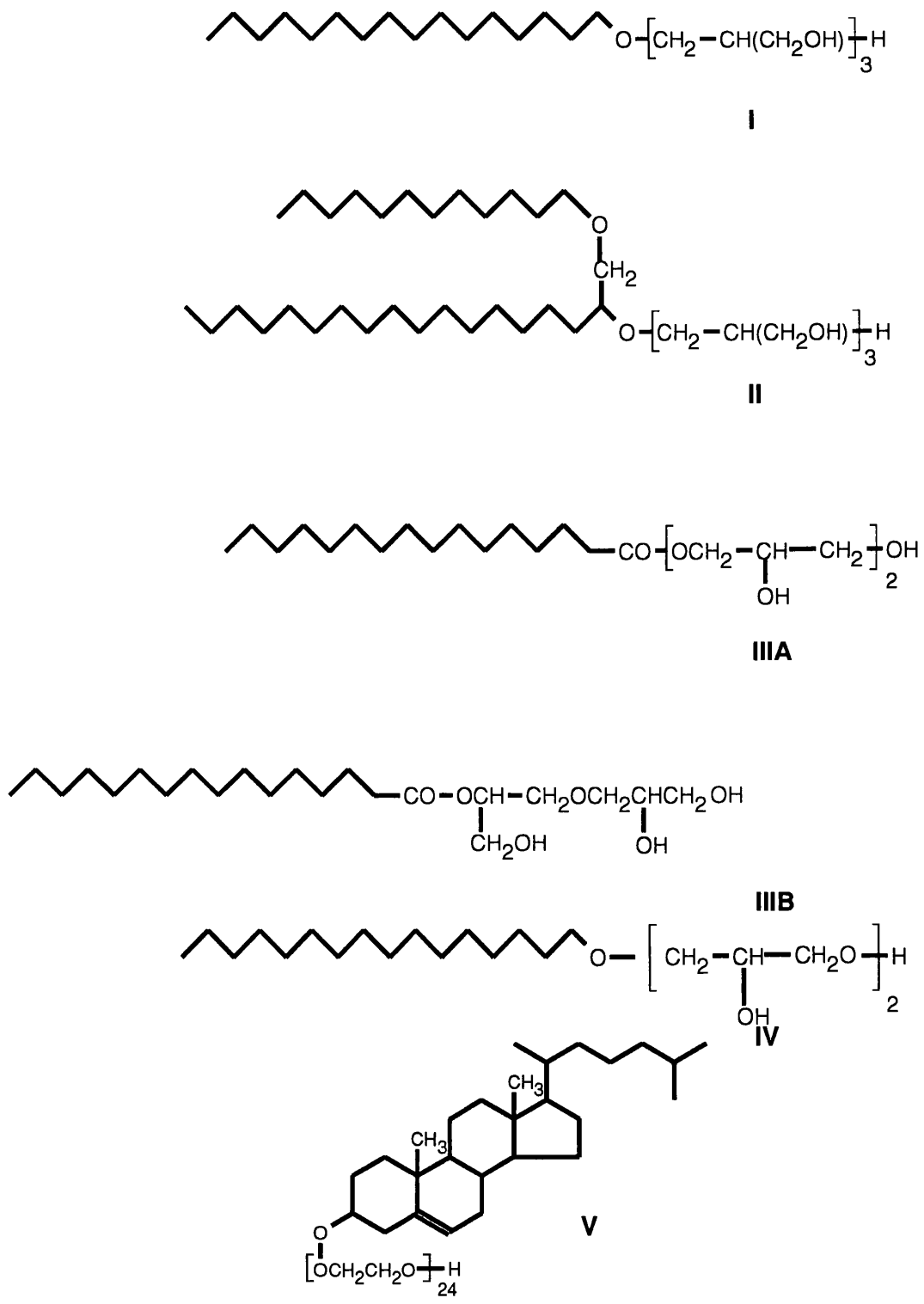

Figure 1.6: L'Oreal non-ionic vesicle forming surfactants and Solulan C24. I = $C_{16}G_3$, II = $C_{16}C_{12}G_7$, III = 92: 8 mixture of A and B (together referred to as surfactant III), IV = $C_{16}G_2$, V = Solulan C24.

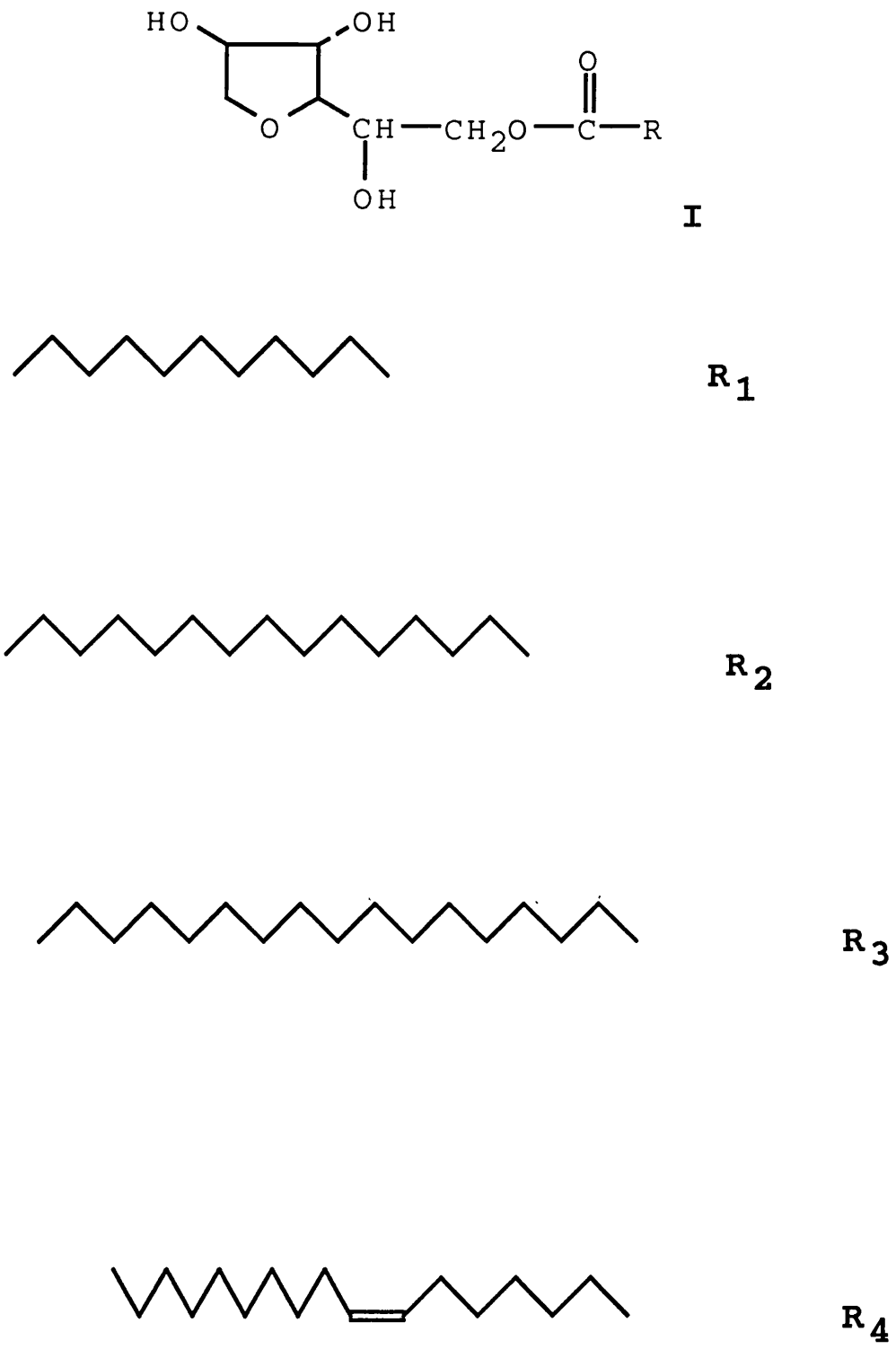

Figure 1.7: Alkyl sorbitan (I) ester vesicle forming amphiphiles (Spans). R1 = sorbitan monolaurate (Span 20), R2 = sorbitan monopalmitate (Span 40), R3 = sorbitan monostearate (Span 60), R4 = sorbitan monooleate (Span 80).

a_0 = hydrophilic head group area. This value is a dimensionless figure derived from the geometry of any particular amphiphile and it predicts the close packing characteristics of the surfactant molecules and ultimately the nature of the structure that will be formed on association. A calculated value of between 0.5 - 1 is predictive of flexible bilayer formation and thus an aggregation into closed vesicles. The CPP is affected by certain environmental factors, which indirectly affect lipid geometry, such as the ionic strength, pH and temperature of the surrounding medium. A number of single chain amphiphiles form bilayer vesicles quite easily, contrary to views held by some authors (Israelachvili, 1992; Menger, 1993), and while the aggregation of monomers into a bilayer structure requires a definite molecular hydrophilic-hydrophobic geometry (Israelachvili, 1992), the packing parameters are often satisfied just as well by single chain synthetic non-ionic surfactants as they are by double chain amphiphiles. Vesicles produced from single chain ionic C_{12} - C_{18} fatty acid and soap mixtures by Hargreaves and Deamer (1978) demonstrated that vesicles could be produced from such single chain amphiphiles. A series of non-ionic single chain surfactants synthesized by L'Oreal (Figure 1.6) have been used in our laboratories to prepare vesicles (niosomes) with a drug delivery objective for a number of years. $C_{16}G_3$ was one of the earliest compounds used (Azmin *et al.*, 1985; Baillie *et al.*, 1985). Relatively stable niosomes could be prepared from the single chain non-ionic surfactants $C_{16}G_3$, $C_{16}G_2$ and surfactant III with the inclusion of cholesterol, by the same methods used to prepare liposomes; these were found to encapsulate and retain solutes (Baillie *et al.*, 1985; Rogerson *et al.*, 1987; Hunter *et al.*, 1988; Rogerson *et al.*, 1989; Florence *et al.*, 1990). $C_{16}G_3$ has been employed in the encapsulation of methotrexate (Azmin *et al.*, 1985), sodium stibogluconate (Baillie *et al.*, 1986; Carter

et al., 1988; Hunter *et al.*, 1988), DOX (Rogerson *et al.*, 1987; Kerr *et al.*, 1988; Rogerson *et al.*, 1988) and haemoglobin (Moser *et al.*, 1989a; Moser *et al.*, 1990). $C_{16}G_2$ has been used to prepare DOX niosomes (Florence *et al.*, 1990) and Sodium stibogluconate niosomes have also been prepared from Surfactant III (Hunter *et al.*, 1988).

The biodistribution of methotrexate niosomes was altered by the encapsulation in the single chain amphiphile $C_{16}G_3$, and there was found to be preliminary evidence of increased delivery of methotrexate to the brain and a slight increase in the oral bioavailability of the compound (Azmin *et al.*, 1985). The *in vivo* evaluation of DOX $C_{16}G_3$ niosomes showed that these DOX niosomes improved tumour localisation and hence tumoricidal activity (Kerr *et al.*, 1988; Rogerson *et al.*, 1988), especially when formulated with equimolar quantities of cholesterol. The administration of cholesterol-free $C_{16}G_3$ DOX niosomes resulted in less tumour localisation of the drug (Rogerson *et al.*, 1988), probably due to their poor latency (potential for retention of encapsulated solutes) (Rogerson *et al.*, 1987). $C_{16}G_3$ DOX niosomes also reduced DOX cardiac levels (Kerr *et al.*, 1988). In cases where improved tumoricidal activity is not actually achieved, as was the case with $C_{16}G_2$ DOX niosomes, there was a reduction in cardiac levels of DOX (Florence *et al.*, 1990). Sodium stibogluconate encapsulated in $C_{16}G_3$ and Surfactant III niosomes increased the efficacy of the drug in experimentally induced leishmaniasis in a murine model (Baillie *et al.*, 1986; Carter *et al.*, 1988; Hunter *et al.*, 1988). The effective suppression of leishmaniasis by sodium stibogluconate niosomes is a result of the rapid uptake of the vesicles by the liver, the site of leishmania infestation. This effect is seen regardless of the surfactant that is

used.

Other monoalkyl surfactants used to prepare niosomes as drug carriers are C_{14} - C_{16} alkyl glucosides, galactosides and mannosides (Kiwada *et al.*, 1985a; Kiwada *et al.*, 1985b; Kiwada *et al.*, 1988). These, however, were found to be rapidly degraded in plasma by a specific heat stable plasma component (Kiwada *et al.*, 1988).

Sorbitan monoalkyl esters and anhydrides (Spans) (Figure 1.7) containing a C_{12} - C_{18} alkyl chain forms stable multilamellar vesicles capable of entrapping solutes and which are proposed as potential drug carriers (Chandraprakesh *et al.*, 1990; Udupa *et al.*, 1993; Yoshioka and Florence, 1994; Yoshioka *et al.*, 1994, Parthasarathi *et al.*, 1994). The pharmacokinetics of methotrexate was altered by encapsulation into large (1.5 - 13.5μm) sorbitan monostearate (Span 60 - Figure 1.5) niosomes with the drug experiencing a longer blood residence time (Chandraprakash *et al.*, 1990; Udupa *et al.*, 1993). Tumoricidal activity was concomitantly increased (Udupa *et al.*, 1993). The encapsulation of vincristine sulphate in Span 60 niosomes decreased the toxicity and improved the anti-cancer activity of the drug (Parthasarathi *et al.*, 1994).

When a non-ionic dialkyl surfactant - $C_{16}C_{12}G_7$ (Figure 1.4) - niosome was compared with $C_{16}G_3$, in the area of encapsulation efficiency and 5(6)-carboxyfluorescein latency, no differences could be found (Baillie *et al.*, 1985). There was also no difference in the pharmacological activity of sodium stibogluconate niosomes formed from dialkyl and monoalkyl surfactants (Hunter *et al.*, 1988). However it was found that while the single chain amphiphile could produce vesicles without the inclusion

of cholesterol in the bilayer, the same could not be said of the dialkyl amphiphile (Rogerson *et al.*, 1989).

C_{16} and C_{18} dialkyl amphphilic amino acids have been used to prepare amino acid vesicles capable of entrapping 5(6)-carboxyfluorescein (Neumann and Ringsdorf, 1986). These vesicles can be converted to peptide vesicles by simple chemical means. Synthetic dialkyl C_{14} - C_{22} polyhydroxyl lipids have also been used to prepare niosomes with encapsulation efficiencies comparable to egg phosphatidylcholine (Assadullahi *et al.*, 1991). Sucrose palmitate stearate, an amphiphilic mixture of mono, di and tri-esters has been used to prepare vesicles encapsulating the cytostatic drug methylglyoxal-bis-guanyl hydrazone (Schenk *et al.*, 1990). This formulation was found to be as efficacious as the free drug. Niosomes have also been produced from poly(oxyethylene) (10) hydrogenated castor oil ether (Tanaka *et al.*, 1990). The head group structure in these vesicle forming surfactants is by no means limited to monosaccharide or amino acid derivatives and compounds possessing neutral crown ether head groups also form niosomes (Echegoyen *et al.*, 1988).

From the foregoing, it becomes apparent that niosomes can be formed from a variety of amphiphiles, but it appears that a minimal alkyl chain length of at least 12 carbons and a head group area in the region of 0.25 - 0.5nm^2 are necessary prerequisites to vesicle formation (Florence, 1993). The molecular requirements conducive to vesicle formation must be assessed not only in relation to environmental factors such as ionic strength, pH and temperature of the medium; but also in relation to the nature of the encapsulating solute. This is especially true for DOX, which interacts with both

neutral and anionic bilayers (Burke and Tritton, 1985; de Wolf *et al.*, 1991a; de Wolf *et al.*, 1991b; Martì *et al.*, 1992). A critical examination of the nature of the encapsulating solute is desirable if we are to exploit fully these amphiphiles as drug carriers. Considerable success has been achieved with niosomal formulations in experimental animals. It is hoped that similar success will be achieved in the clinic at some time in the future

Certain physicochemical properties of $C_{16}G_2$ (Figure 1.6) and monoalkyl sorbitan (Figure 1.7) niosomes have been evaluated in this work and are discussed in Chapter 2. We have also studied the biodistribution of intravenously injected DOX sorbitan monostearate niosomes and have assessed the tumoricidal activity of the said preparation. Additionally, the tumoricidal activity of DOX $C_{16}G_2$ niosomes was evaluated in a murine tumour model. Details on the biodistribution of DOX niosomes following intravenous administration and the tumoricidal activity of DOX niosomes are discussed in Chapter 5.

1.7 THE INTRAPERITONEAL ADMINISTRATION OF DOXORUBICIN VESICULAR DELIVERY SYSTEMS

The intraperitoneal administration of antineoplastic agents is considered important when abdominal metastasis following bowel resection is to be avoided. Unfortunately the intraperitoneal administration of DOX solution is associated with marked local toxicity and is not recommended as a general strategy (Demicheli *et al.*, 1985). Mayhew and co-workers (1990) have studied the intraperitoneal administration of DOX liposomes in mouse colon 26 tumours, and report that although the liposome

formulation conferred no therapeutic advantage to the DOX dose when both liposomal DOX and DOX solution were administered at what the authors describe as equitoxic doses, liposomal DOX was generally less toxic than DOX solution.

We have also studied in this work the biodistribution of DOX niosomes prepared from $C_{16}G_2$ (Figure 1.6) on intraperitoneal administration to mice and characterised an adverse response to the formulation following administration by the same route. These results are discussed and presented in chapter 4.

1.8 DOXORUBICIN RESISTANCE

Apart from the toxic effects of DOX outlined above, another problem associated with DOX chemotherapy is the development of DOX resistance. DOX along with a few other compounds of natural origin, on continued patient exposure, causes chemotherapeutic resistance to develop although, in certain cases the resistance is intrinsic to host tissue, being present without prior chemotherapeutic stimulus. Its influence is on a broad spectrum of anticancer agents, most of natural origin and it is for this reason that this reaction is termed "multi-drug resistance". Once this non-susceptibility develops, the prognosis for the patient is poor (Doyle, 1993).

1.8:1 MECHANISMS OF MULTIDRUG RESISTANCE

The mechanisms of multidrug resistance are as diverse as they are poorly understood, and while a problem is posed to data interpretation by the non-uniformity of the various biological systems used, it is clear that a number of drug resistance

mechanisms are operating in any single situation (Volm and Mattern, 1993).

The most consistent finding in cells exhibiting multidrug resistance is the over expression of a 170 kilodalton membrane glycoprotein termed P-gp. This was found to be common to multidrug resistant cells (Riordan and Ling, 1979) and later correlated with the amplification of a family of multidrug resistant genes (Riordan *et al.*, 1985) termed the MDR1 gene. The over expression of this gene has been encountered in human tumours that are resistant to chemotherapy (Bourhis and Bénard, 1990; Areci, 1993). This membrane protein P-gp is deemed to act as an energy dependant pump, expelling intracellular drug, the kinetics of which have been described (Dordal *et al.*, 1992), or by creating membrane pores for eventual drug efflux (Beck, 1987). A lower level of DOX associated with the cell membrane is observed in some resistant cells and thus any membrane mediated cytotoxicity (Awasthi *et al.*, 1992) might also be decreased. Intracellular drug concentrations may also be decreased by an indirect mechanism of action, whereby the intracellular pH is raised by as yet undefined cellular processes to discourage intracellular pH dependant sequestration and encourage cellular efflux of largely basic drugs (Roepe, 1992). Additionally intracellular drug binding/sequestration within the cell which prevents the molecule reaching its site of activity within the nucleus (Beck, 1987; Boicchi and Toffoli, 1992; Sognier *et al.*, 1992; Doyle, 1993) is the hypothesis favoured by some to account for drug resistance, disregarding the action of the efflux pump. Direct evidence of a shift from a nuclear localisation to an extranuclear site was obtained in studies where the concentration of DOX was quantified in nuclear and cytoplasmic sites. There was a clear reduction in the ratio of nuclear to cytoplasmic

DOX quantities as cells went from being susceptible to resistant (Keizer *et al.*, 1989; Schuurhuis *et al.*, 1991; Lange *et al.*, 1992). Although these studies showed no apparent correlation between the observation of an increased cytoplasmic to nuclear ratio and the overexpression of P-gp. It is quite likely that the efflux mechanism and the diversion from nuclear sites mechanism may both be at work at different stages of the development of resistance or in different kinds of multi drug resistance syndromes. However there is doubt as to which is the major mechanism of multidrug resistance.

The expression of P-gp is by no means essential to the development or existence of the multidrug resistance syndrome and the level of P-gp expression is not the only marker of multidrug resistance (Lee *et al.*, 1989; Schott *et al.*, 1993) as in some cases its level bears no correlation to the decreased accumulation of intracellular DOX (Kato *et al.*, 1990; Ramachandran *et al.*, 1993) or presence or absence of clinical resistance (Ideguchi *et al.*, 1991). These findings have led some workers to propose alternative mechanisms of multidrug resistance, one of which is the non P-gp mediated energy dependant drug export mechanism which prevents the drug accumulating at the nucleus (Doyle, 1993). Increased free radical protection is also observed in some resistant cells, specifically increased levels of the glutathione (GSH) detoxification system - GSH peroxidase and GSH S-transferase (notably GSH S-transferase π) (Lee *et al.*, 1989; Nair *et al.*, 1989; Benchekroun *et al.*, 1993) . Equivocal results however were obtained on the correlation between the absence of drug induced lipid peroxidation and multidrug resistance (Benchekroun *et al.*, 1993). An ability to detoxify DOX in certain cell lines to an inactive metabolite is also thought to

contribute to the drug resistance of such cell lines (Zhang *et al.*, 1992). Another of the less well studied mechanisms of multidrug resistance is a resistance to topoisomerase II inhibitors (Doyle, 1993).

1.8:2 MODULATION OF MULTIDRUG RESISTANCE: THE ROLE OF DRUG DELIVERY SYSTEMS

Various intervention procedures have been employed in cases where drug resistance is established, namely the use of chemical modulators like verapamil, which interact with P-gp (Solary *et al.*, 1991) and other calcium entry blockers (Bruno and Slate, 1990). Unfortunately, the use of verapamil in the clinical management of resistant small cell lung cancer patients showed no significant improvement in survival (Doyle, 1993). The combined depression of DOX and verapamil on cardiovascular function comes to mind. The removal of the basic centre in DOX reversed the DOX resistance and resulted in the intracellular accumulation of the drug (Priebe *et al.*, 1993). The authors attribute this to the abolition of the P-gp binding site. However the proposal that certain acid lysozymes in resistant cells may bind the drug and extrude it to the cells exterior (Doyle, 1993) is apparently supported by this evidence.

A drug delivery approach to the problem of multidrug resistance has been mounted, using in turn: surfactants, nanoparticles and liposomes. The surfactant Cremophor EL (a polyoxyethylated form of castor oil) reverses daunorubicin resistance *in vitro* by supposedly altering the fluidity of the cell membrane and increasing the intracellular concentration of daunorubicin (Woodcock *et al.*, 1992). DOX loaded polyisohexylcyanoacrylate nanospheres delivered the same amount of DOX to resistant

cells as did free DOX to sensitive cells (Cuvier *et al.*, 1992), resulting in comparable levels of cell growth inhibition. A phase I clinical trial of these nanospheres in patients with refractory neoplastic disease reports the occurrence of a grade 2 allergic reaction (World Health Organisation criteria) and dose limiting myelosupression (Kattan *et al.*, 1992). Cardiac toxicities were not reported although none of the patients exceeded a maximum cumulative dose of 180 $mg.m^{-2}$.

Empty liposomes appear to interact with P-gp and partially overcome resistance *in vitro* (Thierry *et al.*, 1992). DOX loaded liposomes *in vitro* are also more effective against resistant cell lines than DOX solution (Thierry *et al.*, 1989: Oudard *et al.*, 1991; Rahman *et al.*, 1992; Thierry *et al.*, 1993), possibly by a direct interaction with P-gp (Rahman *et al.*, 1992). A combination of verapamil and DOX loaded liposomes produced favourable results *in vitro* with evidence of a synergistic relationship in occurrence (Sadasivan *et al.*, 1991). *In vivo*, the activity of DOX liposomes was retained and the formulation improved the effectiveness of DOX in a refractory mouse tumour (Mickisch *et al.*, 1992). Following on from the success of these liposome and non-ionic surfactant formulations in improving the susceptibility of these resistant cell lines, it was deemed appropriate to subject niosome formulations to a similar test. To this aim, we have studied the activity of DOX niosomes of various composition, size and vesicular DOX load against a resistant human ovarian carcinoma cell line *in vitro*. The ovarian carcinoma cell line had been made resistant by repeated *in vitro* exposure to DOX. Data and discussions on this study are presented in chapter 3.

1.9 VESICLE TO MICELLE PHASE TRANSITIONS

While seeking the optimum DOX niosome formulation, various lipid compositions were examined, one of which gave rise to the production of large discoid structures previously observed by Cable and Florence (1988).

Totally new structures can be formed by adding an amphiphilic compound with different molecular aggregate packing parameters to a stable system of amphiphilic aggregates (Israelachvili, 1992). The addition of critical amounts of soluble surface-active molecules to vesicular dispersions of phospholipids leads to the breakdown or solubilization of the vesicles and the formation of a mixed micellar phase. Such vesicle to micelle transitions, of sonicated egg yolk phosphatidylcholine liposomes, have been achieved by the addition of non-ionic surfactants of the polyoxyethylene cetyl ether class (Kim and Kim, 1991). In this system a region occurs where lamellar and mixed micelles coexist. In studies of the vesicle-micelle transition in cholate-phosphatidylcholine systems, Walter and others (1991) identified structures intermediate between vesicles and micelles. On increasing the bile salt concentration, more multilamellar vesicles were detected, but in addition "open" vesicles, large (20 - several hundred nanometres in diameter) bilayer sheets, and long (150 - 300nm) flexible cylindrical vesicles were seen (Walter *et al.*, 1991). Earlier studies (Small *et al.*, 1969) of the phase behaviour of phosphatidylcholine in cholate-water systems led to the hypothesis of an intermediate discoidal mixed micelle, a view later substantiated by the more recent studies (Walter *et al.*, 1991).

In the current work, non-ionic surfactant vesicles were formed from $C_{16}G_2$,

dicetylphosphate (DCP) and cholesterol and solubilized by the soluble surfactant Solulan C24 (a cholesteryl polyoxyethylene ether - Figure 1.6). The resulting phase transitions were studied by turbidometric means. Large disc shaped structures, as a distinguishable phase in the vesicle to micelle transition phase diagram of this system, were observed. Vesicle to micelle transitions of sonicated vesicles prepared from $C_{16}G_2$ have been studied using the detergent octylglucoside (Lesieur *et al.*, 1990; Seras *et al.*, 1992), but structures similar to the ones identified in the present study were not reported in the $C_{16}G_2$-octylglucoside study. Disc shaped structures have been prepared from amphotericin and cholesteryl sulphate (Guo *et al.*, 1991), however these amphotericin disc shaped structures are not thought to be similar to the ones reported here. Discoid structures have also been identified in a C_{18} dialkyl polyoxyethylene (15 oxyethylene units) aqueous dispersion (Okahata *et al.*, 1981). The vesicle to micelle transition of the $C_{16}G_2$ - Solulan C24 system and the discoid structures so produced are discussed in chapter 2.

1.10 OUTLINE OF WORK

The objective of the work described in this thesis was to define the applicability of niosomes to drug targeting. DOX was used as the model drug and the non-ionic surfactants used were $C_{16}G_3$, $C_{16}G_2$ and Spans 20, 40, 60 and 80, the latter chosen because of their use in foodstuffs and pharmaceuticals. The task was subdivided as follows. Vesicle size, encapsulation efficiency and latency were initially studied. The optimisation of these physico-chemical characteristics for the eventual *in vivo* study was the goal of this initial phase of the work. In the quest for an optimum vesicle,

a transition from a vesicle to a novel discoid structure was noted and this transition and the structures produced therefrom were defined. The clinical problem of multidrug resistance, already discussed above was approached from a drug delivery perspective. It was in this respect that niosomes were tested *in vitro* against a synthetically produced resistant cell line. The *in vivo* pharmacokinetic investigations were aimed at two broad fronts, the first entailing examining the fate of DOX niosomes on intravenous injection. Particular attention was paid to the persistence of the niosomes in the vascular space and the altered metabolite profile of the drug on encapsulation. The second area of interest was the fate of niosomes after intraperitoneal injection. An adverse reaction was observed in these studies, namely an inflammatory response in the lung tissue. The pharmacodynamic activity of DOX niosomes was also studied in a variety of murine tumour models and the issue of model selection was raised by the data obtained from these investigations.

The ultimate destination for any drug formulations is the patient, and specifically in this case the cancer patient. Derived benefits are principally an increased incidence of cures from the disease and a better quality of life. The acceptability of any pharmaceutical is unfortunately not simply limited to these qualities, as the issue of production costs also bears considerable influence. The significance of the work presented in this thesis on perceived patient benefits are summarised in the last chapter of the thesis.

CHAPTER TWO

THE PHYSICOCHEMICAL PROPERTIES OF DOXORUBICIN NIOSOMES AND SOME VESICLE TO MICELLE TRANSITIONS

2.1 THE NEED FOR AN OPTIMUM, SIZE, ENCAPSULATION EFFICIENCY AND LATENCY

The size of the administered vesicles affects their disposition *in vivo*, in as much as the extravasation of vesicles to certain tissues is limited by the sheer size of these vesicles (Hwang, 1987). Capillaries can be categorized as being continuous e.g. in the dermis, fenestrated - found in the exocrine glands and kidney and discontinuous (sinusoids) - found in the liver and spleen (Clough, 1991). Continuous capillary membranes permit the transport of particles of less than 10 nm in diameter, whereas the fenestrated capillaries permit the transport of particles in the upper size range of about 30 nm. Discontinuous or sinusoidal capillaries on the other hand permit the transport of particles of up to 100 nm (Hwang, 1987). Liposomes larger than 500 nm are not believed to extravasate and are thus removed from the vascular space by the phagocytic cells of the RES (Hwang, 1987). Tumour tissue differs from normal host tissue in that it is highly heterogenous, consisting of continuous, fenestrated and sinusoidal capillaries in one anatomical unit as well as capillary sprouts and certain blood channels that do not possess an endothelial lining (Jain, 1990). The heterogeneity of tumour vasculature is doubtless responsible for the higher permeability to macromolecules observed in studies using albumin, fibrinogen (Peterson and Applegren, 1973) and dextran (Nugent and Jain, 1984). An advantage of particulate drug delivery to neoplastic tissue is the opportunity to exploit this inherent leakiness in tumour tissue. Extravasation of silver enhanced colloidal gold particles (80 - 100 nm in diameter) has been observed in experimental murine neoplasms (Huang *et al.*, 1992). This extravasation could be especially promoted if circulation times could be enhanced. On a comparative basis smaller liposomes for example circulate for longer than larger liposomes (Hwang, 1987; Woodle and Lasic,

1992; Gabizon *et al.*, 1994). In addition, a hydrophilic surface promotes longer circulation times by avoiding the action of blood opsonins and thus preventing particle recognition by the RES (Allen *et al.*, 1991; Woodle and Lasic, 1991; Woodle *et al.*, 1992; Lasic 1992). While the size of the administered particle is important, an optimum size must not be gained at the expense of maximal drug encapsulation. This refers to the niosome payload. The lipid/surfactant level - as with all excipients, must be kept to a minimum in the majority of cases (Cullis *et al.*, 1987).

2.1:1 SIZE REDUCTION OF NIOSOMES

In this chapter are presented attempts to reduce vesicle size by well established means e.g. sonication (Baillie *et al.*, 1985; Florence, 1993), microfluidization (Mayhew *et al.*, 1984; Gregoriadis *et al.*, 1990; Vemuri *et al.*, 1990) and homogenisation (Brandl *et al.*, 1993). The surfactants used were the L'Oreal surfactants $C_{16}G_3$, $C_{16}G_2$ (Figure 1.6) and the Span surfactants (Figure 1.7). The Span surfactants were studied to enable the product make a smooth transition from the bench to the clinic, as these surfactants are already established pharmaceutical excipients and are used in foodstuffs.

The head group area, according to the critical packing parameter derived by Israelachvili (1985, 1992) - see section 1.6, also determines to some extent vesicle size, in that the larger its contribution to the overall parameter (within certain restrictions of course) the larger the vesicle curvature and, in effect, the smaller the vesicle size. This particular characteristic was exploited and the head group area was manipulated in order to reduce vesicle size. Specifically this was carried out by a

progressive increase in the level of Solulan C24 (a compound with 24 polyoxyethylene units within its structure - Figure 1.6), in the formulation.

There are various methods of determining vesicle size - namely light scattering, electron microscopy and gel filtration (Schurtenberger and Hauser, 1993). In this work, vesicle size in the submicron range was measured using dynamic light scattering (photon correlation spectroscopy). This method has been reviewed by Phillies (1990). Basically the instrumentation is designed to obtain measurements on the diffusion of colloidal particles in any given dispersion. A laser beam records this diffusion as temporal fluctuations in light scattering data. These values can then be computed to give values of particle size - typically expressed as z-average mean hydrodynamic diameter. Static light scattering was used to measure the size of the multilamellar vesicles with size distributions greater than a micron. With the static light scattering procedure, the intensity of scattered light is recorded and this is used to compute the radius of the particle (Schurtenberger and Hauser, 1993).

2.1:2 THE OPTIMIZATION OF NIOSOME ENCAPSULATION EFFICIENCY

Details are presented on efforts to obtain an optimum encapsulation efficiency in conjunction with an optimum particle size.

Specifically DOX encapsulation efficiency was first studied as a function of overall lipid/surfactant level (referred to hereafter for simplicity as total lipid), in order to determine an optimum initial DOX/total lipid ratio. The method of transmembrane gradients has been shown to yield improved encapsulation of basic drugs like DOX

(Mayer *et al.*, 1985; Haran *et al.*, 1993; Montero *et al.*, 1993; Praet *et al.*, 1993). In this work we have loaded DOX by an active trapping method involving a transmembrane pH gradient.

A preliminary comparison was made between the encapsulation efficiency of phosphatidylcholine liposomes, $C_{16}G_2$ niosomes and Span 60 niosomes with the use of pH gradients. Final molar DOX/phospholipid ratios of 0.05 have been reported with phosphatidylcholine, phosphatidylethanolamine liposomes in response to a pH gradient (Praet *et al.*, 1993).

The 5(6)-carboxyfluorescein and DOX latency of certain formulations was also studied in order to gain some knowledge of the stability of these formulations at room temperature.

2.2 $C_{16}G_2$ - SOLULAN C24 VESICLE TO MICELLE TRANSITIONS

The incorporation of increasing amounts of Solulan C24 into $C_{16}G_2$ vesicle formulations (ostensibly to reduce vesicle size, by increasing vesicle curvature), led to the formation of large discoid structures similar to those previously observed by Florence and Cable (1988) in $C_{16}G_3$ - Solulan C24 systems. The physicochemical characteristics of these structures were studied, with a view to examining the possibility of utilising these novel structures as drug carriers. This is considered especially relevant as amphotericin B in combination with the sterol cholesteryl sulphate produces a stable discoid structure (admittedly in the colloidal size range)

with a therapeutic index 4 - 6 fold higher than the free drug (Guo *et al.*, 1991). Geometrically similar structures have been observed in egg phosphatidylcholine - cholate mixtures (Walter *et al.*, 1991) and in C_{18} - dialkyl polyoxyethylene (15 polyoxyethylene units) aqueous dispersions (Okahata *et al.*, 1981).

2.3 MATERIALS

The materials used in the various experiments discussed in this chapter are as given in Table 1. All solvents used for HPLC analysis were of HPLC grade. All other reagents and chemicals were of analytical grade, unless otherwise stated. All materials were used as obtained from suppliers without further purification and the water source was from an ultra high quality reverse osmosis water purifier (Elgastat UHQ PS - Elga UK). Equipment sources are stated within relevant portions of the text.

METHODS

2.4 THE PHYSICOCHEMICAL PROPERTIES OF $C_{16}G_3$, $C_{16}G_2$, AND SPAN SURFACTANT NIOSOMES

2.4:1 GENERAL METHODS FOR THE PREPARATION OF NIOSOMES

Lipids were dissolved in chloroform, and the solvent removed under reduced pressure at 60°C, in a round bottomed flask. Residual organic solvent was removed by drying the lipid film under a stream of nitrogen for 20 min. The lipid film so obtained was then hydrated at 60°C (75°C for Span surfactant niosomes) for 1 h with constant shaking on a mechanical shaker, with either water or DOX solution in phosphate buffered saline (PBS), (pH 7.4), (NaCl 140 mM, Na_2HP0_4

Table 1: Materials used in the study of the physicochemical characteristics of niosomes.

MATERIAL	SOURCE
$C_{16}G_2$	Donated by L'Oreal, France.
$C_{16}G_3$	Donated by L'Oreal France.
5(6)-carboxyfluorescein (CF)	Sigma Chemical Company (UK) Ltd.
Chloroform	Rathburn Chemicals, UK.
Cholesterol	BDH Laboratory Supplies, UK.
Dicetylphosphate (DCP)	Fluka Chemika, Germany.
Disodium hydrogen phosphate	BDH Laboratory Supplies, UK.
Doxorubicin hydrochloride	Donated by Mr P. Launchbury and Dr A. Suarato, Farmitalia Carlo Erba, Italy.
Isopropanol	Rathburn Chemicals Ltd, UK
Potassium chloride	BDH Laboratory Supplies, UK.
Sephadex G50	Pharmacia (UK), Ltd.
Sodium Chloride	BDH Laboratory Supplies, UK.
Sodium dihydrogen phosphate	BDH Laboratory Supplies, UK.
Solulan C24	D.F. Anstead, UK.
Span 20	Fluka Chemika, Germany.
Span 40	Fluka Chemika, Germany.
Span 60	Fluka Chemika, Germany.
Span 80	Fluka Chemika, Germany.

0.18 mM, $NaH_2PO_4.2H_2O$ 3.2mM, KCl 2.7 mM - pH adjusted to 7.4 with 1 M NaOH). The lipid dispersion was sonicated using an MSE PG100 150W probe sonicator with the instrument set at 15% (40% for Span surfactant niosomes) of its maximum power output. Sonication was usually carried out in 10 30 s bursts with 30 s in between each burst for cooling. The temperature of the dispersion during sonication was 40°C. The dispersion was then left to cool to room temperature.

2.4:2 THE REDUCTION OF NIOSOME SIZE BY THE MICROFLUIDIZATION OF $C_{16}G_3$ NIOSOMES

A 5 mL dispersion $C_{16}G_3$, cholesterol, DCP (47.5: 47.5: 5) niosomes (150 µmol total lipid) was diluted to 28 mL with water and passed through a microfluidizer 100™, (donated by Microfluidizer Corp, USA). Microfluidization was carried out at an operating pressure of 0.55 MPa and a flow rate of 48 $mL.min^{-1}$. At regular intervals samples were obtained from the microfluidizer efflux and sized as described below.

2.4:3 THE REDUCTION OF $C_{16}G_2$ NIOSOME SIZE BY THE INCORPORATION OF INCREASING AMOUNTS OF SOLULAN C24 INTO THE BILAYER

Niosomes were prepared from the 150 µmol of lipid in the following molar proportions: $C_{16}G_2$, cholesterol, Solulan C24 (45: 45: 10) (40: 40: 20) (35: 35: 30) (30: 30: 40) (25: 25: 50) and 10 mL of water. These niosomes were sized as described below.

2.4:4 THE REDUCTION OF $C_{16}G_2$ NIOSOME SIZE BY HOMOGENISATION

DOX niosomes were prepared from $C_{16}G_2$, cholesterol, Solulan C24 (30: 30: 40) and

DOX in PBS in an initial DOX/total lipid ratio of 0.0115. 10 mL of the unsonicated dispersion (30 mM lipid) was diluted to 100 mL with PBS (pH 7.4). The diluted dispersion was then passed through a Westfalia Separator homogenizer at 60MPa pressure. Homogenised material was collected at various time intervals and sized as described below. The same procedure was carried out using lipid films prepared from the following mixtures of lipids: a) $C_{16}G_2$, cholesterol, Solulan C24 (45: 45: 10) and b) $C_{16}G_2$, cholesterol, DCP (47.5: 47.5: 5). The encapsulation efficiency of these formulations was determined as described below.

2.4:5 SIZING OF SUBMICRON NIOSOME DISPERSIONS

Sonicated vesicular dispersions were sized by photon correlation spectroscopy (PCS) on a Malvern Autosizer 2c, at a temperature of 25°C by diluting 20 µL of the dispersion (15 - 30 mM lipid, 0 - 2.24 mM DOX) to 4 mL in doubly filtered (0.22 µm pore size) water. Results are expressed as the z-average mean diameter.

2.4:6 SEPARATION OF UNENCAPSULATED MATERIAL, ASSAY OF NIOSOMES FOR DOXORUBICIN CONTENT AND THE DETERMINATION OF DOXORUBICIN ENCAPSULATION EFFICIENCY

1.5 mL of the dispersion (15 - 225 mM total lipid and 0.35 - 5.2 mM DOX) was applied to a 400 x 10 mm Sephadex G50 column. The void volume containing the vesicles was eluted with PBS (pH 7.4) into a 10 mL volumetric flask. To the flask was added 1 mL isopropanol to disrupt the niosomes. The volume was then made up with PBS (pH 7.4). In the event of this solution being too concentrated, further dilutions were made as appropriate. A calibration plot was produced by diluting stock solutions of DOX with PBS (pH 7.4) whilst ensuring that the final dilutions contained

10%v/v isopropanol. The fluorescence of these solutions was measured on a Perkin-Elmer LS-3 fluorescence spectrometer (excitation 480 nm, emission 560 nm). Encapsulation efficiency was calculated and expressed as a percentage of the hydrating solute actually encapsulated and as the molar ratio of encapsulated solute to initial total lipid.

2.4:7 THE OPTIMIZATION OF DOXORUBICIN ENCAPSULATION EFFICIENCY BY VARYING THE INITIAL LEVEL OF TOTAL LIPID

Niosomes were prepared by hydrating 75 - 450 µmol total lipid in the molar proportion $C_{16}G_2$, cholesterol, Solulan C24 (45: 45: 10) and $C_{16}G_2$, cholesterol, Solulan C24, DCP (42.75: 42.75: 9.5: 5) with 2 mL 3.45 mM DOX in PBS (pH 7.4). The dispersions were assayed for entrapped DOX and niosome encapsulation efficiency computed.

2.4:8 SIZE AND ENCAPSULATION EFFICIENCY OF SPAN SURFACTANT NIOSOMES

DOX niosomes were prepared by hydrating Span surfactants (Span 20, 40, 60 and 80) in the ratio Span surfactant, cholesterol, Solulan C24 (45: 45: 10) with DOX in PBS. Initial DOX/total lipid ratios were 0.029. Unsonicated niosomes were sized as described below and sonicated niosomes were sized and assayed for encapsulation efficiency in the usual way.

2.4:9 SIZING OF MULTILAMELLAR SPAN SURFACTANT VESICLES

Multilamellar vesicles were sized on a Malvern series 2600 droplet and particle sizer, by diluting 100µL of the dispersion (60 mM total lipid, 0.42 - 0.66 mM DOX) to 30 mL with water. Results are expressed as volume mean diameter.

2.4:10 OPTIMISATION OF DOXORUBICIN ENCAPSULATION EFFICIENCY BY LOADING NIOSOMES USING TRANSMEMBRANE PROTON GRADIENTS

Method 1: DOX Niosomes were prepared from $C_{16}G_2$, cholesterol, Solulan C24 (45: 45: 10) and DOX in tris buffered saline (trizma HCl 10 mM, NaCl 140 mM, adjusted to pH 4.0 with 1 M HCl - TBS) (pH 4.0). The initial molar ratio of DOX/total lipid was 0.069. After sonication the pH of the dispersion was adjusted from 6.13 to 7.2 with 1 M NaOH and left in the dark at 22°C for 24 h. Similarly DOX niosomes were also prepared from Span surfactants (Span 40 and 80) from lipid proportions of Span surfactant, cholesterol, Solulan C24 (45: 45: 10). The initial DOX/total lipid ratio in these cases was 0.029. Smaller initial DOX/total lipid ratios could be used with the Span surfactants as the encapsulation efficiency with these surfactants was superior to those obtained with $C_{16}G_2$. Sizing and the assay of encapsulated material was carried out in the usual fashion, except that the gel filtration eluate was TBS (pH 7.4).

Method 2: DOX niosomes were prepared from $C_{16}G_2$, cholesterol, Solulan C24 (45: 45: 10) and 1.5 mL TBS (pH 4.0). To the ensuing dispersion was added DOX in TBS (pH 4.0) in the ratio DOX/total lipid 0.029 or 0.035 and the pH adjusted upwards from 6.2 to 7.3. The dispersion was incubated at 60°C for 1 h and left to cool slowly overnight, protected from light. Similarly DOX niosomes were also prepared from Span 60 and phosphatidylcholine using lipid proportions - Span 60, cholesterol, Solulan C24 (45: 45: 10) and phosphatidylcholine, cholesterol, Solulan C24 (45: 45: 10) respectively. Initial DOX/lipid ratios of 0.029 were used in both the latter cases. Sizing and the assay for unentrapped drug was carried out in the usual way.

2.4:11 MEASUREMENT OF THE RELEASE OF 5(6)-CARBOXYFLUORESCEIN (CF) AND DOX FROM $C_{16}G_2$ NIOSOMES

a) CF niosomes were prepared from $C_{16}G_2$, cholesterol and Solulan C24 (30: 30: 40) at an initial CF (in PBS)/lipid ratio of 0.27. Assay was carried out as described under the assay of DOX, except that CF standards were used in conjunction with a fluorescence excitation of 484 nm and emission of 516 nm.

4 mL of CF loaded niosomes (45.6 μM CF), contained in 100 mm of dialysis tubing (Visking 20/32), secured 10 mm from either end with dialysis clips, were placed in each of 3 stoppered 250 mL conical flasks, the latter containing 100 mL PBS (pH 7.4). 3 other flasks contained controls - 4 mL CF (45.6 μM) in dialysis tubing. The flasks were placed in a shaking water bath (25 ± 1°C) and at regular intervals, samples of PBS external to the dialysis tubing were sampled and their fluorescence measured. Samples were returned to the flask after measurement to maintain a constant volume of dialysis medium. CF efflux into the dialysis medium was expressed as a percentage of the total initial aqueous marker released with time.

b) DOX niosomes prepared from $C_{16}G_2$, cholesterol, Solulan C24 (30: 30: 40) and with a DOX/total lipid ratío 0.023 were used to measure the DOX efflux from $C_{16}G_2$ niosomes. The procedure outlined above for the CF niosomes was generally followed except that DOX niosomes (0.033 mM) were used in place of CF niosomes and DOX solution (0.031 mM) was used as control.

2.5 VESICLE TO MICELLE TRANSITIONS IN THE $C_{16}G_2$ - SOLULAN C24 SYSTEM

2.5:1 SOLUBILIZATION OF VESICLES USING SOLULAN C24

Niosomes prepared from $C_{16}G_2$, cholesterol and DCP (69: 29: 2) (initial total lipid = 15 mM) were diluted to produce dispersions containing total lipid concentrations of 1.5 mM, 3.0 mM and 7.5 mM. These dispersions were incubated with various proportions of 15 mM Solulan C24 in a shaking water bath at a temperature of 74°C for 1 h. Once the mixtures had cooled to room temperature, their absorbance was measured on a Shimadzu multipurpose recording spectrophotometer with the wavelength set at 350 nm.

2.5:2 SIZE GROWTH STUDY

Lipid aggregates were prepared by hydrating 0.3mmol $C_{16}G_2$, cholesterol, Solulan C24, DCP (49: 19.5: 29.5: 2) with 10 mL 65 μM CF in PBS (pH 7.4). This was followed by probe sonication in 10 X 1 min bursts with the instrument set at 20% of its maximum output and with a 30 s cooling period in between each burst. The hydration and initial sonication temperature was 55-60°C. Once the dispersion had cooled to room temperature samples were carefully withdrawn and sized on a Malvern series 2600 droplet and particle sizer (M4.4) using PBS (pH 7.4) as the diluent.

2.5:3 PREPARATION OF DISCOMES

$C_{16}G_2$ (95.6 mg), cholesterol (37.7 mg), Solulan C24 (212.8 mg) and DCP (5.5 mg) - molar proportions 49: 19.5: 29.5: 2 were hydrated with either 8 mM CF in PBS (pH 7.4) or with PBS (pH 7.4) alone and then sonicated as described above. The dispersion containing PBS alone will be referred to as empty discomes. The

dispersions were left to stand at room temperature for at least 18 h and the discomes containing CF were subsequently dialysed in 150 mm of dialysis tubing (Visking 20/32), clipped 10 mm from each end with dialysis clips, for 80 h against 800 mL of PBS (pH 7.4) at a temperature of 4°C. Dialysis was carried out in the dark. The dialysis medium was changed 6 times and the removal of CF not encapsulated by the lipid aggregates was assumed to be complete when the fluorescence in the dialysis medium had reached a limiting value. Fluorescence was measured as previously described for CF. Fluorescence photomicrographs of these discomes were recorded (Nikon Microphot FXA equipped with a fluorescent light source). Discomes were assayed as previously described for CF niosomes. Entrapment volumes were calculated as litres of hydrating solution per mole of lipid used initially. It was assumed that the aqueous solution entrapped by the lipid aggregates was at the same concentration as the solution used to hydrate the lipids initially and also that there was no loss of lipid during the procedures.

2.5:4 THE RELEASE OF CF FROM DISCOMES AT ROOM TEMPERATURE

The release of CF from CF loaded discomes, empty discomes + CF or CF solution was assessed in a similar manner to that described for CF niosomes.

2.5:5 TURBIDITY MEASUREMENTS ON $C_{16}G_2$ DISCOMES AND NIOSOMES AS A FUNCTION OF TEMPERATURE

$C_{16}G_2$, cholesterol and Solulan C24 in the following proportions, a) 50: 40: 10; b) 50: 30: 20 and c) 50: 20: 30, present as films that had been prepared by the evaporation of suitable chloroform solutions under vacuum were hydrated with water (150 µmol lipid: 10 mL water). They were then sonicated as describe previously. Microscopic

examination of the dispersions after sonication revealed discomes in the 20 and 30% Solulan C24 preparations. Turbidity measurements were carried out on all three samples on a Sigma ZWSII spectrophotometer at temperatures of 30°C and 37°C at 350 nm.

RESULTS AND DISCUSSION

2.6 THE PHYSICOCHEMICAL PROPERTIES OF $C_{16}G_3$, $C_{16}G_2$ AND SPAN SURFACTANT NIOSOMES

As a necessary preliminary to any *in vivo* investigation, certain characteristics of the niosome formulation must be optimised. Efforts described in this chapter focus on particle size and encapsulation efficiency.

2.6:1 MICROFLUIDIZATION OF $C_{16}G_3$ NIOSOMES

Microfluidization techniques have been used in the preparation of liposomes (Mayhew *et al.*, 1984; Gregoriadis *et al.*, 1990; Vemuri *et al.*, 1990) and microemulsions (Washington and Davis, 1988). The technique involves pumping a stream of the vesicle dispersion into an "interaction chamber" under high pressure, where it is divided into two separate streams. These two streams are then forced to collide with one another at a high velocity. These collisions produce shear forces capable of reducing vesicle size and size distribution (Mayhew *et al.*, 1984). This work is the first report of the effect of microfluidization on niosome size (Figure 2.1). There is efficient size reduction of $C_{16}G_3$ niosomes suspended in water after the first 3.4 cycles (2 min) with z-average mean diameters falling from 95 nm to 83 nm. Thereafter the fall in size is gradual reaching about 69 nm after 34.3 cycles (20 min). Any large size

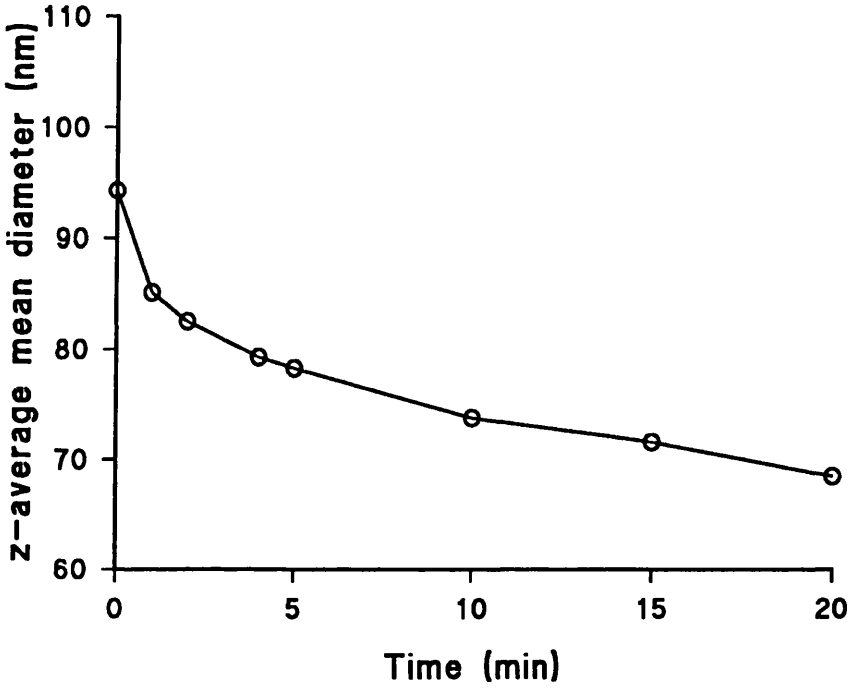

Figure 2.1: The effect of microfluidization at a pressure of 0.55 MPa and a flow rate of 48 mL min^{-1} on the size of $C_{16}G_3$, cholesterol, DCP (47.5: 47.5: 5) niosomes. 1 cycle = 35 s.

reduction is minimal after 5.1 cycles. These findings are in accordance with previously published data on dehydration-rehydration phosphatidylcholine liposomes entrapping maltose and suspended in water (Gregoriadis *et al.*, 1990). In these studies maximal size reduction was obtained after 3.5 cycles, sizes fell from 464 nm to 150 nm with only minimal size reduction obtained on prolonging the procedure to 10.6 cycles, whereas if these same vesicles were suspended in PBS (pH 7.4), the procedure was maximally effective after 10.6 cycles, due to flocculation, which reduces the efficiency of the procedure. Size reduction of metaproterenol PC liposomes was also found to be maximal after 3 cycles, particle size fell from 640 nm to 180 nm (Vemuri *et al.*, 1990). While the initial niosome size in this work was a little under 100 nm, the size of liposomes used in the other studies was much greater 640 nm (Vemuri *et al.*, 1990) and 464 nm (Gregoriadis *et al.*, 1990). A critical radius has been defined by Israelachvili (1985, 1992), below which a vesicle bilayer may not curve without unfavourable energetic constraints - notably the head group in the outer monolayer is unable to achieve an optimal head group area. The energy barrier that needs to be surmounted to reach ever smaller vesicle sizes will increase as this critical radius is approached. It is for this reason that the % size reduction obtained in this study is not as large as the reduction in size quoted in previous reports. The polydispersity of the $C_{16}G_3$ niosome suspension changed only minimally falling from 0.34 to 0.31 after 34.3 cycles (20 min). Similar small changes in polydispersity were recorded with metaproterenol loaded PC liposomes as the polydispersity fell only 1.25% per cycle (Vemuri *et al.*, 1990). This is contrary to earlier findings (Gregoriadis *et al.*, 1990) which report the production of narrower size bands with the technique. It is concluded that while efficient niosome size reduction of $C_{16}G_3$ niosomes is possible

after 3 microfluidization cycles, the reduction in polydispersity of the dispersion is minimal.

2.6:2 SOLULAN C24 IN $C_{16}G_2$ NIOSOMES

Solulan C24 (Figure 1.6) is a relatively hydrophilic cholesterol derivative that has been used experimentally in pharmaceutical formulations to solubilize (Tasset *et al.*, 1990) and enhance paracellular transport (Drewe *et al.*, 1993) of various pharmaceuticals. It is used here in attempts to reduce vesicle size to an optimum minimum, based on the principle of the critical radius being dependant on molecular geometry of the bilayer lipids.

The critical packing parameter (CPP) (Israelachvili 1985, 1992) can be used to compute a critical radius R_c:

$$R_c = l_c / (1-v/a_0 l_c) \qquad 2.1$$

The terms of the equation are defined in section 1.6. From equation 2.1, it can be seen that, the larger the optimum headgroup area (a_0) in relation to the critical chain length (l_c), the smaller the value of the critical radius.

The increasing incorporation of Solulan C24 into $C_{16}G_2$ niosomes results in the production of progressively smaller niosomes (Figure 2.2) - falling from 83 nm to 48 nm in diameter. Solulan C24 is a highly hydrophilic compound and its incorporation into the bilayer in increasing amounts, increases the net headgroup area of the lipid/ surfactant aggregates, resulting in a reduction in niosome size. Similar results were obtained when niosomes were produced from the dialkyl surfactant $C_{30}G_7$, cholesterol

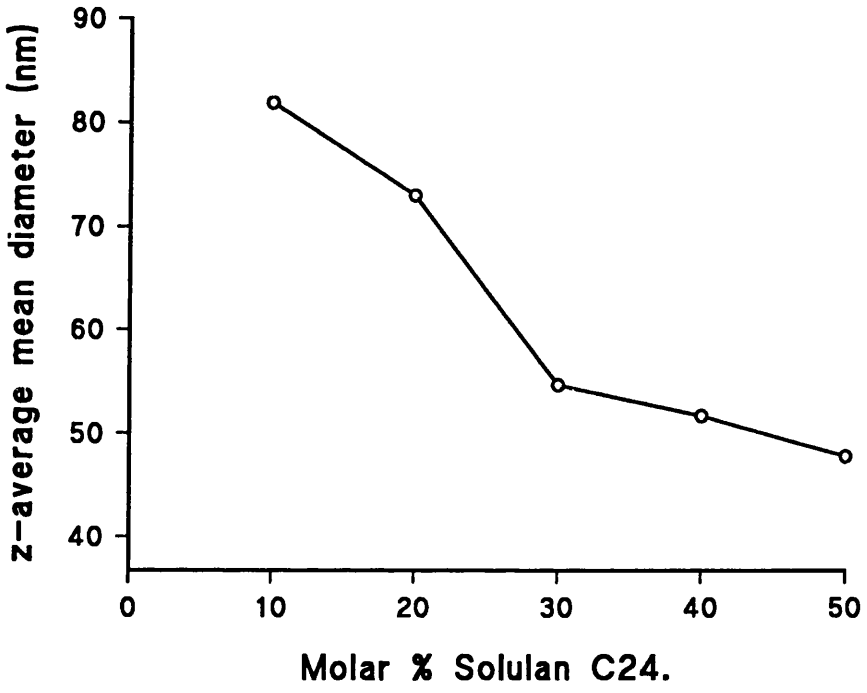

Figure 2.2: The effect of increasing Solulan C24 content in niosome formulations on vesicle size. Niosomes, consisted apart from Solulan C24, of a 1: 1 molar ratio of $C_{16}G_2$ and cholesterol.

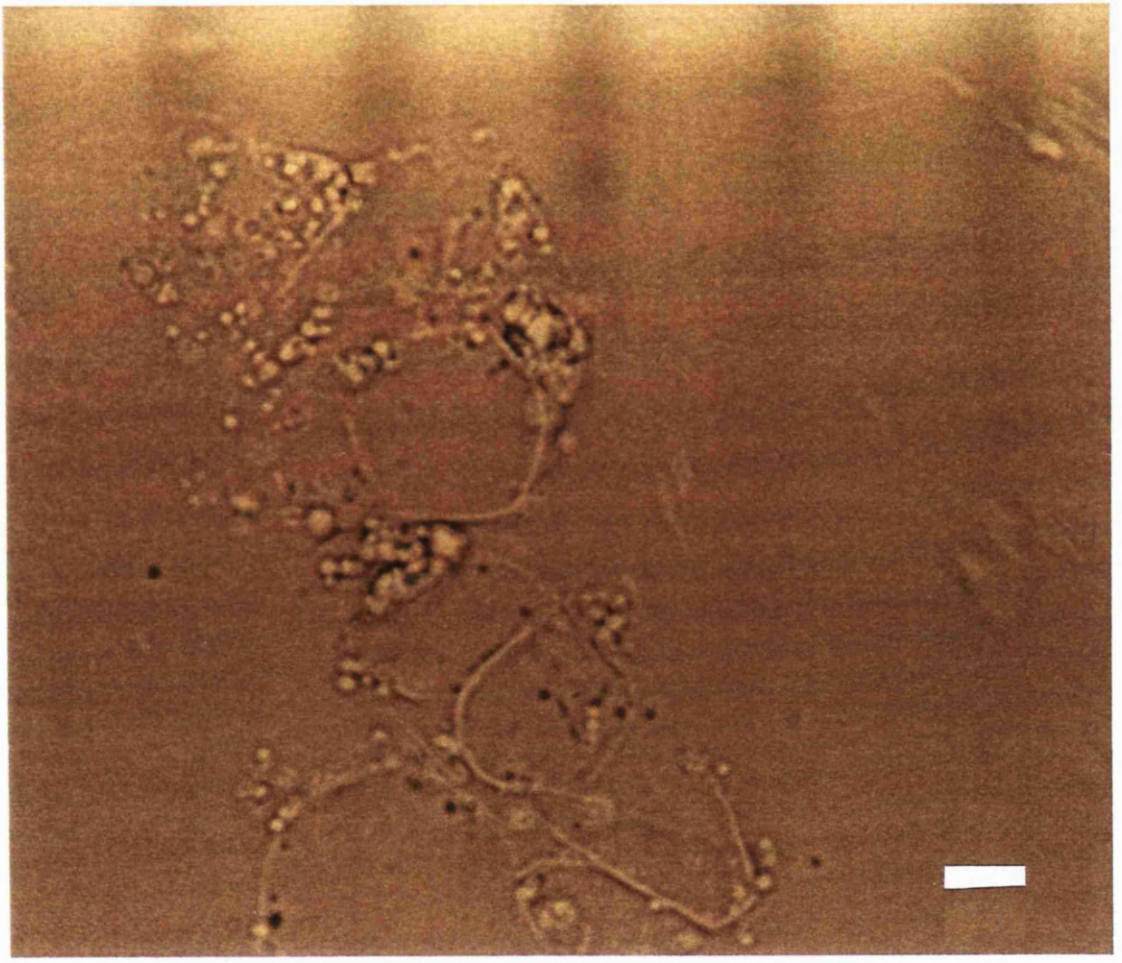

Figure 2.3: Photomicrograph (X1000) DOX $C_{16}G_2$, cholesterol, Solulan C24 (30: 30: 40) niosomes that had been left to stand at 4°C for 70 days, photographed under a fluorescent light source. Large (20 - 30 μm) irregular shaped structures are seen. Niosome dispersion had a z-average mean of 85 nm when freshly prepared. Bar = 10 μm.

and Solulan C24 (molar proportions - 50: 50-X: X) (Cable, 1989). In this work it was essential that the an equimolar ratio of $C_{16}G_2$, cholesterol was maintained for niosomes to form. When the molar ratio of $C_{16}G_2$ was fixed at 50% and the ratio of cholesterol, Solulan C24 was varied in the order 50-X: X (in a manner similar to Cable, 1989); large disc shaped structures were formed once the level of Solulan C24 exceeded 10 mole %. Cable and Florence (1988) observed similar disc shaped structures with $C_{16}G_3$, cholesterol, Solulan C24 in the molar proportions (50: 50-X: X). A partial explanation for these phenomenon can be sought from a consideration of the influence of the CPP (Israelachvili, 1985, 1992) on the nature of lipid aggregate that is ultimately formed. It is plausible that when the mole % of $C_{16}G_2$ is fixed at 50, the continued reduction in cholesterol content experienced as the mole % of Solulan C24 is increased, would decrease the hydrocarbon volume (v) and critical chain length (l_c) components in favour of an increase in head group volume (a_0). This reduction in v and l_c and increase in a_0 would be greater when cholesterol (a largely hydrophobic molecule) is replaced by Solulan C24 than when both $C_{16}G_2$ and cholesterol are replaced by Solulan C24 - as is the case where $C_{16}G_2$ and cholesterol are present in equimolar ratio. At such a point when the critical packing parameter no longer fell between the limits of 1/2 - 1, but had decreased far beyond this value, alternative structures to conventional vesicles would then predominate in the dispersion. It is observed that the higher mole % Solulan formulations prepared in the present work(equimolar $C_{16}G_2$, cholesterol) are relatively unstable and when left to stand large apparently flat structures are observed (Figure 2.3), similar to the disc shaped structures characterized in section 2.7 of this work.

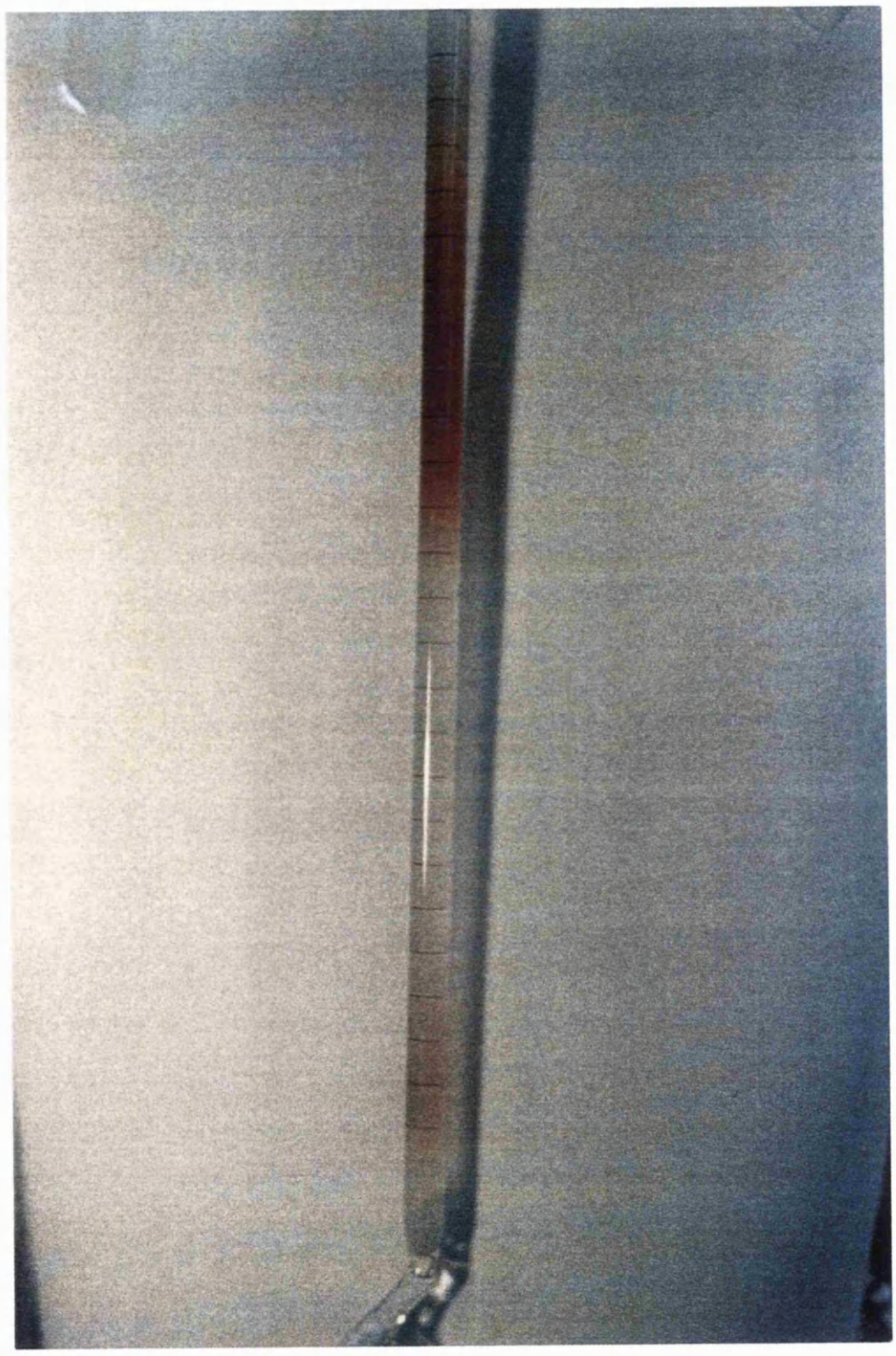

Figure 2.4: The separation of DOX niosomes $C_{16}G_2$, cholesterol, Solulan C24 (45: 45: 10) on a Sephadex G50 gel filtration column (400 mm X 10 mm). A = unencapsulated DOX solution, B = DOX niosomes.

2.6:3 SEPARATION OF DOX NIOSOMES BY GEL FILTRATION

After the preparation of DOX loaded niosomes the separation of unentrapped drug solution is both efficient and quick,as shown in Figure 2.4. This method of niosome purification is faster than previously reported dialysis methods (Baillie *et al.*, 1985; Cable 1989) taking only 3 - 4 min as opposed to 80 h used for dialysis. The gel may be reused after washing and the size of the column adjusted to meet the requirements of the sample. The disadvantage of this method is the dilution of the sample by passage through a gel filtration column. However, where a concentrated sample is desired, this can be obtained by subsequent dialysis against solid polyethylene glycol 6,000 at 4°C for 2 - 3 h.

2.6:4 DOX NIOSOME MORPHOLOGY

Microscopic examination of the various niosome dispersions yielded many interesting structures. Apart from the large irregular shaped structures seen when DOX $C_{16}G_2$, cholesterol, Solulan C24 (30: 30: 40) niosomes were left to stand (Figure 2.3), there were tubular and helical structures (Figure 2.5), seen with the incorporation of 5 mole % DCP and the large unilamellar niosomes seen with the incorporation of sodium dicetylphosphate (NaDCP - Figure 2.6). Helical and tubular liposomes have been reported with the helical liposomes forming in response to Ca^{2+} (Lin *et al.*, 1982). The Ca^{2+} are believed to serve as the foci for periodic membrane-membrane attachment converting tubular vesicles to helices. Self assembling lipid helices have also been synthesized by the attachment of the nucleoside cytidine to phospholipids (Yanagawa *et al.*, 1989). The tubular and in some cases helical structures reported in this work were often visualised in lipid dispersions, mixed with the more commonly

observed spherical vesicles. Flexible bilayers were also observed and vesicles were seen to alter their shape. The association of monomers into bilayer aggregates is a dynamic phenomenon and the final structure visualised is merely the distribution about some mean (Israelachvili 1992). The presence of flexible bilayers in the dispersion and the tubular and helical structures photographed serves to emphasize this fact. The principle features of a niosome dispersion that promote the formation of tubular and helical structures as opposed to the commonly observed spherical aggregates remains to be elucidated.

Large (10 μm) unilamellar niosomes (Figure 2.6) were obtained after sonication of DOX $C_{16}G_2$, cholesterol, NaDCP (47.5: 47.5: 5) niosomes. DOX can be seen as fluorescence in the bilayer. The production of large unilamellar vesicles (LUV's - ≈ 1 μm in diameter) is usually by detergent dialysis (Philpott and Liautard, 1993) in which detergent is removed from a mixed micelle system to produce LUV's. Alternatively LUV's may be prepared from cochleate cylinders (swiss roll type cylinders of phospholipid sheets). Cochleate cylinders are calcium-phospholipid complexes, which form LUV's (0.2 - 4.0 μm) on chelation of Ca^{2+} (Gould-Fogerite and Manino, 1993). The structures shown in Figure 2.6 are larger than conventional LUV's and are produced by simply hydrating and sonicating $C_{16}G_2$-NaDCP lipid films with DOX solution. These large unilamellar niosomes were not seen when NaDCP was omitted from the formulation. It is surprising that even after sonication such a large size is maintained.

At the pH used (pH 7.4), the phosphate groups would be ionized and the electrostatic

Figure 2.5a

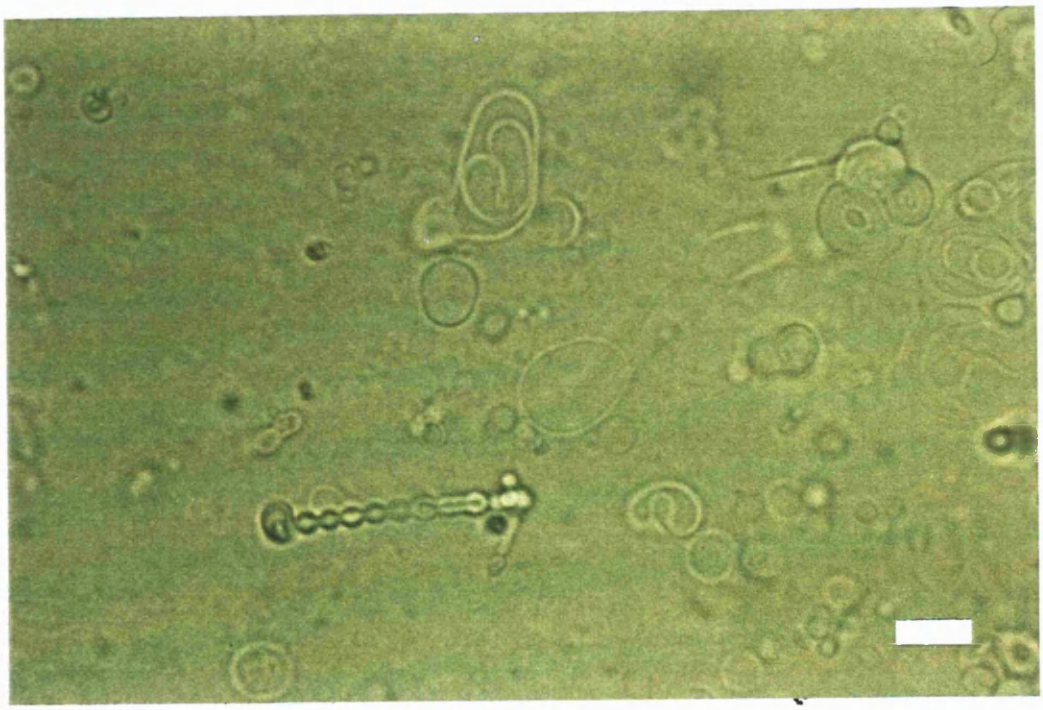

Figure 2.5b

Figure 2.5a Photomicrographs (X500) & 2.5b (X1000) DOX niosomes prepared from $C_{16}G_2$, cholesterol, DCP (47.5: 47.5: 5) showing tubular and helical structures. Bar = 20 μm & 10 μm respectively.

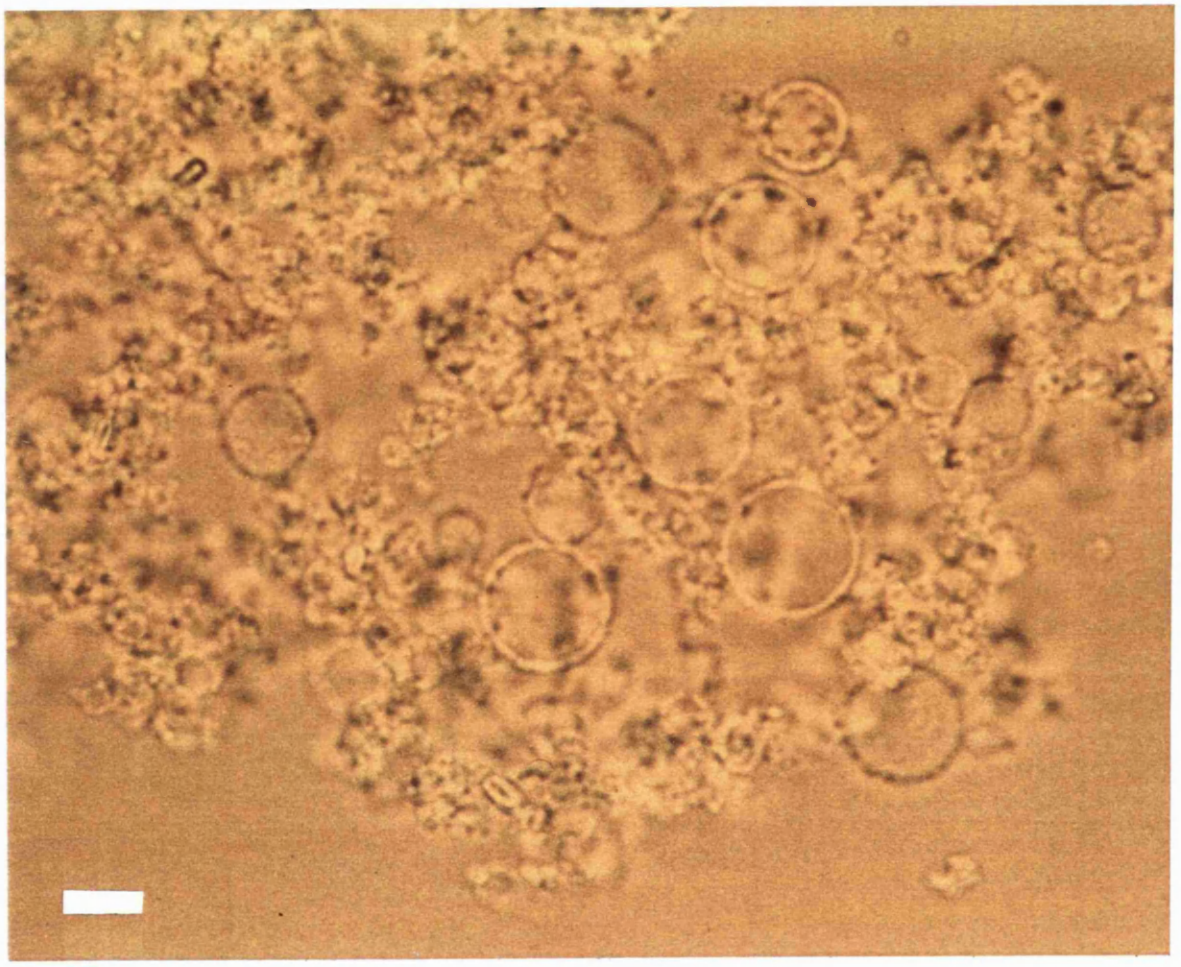

Figure 2.6: Photomicrograph (X1000) of large unilamellar DOX $C_{16}G_2$, cholesterol, sodium dicetyl phosphate (NaDCP) (47.5: 47.5: 5) niosomes photographed under a fluorescent light source and showing drug fluorescence in the bilayer. Bar = 10 µm.

association of DOX, an amine and the membrane would account for the bilayer fluorescence. DOX is known to associate with anionic and neutral bilayers (Burke and Tritton, 1985; de Wolf *et al.*, 1991; de Wolf *et al.*, 1991b; Martí *et al.*, 1992).

2.6:5 HOMOGENIZATION OF DOXORUBICIN $C_{16}G_2$ NIOSOMES

High pressure homogenization is a size reduction process whereby bubbles of gas are created in the dispersion which on implosion generate high local stress and ultimately bilayer shear (Brandl *et al.*, 1993). The homogenisation at a pressure of 60 MPa of $C_{16}G_2$, cholesterol, Solulan C24 (30, 30, 40) niosomes reduced vesicle size of multilamellar vesicles (11.3 μm) to 32 nm after 20 homogenisation cycles (Figure 2.7). However after only 5 cycles vesicle size had been reduced to 50 nm, once again indicating that the procedure did not require prolonged periods of operation to be effective. This 5 cycle optimum is in accordance with published findings (Brandl *et al.*, 1993) in which liposomes of diameter of 16 - 90 nm were produced from hand-shaken multilamellar vesicles, after 5 homogenisation cycles at pressures of 140MPa. Niosomes containing 10 mole % of Solulan were on the whole slightly larger than niosomes containing 40% Solulan C24 (Figure 2.7), as previously discussed and the 10% Solulan niosome size was reduced from an initial value of 11.1 μm to 70 nm after only 5 cycles at 60 MPa pressure. The polydispersity of the 40% Solulan C24 DOX $C_{16}G_2$ niosomes was decreased from 0.42 after 5 cycles to 0.26 after 20 cycles, while the polydispersity of 10% Solulan C24 $C_{16}G_2$ niosomes remained largely unchanged between 5 and 20 homogenization cycles. However, it must be stated that with all preparations homogenized, there was a narrowing of the size distribution on going from the hand-shaken multilamellar niosomes to the homogenized niosomes.

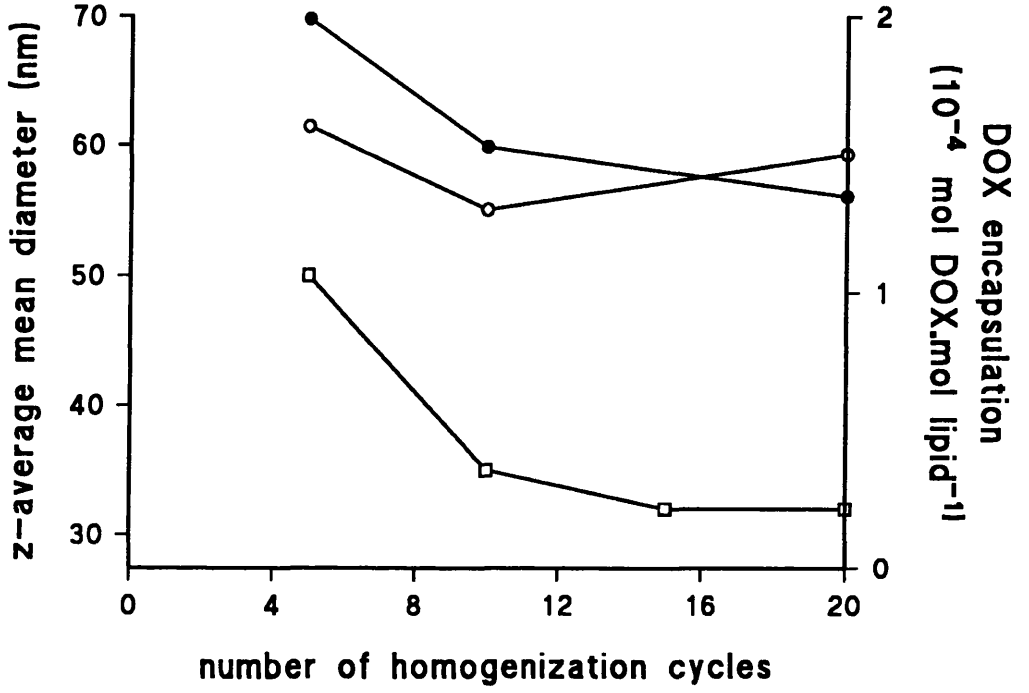

Figure 2.7: The homogenisation of DOX multilamellar niosomes at 60 MPa pressure. ● = $C_{16}G_2$, cholesterol, Solulan C24 (45: 45: 10) niosome size, O = $C_{16}G_2$, cholesterol, Solulan C24 (45: 45: 10) niosome encapsulation efficiency, □ = $C_{16}G_2$, cholesterol, Solulan C24 (30: 30: 40) niosome size.

The encapsulation efficiency of the homogenized 10% Solulan C24 niosomes generally followed size trends. The direct relationship between encapsulation efficiency and vesicle size in any given formulation is generally acknowledged and experimental data has been presented in the past in support of this logical assumption (Vemuri *et al.*, 1990). When the formulation is slightly altered however encapsulation efficiency values may alter drastically. Table 2.2 gives the encapsulation efficiencies of two different $C_{16}G_2$ niosome formulations. The substitution of 5% DCP for 10% Solulan C24 alters the encapsulation efficiency increasing it 10 fold. This increase is not related to vesicle size, as both vesicles are similarly sized (78 nm - DCP and 70 nm - Solulan C24). It appears that DOX forms a more efficient association with DCP containing bilayers than it does with Solulan C24 bilayers. At the working pH DOX is still ionized at its 3' amino group (pKa = 7.2 - 7.4) (Bouma *et al.*, 1986). DOX would thus form an electrostatic association with anionic phosphate groups in the bilayer membrane. DOX has been known to associate with anionic bilayers (Figure 2.6) in both the charged and uncharged form (de Wolf, 1991, de Wolf *et al.*, 1993) and specifically with phosphate headgroups (Dupou-Cézanne *et al.*, 1989; de Wolf *et al.*, 1991a). It is interesting that this increased encapsulation efficiency did not lead to an increase in vesicle size. It appears that the CPP of this particular DOX-DCP aggregate, assuming an association between DOX and the bilayer, was not sufficiently altered to give rise to larger sized vesicles. DOX molecules are thought to penetrate the bilayer and interact with the hydrophobic portion of the membrane (de Wolf *et al.*, 1993).

Table 2.2: The effect of vesicle formulation on the DOX encapsulation efficiency and size of homogenized $C_{16}G_2$ niosomes. Initial DOX/lipid ratio = 0.0115

Niosome lipid composition	number of homogenization cycles	z-average mean diameter (nm)	encapsulation efficiency (mol DOX.mol lipid^{-1})	initial size of niosomes (μm)
$C_{16}G_2$, cholesterol, DCP (47.5: 47.5: 5)	5	78	0.00174	6.4
$C_{16}G_2$,cholesterol, Solulan C24 (45: 45: 10)	5	70	0.00016	11.1

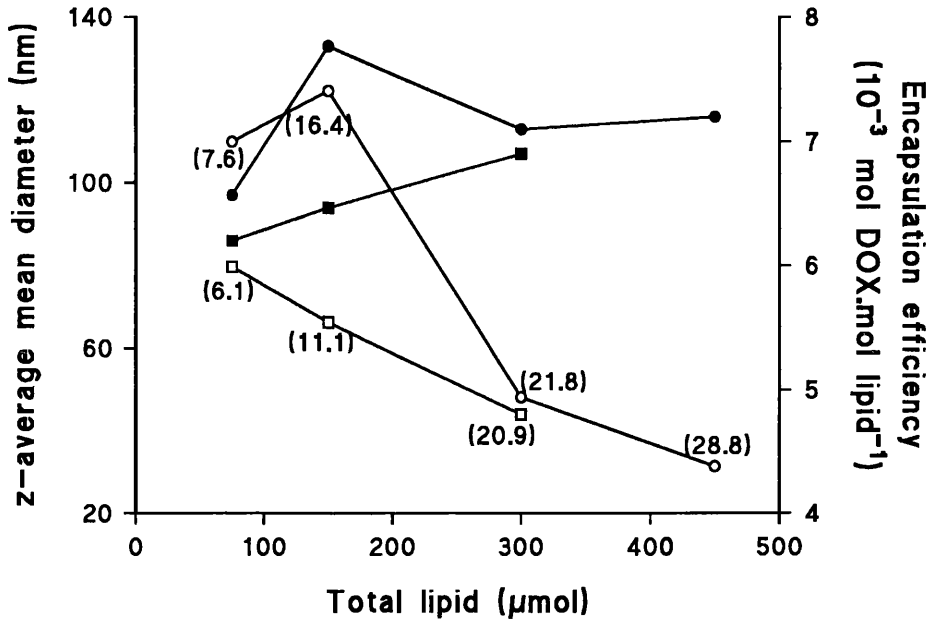

Figure 2.8: The effect of total amount of lipid on the size and encapsulation efficiency of $C_{16}G_2$ niosomes. ● = $C_{16}G_2$, cholesterol, Solulan C24 (45: 45: 10) niosome size; ○ = $C_{16}G_2$, cholesterol, Solulan C24 (45: 45: 10) niosome DOX encapsulation efficiency; ■ = $C_{16}G_2$, cholesterol, Solulan C24, DCP (42.75: 42.75: 9.5: 2) niosome size; □ = $C_{16}G_2$, cholesterol, Solulan C24, DCP (42.75: 42.75: 9.5: 2) niosome DOX encapsulation efficiency. Figures in parenthesis are the percentages of DOX actually encapsulated.

2.6:6 THE EFFECT OF THE LEVEL OF LIPID ON THE DOXORUBICIN ENCAPSULATION EFFICIENCY OF $C_{16}G_2$ NIOSOMES

Figure 2.8 presents interesting observations on the influence of total initial lipid on niosome size when $C_{16}G_2$-Solulan C24 niosomes are formulated with and without DCP. As the amount of lipid in the DCP niosomes is increased there is an almost linear increase in vesicle size. With non-DCP, the particle size increased on increasing the total lipid from 75 μmol to 150 μmol and fell thereafter as the level of lipid was increased to a value of 300 μmol. The relationship between vesicle size of elastic bilayers is defined by the equation given below (Israelachvili, 1992):

$$M = (C^{\alpha})^{1/2} \qquad (2.2)$$

M = mean aggregation number, which determines vesicle size

C = amphiphile concentration

α = an amphiphile interaction parameter, that depends on the strength of the various molecular interactions.

For elastic bilayers, this interaction parameter defines the effect the repulsive forces between the headgroups and the repulsive forces between hydrocarbon chains have on vesicle curvature. If chain repulsion dominates headgroup repulsion, these chain repulsion forces oppose bilayer bending and polydisperse and larger vesicles result from increased levels of lipid. With the DCP niosomes, this appears to be the case. With the non-DCP, when lipid levels above 150 μmol are used, niosome size fails to rise. The most likely explanation for this is the fact that at a high enough lipid level, the geometry of the individual monomers not withstanding, non-vesicular structures (bilayer sheets etc) will be formed from individual monomers because of insufficient hydrating solvent, space constraints or the attractive forces between vesicles

(Israelachvili, 1992). The attractive forces between DCP niosomes will be less than the attractive forces between non-DCP containing niosomes because of the presence of electrostatic repulsions, hence non vesicular structures would form more readily in the non-DCP dispersion than in the DCP dispersion.

The percentage of solute actually encapsulated (Figure 2.8 - figures in parentheses) was directly proportional to the level of initial lipid, irrespective of bilayer composition. A correlation coefficient (r) of 0.97 was calculated for these parameters. However the encapsulation efficiency (expressed as the number of moles of DOX encapsulated per mole of lipid) was progressively decreased as the level of lipid was increased (Figure 2.8). This is especially true for the non-DCP niosomes. The increase in encapsulation efficiency observed with the non-DCP niosomes on increasing the lipid level from 75 to 150 µmol appears to follow the observed increase in size. When initial lipid levels above 150 µmol are employed, encapsulation efficiency drops drastically from a DOX/lipid ratio of 0.0074 for 150 µmol lipid to 0.0049 for 300 µmol lipid. Once again this is thought to be due to the production of a lower proportion of niosomes in this formulation as the amount of initial lipid is increased. With the DCP niosomes, as the proportions of niosomes produced with increasing lipid are thought to change only minimally for reasons of surface charge and attendant electrostatic repulsions, the final DOX/lipid ratio also changes only minimally; falling from 0.055 for 150 µmol lipid to 0.048 for 300 µmol lipid.

The addition of DCP to $C_{16}G_2$-Solulan C24 niosomes did not increase entrapment efficiencies as was noted with the replacement of 10% Solulan C24 by 5% DCP in

$C_{16}G_2$ niosomes (Table 2.2). It can only be assumed that the presence of Solulan C24 in the bilayer in conjunction with DCP, reduced the association of DOX with the bilayer. It is possible that the bulky Solulan C24 headgroup, would resist the incorporation of the DOX glycoside into the bilayer.

It is concluded that an initial optimum lipid concentration in a solution of 0.0035M DOX for efficient entrapment is in the region of 0.075M (initial DOX/lipid ratio = 0.046) for non DCP $C_{16}G_2$-Solulan C24 niosomes and 0.038M (initial DOX/lipid ratio = 0.092) for DCP $C_{16}G_2$-Solulan C24 niosomes and yields niosomes with DOX/lipid ratios of 0.0074 and 0.0060 respectively.

2.6:7 SIZE AND ENCAPSULATION EFFICIENCY OF SPAN SURFACTANT NIOSOMES

Span surfactants, are sorbitan monostearate esters (Figure 1.7), although they are usually commercially supplied as impure mixtures of the anhydrides and esters. The Span surfactants differ from each other in the nature of the hydrocarbon chain. Span 20 has a C_{12} acyl chain, Span 40 a C_{16} acyl chain, Span 60 a C_{18} acyl chain and Span 80 an unsaturated (cis) C_{18} acyl chain. These surfactants were studied as vesicle forming surfactants to enable the data generated on the bench to be utilized in future clinical trials, without the added worry of toxicological profiling of the fairly novel L'Oreal surfactants.

Size distributions of empty unsonicated multilamellar Span surfactant niosomes showed no dependence on acyl chain length (Figure 2.9), with volume distribution mean diameters ranging from 10 - 20 μm. The size of Span 60 niosomes (volume

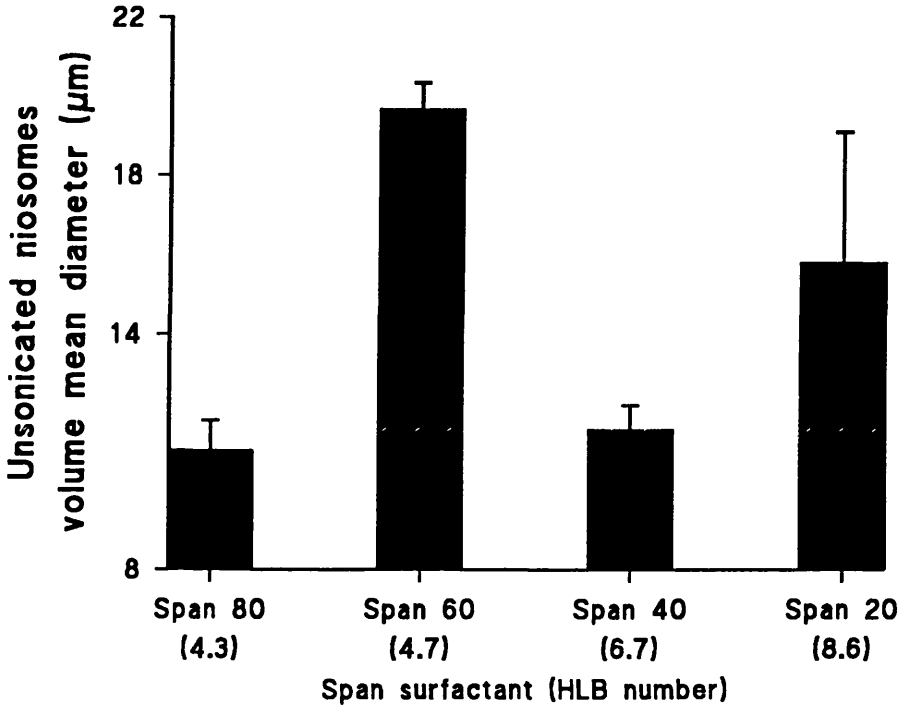

Figure 2.9: The size of *unsonicated* Span surfactant, cholesterol, Solulan C24 (45: 45: 10) niosomes. Niosomes were prepared by hydrating lipid films with water.

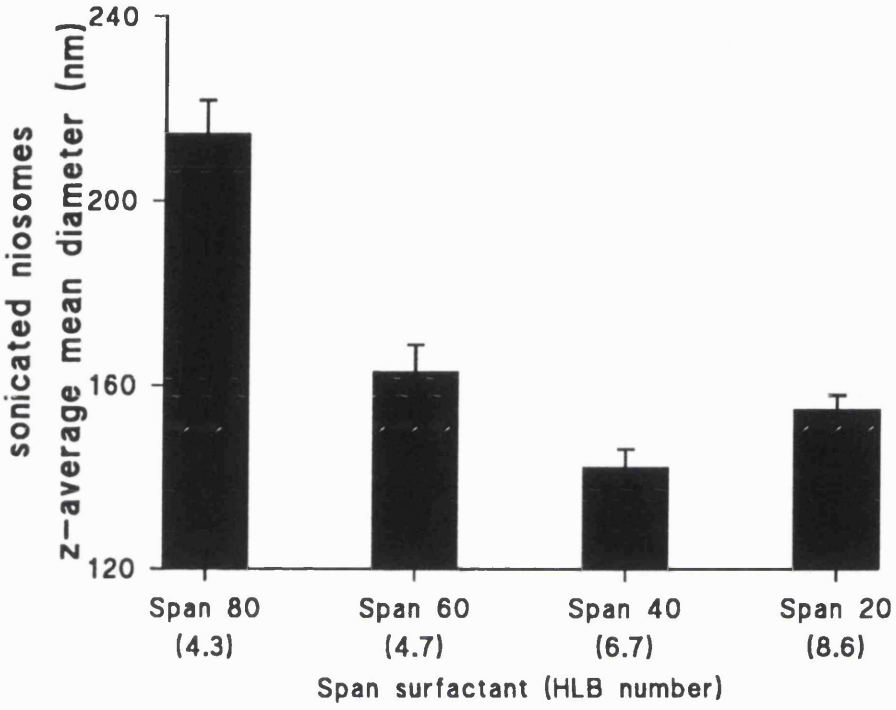

Figure 2.10: The size of *sonicated* Span surfactant, cholesterol, Solulan C24 (45; 45; 10) niosomes. Niosomes were prepared by hydrating lipid films with water.

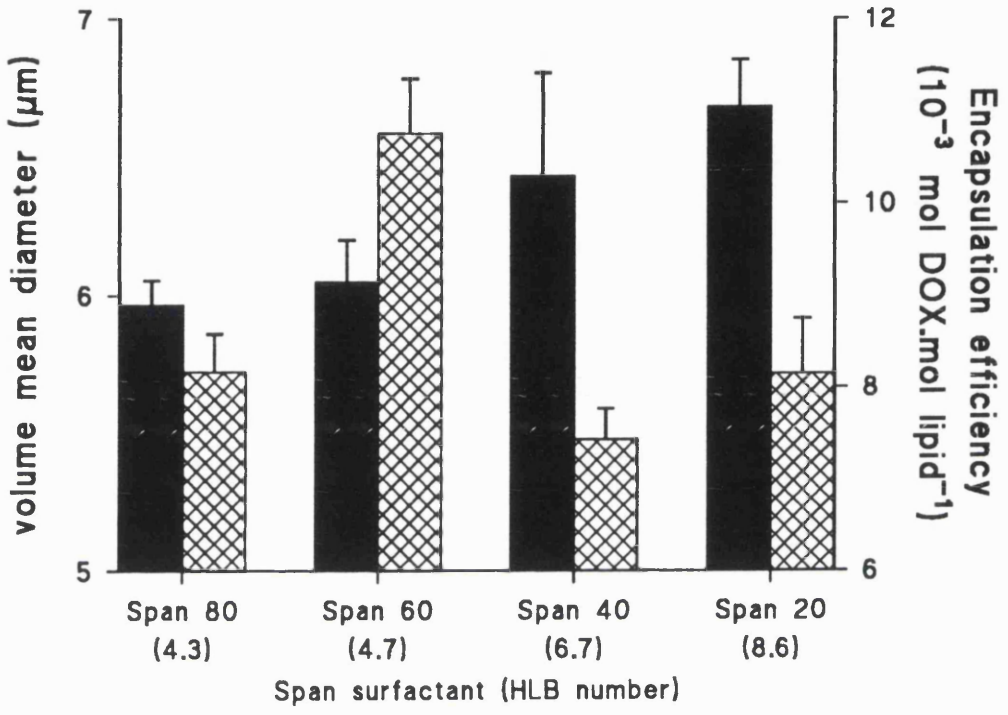

Figure 2.11: The size (solid bars) and encapsulation efficiency (hatched bars) of DOX containing *unsonicated* Span surfactant, cholesterol, Solulan C24 (45: 45: 10) niosomes.

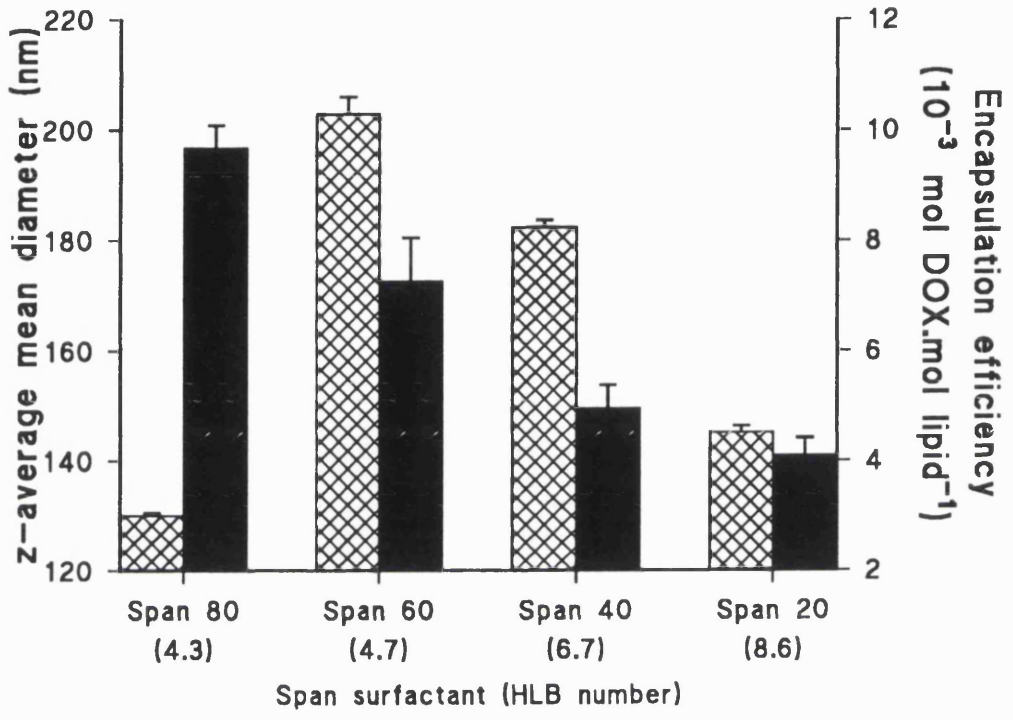

Figure 2.12: The size (solid bars) and encapsulation efficiency (hatched bars) of DOX containing *sonicated* Span surfactant, cholesterol, Solulan C24 (45: 45: 10) niosomes.

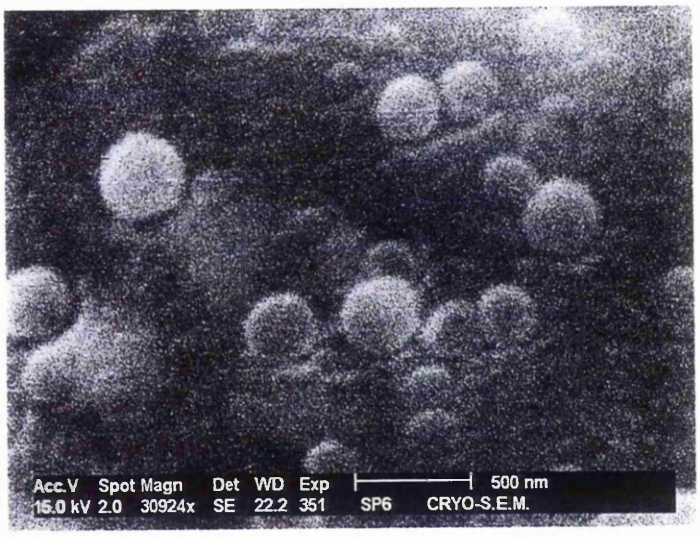

Figure 2.13: Scanning electron micrograph (X30924) of DOX containing Span 60, cholesterol, Solulan C24 (45: 45; 10) niosomes. Bar = 500 nm.

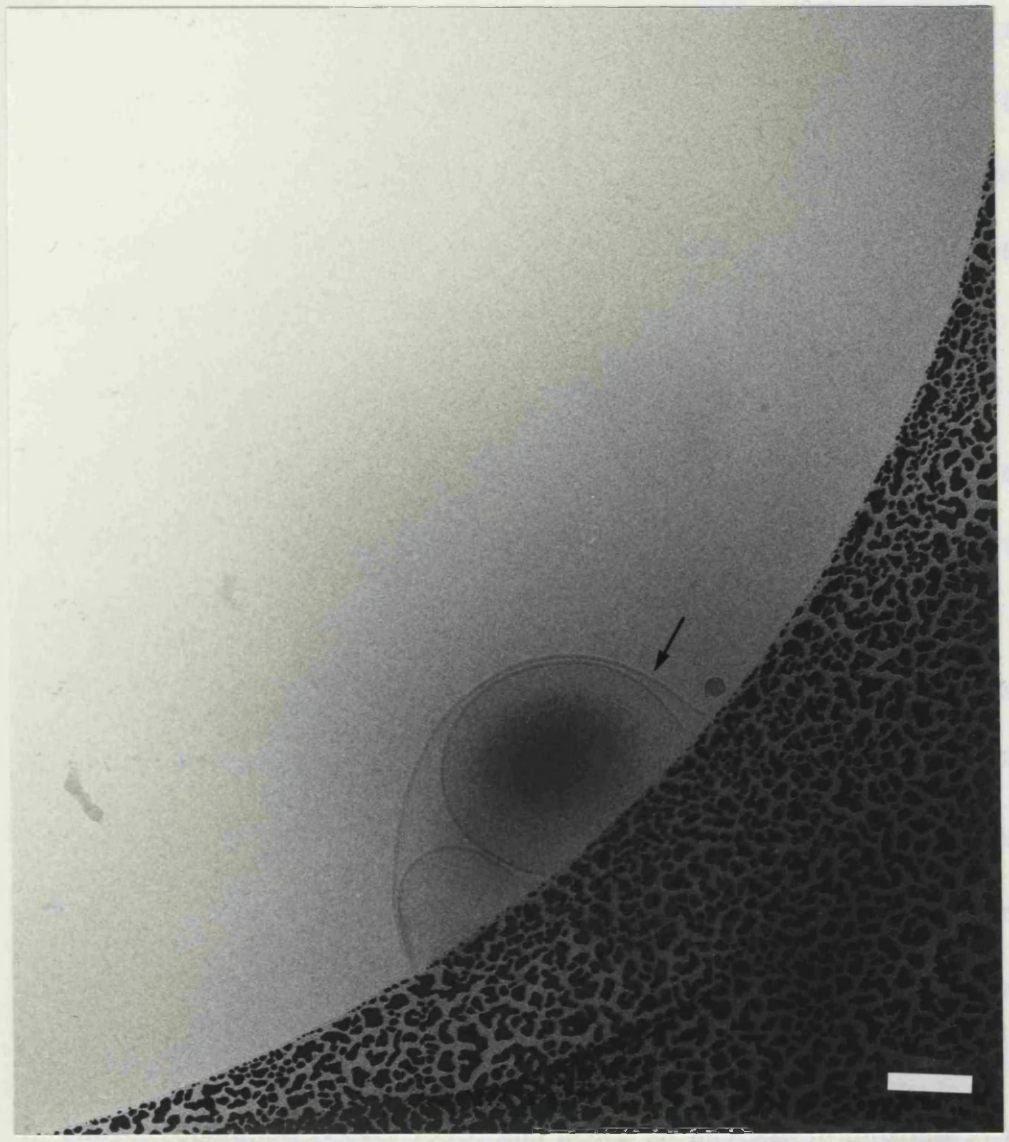

Figure 2.14: Cryo-transmission electron micrograph (X450,000) of DOX Span 20, cholesterol, DCP (47.5: 47.5: 5) niosomes. Bar = 20 nm

mean diameter = 19.7 μm), especially and to a lesser extent Span 20 (volume mean diameter = 16.1 μm) niosomes was shifted to somewhat higher values than those of Spans 40 and 80 niosomes (volume mean diameters of 11.6 and 10.4 μm respectively). While no obvious trends can be found in the sizes of the unsonicated niosomes, sonicated empty Span surfactant vesicles show a progressive increase in size as HLB values are reduced (Figure 2.10). HLB values are a measure of the ratio of hydrophilic to lipophilic regions of any amphiphile. Higher HLB numbers define higher hydrophilicity and vice versa. It is generally accepted for liposomes that the more hydrophilic the amphiphile the smaller the resulting vesicles (Cevc, 1993). The increase in acyl chain length on going from Span 20 to Span 60 would result in an increased CPP (equation 1.1 - Israelachvili, 1992) as the value v/l_c increases. This ultimately leads to a larger vesicle size. With Span 80, the cis unsaturation would further reduce l_c (Israelachvili, 1992), once again increasing the CPP further and concomitantly, vesicle size. When unsonicated Span surfactant niosomes are loaded with DOX, niosome size seemed to increase as HLB number decreased (Figure 2.11), although the size distributions of all Span surfactant niosomes were all fairly similar (volume mean diameters 5.7 - 6.9 μm). This increase in size, with increasing HLB number, could be attributed to an increase in bilayer hydration associated with the more hydrophilic amphiphiles. Increased bilayer hydration would lead to an increase in bilayer separation (Cevc, 1993) and hence an increase in niosome size. It is not clear why a similar size trend was not observed when empty niosomes were formed and the exact reason why empty unsonicated multilamellar niosomes were larger than drug loaded unsonicated multilamellar niosomes is also unclear. However, what does become apparent is the fact that DOX interacts with the bilayer to change the vesicle

forming properties of these surfactants, resulting in the different size distribution profiles between empty and DOX containing niosomes.

The encapsulation efficiencies of these unsonicated DOX Span surfactant niosomes were similar (final molar DOX/lipid ratios of 0.0074 - 0.0082), with the notable exception of the Span 60 niosomes (final molar DOX/lipid ratio = 0.0108). It appears that DOX does seem to show a predilection for Span 60 niosomes, which appeared not to be dependant on niosome size. DOX has been shown to interact with zwitterionic phospholipids at neutral pH (Martí *et al.*, 1992) and hydrophobic interactions between DOX and acyl phospholipid chains have been reported (Burke and Tritton, 1985; de Wolf *et al.*, 1993). It is possible that DOX would associate favourably with Span 60 niosome bilayers by virtue of hydrophobic and hydrophilic (hydrogen bonding) interactions, probably because of some particular molecular packing characteristics. Alternatively the Span 60 bilayer would be present in the gel phase at room temperature (Yoshioka *et al.*, 1994) and not the liquid crystal phase. This would encourage solute retention. This particular observation does indeed deserve further study.

The picture was clearer somewhat with the sonicated DOX Span surfactant niosomes as niosome size was inversely proportional to Span surfactant HLB, for reasons advanced above. Encapsulation efficiencies followed size trends, increasing with size, except for niosomes formed from the unsaturated surfactant Span 80. Unsaturation, increases chain fluidity, thus increasing the permeability of the bilayer to solutes (Cohen, 1975). Unsaturation of long chain fatty acid bilayers, makes the resulting

bilayers more leaky and less able to retain solutes. (Gebicki and Hicks, 1976).

Scanning electron micrographs of DOX loaded Span 60 niosomes are shown in Figure 2.13. Distinct spheres may be seen of about 100 - 300nm diameter. Figure 2.14 is a cryo TEM of 120nm Span 20-DCP niosomes loaded with DOX. Delicate bilayer detail may be seen as well as an electron dense region in the vesicle interior (presumably drug). Vesicles within vesicles are also seen. Micrographs obtained by the cryo TEM procedure differ markedly from the "onion like" structures normally seen with transmission electron microscopy and could offer new insights into vesicular microstructure.

It is concluded that surfactant molecule geometry plays very little part in predicting vesicle size of empty unsonicated multilamellar Span surfactant niosomes, although interfacial energy must change with surfactant structure. Any changes in this parameter are not reflected in vesicle size. DOX associates with Span surfactant bilayers to alter the size profile of unsonicated Span surfactant niosomes. DOX appears to form a particularly favourable association with Span 60 niosomes and Span surfactant geometry serves as a useful prediction to the size profile of Span surfactant sonicated niosomes. Detailed molecular modelling studies may provide a working hypothesis for this association which could then be tested in future work. The unsaturation in the Span 80 acyl chain reduces the propensity of DOX to associate with the niosomes, probably by altering the order of acyl chains in the bilayer and producing a leakier niosome.

2.6:10 THE OPTIMIZATION OF DOX ENCAPSULATION EFFICIENCY

The remote loading of weak anionic and cationic drugs into vesicles has been used to entrap vinblastine dibucaine, chlorpromazine as well as DOX (Cullis *et al.*, 1987). Briefly a transmembrane gradient is set up using either protons (Harrigan *et al.*, 1993; Montero *et al.*, 1993; Partharsarathi *et al.*, 1994), NH_4^+ (Haran *et al.*, 1993; Lasic *et al.*, 1992) or K^+ (Mayer *et al.*, 1985: Praet *et al.*, 1993). The drug then accumulates in the interior of the niosome in response to this gradient, sometimes even precipitating in the interior of the vesicle (Cullis *et al.*, 1987) or forming a thermodynamically stable gel (Lasic *et al.*, 1992). Extremely high levels of entrapment are obtained with this method (Cullis *et al.*, 1987).

2 methods of remote loading were used. Method 1 involved the initial formation of DOX loaded niosomes with an internal pH of 4.0 and an external pH of 7.0 - 7.6. Method 2 required that empty niosomes would be formed encapsulating a suitable buffer at pH 4.0. DOX solution at a pH of > 7.0 was then introduced exterior to the niosomes and allowed to incubate with the niosomes at an elevated temperature. The primary 3′ amine in the DOX molecule has a pKa of about 7.2 - 8.99, while the acidic C6 and C10 phenol functions have pKa's of between 8.53 - 10.16 (Bouma *et al.*, 1986). At pH 4.0 the amino group would thus be protonated and at pH 9.0 the phenolic functions would be ionic. At pH 7.0 however ionisation of both functions would be suppressed. The unionized DOX molecule exterior to the niosome would then traverse the membrane in response to the pH gradient and once inside the niosome the molecule would become protonated, effectively trapping it within the niosome; as the work required to place an ionic drug into the hydrophobic membrane

Table 2.3: The effect of transmembrane proton gradients on the encapsulation efficiency of $C_{16}G_2$ DOX niosomes. Lipid composition = $C_{16}G_2$, cholesterol, Solulan C24 (45: 45: 10)

Proton gradient[1] method used	encapsulation efficiency (mol DOX.mol lipid^{-1})	initial molar DOX/lipid ratio	Initial concentration of DOX in medium external to preformed empty niosomes (mg mL^{-1})	z-average mean diameter (nm)
method 1	0.026	0.070	-	-
method 2	0.010 0.005	0.043 0.034	1.5 0.67	167 199
no proton gradient used	0.003 0.007 0.007	0.038 0.259 0.230	- -	153 74 61

[1]See methods text for the different transmembrane proton gradient methods used.

Table 2.4: The effect of transmembrane proton gradients on the DOX encapsulation efficiency of Span surfactant niosomes.

Niosome lipid composition	Initial molar DOX/lipid ratio	Transmembrane gradient method used[1]	Initial DOX concentration external to niosomes in method 2 (mg mL^{-1})	Final molar DOX/lipid ratio (mean ± sd)	z-average mean diameter (nm)
Span 40, cholesterol, Solulan C24 (45: 45: 10)	0.029	no transmembrane gradient used	-	0.0034 ± 0.0008	187
Span 40, cholesterol, Solulan C24 (45: 45: 10)	0.029	method 1	-	0.0082 ± 0.0002	150
Span 80, cholesterol, Solulan C24 (45: 45: 10)	0.029	no transmembrane gradient used	-	0.0026 ± 0.0003	210
Span 80, cholesterol, Solulan C24, (45: 45: 10)	0.029	method 1	-	0.0030 ± 0.0007	197
Span 60, cholesterol, Solulan C24 (45: 45: 10)	0.029 0.034 0.043 0.020 0.043	method 1 method 2 method 2 method 2 method 2	- 0.67 1.5 1.75 2.00	0.0103 ± 0.0006 0.0095[2] 0.0128[2] 0.0144[2] 0.0151[2]	173 182 174 171 212

[2]These values represent single determinations.

Table 2.5: The DOX encapsulation efficiency of niosomes and liposomes using the method of transmembrane gradients (method 2)[1].

Lipid/ composition	Initial DOX/lipid molar ratio	Initial concentration of DOX external to the vesicles (mg mL^{-1})	Final DOX/lipid molar ratio	z-average mean diameter (nm)
Span 60, cholesterol, Solulan C24 (45: 45: 10)	0.034	0.67	0.00954	182
$C_{16}G_2$, cholesterol, Solulan C24 (45: 45: 10)	0.034	0.67	0.00524	199
PC, cholesterol, Solulan C24 (45: 45: 10)	0.034	0.67	0.00331	188

core for eventual travel out of the vesicle is rather large (Gennis, 1989). DOX encapsulated in phospholipid vesicles in response to transmembrane proton gradients is found to be 99% associated with the inner portion of the bilayer (Harrigan *et al.*, 1993).

The method relies on a pH gradient as bilayer membranes are highly permeable to protons (H_3O^+) (Gennis, 1989). The entrapment although high, could be undermined by the movement of protons across the membrane. For this reason, formulations were always freshly prepared. After storing the formulation at 4°C for 14 days about 50% of entrapped drug was found to have leaked out of the niosomes and two bands were seen on a Sepharose 2B gel filtration column.

With the $C_{16}G_2$ niosomes, the remote loading by exploiting transmembrane gradients increased encapsulation (Table 2.2). This finding was in accordance to published findings (Cullis *et al.*, 1987; Harrigan *et al.*, 1993; Montero *et al.*, 1993). Admittedly encapsulation was largely dependant on the initial ratio of DOX/lipid and while initial molar ratios of DOX/lipid of 0.230 - 0.259 yielded final molar DOX/lipid ratios of 0.007 when no gradient was used. Use of a gradient transformed an initial molar DOX/lipid ratio of 0.043 into a final molar DOX/lipid ratio of 0.010. The remote loading method 2 showed that encapsulation depended largely on the concentration of DOX external to the empty niosomes at the start of the remote loading procedure. The higher external concentration of 1.5 mg mL^{-1} gave an encapsulation efficiency of 0.0095 mol DOX.mol $lipid^{-1}$, whereas the corresponding value for an initial exterior concentration of 0.067 mg mL^{-1} gave an encapsulation efficiency of 0.0055 mol DOX.

mol lipid^{-1}. Initial DOX/lipid ratios were comparable with both higher and lower external concentration method 2 procedures (Table 2.3) being 0.043 and 0.034 respectively.

It is obvious that the higher concentration gradient generated by having a higher concentration of DOX external to the niosomes encouraged the migration of DOX from the exterior to the interior of the niosomes as dictated by the laws of diffusion (Gennis, 1989).

The story repeats itself almost verbatim for the Span surfactants (Table 2.4). With Span 40 niosomes encapsulation virtually increased 2.5 fold on changing from a method that did not to a method that did rely on transmembrane proton gradients. Encapsulation efficiency increased from 3.36 to 8.24 mmol DOX.mol lipid^{-1}. With Span 80 niosomes however such differences in encapsulation efficiency were not apparent on shifting from a method that did not utilize transmembrane gradients to one that did (method 1 - in which there is an initial quantity of DOX within the niosome before the remote loading procedure commenced) (Table 2.4). It appears that the unsaturation within Span 80 once again resists any gains that can be achieved from the use of transmembrane proton gradients. It is known that the unsaturation of acyl surfactant chains increases chain fluidisation (Cevc, 1993) and hence membrane permeability (Cohen, 1975). It appears that Span 80 operates within the membrane in a similar manner, causing any encapsulated material to leak out. The incorporation of cholesterol into the bilayer decreases membrane fluidity and tends to decrease non-ionic surfactant bilayer permeability to DOX (Baillie *et al.*, 1985; Rogerson *et al.*,

1987).

The data on the remote loading of Span 60 niosomes (Table 2.4) demonstrate that the encapsulation efficiency of the method 2 process is determined principally by the concentration of DOX external to the niosomes at the start of the procedure. A correlation coefficient (r) of 0.996 was calculated for these two variables. High DOX concentrations in buffer solutions forms a viscous unmanageable solution (Hayakawa *et al.*, 1991). However high entrapment (0.1 - 0.42 mol DOX.mol lipid^{-1}) has been achieved by other authors (Haran *et al.*, 1993) using ammonium sulphate gradients and external DOX to empty liposome concentrations of up to 11.6 mg mL^{-1} (using DOX sucrose solutions). In this method DOX is said to precipitate within the liposomes. In the current work, however, there was no correlation between the initial DOX/lipid ratio and the eventual encapsulation efficiency (r = -0.021), when the concentration of DOX external to the niosomes at the start of the procedure was not considered.

A comparison between the encapsulation efficiencies of $C_{16}G_2$ niosomes, Span 60 niosomes and egg phosphatidylcholine vesicles showed that the phospholipid vesicles encapsulated poorly compared to the niosomes (Table 2.5) although all vesicles were of comparable size. Egg phosphatidylcholine forms comparatively fluid membranes which would reduce solute retention. Additionally, DOX in response to proton gradients accumulates in the inner monolayer (Harrigan *et al.*, 1993) and it is conceivable that any molecular geometry characteristics of the various monomers would affect the accumulation of DOX at this site. It appears that all the data so far presented point to a unique association of Span 60 niosomes and DOX.

In conclusion the use of transmembrane gradients increased encapsulation efficiency, except with the use of Span 80 niosomes. Optimum encapsulation could be achieved by increasing the concentration of DOX external to the niosomes, when employing method 2.

2.6:11 THE LATENCY OF $C_{16}G_2$ NIOSOMES

The aqueous marker CF is commonly used to measure solute release from various vesicular structures (Weinstein *et al.*, 1977; Ralston *et al.*, 1980). In a preliminary experiment the release of this aqueous solute from $C_{16}G_2$, cholesterol, Solulan C24 (30: 30: 40) niosomes was measured over 24h. 97% of the aqueous marker CF (Figure 2.15) was retained after 24h and in a similar experiment it was found that 90% of encapsulated DOX (Figure 2.16) was retained after 6h at room temperature. The release of an aqueous solute from vesicles is determined by the permeability of the vesicle bilayer. Permeability typically decreases with the ability of the solute to form hydrogen bonds, showing that dehydration of the solute must take place before the solute may traverse a bilayer membrane (Cohen, 1975). CF is a highly polar compound (Figure 2.17) and at pH 7.4 is fully ionized as shown in Figure 2.17, quite unlike the DOX molecule which does not experience full ionization at neutral pH. The more polar compound CF thus enjoys less permeability to the membrane, for reasons of enhanced bonding of this molecule with water.

Permeability also decreases with increasing cholesterol content (Cohen, 1975; Baillie *et al.*, 1985; Rogerson *et al.*, 1987; Florence *et al.*, 1990; Sada *et al.*, 1990; Florence, 1993). Cholesterol tends to decrease the fluidity of the membrane thus decrease the

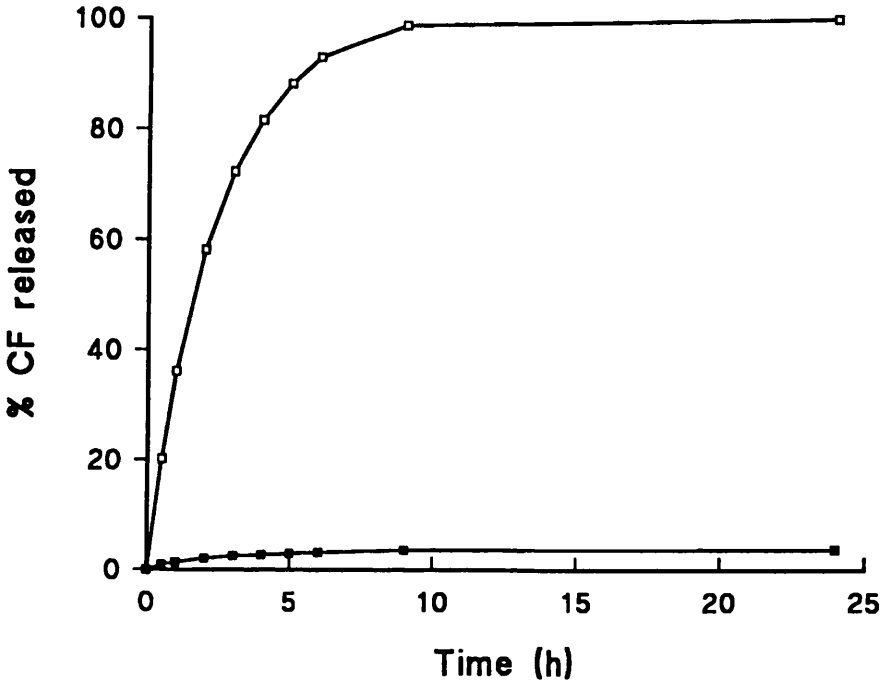

Figure 2.15: The release of CF from $C_{16}G_2$, cholesterol, Solulan C24 (30: 30: 40) niosomes at room temperature (22°C). □ = 45.6μM CF solution, ■ = 45.6μM CF in niosomes. Each point represents the mean of 3 measurements.

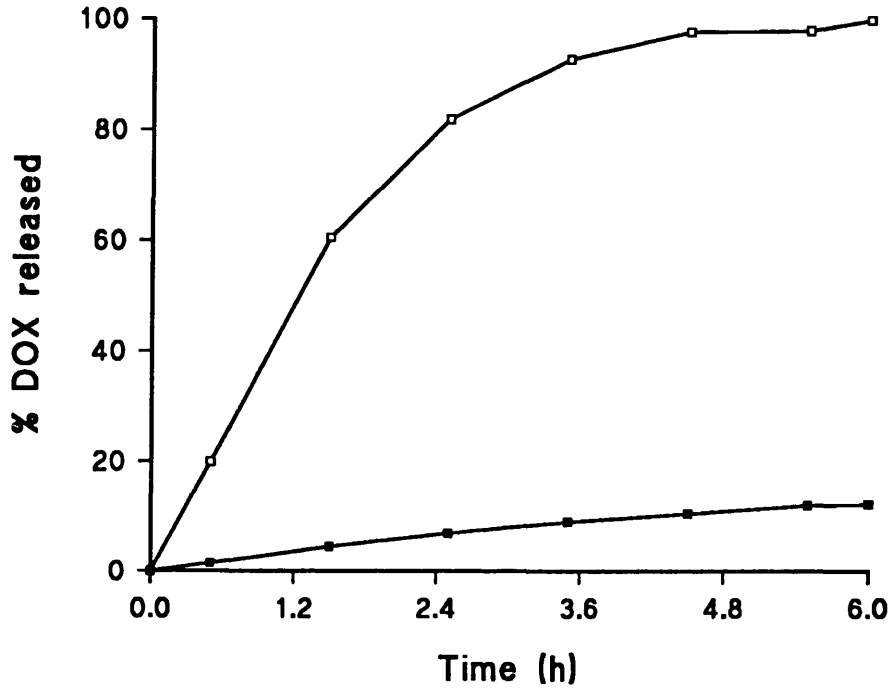

Figure 2.16: The release of DOX from $C_{16}G_2$, cholesterol, Solulan C24 (30: 30: 40) niosomes at room temperature (22°C). □ = 0.031mM DOX solution, ■ = 0.033mM DOX in niosomes. Each point represents the mean of three measurements.

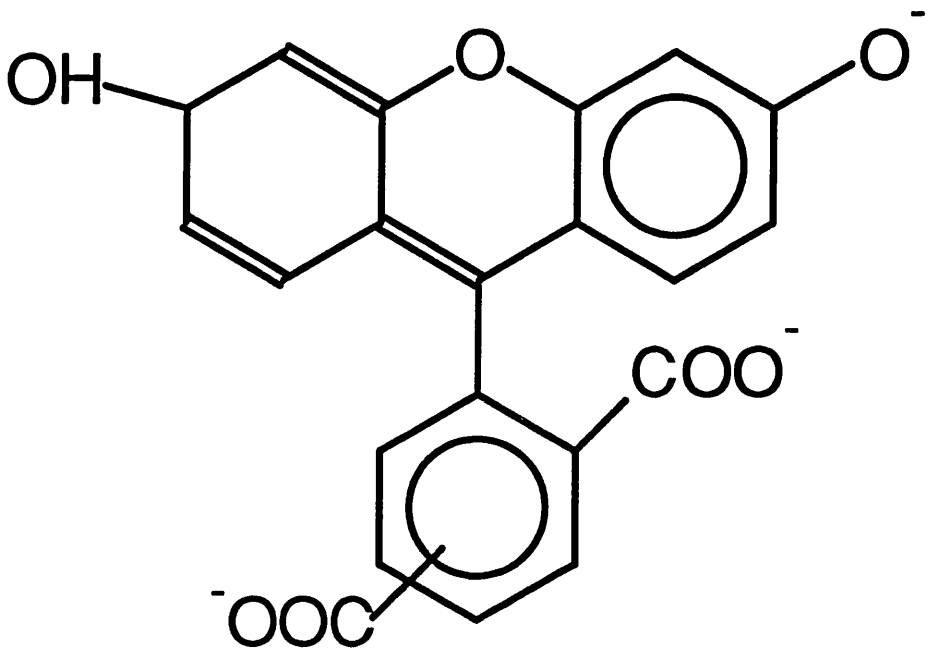

Figure 2.17: 5(6)-carboxyfluorescein (CF) at pH 7.4.

ease with which substances traverse the membrane (Gennis, 1989). In the present work niosomes were formulated with a 1: 1 ratio of surfactant to cholesterol. As membranes pass from a liquid crystalline to a gel state or as the vesicle becomes smaller in size (Niven *et al.*, 1991) they tend to become less permeable (Cohen, 1975).

The release of DOX from these $C_{16}G_2$ niosomes is in accordance with published values of between 0.5 - 10% after 6 h (Rogerson *et al.*, 1987; Florence *et al.*, 1990). Release of DOX and CF from $C_{16}G_2$ niosomes was minimal and these niosomes were fairly stable over 6 and 24 h periods respectively at room temperature.

2.7: VESICLE TO MICELLE TRANSITIONS IN THE $C_{16}G_2$ - SOLULAN C24 SYSTEM

2.7:1 SOLUBILIZATION OF VESICLES USING SOLULAN C24 AND THE PREPARATION OF DISCOMES

Following the report of disc like structures found in $C_{16}G_3$ - Solulan C24 niosomes by Cable and Florence (1988) and the observation of similar structures in $C_{16}G_2$ - Solulan C24 systems, the solubilization of $C_{16}G_2$ niosomes by Solulan C24 was studied. The change in turbidity of the niosomes on incubation with Solulan C24 was measured. Turbidity measurements on the vesicle dispersions (Figure 2.18) expressed as a function of the Solulan C24 concentration gave plots that are similar in shape and can be largely characterized by three break-points as indicated by the arrows. These break-points indicate a distinct change in the nature of the dispersion. Turbidity titrations of vesicles with soluble surfactants are used to characterize the solubilization of vesicle bilayers by such soluble surfactants by way of turbidity vs surfactant

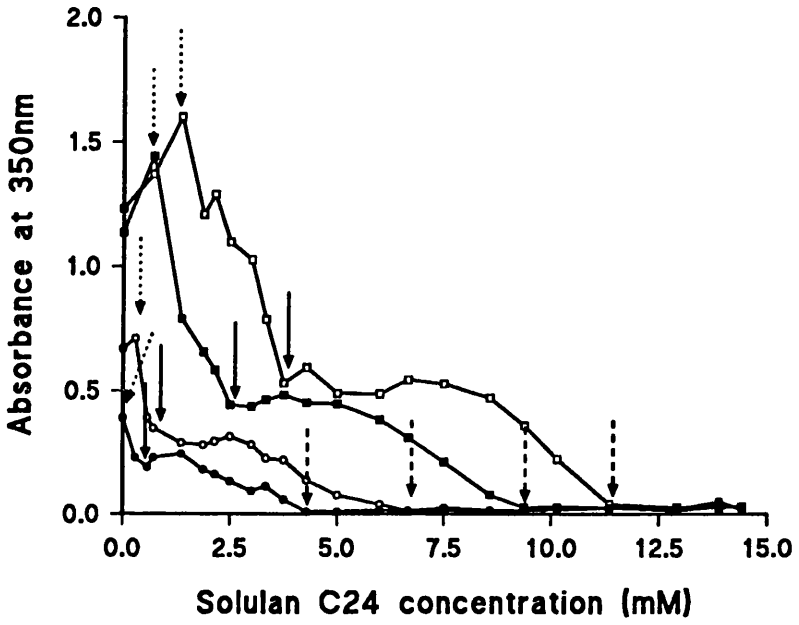

Figure 2.18: Turbidity measurements on $C_{16}G_2$, cholesterol, DCP (69: 39: 2) niosomes incubated with Solulan C24 at 74°C for 1h. ● = niosome total lipid concentration - 1.5mM; ○ = niosome total lipid concentration - 3.0mM; ■ = niosome total lipid concentration - 7.5mM; □ = niosome total lipid concentration - 15mM. Arrows indicate points of distinct change in the nature of the dispersion. Dotted arrows indicate the start and hatched arrows indicate the end of the micellization process. The solid arrows indicate similar troughs in all four plots.

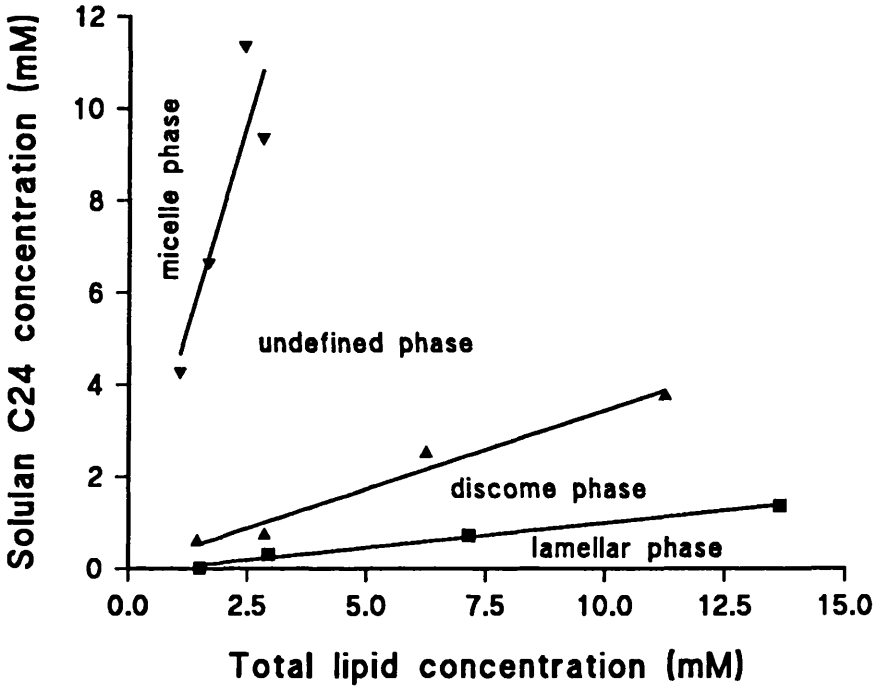

Figure 2.19: Vesicle to micelle transition phase diagram for $C_{16}G_2$, cholesterol, DCP (69: 39: 2) niosomes solubilized with Solulan C24.

concentration plots (Jackson *et al.*, 1982; Paternoste *et al.*, 1988; Almog *et al.*, 1990; Lesieur *et al.*, 1990; Kim and Kim, 1991; Walter *et al.*, 1991). Plots of Solulan C24 concentration vs total lipid concentration at these identified break-points yield straight line plots (Figure 2.19) that effectively describe the partial phase diagram of the system. A novel phase was identified which we have called the "discome" phase. This phase consisted of large disc shaped structures (11-60 μm volume mean diameter) (Figures 2.20a&b). Freeze fracture electron micrographs of the discome dispersion revealed (Figure 2.21) large flat vesicular structures, confirming the discoid shape. The equations that describe the straight line plots in Figure 2.19 are:

1. micelle/undefined phase: $y = 3.540x + 0.848$ ($r = 0.89$)
2. undefined/discome phase: $y = 0.343x + 0.015$ ($r = 0.98$)
3. lamellar/discome phase: $y = 0.108x - 0.089$ ($r = 0.99$).

The structures identified in the present study are unique by virtue of their large size. The large sizes of the aggregates is unexpected in a sonicated lipid dispersion. Discomes are also unique because they possess asymmetric structures within their population. They are formed when Solulan C24, $C_{16}G_2$, cholesterol and DCP are hydrated in the following proportions 29.5: 49: 19.5: 2 and the resulting dispersion sonicated. They form slowly from the original smaller aggregates in the sonicated dispersion.

The size of the discomes is, to some extent, dependent on the Solulan C24 concentration in the system. Discomes produced when $C_{16}G_2$, cholesterol, DCP niosomes (69: 39: 2) were incubated with Solulan C24 in the ratio total lipid: Solulan

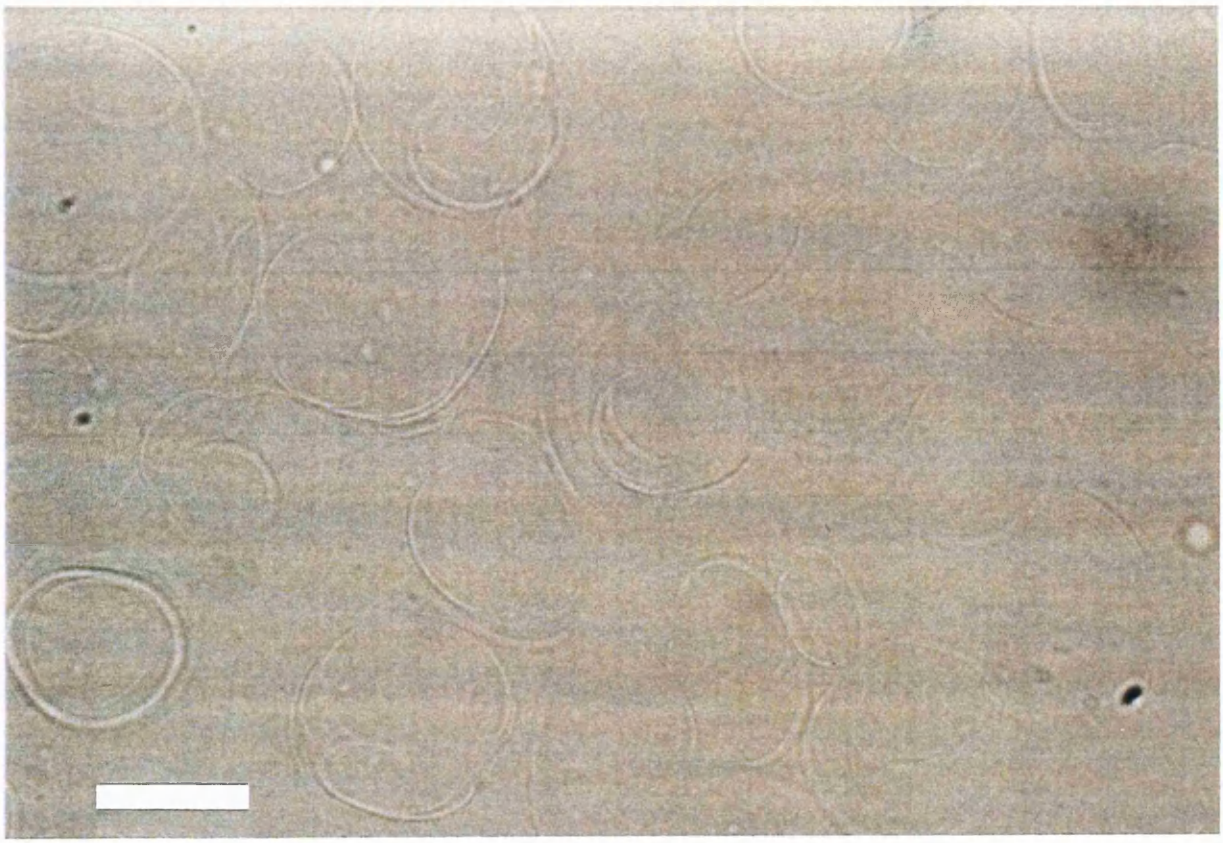

Figure 2.20a: Photomicrograph (X800) of discomes produced by incubating $C_{16}G_2$, cholesterol, DCP (69: 39: 2) niosomes with Solulan C24 in the proportions total niosome lipid: Solulan C24 - 12.86: 2.14. Bar = 25 μm.

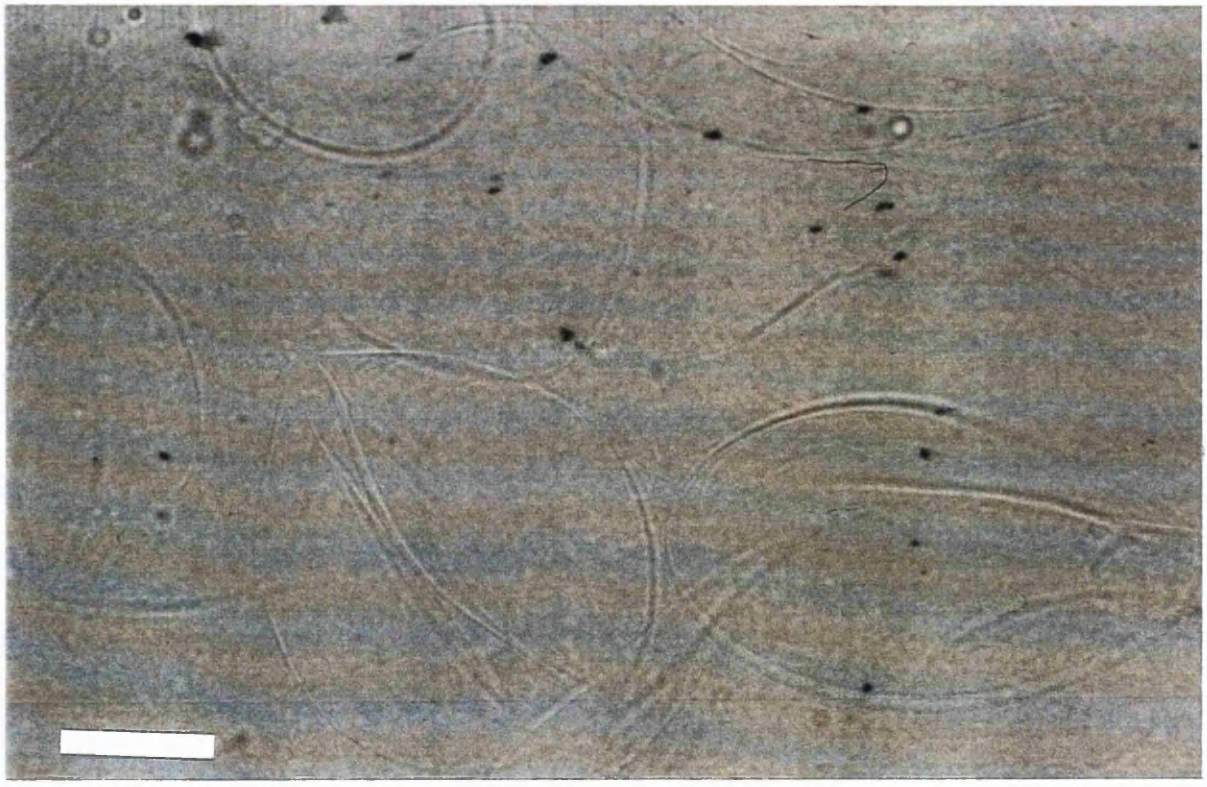

Figure 2.20b: Photomicrograph (X800) of discomes produced by incubating $C_{16}G_2$, cholesterol, DCP (69: 39: 2) niosomes in the proportion total niosome lipid : Solulan C24 - 10.71: 4.29. Bar = 25 μm.

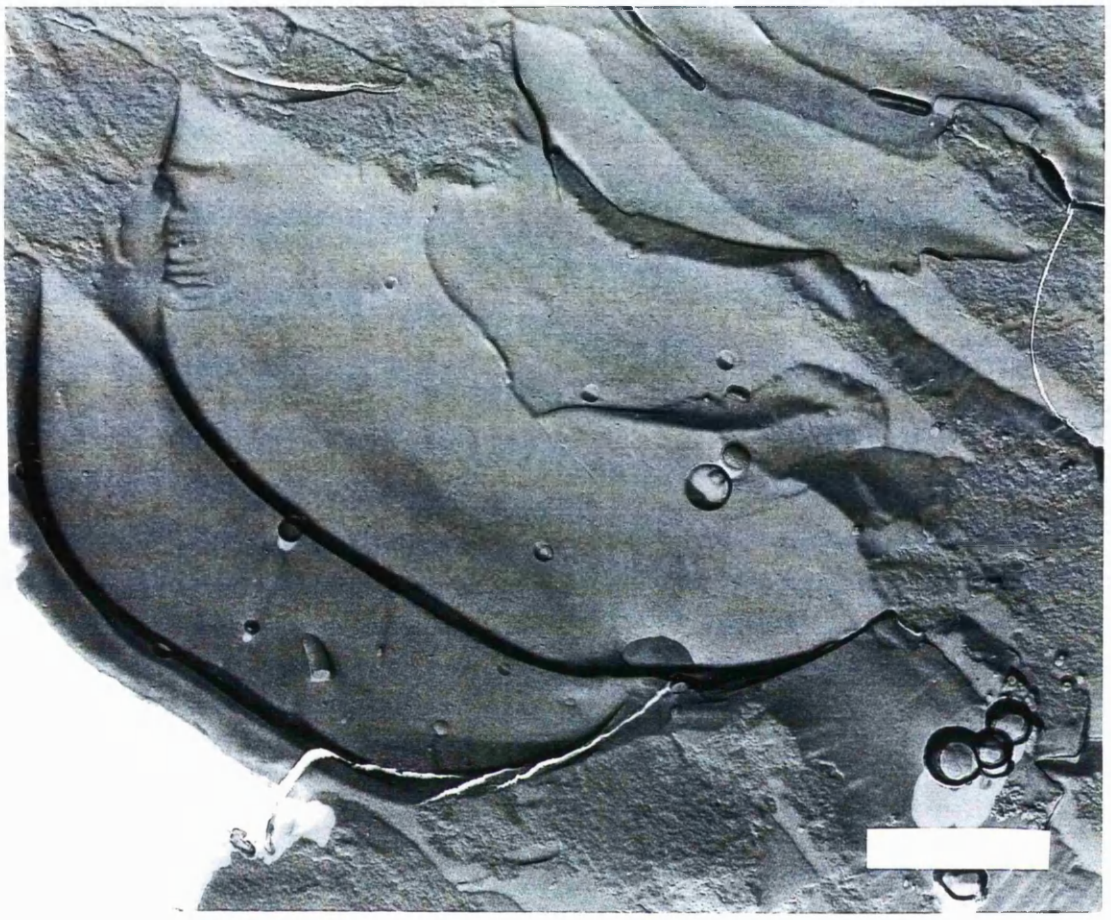

Figure 2.21: Freeze fracture micrograph (X24000) of a discome suspension produced by hydrating $C_{16}G_2$, cholesterol, Solulan C24, DCP (49: 19.5: 29.5: 2) with a CF solution. Large flat vesicular structures are apparent. Bar = 1 μm.

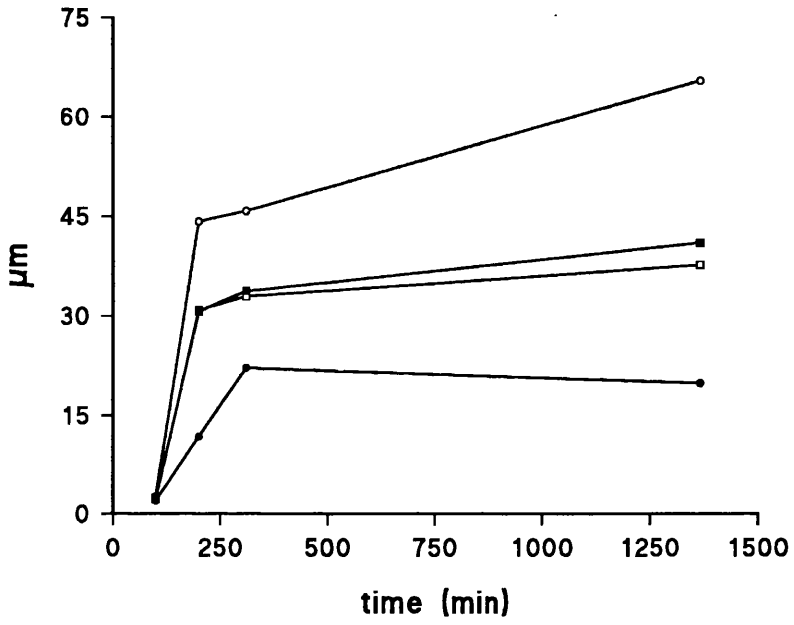

Figure 2.22: Growth of niosomes produced by the sonication of $C_{16}G_2$, cholesterol, Solulan C24, DCP (49: 19.5: 29.5: 2). Size distribution data is expressed as: volume distribution mean diameter (■) and % undersize (% undersize refers to a specified diameter beneath which a certain % of the particle population fall); 90% undersize (○), 50% undersize (□), 10% undersize (●).

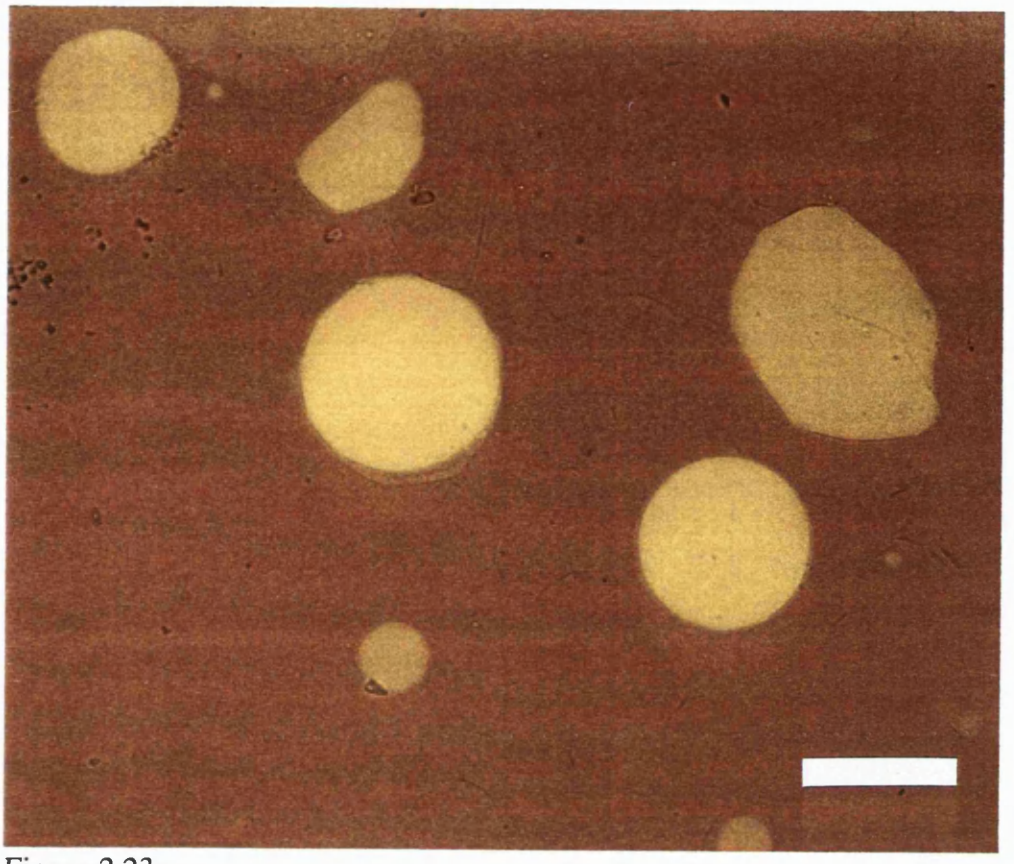

Figure 2.23a

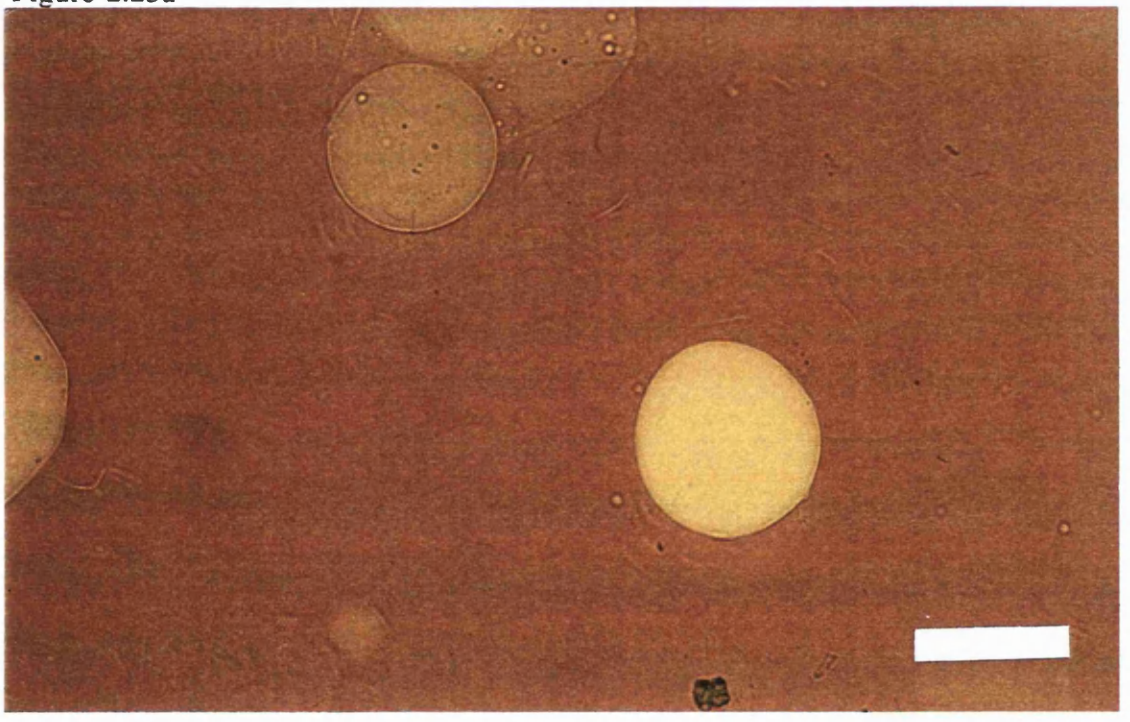

Figure 2.23b

Figure 2.23a&b: Photomicrograph (X200) of CF loaded discomes produced by the hydration and sonication of $C_{16}G_2$, cholesterol, Solulan C24, DCP (49: 19.5: 29.5: 2) with CF. Bar = 50 μm.

C24 (12.86: 2.14) (Figure 2.20a), show smaller structures than the discomes produced when niosomes were incubated with Solulan C24 in the ratio of total lipid: Solulan C24 (10.71: 4.29) (Figure 2.20b). Volume distribution mean diameters of both dispersions of 17.75 μm and 53 μm respectively were recorded. The turbidity of the dispersions, however, decreases with increasing Solulan C24 concentration (Figure 2.18). This decrease in turbidity with increase in size is explained by the accompanying decrease in the number of the particles leading to a lower light scattering. The increase in size of the discomes that accompanies the increase in the level of Solulan C24 in the system is due to the fact that Solulan C24 is a much larger molecule (molecular weight = 1443) with a greater surface area than the other molecules in the system ($C_{16}G_2$ molecular weight = 390, cholesterol molecular weight= 386.7); the inclusion of Solulan C24 in the lipid membrane would thus give rise to larger structures due to the inherent large bulk of the Solulan C24 molecule. Solulan C24 is also a relatively hydrophilic molecule. It contains 24 oxyethylene units and would thus be well hydrated. The added bulk created by the associated water molecules would lead to an increase in the hydrophilic head group cross-sectional area and in turn to an increase in volume of the non-ionic surfactant aggregates produced in these systems of increasing Solulan C24 content. The molecules of hydration (H_2O) when also incorporated into the discome membrane in increasing quantity would be expected to yield structures with decreasing light density. The equations describing the straight lines in the partial phase diagram can be used to describe quantitatively the solubilization process in the fashion of Levy and associates (1990):

$$[D_T] = R_{eff}[L] + D_W$$

where L and D_T are the total lipid ($C_{16}G_2$, cholesterol and DCP) and Solulan C24

concentration respectively, D_w is the Solulan C24 concentration in the continuous phase and R_{eff} is the effective Solulan C24: lipid ratio at which the phase transitions occur. The transition from lamellar to discome phase occurs at an effective Solulan C24 : lipid ratio of 0.108 or alternatively at a Solulan C24 mole fraction of 0.1 within the lipid aggregates. The transition from discome to the undefined phase occurs at an effective Solulan C24 : lipid ratio of 0.343 or a Solulan C24 mole fraction of 0.25 within the lipid aggregates. The transition from the undefined phase to the micellar phase occurs at a Solulan C24 : lipid ratio of 3.540 or a Solulan C24 mole fraction of 0.78 within the lipid aggregates. It follows, therefore, that the formation of discomes is only favoured if the mole fraction of Solulan C24 in the lipid aggregates lies between approximately 0.1 and 0.25. A Solulan C24 level within the lipid aggregates above a mole fraction of 0.25 does not yield discomes; once the Solulan C24 mole fraction within the lipid aggregates reaches 0.78 the formation of mixed micelles is favoured and an isotropic liquid is obtained. Size measurements on the mixed micellar dispersion gave a z-average mean hydrodynamic diameter of 3.9 nm (Malvern automeasure 4700V4).

A $C_{16}G_2$: cholesterol molar ratio of 7: 3 favours the formation of discomes. Increasing the cholesterol level in the vesicular dispersion above this, prior to challenge with Solulan C24, suppresses the production of discomes. In order to prevent the formation of discomes and produce conventional vesicular dispersions which nevertheless incorporate Solulan C24 in the bilayer, a molar ratio of $C_{16}G_2$: cholesterol of 1: 1 is optimal. This was found to be the case (Section 2.4) when niosomes were prepared from $C_{16}G_2$, cholesterol, Solulan C24 (30: 30: 40). The role

of cholesterol in preventing the insertion of octylglucoside into the bilayer of $C_{16}G_2$ vesicles during the micellization of these vesicles has been reported (Lesieur *et al.*, 1990). It is clear that the low mole fraction of cholesterol in the vesicular dispersion prior to their challenge with Solulan C24 facilitates the production of discomes by making the vesicular bilayer more permeable to the Solulan C24 molecules. The solubilization of non-ionic surfactant vesicles by Solulan C24 can be said to proceed in the following manner. As the Solulan C24 concentration in the system increases, it partitions progressively between the continuous phase and the bilayer until a critical level is reached in the vesicular bilayer phase and the vesicular phase gives rise to the discome phase. The partitioning of Solulan C24 within the discome membrane and continuous phase proceeds until eventually the level of Solulan C24 in the discomes leads to their breakdown to give other aggregates. Finally solubilization is complete with the production of mixed micelles.

When discomes are prepared by hydrating appropriate lipid mixtures e.g. $C_{16}G_2$, cholesterol, Solulan C24 and DCP (49: 19.5: 29.5: 2) with 8mM CF (Figure 2.23a&b), it appears that the dispersion attains equilibrium relatively slowly. It is possible that discome formation may be limited by kinetic processes as well as by the nature of the lipid mixture. The change in size of the dispersion immediately after sonication corroborates this assumption. An increase in size is experienced by the non-ionic surfactant particles after sonication (Figure 2.22). Most of the growth takes place in the first 5 h after sonication with little change thereafter. This increase in size is accompanied by an easily distinguishable change in the turbidity of the dispersion, with the discomes eventually forming a loose sediment in what was previously an

almost clear dispersion. It is possible that the formation of discomes may be limited by the time taken for the system to achieve an optimum distribution of Solulan C24 within the bilayer, hence the slow attainment of a discome like size (Figure 2.22). The rate limiting step to the solubilization of $C_{16}G_2$ niosomes by octylglucoside is said to be the actual insertion of the detergent molecules into the bilayer (Seras *et al.*, 1992).

Discomes (Figure 2.23a&b) are different from the bilayer sheets reported in the transition from vesicle to micelles in the phosphatidylcholine-sodium cholate system reported by Walter and others (1991). They are also different from the discoid micelles found in phosphatidylcholine-octylglucoside vesicle to micelle transitions (Levy *et al.*, 1990). Discomes are much larger than both of these structures and in addition, they appear in the main to be oval in shape. Asymmetric structures are also observed (Figure 2.23), atypical to the spherical bilayer conformations usually predicted by various theoretical models (Lipowsky, 1991). This observed asymmetry could be the result of a grossly heterogenous distribution of monomers within the bilayer. A heterogenous distribution of detergent molecules during $C_{16}G_2$ - octylglucoside vesicle to micelle transitions has been postulated (Lesieur *et al.*, 1990).

Discomes loaded with CF could be visualised under the light microscope using a fluorescent light source (Figures 2.23a&b). They were largely similar in structure to the discomes obtained by Solulan C24 solubilization of the $C_{16}G_2$ niosomes (Figures 2.20a&b). The different methods of preparation of the discomes: viz Solulan C24 vesicle solubilization (Figures 2.20a&b) and the hydration of a lipid film (Figures

2.23a&b) did not appear to affect the discome structure. Discomes encapsulating water (Figures 2.20a&b) and discomes encapsulating a buffered CF solution (Figures 2.23a&b), were also similar in structure.

The solubilization of liposomes by various detergents namely octylglucoside (Jackson *et al.*, 1982; Almog *et al.*, 1990), octaethylene glycol mono-n-dodecyl ether (Levy *et al.*, 1990) and polyoxyethylene cetyl ethers (Kim and Kim, 1991) at room temperature produced transition phase diagrams consisting of essentially 3 phases, the lamellar phase, the micellar phase and a region where lamellae and micelles are coexistent. The region of transition of vesicles to spherical micelles in the PC-cholate system has been described as consisting of "open" vesicles and bilayer sheets from which develop cylindrical micelles (Walter *et al.*, 1991). Solubilization of $C_{16}G_2$, cholesterol rich vesicles using the detergent octylglucoside has been described as consisting of essentially 3 stages: namely a lamellar phase, a micellar phase, and a phase in which octylglucoside penetrates the vesicle membrane - attains a level of saturation, albeit non-homogeneous distribution within the membrane and is then distributed throughout the membrane; and micellization results. In the present study, the micellization of niosomes studied at elevated temperatures by multiple sample preparation as opposed to the titrimetric methods used elsewhere (Walter *et al.*, 1991; Kim and Kim, 1991; Jackson *et al.*, 1982) produced a novel phase consisting of large stable discomes in addition to the lamellar phase, micellar phase and the third phase which marks the transition from discomes to micelles.

2.7:2 THE CARBOXYFLUORESCEIN ENCAPSULATION EFFICIENCY AND CARBOXYFLUORESCEIN RELEASE FROM DISCOMES *IN VITRO*

Discomes are able to encapsulate and retain an aqueous volume. The CF aqueous entrapment efficiency of discomes showed considerable batch-to-batch variation. A mean value (n=3) of 1.2009 ± 0.97 litres of hydrating solution per mole of lipid used was obtained. This represents a percentage entrapment of about 3.603 ± 2.916%.

The discomes retain about 50% of their aqueous volume marker over a 24 hour period at room temperature (Figure 2.24). A mixture of empty discomes and CF that had been incubated with CF at room temperature for 1 h showed a virtually identical release profile with a CF solution of similar concentration. This is evidence that CF is not adsorbed on the surface of the discomes to any significant degree and that any CF associated with the discomes must be encapsulated within the discome interior.

2.7:3 PROLONGED DIALYSIS AT ROOM TEMPERATURE

An apparently oligolamellar non-ionic surfactant aggregate was produced after dialysis of a dispersion of CF loaded discomes at room temperature for 80 h (Figure 2.25). Entrapment of CF is still evident in this particle as indicated by the fluorescence exhibited. It is interesting that while the separation of the entrapped solute from the unentrapped solute by dialysis of these discomes at 4°C did not appear to change their morphology (Figures 2.23a&b), dialysis at room temperature for prolonged periods does affect the morphology of the discomes (Figure 2.25). In the latter figure, an oligolamellar lipid aggregate is formed with the retention of the entrapped CF. It seems that the discome structure collapses to produce conventional multilamellar

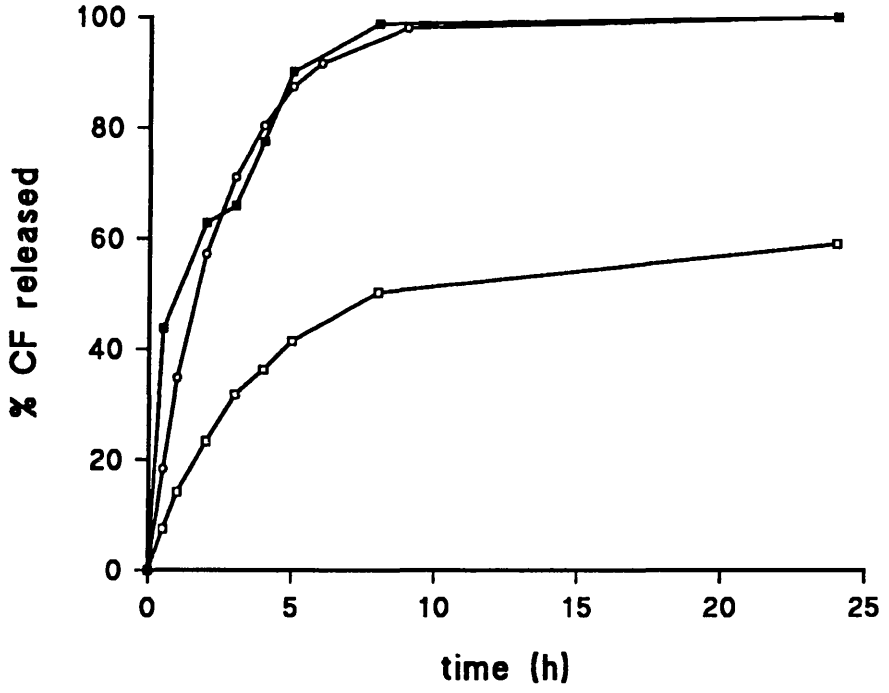

Figure 2.24: In vitro release of CF from discomes. □ = 65μM CF in discomes, ■ = 65μM CF solution, O = 65μM CF + empty discomes.

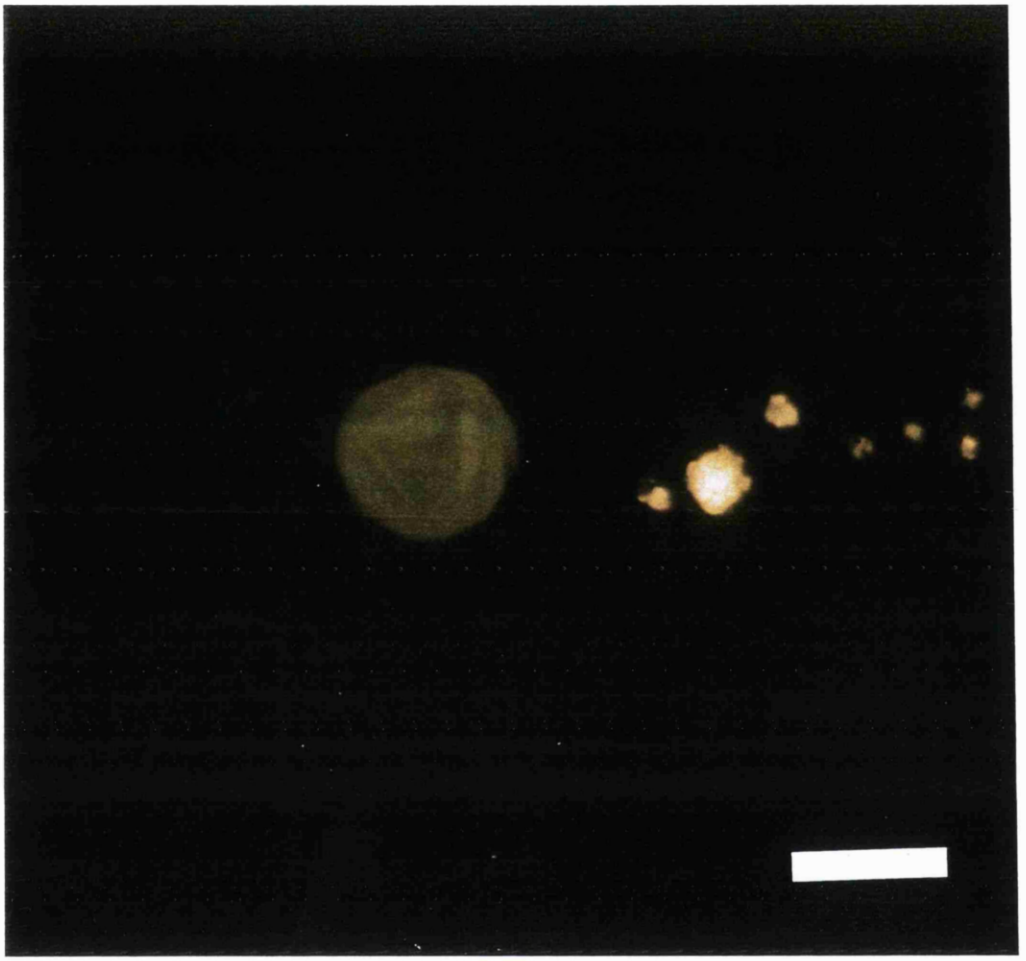

Figure 2.25: Photomicrograph (X200) of CF loaded discomes produced by hydration and sonication of $C_{16}G_2$, cholesterol, Solulan C24, DCP (49: 19.5: 29.5: 2) which had been dialysed at room temperature for 80 h. Bar = 100 μm.

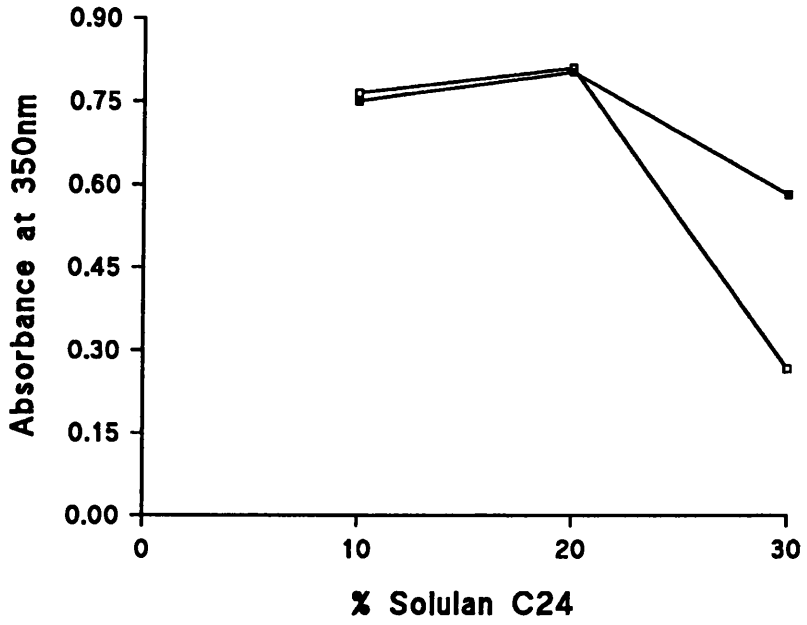

Figure 2.26: Turbidity measurements on niosomes and discomes containing various proportions of Solulan C24, at 30 and 37°C. ■ = 30°C, □ = 37°C.

vesicles as a result of the loss of Solulan C24 from the lipid aggregates through prolonged dialysis at room temperature, a process not significant at 4°C. The removal of detergent from mixed micelles by dialysis results in the production of unilamellar vesicles (Lesieur *et al.*, 1990; Almog *et al.*, 1990; Philpott and Liautard, 1993) and a similar process of detergent depletion seems to be operating here. It is conceivable that the discomes are formed from a lipid bilayer although the exact nature of the discome membrane requires further investigation.

2.7:4 TURBIDITY OF THE DISCOME DISPERSION AS A FUNCTION OF TEMPERATURE

Turbidity data of three non-ionic surfactant vesicle dispersions containing 10, 20 and 30% Solulan C24 respectively and taken at 30°C and 37°C are shown in Figure 2.26. The 20 and 30% Solulan C24 non-ionic surfactant vesicle dispersions when viewed under the light microscope were seen to contain discomes. The 30% Solulan dispersion showed marked loss of turbidity when the temperature was raised from 30 to 37°C, an indication of the instability of the dispersion at the higher temperature, although discomes could still be seen under the light microscope when smears were taken from a dispersion at 40°C. Discomes are stable for up to 6 months when stored at 4°C.

In conclusion novel disc shaped structures, discomes have been identified as part of the $C_{16}G_2$ - Solulan C24 vesicle to micelle phase transition. These discomes are able to encapsulate and retain aqueous solutes. It is envisaged that these discomes might be of use as drug delivery vesicles in the field of ophthalmology where their large size and minimum opacity might prove advantageous.

CHAPTER THREE

THE EVALUATION OF DOXORUBICIN NIOSOMES AGAINST A RESISTANT HUMAN OVARIAN CANCER CELL LINE

3.1DRUG DELIVERY INITIATIVES AND MULTIDRUG RESISTANCE

The multidrug resistance syndrome is commonly linked with the overexpression of a membrane glycoprotein (P-gp) (Riordan and Ling, 1979) and energy driven drug efflux (Beck, 1987). Decreased intracellular drug accumulation at nuclear sites (Schuurhuis *et al.*, 1991), the increased protection from free radical damage (Benchekroun *et al.*, 1993) and a decreased susceptibility to topoisomerase II inhibition (Doyle, 1993) have all been found in multidrug resistant cell lines.

Multidrug resistance has been modulated by liposomal encapsulation *in vitro* (Thierry *et al.*, 1989; Oudard *et al.*, 1991; Sadasivan *et al.*, 1991; Rahman *et al.*, 1992; Thierry *et al.*, 1993) and the effects of multidrug resistance gene amplification has been modulated in a transgenic mouse model *in vivo* (Mickisch *et al.*, 1992). The cytotoxic action of empty liposomes on resistant cells, overexpressing P-gp is greater than its action on sensitive cells, and an interaction between P-gp and empty liposomes has been proposed (Thierry *et al.*, 1992). Non-ionic surfactants with polyoxyethylene head groups also reverse multidrug resistance in vitro and in vivo (Woodcock *et al.*, 1992). The polyoxyethylene derivative of sorbitan monooleate, Tween 80, increased the accumulation of DOX in 'primary' and 'metastatic' cell lines (Bar-Shira-Maymon *et al.*, 1992) although this surfactant was inactive against a resistant human bladder cancer cell line not demonstrating typical decreased intracellular drug accumulation (Usansky *et al.*, 1991).

This chapter presents data from experiments performed to assess the activity of DOX niosomes of various compositions against a human ovarian cancer cell line CH1

DOX^R. CH1 DOX^R was made resistant to DOX *in vitro* by repeated exposure of the susceptible parent line to DOX. This resistant cell line exhibited a 230 fold lowered sensitivity to DOX compared to the parent line although the exact mechanism of DOX resistance has not been elucidated.

3.2 MATERIALS

Materials are as stated in chapter 2, but additional materials used in this study are given in Table 3.1.

3.3: METHODS

3.3:1 PREPARATION OF NIOSOMES

Niosomes were prepared from the lipid proportions and the DOX/lipid molar ratios shown in table 3.2. Niosomes were sized and analyzed in the usual way.

3.3:2 THE EVALUATION OF DOXORUBICIN NIOSOMES

A human ovarian cancer cell line (CH1) and its experimentally resistant subline (CH1 DOX^R) were grown as monolayers in Dubecco's modified eagles medium + 10% fetal calf serum in a humidified environment with 10% CO_2. Exponentially growing cells were harvested from T80 flasks by washing cells with 5 mL Earle's balanced salt solution and incubating for 4 min at 37°C with 0.5%w/v trypsin to dislodge cells from flask surface. Cells were then suspended in 5 mL Dubecco's modified eagles medium and centrifuged at 500 g for 5 min. The pellet was resuspended in this medium and

Table 3.1: Materials and sources

MATERIAL	SOURCE
CH1 ovarian cancer cell line	Donated by Dr Lloyd Kelland, Institute for Cancer Research, Royal Marsden hospital, Sutton, UK.
CH1 DOX^R ovarian cancer cell line	Donated by Dr Lloyd Kelland, Institute of Cancer Research, Royal Marsden Hospital, Sutton, UK.
Dubecco's modified eagles medium	Sigma Chemical Company, UK.
Earle's balanced salt solution	Sigma Chemical Company, UK.
Fetal Calf Serum	Sigma Chemical Company, UK.
Trizma hydrochloride	Sigma Chemical Company, UK.
Trypsin	Sigma Chemical Company, UK.

Table 3.2: Lipid molar proportions and initial DOX/lipid molar ratios used to prepare niosomes for the *in vitro* evaluation of DOX niosomes against a resistant human ovarian cancer cell line.

LIPID MOLAR RATIO	INITIAL DOX/LIPID RATIO
$C_{16}G_2$, cholesterol, NaDCP (47.5: 47.5: 5)	0.008
$C_{16}G_2$, cholesterol, Solulan C24 (45: 45: 10)	0.038
Span 60, cholesterol, Solulan C24 (45: 45: 10)	0.017

diluted to obtain a cell density of 3.125 X 10^5 cells.mL^{-1}. The growth inhibitory concentration for 50% of the cell population (IC_{50}) was determined by seeding cells in a 96 well microculture plate at a density of 5,000 cells per well (160 µL cell suspension per well), to which was added 40 µL of either of the DOX formulations described above, in varying concentration. DOX formulations were added 24 h after seeding cells in microculture plates. DOX solution was used as control. Cells were incubated for 96 h at 37°C in an 8% CO_2 environment. At the end of this period cells were assayed for viability, using a colorimetric assay (Skehan *et al.*, 1990). Cell growth medium was replaced with cold trichloroacetic acid (TCA) and left on ice for 30 min. TCA was then replaced with methanol, which was left in place for 5 min and cells were subsequently washed thoroughly with water. Fixed, previously viable, cells were then stained with 0.4% sulphorhodamine B (SRB) dissolved in 1% acetic acid, air dried and the dye solubilized with the addition to each well of 100 µL unbuffered tris base. Optical density (O.D.) was read at 540 nm (492 nm if O.D. readings are too high). Results are expressed as percentage survival of the cell population against drug concentration (Figure 3.1).

3.4: RESULTS AND DISCUSSION

The size, DOX/lipid ratio of the niosomes used in this study are given in Table 3.3 as are the calculated IC_{50} values (i.e. concentrations at which cell growth is inhibited in 50% of the cell population). Although there appeared to be cross resistance when $C_{16}G_2$ niosomes were used, DOX Span 60 niosomes were more active against the resistant ovarian cancer cell line CH1 DOX^R than DOX solution (Figure

Table 3.3: Characteristics of niosomes used against the CH1 DOX^R cell line and their corresponding IC_{50} values.

DOX formulation used	IC_{50} against CH1 (μM)	IC_{50} against CH1 DOX^R (μM)	z-average mean diameter (nm) of niosomes	Final molar DOX/lipid ratio in the formulation
DOX solution	0.0013	0.3	-	-
$C_{16}G_2$, cholesterol, NaDCP (47.5: 47.5: 5)	0.003	0.22	520	0.0028
$C_{16}G_2$, cholesterol, Solulan C24 (45: 45: 10)	0.0035	0.19	154	0.0032
Span 60, cholesterol, Solulan C24 (45: 45: 10)	0.0043	0.087	161	0.0105

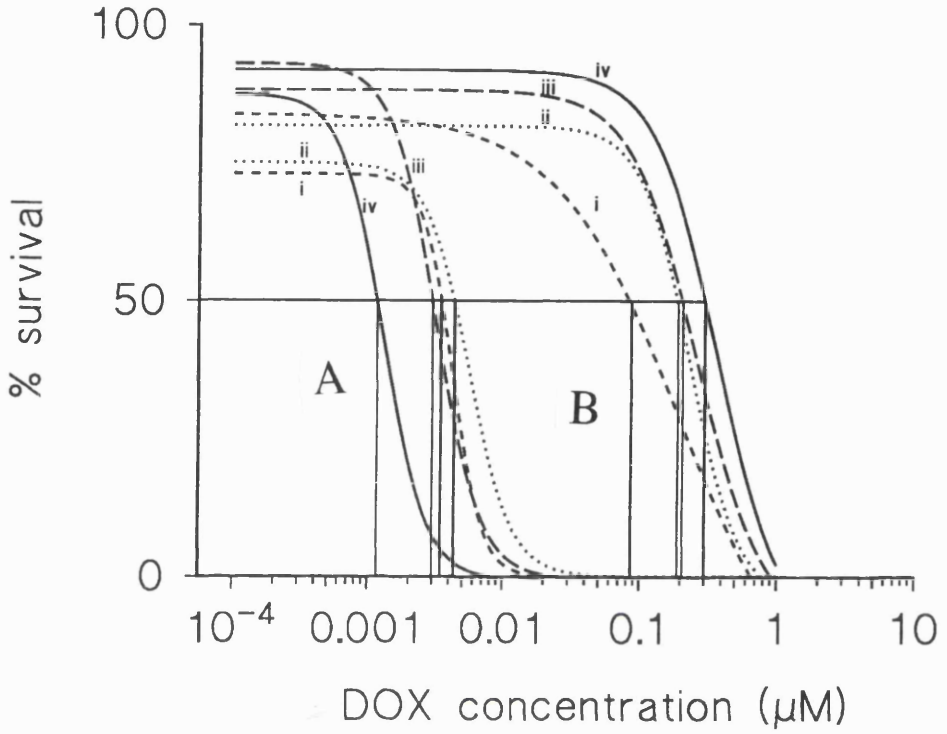

Figure 3.1: The activity of DOX niosomes against a resistant ovarian cancer cell line CH1 DOX^R (B) and its susceptible parent line - CH1 (A). i) Span 60, cholesterol, Solulan C24 (45: 45: 10) niosomes; ii) $C_{16}G_2$, cholesterol, Solulan C24 (45: 45: 10) niosomes; iii) $C_{16}G_2$, cholesterol, NaDCP (47.5: 47.5: 5) niosomes; iv) DOX solution.

3.1). However DOX niosomes were generally less active than DOX solution against the parent susceptible cell line CH1. The most active formulation against the resistant cell line CH1 DOX^R, Span 60 niosomes was the least active formulation against the susceptible cell line (Table 3.3). The use of DOX niosomes against the resistant CH1 DOX^R cell line resulted in a 3.5 fold increase in sensitivity with Span 60 niosomes and a 1.6 and 1.4 fold increase in sensitivity with the $C_{16}G_2$-Solulan C24 and $C_{16}G_2$-NaDCP niosomes respectively. These values could have been influenced by the lipid formulation, DOX load and/or niosome size. From Table 3.3, it appears that the Span 60 niosomes, which had a higher DOX load, were also the most active against the resistant cells. Each niosome with a larger payload on association with the cells would deliver more of drug to the cell than niosomes with a smaller payload. In a similar experiment involving DOX phosphatidylcholine-cardiolipin (PC-CL) liposomes and a resistant human ovarian carcinoma SKVLB cell line DOX sensitivity was increased 9.6 fold by encapsulation in liposomes (Thierry *et al.*, 1992). Studies with resistant chinese hamster LZ cells and a resistant human breast cancer MCF-7/ADR cell line showed that PC-CL DOX containing liposomes increased the sensitivity of these cells to DOX by 9 and 3 fold respectively (Thierry *et al.*, 1993). A value of a 7 fold increase in sensitivity with the LZ cell line and DOX PC-CL liposomes was also reported (Thierry *et al.*, 1989). The sensitization to DOX by liposomal encapsulation experienced by MCF-7/ADR cell line was comparable to that obtained in this study with Span 60 niosomes and the resistant ovarian cancer cell line CH1 DOX^R (3.0 and 3.5 respectively). Sadasivan and associates (1991) have quantified the sensitization to DOX encountered on liposomal encapsulation by computing a value called the relative resistance index (RR).

$$RR = IC_{50} \text{ resistant cells}/IC_{50} \text{ sensitive cells} \qquad (3.1)$$

DOX liposomes prepared from phosphatidylcholine-phosphatidylserine (PC-PS) reduced this value from 80 to 32 in a resistant variant of a human preleukemic cell line HL60R (Sadasivan *et al.*, 1991), P-gp overexpression was confirmed in this cell line. A computation of similar RR values with the Span 60 niosomes used in this work revealed a reduction in this value from 230 to 20, clearly larger than the value obtained with DOX PC-PS liposomes. When the IC_{50} values of DOX PC-CL liposomes and free DOX were compared for HL-60R cells not expressing P-gp, no sensitization to DOX was observed with the use of the encapsulated material (Thierry *et al.*, 1992). On the contrary, alternative HL-60R cell lines resistant to vincristine and with attendant overexpression of P-gp showed that DOX PC-CL liposomes increased the susceptibility of these cells to DOX 5 fold. Work with a colon cancer cell line SW620/R overexpressing P-gp showed a 1.4 fold increase in sensitivity with the use of PC-CL liposomal DOX (Oudard *et al.*, 1991). The number of different cell lines used in these various studies make it extremely difficult for any meaningful comparisons to be made and the systematic characterisation of the exact processes that lead to multidrug resistance would help future studies in this area.

While the amplification of the multidrug resistance gene and the overexpression of P-gp were not confirmed for the cell line used in this work, it appears that in many of the earlier reports cited above, confirmation of P-gp overexpression was linked to the ability of vesicular drug delivery to modulate this resistance. In certain cases the increased susceptibility of the resistant variant was associated with an increased

accumulation of DOX within the cell (Thierry *et al.*, 1989; Oudard *et al.*, 1991; Rahman *et al.*, 1992). This suggests that these vesicles may interact with P-gp and in some way change its function in resistant cell lines (Thierry *et al.*, 1989; Oudard *et al.*, 1991; Rahman *et al.*, 1992), preventing drug efflux. A specific binding of liposomes to P-gp has been reported (Rahman *et al.*, 1992; Thierry *et al.*, 1992). P-gp, apart from being responsible for the much vaunted energy dependant efflux mechanism (Beck, 1987), is also thought to alter membrane function by an alteration of membrane structure (Awasthi *et al.*, 1992). A reduced DOX accumulation in the lipid fraction of the membrane is found in some DOX resistant cells (Awasthi *et al.*, 1992). The interaction of surfactants with cell membranes in resistant cell lines also alters membrane fluidity and P-gp function (Woodcock *et al.*, 1992) while the interaction of empty PC-CL liposomes with P-gp is believed to be responsible for the increased susceptibility of these resistant cells to empty liposomes (Thierry *et al.*, 1992). It is possible that the surfactants present in the Span 60 niosome formulation would interact with the cell membrane increasing its retention of DOX.

In a resistant human bladder cancer cell line, resistance was associated with altered cellular distribution of the drug (Usansky *et al.*, 1991; Thierry *et al.*, 1993) and the modulation of resistance found a change in the intracellular drug distribution in favour of nuclear sites (Thierry *et al.*, 1993). It is not known whether the niosomes are taken up intact into the intracellular space, but the association of DOX with niosome membrane surfactants (Figure 2.6) may alter the intracellular distribution of the drug and reduce DOX resistance this way.

Largely the action of these vesicle formulations on the parent susceptible lines was unchanged by the encapsulation of DOX (Thierry *et al.*, 1993; Oudard *et al.*, 1991) and in our case, encapsulation actually decreased the sensitivity of the parent line CH1 to DOX, reducing the activity on niosomal encapsulation by 3.3, 2.7 and 2.3 fold for the Span 60 niosomes, $C_{16}G_2$-Solulan C24 and $C_{16}G_2$-NaDCP niosomes respectively.

Liposomal DOX preferentially lowers the white blood cell count of MDR-transgenic mice *in vivo* (Mickisch *et al.*, 1992). This mouse model expresses the multidrug resistance gene in the bone marrow. Measurements of white blood cell count relate directly to the level of multidrug resistant gene expression. In addition the use of the polyoxyethylene surfactant Cremophor in conjunction with DOX increased the survival time of mice bearing a resistant P388 transplantable tumour (Woodcock *et al.*, 1992).

These data suggest that drug delivery may have a role to play in the modulation of multidrug resistance. The encouraging results obtained with Span 60 niosomes in this report demonstrate a need for *in vivo* evaluation of this formulation against a multidrug resistant neoplasm. It is hoped that this may be done at some future date.

CHAPTER FOUR

THE INTRAPERITONEAL ADMINISTRATION OF DOXORUBICIN $C_{16}G_2$ NIOSOMES

4.1 THE INTRAPERITONEAL ADMINISTRATION OF DOXORUBICIN NIOSOMES

The intraperitoneal administration of DOX vesicles has received scant attention from drug delivery scientists. There are two reasons why the intraperitoneal administration of DOX may be considered important. The first is the already stated objective (Chapter 1), the achievement of prophylaxis following bowel resection of a carcinoma. The second is to target metastasis by increasing the concentration of drug present in the lymphatics. Metastases travel from their site of origin to their new site via the lymphatics and the peritoneal cavity is drained by the lymphatics (Hirano *et al.*, 1985).

This chapter describes investigations into the intraperitoneal administration of DOX niosomes prepared from $C_{16}G_2$, cholesterol and Solulan C24 to healthy, non-tumour bearing mice. To our knowledge this is the first report of intraperitoneal administration of DOX niosomes.

4.2 MATERIALS

The materials and sources used in the intraperitoneal study are as described in previous chapters. Additional materials and sources are as given in Table 4.1.

4.3 METHODS

4.3:1 NIOSOME PREPARATION

The study was divided into two parts, namely a pharmacokinetic study in which

Table 4.1: Materials and sources

MATERIAL	SOURCE
AKR mice	Harlan Olac, UK.
C_{18} microbondapak reverse phase HPLC column	Waters, Millipore, UK
Epirubicin	Sigma Chemical Company, UK.
Orthophosphoric acid	BDH Laboratory Supplies, UK.
Rat and Mouse standard Expanded diet	B & K Universal, UK
Silver nitrate	BDH Laboratory Supplies, UK.

plasma was assayed after the intraperitoneal administration of the DOX niosomes and a study in which tissue histology was studied in animals administered DOX niosomes intraperitoneally or intravenously. For the pharmacokinetic study, niosomes were prepared in the usual way from the lipid composition, $C_{16}G_2$, cholesterol, Solulan C24 (45: 45: 10) and a DOX/lipid molar ratio of 0.069. Niosomes were then filtered through a 0.22 μm filter, concentrated in an Amicon concentration cell for 22 h, and aseptically passed through a sterile 0.22 μm filter. Empty niosomes were prepared in a similar manner to drug loaded niosomes, but without the incorporation of the drug.

For the histological study, niosomes were prepared from the DOX/lipid combinations given above using the remote loading procedure previously described (method 1 - Chapter 2). This dispersion was not aseptically passed through sterile 0.22 μm filters. Separation of unentrapped drug from all niosomes was as already stated in Chapter 2. Empty niosomes containing TBS (pH 4.0) for the histology study were prepared by adjusting the pH to 7.2 post-sonication. All niosomes were concentrated to the required level by dialysis over solid PEG 6000. Niosomes were assayed in the usual way.

4.3:2 ANIMAL HUSBANDRY

Male AKR mice, 5-8 weeks old and mean weight 25 g, were housed in groups of 3, in suspended plastic cages at 19-23°C with a 12 h light-dark cycle. A conventional diet and water were available *ad libitum.*

4.3:3 PHARMACOKINETIC STUDY

78 mice were divided into 4 groups of 18 animals each (groups 1-4), and a group of 6 animals (group 5). Groups 1-3 were dosed intraperitoneally with DOX niosomes at dose levels of 2.5, 5.0 and 10.0 mg kg^{-1}. Group 4 received a solution of DOX in TBS (pH 4.0) intraperitoneally at a dose level of 10 mg kg^{-1}. Group 5 received no treatment. The dose volume was 1.6 - 2.0 mL injected slowly over 60 s. Three mice were killed by halothane overdose from each of groups 1-4 at 30 min, 1, 2, 4, 8 and 24 h post-dosing. The mice in group 5 were killed at the start of the experiment. Blood was collected by cardiac puncture following a thoracotomy incision, into lithium heparinized tubes. Plasma was separated from other blood components by centrifugation at 500 g and stored at -44°C. Hearts were removed, foil wrapped, placed in liquid nitrogen and also stored at -44°C.

4.3:4 ANALYSIS OF PLASMA SAMPLES FOR DOX

Analysis was performed by a modification of the method of Cummings and associates (1984). Plasma (0.1 mL) was extracted with 5 mL of isopropanol: chloroform (1: 2), the solvent evaporated under reduced pressure at 50°C and the residue reconstituted in 0.2 mL of mobile phase (isopropanol 170: 5 mM phosphoric acid 500) containing 0.4 μg mL^{-1} of epirubicin as internal standard. Analysis was performed using a C_{18} Microbondapak reverse phase HPLC column, with the mobile phase driven by a Waters 501 solvent delivery system. Fluorescence was measured with a Waters 470 scanning fluorescence detector (excitation 480 nm, emission 560 nm) and the peak area quantified using a Waters 746 data module.

4.3:5 ANALYSIS OF HEART TISSUE FOR DOX

Analysis of solid tissue was by the method of Cummings and McArdle (1986). Thawed hearts were weighed and homogenised in 3 mL of PBS (pH 7.4) and 200 µL of 33% $AgNO_3$ was added to 1 mL of the homogenate. The mixture was extracted with 5 mL of isopropanol: chloroform (1:2) and the organic phase evaporated under reduced pressure at 50°C. The residue was reconstituted in 1.0 mL mobile phase (as above). Analysis for DOX was performed as described above.

4.3:6 HISTOLOGY

30 mice were divided into 10 equal groups and dosed as shown in Table 4.2. At 6h post-dosing, mice were killed by halothane overdose, the organs examined and the heart, spleen, kidneys and liver removed weighed and placed in 10% buffered formalin. The lungs were inflated *in situ*, removed and placed in 10% buffered formalin. Histological sections were prepared and stained with haematoxylin and eosin and photomicrographs of these sections were recorded (Nikon Microphot FXA).

4.3:7 PHARMACOKINETIC PARAMETERS

Areas under the concentration time curves (AUCs) were calculated using the linear trapezoidal rule. The time of maximum tissue level (t_{max}) and the maximum tissue level (C_{max}) were estimated by visual inspection of the curves.

4.3:8 STATISTICAL ANALYSIS

Results are expressed as means ± s.e.m. Statistical analysis was carried out using ANOVA one-way analysis of variance.

Table 4.2: The dosing of mice used in the histology study

GROUP NUMBER	FORMULATION ADMINISTERED AND ROUTE OF ADMINISTRATION
1	0.2 - 0.4 mL DOX niosomes 12 mg kg^{-1} intraperitoneally
2	0.2 - 0.4mL DOX niosomes 12 mg kg^{-1} intravenously
3	0.2 - 0.4 mL empty niosomes intraperitoneally
4	0.2 - 0.4mL empty niosomes intravenously
5	0.2 - 0.4 mL DOX solution 12 mg kg^{-1} intraperitoneally
6	0.2 - 0.4mL DOX solution 12 mg kg^{-1} intravenously
7	0.2 - 0.4 mL TBS (pH 4.0) intraperitoneally
8	0.2 - 0.4mL TBS (pH 4.0) intravenously
9	no treatment
10	DOX niosomes 12mg kg^{-1} intraperitoneally. Dose was diluted to 1.8 - 2.0 mL with empty niosomes.

4.4 RESULTS AND DISCUSSION

4.4:1 PHYSICAL CHARACTERISTICS OF DOX NIOSOMES

The niosomes used in the pharmacokinetic study and the histological study had a mean size of approximately 100 nm. The DOX concentration of the niosomal dispersion for the pharmacokinetic study was 0.12 mg mL^{-1} while the concentration for the histological study was 0.93 mg mL^{-1}. The dispersion for the histological study was concentrated to the above level to allow for the intravenous administration of DOX to mice at a dose level of 12.0 mg kg^{-1}.

4.4:2 PHARMACOKINETIC STUDIES - PLASMA

Plasma levels of DOX following intraperitoneal administration of DOX niosomes and free drug at 10.0 mg kg^{-1} are shown in Figure 4.1a. The encapsulation of DOX niosomes more than doubled the area under the plasma level time curve (Table 4.3). Peak plasma levels are attained at 0.5 h post-dosing for the free drug (10 mg kg^{-1}) and at 2.0 h for the same dose of niosome encapsulated DOX (Table 4.3). Peak plasma levels (C_{max}) were similar for the free drug and the niosome preparation at the dose level of 10.0 mg kg^{-1}, being (mean ± s.d.) 531 ± 671 and 575 ± 300 ng mL^{-1}, respectively (Table 4.3). These are particularly large standard errors about the mean showing the extent of individual variation in niosomal DOX pharmacokinetics. There is considerable individual variation in free DOX plasma pharmacokinetic data (Speth *et al.*, 1988).

Intraperitoneally administered liposomes are said to survive and exit, largely intact, from the peritoneum to the vascular space and exert their depot effect from within the

blood compartment (Kirby and Gregoriadis, 1980, 1983; Titulaer *et al.*, 1990; Allen *et al.*, 1993), but it is not clear whether the niosomes remain within the peritoneum and slowly release their contents or whether they survive and exit intact from the peritoneum to release DOX from within the central compartment. The transport of intraperitoneally administered particulate drug delivery systems from the peritoneum proceeds through the lymphatics of the diaphragm through to the thoracic lymph (Olin and Saldeen, 1964; Tsilibary and Wissig, 1983; Hirano *et al.*, 1985), from where they are emptied into the blood stream. This transport system is slower for particulate drug formulations than for drug in solution (Hirano *et al.*, 1985; Maincent *et al.*, 1992; Kresta *et al.*, 1992) and the opening of the terminal lymphatics is governed by conditions within the diaphragm (Tsilibary and Wissig, 1983). Results in Table 4.3 indicate that the clearance of free DOX from the peritoneal cavity is more efficient than the clearance of DOX niosomes in accordance with reported kinetics of lymphatic transport from the peritoneum (Hirano *et al.*, 1985; Maincent *et al.*, 1992; Kresta *et al.*, 1992) and phosphtidylcholine-phosphatidylglycerol (PC-PG) liposomal data (Mayhew *et al.*, 1990).

Figure 4.2 illustrates the plasma levels of the cytotoxic after the intraperitoneal dosing of DOX niosomes at 2.5, 5.0 and 10.0 mg kg^{-1}. The various plasma pharmacokinetic parameters are set out in Table 4.3. Despite considerable individual variation in the results, there was a dose-related response in the peak plasma concentrations of DOX for the niosome formulations administered at 2.5, 5.0, 10.0 mg kg^{-1} (Figure 4.1b, Table 4.3).

When DOX was administered at a dose of 10.0 mg kg^{-1}, either in the free or encapsulated form, the elimination of the drug from the plasma compartment was biphasic (Figure 4.1a). This pattern of elimination also applied in essence to the niosomal preparation given at 5.0 mg kg^{-1} (Figure 4.1b). With the 10 mg kg^{-1} niosome dose, elimination appeared to be preceded by the appearance of a plateau in the plasma level time curve at the point of peak drug concentration.

In vitro data point to the encapsulation of DOX in niosomes being protective against the processes of elimination (Rogerson *et al.*, 1987). This protection was not evident when the drug was administered intraperitoneally as PC-PG liposomes (Mayhew *et al.*, 1990) and in contrast to the present observations with niosomes, Mayhew and associates (1990) showed that there was no change in the area under the plasma level time curve when free drug or the drug encapsulated in PC-PG liposomes were given by the intraperitoneal route. The increased levels of DOX in the plasma following the intraperitoneal administration of DOX in $C_{16}G_2$-cholesterol-Solulan C24 ($C_{16}G_2$-SOL) niosomes, in contrast to no such increase observed with PC-PG DOX liposomes (Mayhew *et al.*, 1990), may be associated with the nature of the lipid membrane of the two vesicles. The lipid membrane of the niosomes in the present study contained a polyoxyethylene derivative (Solulan C24; MW = 1443). In contrast the liposomal membrane used in the study by Mayhew and others (1990) did not have a significant hydrophilic component. Decreased clearance of xenobiotics from the plasma compartment has been associated with the polyoxyethylene component of vesicular membranes by many authors (Klibanov *et al.*, 1990; Blume and Cevc, 1990; Senior *et al.*, 1991; Allen *et al.*, 1991; Lasic *et al.*, 1991; Woodle and Lasic, 1992), and it has

been proposed that the reduced clearance is related to the process of steric hindrance which acts against the phagocytic mechanisms of the reticuloendothelial system (Lasic *et al.*, 1991).

With the lowest niosome dose (2.5 mg kg^{-1}), there was a peak plasma level at 0.5 - 1h, followed by a decline and then a further sustained rise starting at 2h post-dosing (Figure 4.1b). A modest rise can also be seen with the free drug administered at 10.0 mg kg^{-1}, between 4 and 24 h post-dosing (Figure 4.1a). A similar, but less clear-cut result is seen in the data of Mayhew and others (1990). It is not certain why various secondary increases in DOX plasma levels occur. It is possible that the secondary rise may be associated with the release of DOX from disrupted vesicles in the peritoneal cavity, or with the release of drug from previously equilibrated tissue stores. Peritoneal macrophages, for instance, have been shown to take up and subsequently release cytostatic levels of DOX following intraperitoneal injection (Storm *et al.*, 1988).

4.4:3 PHARMACOKINETIC STUDIES - HEART

Levels of DOX in heart tissue following the administration of the free drug and the niosomal formulation at 10 mg kg^{-1} are shown in Figure 4.2a. DOX levels in cardiac tissue after giving the niosomal preparation at 2.5, 5.0 and 10.0 mg kg^{-1} are presented in Figure 4.2b. Pharmacokinetic parameters for cardiac tissue are set out in Table 4.4. However, in contrast to the results for plasma, levels of DOX in the heart tissue appeared to be unrelated to the dose levels of the drug administered as the niosome preparation. This finding applied to the results for the AUC, the t_{max} and the C_{max}

(Table 4.4). However, the peak cardiac tissue concentration was similar in animals receiving the free drug at 10.0 mg kg^{-1} and in mice given DOX niosomes at this dose level, the levels being 2.60 ± 1.69 and 1.54 ± 0.51 μg ml^{-1} respectively, although not much can be deduced from this as the standard errors about the mean for both values are large. Cable (1989) demonstrated that the administration of DOX niosomes intravenously was associated with decreased cardiac levels when compared to the administration of an identical dose of the free drug.

The general insensitivity of cardiac levels to DOX dose were unexpected, These cardiac levels may be related to the fluid imbalance suffered by these animals, as seen by the fluid accumulation in the pleural cavity, and the congested pulmonary blood vessels (Figure 4.5).

4.4:4 CLINICAL SIGNS AND GROSS PATHOLOGY

Animals dosed intraperitoneally with DOX niosomes at 5.0 and 10.0 mg kg^{-1} showed, between 4 and 8 h post dosing, signs of inactivity and depressed behaviour, a hunched posture, piloerection and laboured breathing. The effects were not clearly evident earlier than 4 h post-dosing. Four animals out of a total of six dosed at 5.0 and 10.0 mg kg^{-1} (2 from each group), and scheduled to be killed at 24h, died between 8 and 24 h post-dosing. The remaining animals (1 from each group), eventually became comatose and were killed at 24 h post-dosing. None of these clinical signs were seen in mice dosed intraperitoneally with DOX niosomes at 2.5 mg kg^{-1}, DOX solution at 10.0mg kg^{-1}, or control animals that received no treatment at all.

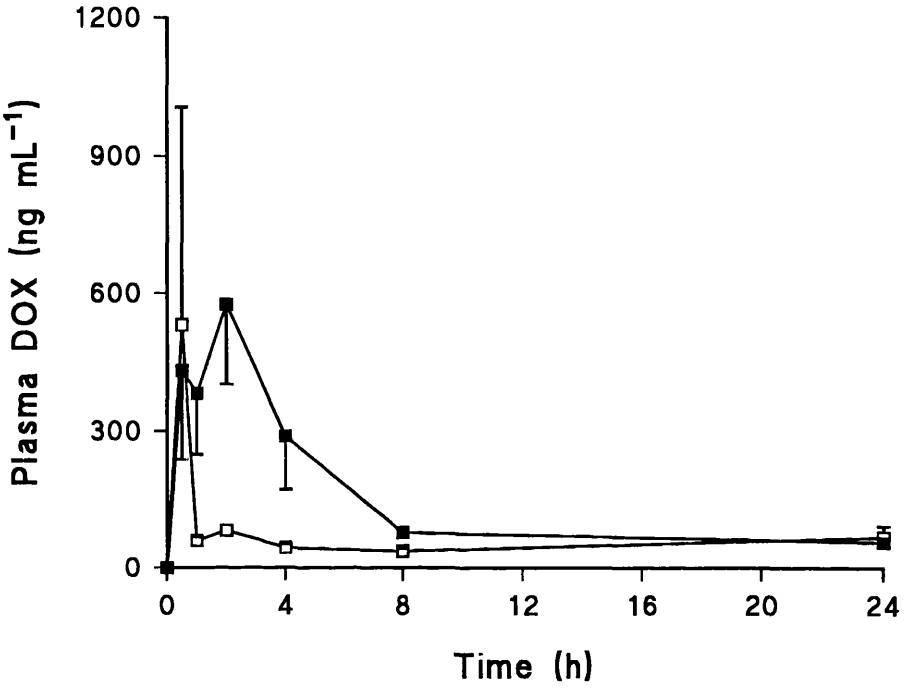

Figure 4.1a: Mean plasma levels (± s.e.) of DOX following intraperitoneal administration of DOX formulations. □ = 10 mg kg^{-1} DOX solution, ■ = 10mg kg^{-1} DOX niosomes.

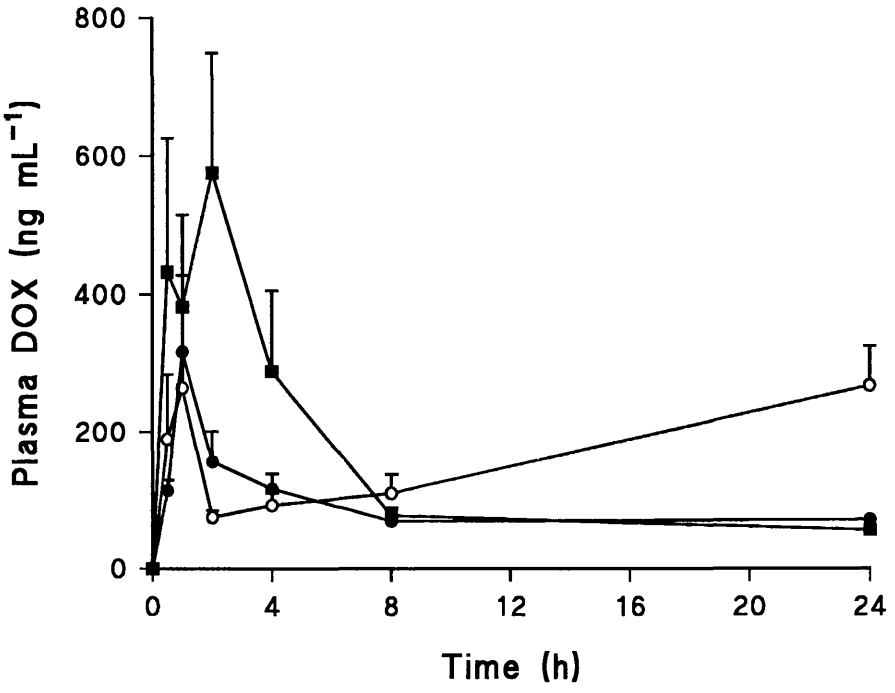

Figure 4.1b: Mean plasma levels (± s.e.) of DOX following intraperitoneal administration of DOX niosomes. ○ = 2.5 mg kg^{-1}, ● = 5mg kg^{-1}, ■ = 10 mg kg^{-1}.

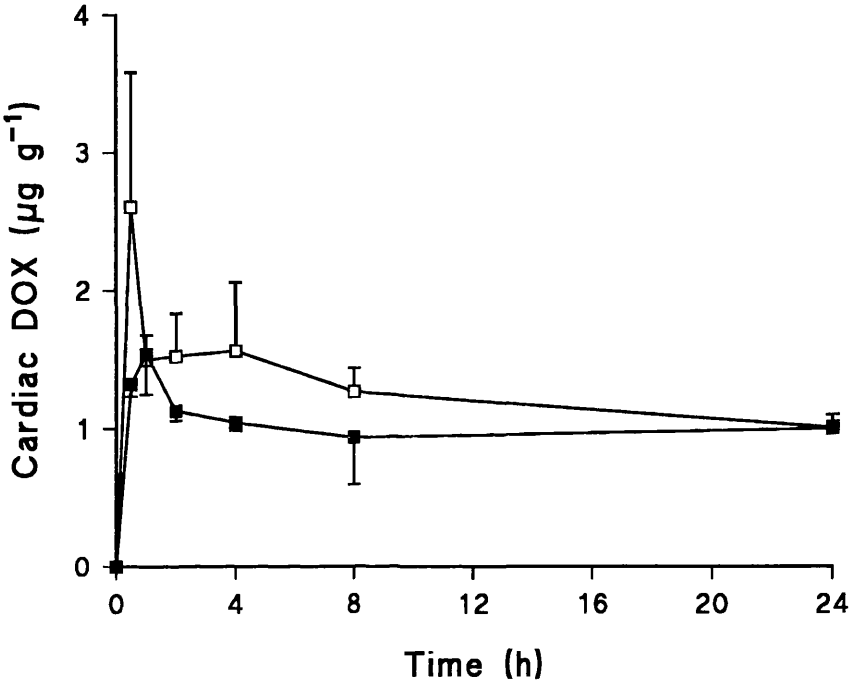

Figure 4.2a: Mean cardiac tissue DOX levels (± s.e.) following intraperitoneal administration of DOX formulations. □ = 10mg kg^{-1} DOX solution, ■ = 10 mg kg^{-1} DOX niosomes.

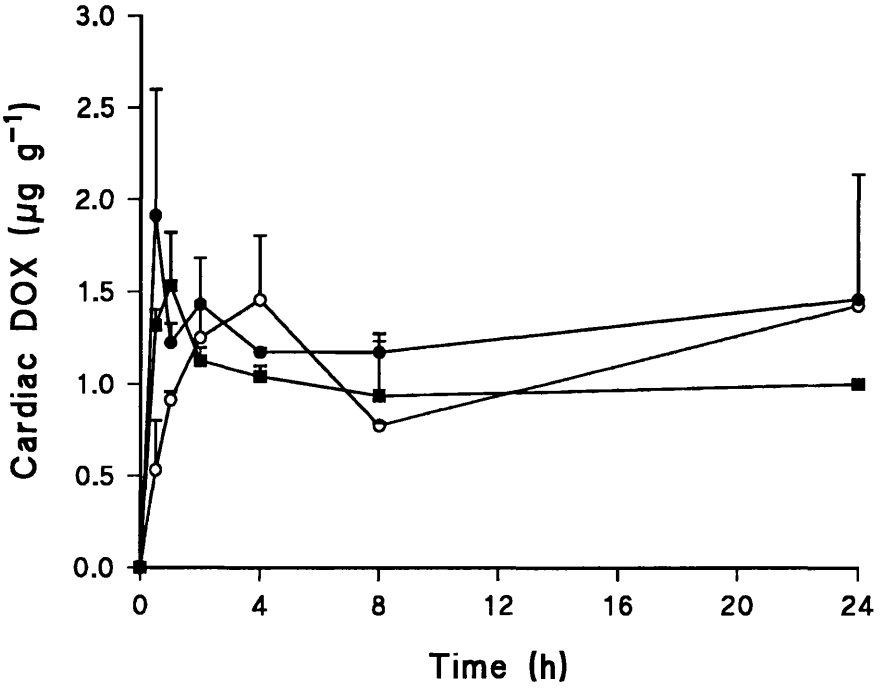

Figure 4.2b: Mean cardiac tissue DOX levels (± s.e.) following intraperitoneal administration of DOX niosomes. ○ = 2.5mg kg^{-1}, ● = 5 mg kg^{-1}, ■ = 10mg kg^{-1}.

Table 4.3: Plasma pharmacokinetic parameters for the solution and niosomal formulations of DOX administered intraperitoneally.

FORMULATION AND DOSE LEVEL OF DOX ADMINISTERED	$AUC^{0.17-24}$ (ng.h mL^{-1})	PEAK PLASMA LEVEL TIME t_{max} (h)	PEAK PLASMA CONCENTRATION C_{max}* (ng mL^{-1})
Solution 10 mg kg^{-1}	1471	0.5	531 ± 671
Niosomes 10mg kg^{-1}	3461	2.0	575 ± 300
Niosomes 5 mg kg^{-1}	2150	1.0	316 ± 156
Niosomes 2.5mg kg^{-1}	3929	1.0	264 ± 282

*Mean ± s.e.

Table 4.4: Cardiac tissue pharmacokinetic parameters for solution and niosomal formulations of DOX administered intraperitoneally.

FORMULATION AND DOSE LEVEL OF DOX ADMINISTERED	$AUC^{0.17-24}$ (µg.h mL^{-1})	PEAK CARDIAC TISSUE LEVEL TIME t_{max} (h)	PEAK CARDIAC CONCENTRATION C_{max}* (µg mL^{-1})
Solution 10 mg kg^{-1}	30.1	0.5	2.6 ± 1.69
Niosomes 10mg kg^{-1}	24.0	1.0	1.54 ± 0.51
Niosomes 5 mg kg^{-1}	31.0	0.5	1.91 ± 1.19
Niosomes 2.5mg kg^{-1}	26.4	4.0	1.46 ± 0.60

*Mean ± s.e.

Figure 4.3: Section of lung (H&E X500) from a mouse given empty niosomes *intraperitoneally* at the same total lipid level as the groups of mice that received DOX niosomes. 6h after dosing the appearance of the tissue is normal.

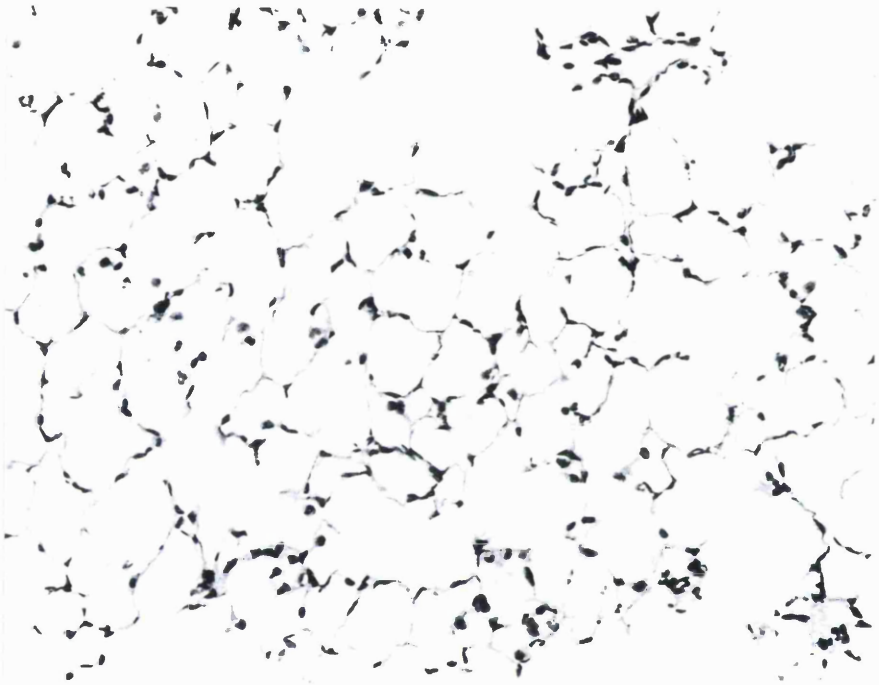

Figure 4.4: Section of lung (H&E X500) from a mouse given 12 mg kg^{-1} DOX niosomes *intravenously*. 6h after dosing the appearance of the tissue is normal.

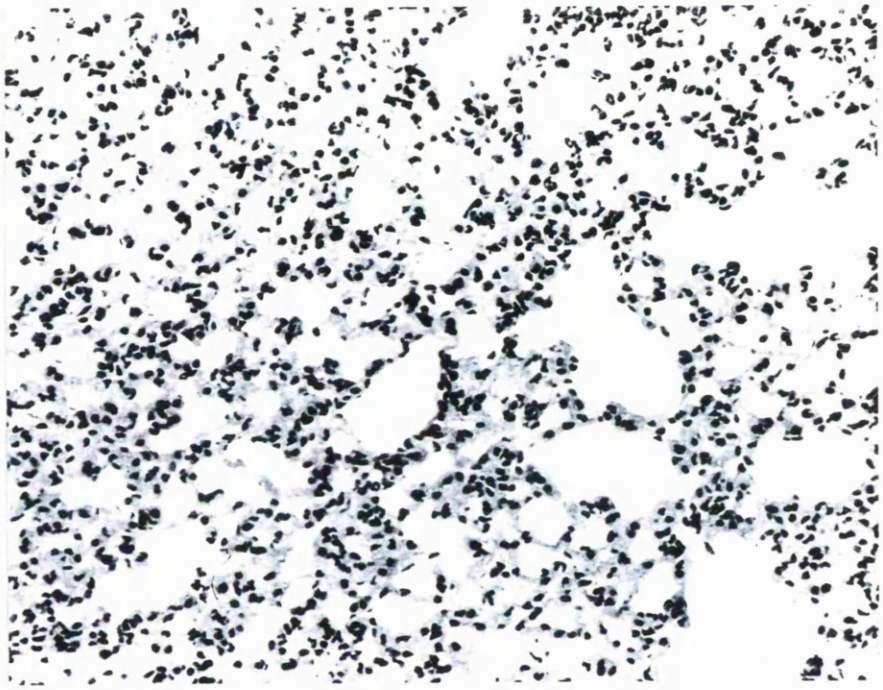

Figure 4.5: Section of lung (H&E X500) from a mouse given 12mg kg^{-1} DOX niosomes *intraperitoneally*. 6h after dosing there is an increase in the cellularity of the alveolar tissue with congestion of the alveolar capillaries and an increase in the number of acute inflammatory cells in the alveolar is evident.

At post mortem examination, the pleural cavities of animals dosed with DOX niosomes at 5.0 and 10.0 mg kg^{-1} intraperitoneally and killed at the 8 and 24 h time points, were found to contain 0.15 - 0.3 mL of a clear, straw coloured fluid. The tissues within the pleural cavity had retained their shiny appearance and there was no evidence of fibrin deposits. This pleural effusion was not seen before the post mortem performed at the 8h time point. The volume of fluid tended to be greater in animals with more pronounced clinical signs. At the 8 and 24 h post mortem examinations, there were no signs of fluid accumulation in the pleural cavity of mice dosed intraperitoneally with DOX niosomes at 2.5 mg kg^{-1} or DOX solution at 10.0 mg kg^{-1}. Control animals that received no treatment also showed no sign of accumulation of fluid in the pleural cavity.

In animals used in the histology study, there was no statistically significant effect on either the absolute or relative weights of the spleen, liver, kidneys or heart in mice treated by the intravenous or intraperitoneal route with empty niosomes, DOX-containing niosomes or DOX solution, in comparison with control mice receiving TBS.

No adverse signs were seen in mice dosed with empty niosomes intraperitoneally, neither were they seen in animals administered with DOX niosomes at 12 mg kg^{-1} or empty niosomes when these were administered by the intravenous route. The early clinical signs seen in some mice at 4 and 8 h, described above in the pharmacokinetic study, (inactivity, hunched posture, piloerection) became evident between 4 and 6 h post-dosing in animals in the histology study given DOX-containing niosomes at 12.0

mg kg^{-1} by the intraperitoneal route, irrespective of whether the mice received the lower (0.2 - 0.4 mL) or the higher (1.8 - 2.0 mL) dose volume. These adverse signs were not observed in mice from any of the other treatment groups. At post mortem, 6 h post-dosing, there was some evidence of fluid accumulation in the pleural cavities of mice treated with DOX niosomes at 12.0 mg kg^{-1} by the intraperitoneal route, whether the mice were administered with the higher or the lower dose volume; but there was no evidence of fluid accumulation in the pleural cavity of mice from any other group. This effusion is considered to be a transudate as there were no associated fibrin deposits.

4.4:5 LUNG HISTOLOGY

The normal histological appearance of the lungs from control mice treated with empty niosomes intraperitoneally is seen in Figure 4.3. Normal histology was also seen in the lungs of mice treated with TBS intraperitoneally or intravenously and from mice treated intravenously with 12.0 mg kg^{-1} DOX niosomes (Figure 4.4). However in mice given DOX niosomes by the intraperitoneal route, at 12.0 mg kg^{-1} and at a dose volume of 0.2 - 0.4 mL, the lungs showed an increase in cellularity of the alveolar tissue. There was also an increase in the number of acute inflammatory cells in the alveolar walls and congestion of the alveolar capillaries (Figure 4.5). These changes were however, not seen in mice dosed intraperitoneally with DOX niosomes at 12.0 mg kg^{-1}, and at a dose volume of 1.8 - 2.0 mL, neither were they seen in the lungs of animals from any other treated group. The larger dose volume used in mice dosed intraperitoneally with DOX niosomes at 12 mg kg^{-1} appeared to reduce the severity of the reaction and although the animals did show the same gross pathological changes

as animals receiving the smaller dose volume these animals dosed with the higher dose volume failed to show the accompanying histopathological changes. There were no histopathological changes observed in the heart, kidney or spleen of any treated mice. DOX encapsulated in PC-PG liposomes, administered intraperitoneally (Mayhew *et al.*, 1990) showed reduced acute toxicity in comparison with free drug. However in the present study, DOX niosomes given intraperitoneally induced significant acute toxic changes, leading to death in some animals.

We are unclear as to the pathological processes which may have induced the clinical signs of toxicity, and the gross and microscopic changes described above. It is considered unlikely that the lung lesion was caused by niosomes becoming trapped in the lungs, as the lungs from mice treated with empty niosomes were normal (Figure 4.3). Furthermore, the niosomes in the preparation, were small ($\approx$ 100 nm), and vesicles of this size are unlikely to become trapped in the lung capillaries. However any accumulation of DOX niosomes in the lungs could give rise to alveolar capillary congestion by a direct action on the lungs. DOX is known to alter the physiological characteristics of cell membranes (Arancia and Donelli, 1991), and its cytotoxicity has been linked to this property. An alternative explanation for the inflammation in the lungs is that this response may have been associated with the accumulation of fluid in the pleural cavity. The most common condition associated with pleural transudates is biventricular cardiac failure. The death of mice within 24 h of receiving the dose adds weight to the possibility of cardiac failure being the cause of slow death. Further support to this hypothesis is furnished by the different pathways expected to be followed by the intraperitoneal and intravenous doses. The transport of particulate

drug delivery systems from the peritoneum by the lymphatics via the thoracic duct (Hirano *et al.*, 1985; Maincent *et al.*, 1992; Oya *et al.*, 1993), would result in the niosomes emptying into the vascular space at the juncture of the left internal jugular vein and the subclavian vein (Guyton, 1981). This pathway could result in a greater targeting to the heart and lungs than either an intraperitoneally administered free drug dose or an intravenous niosome dose. However if this is the case, similar effects should be observed by DOX liposomes, but DOX PC-PG liposomes are actually less toxic by the intraperitoneal route than an equivalent dose of DOX solution by the same route (Mayhew *et al.*, 1990). Additionally the heart levels of DOX were actually similar for the free drug and the niosomal formulation (Table 4.4).

Although the heart is the most common target organ of DOX toxicity, histological examination of this organ in mice 6 h after dosing showed no evidence of a cardiac lesion in any of the animals treated. However 6 h may have been too early for a cardiac injury to have become apparent morphologically. A possible sequence of events to account for the observed changes may be that DOX caused cardiotoxicity, leading to a slow cardiac failure over a 24 h period with the accumulation of a pleural effusion and an associated pulmonary inflammation, but this seems unlikely as DOX levels in the heart tissue were similar in mice given either the free drug or the niosome preparation intraperitoneally (Table 2), and the animals dosed with the free compound showed no evidence of any of the toxic changes discussed above.

In conclusion, the administration of DOX niosomes by the intraperitoneal route showed that DOX niosomes were cleared more slowly from the peritoneal cavity than

the free drug and also yielded higher plasma levels than the free drug. DOX was also found to cause an inflammatory response in the lungs of male AKR mice. This lesion was postulated to be the result of biventricular cardiac failure or due to the result of a direct action of the formulation on the lung.

CHAPTER FIVE

NIOSOMAL DOXORUBICIN DISTRIBUTION, METABOLISM AND TUMORICIDAL ACTIVITY IN MICE

5.1 DOXORUBICIN DISTRIBUTION IN NIOSOMES AND THE USE OF TUMOUR MODELS

Niosomes offer an alternative to liposomes in the field of drug delivery (Florence *et al.*, 1990) and DOX containing $C_{16}G_3$ niosomes have been evaluated in various tumour models. Improved tumour localisation and tumoricidal activity of the cytotoxic was reported (Rogerson *et al.*, 1988; Kerr *et al.*, 1988). This chapter describes efforts to assess the tumoricidal activity of the various niosomal formulations, using a variety of murine tumour models. Murine tumour models although being readily accessible to the experimentalist are limited when it comes to the extrapolation of findings to the clinical situation. It is in this respect that problems of correct data interpretation abound (Martin *et al.*, 1986; Siemann, 1987; Denekamp, 1992). These tumour models thus serve as a convenient starting point for any tests on new drugs/ novel formulations and data generated from these studies should be viewed purely in this respect. Clinical data is hence the overriding objective to any therapeutic evaluation programme. Future efforts within the broad framework of a niosomal drug delivery initiative will thus focus keenly on this area.

Niosomal encapsulation of DOX resulted in altered drug pharmacokinetics. Heart levels were decreased (Kerr *et al.*, 1988; Florence *et al.*, 1990) and blood levels increased (Kerr *et al.*, 1988; Rogerson *et al.*, 1988; Florence *et al.*, 1990). Numerous studies have examined the effect of novel drug delivery systems on drug pharmacokinetics but few reports deal with the impact of drug encapsulation on the level of metabolic activity. Altered metabolite formation from a quantitative and/or qualitative point of view may seriously interfere with the goal of novel drug delivery

therapeutics. The use of a microencapsualted digoxin formulation designed to avoid gastric hydrolysis resulted in increased reductive inactivation of the drug (Magnusson *et al.*, 1984). The encapsulation of DOX in niosomes, subsequent to increased plasma levels has been found to result in increased reductive glycosidic cleavage, giving rise to elevated liver level time curves for the DEOXONE and 7-deoxydoxorubicinol metabolites (Rogerson *et al.*, 1988; Kerr *et al.*, 1988). However when DOX is administered in solution in escalating doses, the dose-standardized level of DEOXONE appears to fall at elevated doses, between 10 and 40 min after dosing. This dose dependence is not observed over a 48 h period. This suggests that the rate of synthesis of this aglycone is reduced at high doses although the elimination kinetics are non capacity-limited (Preiss *et al.*, 1989). Unlike the present work, the increased levels of DEOXONE previously found on niosomal administration (Rogerson *et al.*, 1988; Kerr *et al.*, 1988), were not assessed in relation to the increased liver/ plasma levels of the parent drug, making an interpretation of the significance of this finding rather difficult. The altered biodistribution of DOX on niosomal encapsulation is reported in this chapter as is the changed metabolic profile.

DOX metabolites were found to be associated with Span 60 niosomes *in vivo*. A niosome metabolite formulation was thus prepared and the release of DOX metabolites from these particles in the presence of plasma was studied, with a view to examining the binding of the various metabolites to a niosome plasma protein mixture.

5.2 MATERIALS

Material sources are given in Table 5.1 and as stated in earlier chapters

METHODS

5.3: METABOLISM AND BIODISTRIBUTION OF DOXORUBICIN IN SPAN 60 NIOSOMES

5.3:1 PHARMACOKINETIC STUDY ON TUMOUR BEARING ANIMALS

Niosomes were prepared by the remote loading method (method 2, Chapter 2). Lipid composition was Span 60, cholesterol, Solulan C24 (45: 45: 10). Initial DOX/lipid ratio was 0.043. The separation of unentrapped material and DOX assay were carried out as previously described.

Female NMRI mice (mean weight 24 g) were implanted subcutaneously a MAC 15A tumour. The day of implantation was taken as day 0. On day 9 mice were administered intravenously with DOX niosomes or DOX solution (0.75 mg mL^{-1}) at a dose of 10 mg kg^{-1} (dose volume calculated on the basis of individual body weight had a mean value of 0.3 mL). At various time points (0, 10 min, 30 min, 1 h, 2 h, 4 h, 8 h, 24 h) 4 mice from each group were killed by halothane overdose and blood collected as described. Plasma was separated from other blood components by centrifugation (500 g X 10 min) and divided into 2 portions. Half the fresh plasma was fractionated over Sepharose 2B as described below and half was stored at -44°C. The liver, heart, tumour and lung tissue were also removed and stored at -44°C until analysis could be performed. In certain cases, where for technical reasons, plasma

Table 5.1: Materials used in the study on the biodistribution and metabolism of DOX contained in Span 60 niosomes

MATERIAL	SOURCE
BALB/c mice	Bantam and Kingman, UK.
7-deoxydoxorubicinone	Donated by Mr P. Launchbury and Dr A. Suarato, Farmitalia Carlo Erba, Italy.
Dimethylformamide (DMF)	BDH Laboratory Supplies, UK.
Doxorubicinol hydrochloride	Donated by Mr Paul Launchbury and Dr A. Suarato, Farmitalia Carlo Erba, Italy.
Doxorubicinolone	Donated by Mr P. Launchbury and Dr A. Suarato, Farmitalia Carlo Erba, Italy.
Doxorubicinone	Donated by Mr P. Launchbury and Dr A. Suarato, Farmitalia Carlo Erba, Italy.
Male nude athymic mice	Donated by Dr Lloyd Kelland, Institute for Cancer Research, Royal Marsden Hospital, Sutton, UK.
NMRI mice	Donated by Professor John Double, Clinical Oncology Unit, University of Bradford, UK.

samples could not be fractionated straight away, they were stored at 4°C for short periods only (not exceeding 2 h).

5.3:2 SEPARATION OF NIOSOME ASSOCIATED AND UNENCAPSULATED DOXORUBICIN IN PLASMA SAMPLES

Male BALB/c mice of mean weight 30.0 g were injected intravenously (IV) with either 5 mg kg^{-1} DOX loaded Span 60 niosomes, 20 mg kg^{-1} DOX solution, or received no drug at all (the latter served as controls). At 0 min (controls) 90 min and 4 h two mice were killed from each group by halothane overdose and blood collected by cardiac puncture following a thoracotomy incision into lithium heparin tubes. Plasma was immediately separated by centrifugation at 500 g. Fresh plasma, so obtained, was fractionated over an 82 mm X 5 mm Sepharose 2B column eluted with TBS (pH 7.4), 25 0.27 ml fractions were collected.

Plasma samples (50-100 µL) originating from tumour bearing animals used in the pharmacokinetic study were passed over an 82 mm X 5 mm Sepharose 2B column. The column was eluted with TBS (pH 7.4). Two fractions were collected, the void volume 1.8 mL (of which the first 0.5 mL were discarded) and a subsequent 3 mL fraction.

5.3:3 HPLC ANALYSIS

HPLC analysis was as previously described (Chapter 4 and Cummings, 1984; Cummings and McArdle, 1986). Extract residues however were reconstituted in 150 µL of mobile phase (5 mM phosphoric acid 500: isopropanol 185), containing 0.4 µg mL^{-1} epirubicin as internal standard. Samples originating from animals which had

been administered with DOX solution were reconstituted in 50 µL of mobile phase. Cloudy dispersions were clarified by filtration through a 0.22 µm filter before HPLC analysis.

5.3:4 ASSAY FOR PLASMA PROTEINS

Plasma obtained from mice which had not been administered with DOX (control mice) (50 µL) was passed over an 82 X 5 mm Sepharose 2B column eluted with TBS (pH 7.4). 25 0.27 mL fractions were collected and each assayed for total protein by the Lowry method (Lowry, 1951).

5.3:5 PHARMACOKINETIC CALCULATIONS

The plasma level time data for the niosome associated and unencapsulated DOX were treated, for the purposes of simplicity, as independent pharmacokinetic events. Non-compartmental methods were used for the calculation of all pharmacokinetic parameters (Gibaldi, 1990). AUC^{0-24} was calculated by the linear trapezoidal rule, while $AUC^{24-\infty}$ was calculated by dividing the 24 h concentration time point by the terminal elimination rate constant (Cp_{24h}/β). Volume of distribution was calculated using the equation given below

$$Vd = \text{dose X } AUMC/(AUC)^2 \qquad (1)$$

where AUMC is the area under the first moment curve with units of $mass.time^2$ mL^{-1}.

5.3:6 STATISTICS

The students t-test was used.

5.4: THE *IN VITRO* RELEASE OF SPAN 60 NIOSOME ASSOCIATED DOX METABOLITES IN THE PRESENCE OF PLASMA

5.4:1 PREPARATION OF DOX METABOLITE SPAN 60 NIOSOMES

150 μmol total lipid in the molar ratio, Span 60, cholesterol and Solulan C24 (45: 45: 10) were dissolved in 10 mL of chloroform. To this solution was added 1 mL of a DMF solution of the following DOX metabolites: DOXONE (2.06 mg mL^{-1}), DXOLONE (0.76 mg mL^{-1}) and DEOXONE (0.36 mg mL^{-1}). The solvent was removed by rotary evaporation at 60°C and the resulting film hydrated with 3 mL DXOL (0.11 mg mL^{-1}) in TBS (pH 7.4) at 70°C for 1 h. The multilamellar dispersion was sonicated in the usual way and unentrapped material separated by gel filtration, Niosomes were sized by PCS as previously described.

5.4:2 ASSAY OF DOX METABOLITE LOADED VESICLES

100 μL of the DOX metabolite loaded vesicles were added to 1 mL of isopropanol and the resulting solution made up to 10 mL with a mixture of isopropanol-5 mM orthophosphoric acid (270: 500). To 200 μL of this solution was added 40 μL of epirubicin (3.6 μg mL^{-1}) dissolved in the same isopropanol-5mM orthophosphoric acid solvent mixture, as internal standard. This resulting solution was clarified by filtration through a 0.45 μm filter and analyzed by HPLC. Calibration plots were prepared from dilutions of the metabolites (nominally 10 ng mL^{-1} - 1600 ng mL^{-1}) in isopropanol-5 mM orthophosphoric acid mixtures (270: 500), plus the internal standard epirubicin. DOX metabolite solutions were then assayed by HPLC as previously described.

5.4:3 THE *IN VITRO* RELEASE OF DOX METABOLITES FROM SPAN 60 NIOSOMES IN THE PRESENCE OF PLASMA

0.4 mL of the DOX metabolite dispersion described above and 0.4 mL of fresh mouse plasma (obtained from female BALB\c mice by cardiac puncture and centrifugation to separate plasma from other blood components) were placed in 60 mm of dialysis tubing (Visking 20/32), with the ends secured 10 mm from each end by dialysis clips. This dialysis tubing was placed in 20 mL PBS (pH 7.4), contained in screw capped bottles, which were in turn set up in a shaking water bath with the temperature set at 37°C. At various time intervals 100 µL aliquots were withdrawn from the liquid external to the dialysis bag. To these aliquots were added 20 µL of a solution of epirubicin (3.6 µg mL^{-1}) in the mobile phase - isopropanol-orthophosphoric acid, as internal standard. These samples were then analysed by HPLC. Results are expressed as a percentage of the initial metabolite mass released with time.

5.5 THE EVALUATION OF THE TUMORICIDAL ACTIVITY OF DOX NIOSOMES

5.5:1 PREPARATION OF $C_{16}G_2$ AND SPAN 60 NIOSOMES

DOX $C_{16}G_2$ niosomes were prepared according to the method utilizing proton gradients (method 1 - Chapter 2). Lipid composition was $C_{16}G_2$, cholesterol, Solulan C24 (45: 45: 10) and DOX/lipid molar ratio was 0.07. They were then assayed and sized in the usual way.

Span 60 niosomes were prepared also according to the method of transmembrane proton gradients (method 2 - Chapter 2). Lipid composition was Span 60, cholesterol,

Solulan C24 (45: 45: 10). Initial DOX/lipid ratio was 0.018. Niosomes were sized and assayed in the usual way. Control niosomes containing TBS alone were also prepared as described previously.

5.5:2 EVALUATION AGAINST A HUMAN TUMOUR XENOGRAFT

Male nude athymic mice (mean weight 22 g) were implanted with a human ovarian carcinoma xenograft (PXN/ 109/ TC) Four weeks later or when tumour mass became palpable, groups of five mice were injected intravenously with 8 mg kg^{-1} DOX Span 60 niosomes. Control mice were injected (0.1 mL) either with DOX solution, TBS, empty niosomes or received no treatment at all. At regular intervals the tumour mass was measured and the animals weighed. 28 days after drug administration mice were killed, and the tumours excised and weighed. Tumoricidal activity was expressed as terminal mean tumour weight.

5.5:3 EVALUATION AGAINST MOUSE ADENOCARCINOMAS (MAC)

Male NMRI mice (n = 7, mean weight 23 g) bearing a MAC 13 solid tumour implanted subcutaneously were injected 2 days after tumour implantation with either 2.5, 5.0 or 10.0 mg kg^{-1} DOX $C_{16}G_2$ niosomes, empty niosomes, TBS or 10 mg kg^{-1} DOX solution (dose volume, 0.1 mL). On day 26 animals were killed and tumours excised and weighed. Tumoricidal activity was assessed from the terminal tumour weight.

A similar experiment was performed using male NMRI mice (n = 5, mean weight 23 g) bearing a subcutaneously transplanted MAC 15A tumour. DOX $C_{16}G_2$ niosomes

and solution (3.9 mg kg^{-1}) and the usual controls were administered intravenously and tumoricidal activity assessed on day 14 in the usual way. Intravenously administered DOX Span 60 niosomes (2.5, 5.0 & 10.0 mg kg^{-1}) were also evaluated in the same tumour model.

5.5:4 STATISTICAL ANALYSIS

Tumoricidal indices were analysed using one way analysis of variance (ANOVA).

RESULTS AND DISCUSSION

5.6 METABOLISM AND DISTRIBUTION OF DOX IN SPAN 60 NIOSOMES

5.6:1 CHARACTERISTICS OF SPAN 60 NIOSOMES.

Span 60 niosomes used in this study had a mean diameter of 235 nm. Encapsulation efficiency was 35% and the final DOX to lipid (surfactant + cholesterol) molar ratio was 0.015. Initial weights of surfactant and cholesterol were used to compute this value. The encapsulation efficiency of the remote loading procedure, utilising a pH gradient, was 0.047 mol DOX.mol $lipid^{-1}$ when phospholipid vesicles were prepared (Montero *et al.*, 1993). These liposomes were of comparable size to the niosomes used in this work. The lower amount of DOX encapsulated in the Span 60 niosomes prepared in this study was due to the fact that less DOX was used initially. Initial DOX/lipid ratio used in this study was 0.043.

5.6:2 SEPARATION OF NIOSOME ASSOCIATED AND UNENCAPSULATED DOX IN PLASMA SAMPLES.

Plasma samples fractionated by passage over Sepharose 2B columns show that the

separation of encapsulated and unencapsulated DOX was achieved by this method (Figure 5.1). Niosomes eluted in the void volume (elution volume 1.4 mL), while unencapsulated DOX eluted later (elution volume 3.4 mL). However while the biological samples from animals administered DOX niosomes showed DOX eluting in the void volume, samples from animals given DOX solution co-eluted with plasma proteins (Figure 5.1).

The plasma samples taken from mice at the 4h time point in the experiment performed to validate the separation procedure, on fractionation, yielded fractions that were beyond the limit of detection in the assay for DOX. The separation method failed to distinguish between plasma protein bound and free DOX.

The therapeutic effect of drug delivery systems is usually a function of the amount of unencapsulated drug available at the diseased site (Hwang, 1987), although this is not always true if extravasation of particulate material occurs followed by cellular uptake. It is essential to quantify the proportion of vesicular drug delivery systems that is actually available in molecular form in vivo. Free doxorubicin is largely plasma protein bound (Speth *et al.*, 1988) (Figure 5.1). Plasma protein bound drug is in dynamic equilibrium with the free drug (Gibaldi, 1991) and can thus be considered to be available in molecular form. Following the administration of DOX niosomes we have been able to quantify the proportion of plasma DOX that had leaked out of the nisosomes *in vivo* and is thus available in molecular form. Our method of separation unlike similar methods (Druckmann *et al.*, 1989; Thies *et al.*, 1990), allows direct quantification of unencapsulated DOX and its metabolites. Although the method of

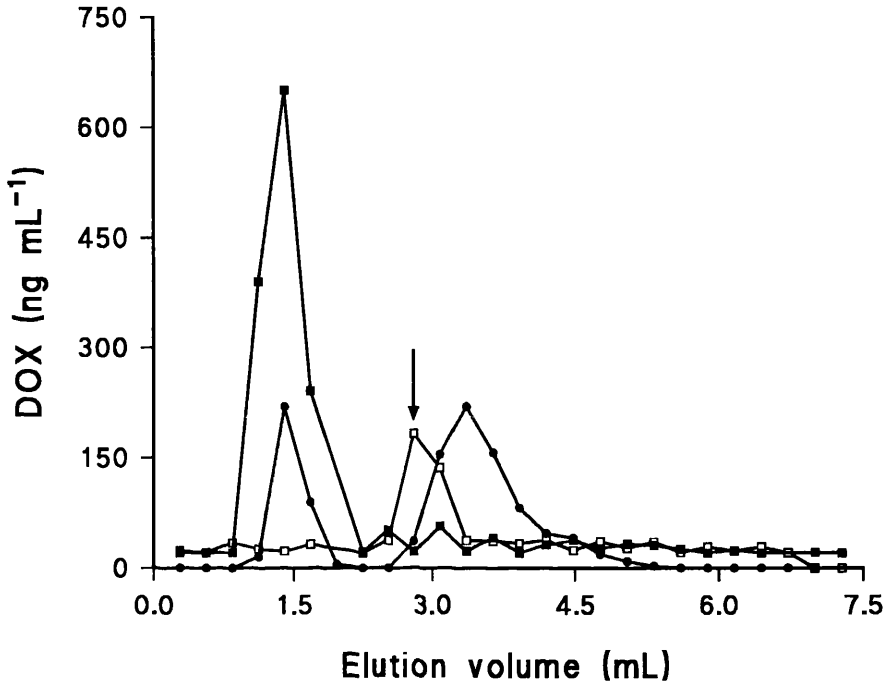

Figure 5.1: Elution profile for various *in vivo* and *in vitro* samples fractionated over an 82 mm X 5 mm Sepharose 2B column. ■ = mouse plasma 90 min after intravenous injection of 5 mg kg^{-1} DOX Span 60 niosomes. □ = mouse plasma 90 min after the intravenous injection of 20 mg kg^{-1} DOX solution, ● = DOX solution + DOX niosomes. Arrow = plasma protein peak. Plasma proteins elute as a coloured distinct band.

Table 5.2: The recovery of DOX and DOX metabolites from Sepharose 2B columns

SAMPLE DESCRIPTION	SAMPLE VOLUME (μL)	SAMPLE CONCENTRATION (μg mL^{-1})	PERCENTAGE RECOVERY
DOX Span 60, cholesterol, Solulan C24 (45: 45: 10) niosomes	100	110	89.5
DOX solution	100	50.0	87.7
DXOL Span 60, cholesterol, Solulan C24 (45: 45: 10) niosomes	100	4.20	66.7
DXOLONE Span 60, cholesterol, Solulan C24 (45: 45: 10) niosomes	100	28.7	79.3
DOXONE Span 60, cholesterol, Solulan C24 (45: 45: 10) niosomes	100	137	79.4
DEOXONE Span 60, cholesterol, Solulan C24 (45: 45: 10) niosomes	100	24.1	83.4

Thies and associates (1990) which utilizes a weak cationic exchanger in association with alcoholic extraction, allows for the separation and quantification of free drug, it is unable to allow for quantification of DOX aglycone metabolites.

5.6:3 PHARMACOKINETIC STUDIES

The area under the plasma level time curve calculated for the study period $AUC^{0.17-24}$ for DOX niosomes was increased 6 fold by niosomal encapsulation (Figure 5.2) - 10.3 and 66.0 μg.h mL^{-1} respectively. Most of the plasma DOX (90%) was still niosome associated, 4 h after dosing and 50% was niosome associated 24 h after dosing (Figures 5.3 and 5.4), indicating hitherto unknown in vivo stability for DOX niosomes.

The various other plasma pharmacokinetic parameters are given in Table 5.3. The clearance and volume of distribution of DOX was decreased quite substantially by niosomal encapsulation, evidence that DOX niosomes are confined to a large extent to the vascular space. The large volume of distribution given for DOX that had exited from niosomes was indicative of the fact that most of the dose was still entrapped in niosomes for a significant portion of the study period. Clearance of DOX that had exited from niosomes was, as expected, similar to that observed for administration of DOX solution.

DOX delivery to the liver was doubled on niosomal encapsulation (Figure 5.5) while delivery of DOX to tumour tissue was increased by 50% (Figure 5.6). DOX delivery to the heart (Figure 5.7), was statistically indistinguishable regardless of the formulation used (students t-test, $p > 0.05$). Lung levels of DOX were increased on

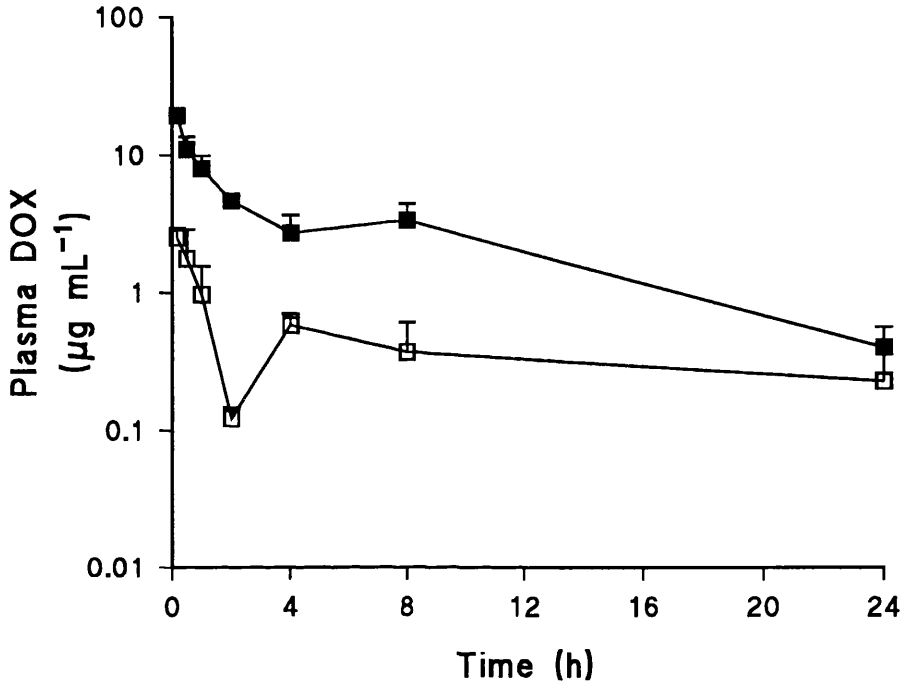

Figure 5.2: Mean plasma DOX (± s.e.) after the intravenous injection of Span 60 niosomes to female NMRI tumour bearing mice. ■ = intravenous 10 mg kg^{-1} DOX Span 60 niosomes, □ = intravenous 10 mg kg^{-1} DOX solution.

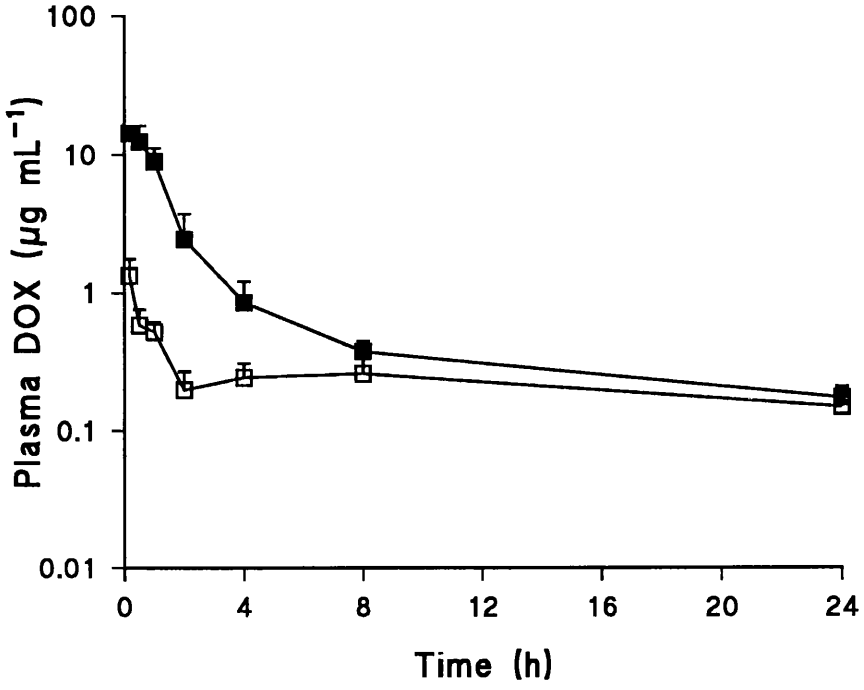

Figure 5.3: Mean plasma DOX (± s.e.) after the intravenous injection of 10 mg kg^{-1} DOX Span 60 niosomes to female NMRI tumour bearing mice. ■ = niosome associated DOX, □ = unencapsulated DOX that had leaked out of the niosomes *in vivo*.

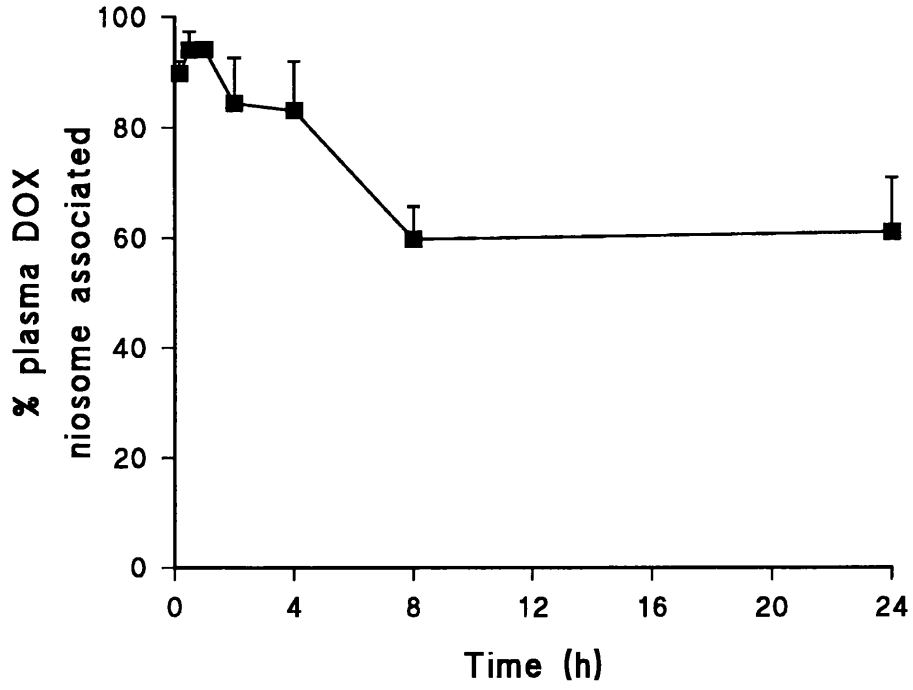

Figure 5.4: Mean percentage of plasma DOX (± s.e.) still encapsulated in niosomes after the intravenous injection of 10 mg kg^{-1} DOX Span 60 niosomes to female NMRI tumour bearing mice.

niosomal encapsulation (Figure 5.8).

It is because the circulating niosomes retain 90% of their payload up to 4h after dosing and 50% 24 h after dosing (Figure 5.4) that the AUC for niosomal DOX is six times that of DOX solution (Figure 5.2). Similar studies with phospholipid vesicles show varying levels of liposome associated DOX depending on the rigidity of the liposome membrane, with phosphatidylcholine and phosphoglycerol vesicles showing 50 - 90% of the drug being vesicular associated with vesicles up to 2 h after dosing (Gabizon *et al.*, 1991) and for the more rigid hydrogenated phosphatidylcholine vesicles 57% of plasma DOX 72 h after dosing (Gabizon *et al.*, 1989).

Examination of the niosome associated DOX curve reveals (Figure 5.3) that in the first hour after dosing, there is a comparatively slow removal of niosome associated DOX. As 90% of plasma DOX is niosome associated during this time, it can be assumed that any change in the concentration of niosome associated DOX is not due to drug leakage but due to the actual removal of intact niosome associated DOX. 40% of the dose is present in the liver 10 min after dosing, suggesting that the liver is the main organ of niosome uptake. [Vesicle dose depletion *in vivo* is primarily a function of splenic and liver uptake (Gregoriadis and Ryman, 1972; Azmin *et al.*1985: Hwang, 1987)]. After the first 1 h plasma clearance of niosome associated DOX is substantially faster than the earlier time points, perhaps due to initial saturation of the uptake processes in the liver, by the high plasma level of niosome associated DOX. The liver data (Figure 5.5), appears to corroborate this view as in the first 1 h after dosing, the liver levels of DOX fall steeply, from an initial high level. Between 2 h

and 8 h, the clearance of doxorubicin niosomes from the plasma slows somewhat, and liver levels of the drug also rise slightly. In the terminal phase the niosomes are cleared by a combination of the uptake processes, the progressive degradation of the niosomes and the release of their contents.

It appears that in the first 8 h after dosing, there are at least two kinetically distinct processes in operation. i) A fast phase operating predominantly in the early part of the curve, which is initially saturated and becomes more efficient after the plasma level of niosome associated DOX falls and ii) a slow uptake process. It is possible that during the phase of the curve when the fast uptake processes are saturated, this slow phase is also saturated. Evidence for a saturable non-Michaelis Menton like uptake process in the liver for phospholipid vesicles has been reported (Kume *et al.*, 1992) and the existence of 2 kinetically distinct uptake processes in the liver has been proposed (Hwang, 1987; Harashima *et al.*, 1992), one of which is thought to be an efflux model (Harashima *et al.*, 1993). From our data it is not possible to verify the existence of an efflux model. The heterogenous nature of the vesicular dispersion in terms of vesicular diameter could be responsible for the existence of a slow and fast uptake mechanism, with the two different mechanisms showing size specificity (Hwang, 1987).

A second dose of DOX niosomes given 24 h after the first should result in even higher blood levels than the first dose as saturation of the uptake mechanisms will be achieved faster when a residual dose of DOX niosomes is present. Toxicity will also be minimized as during the first 4 h most of the drug is associated with the niosomes.

The released DOX (Figure 5.3), shows typical biexponential clearance kinetics. In the terminal elimination phase, the curve plateaus, due to the input from degraded DOX niosomes.

The presence of a polyoxyethylene moiety (Solulan C24 - MW = 1443), within the membrane failed to divert the niosomes away from the liver. Polyoxyethylene (polyethylene glycol, PEG - MW = 1000-5000) within phospholipid vesicles results in less vesicular uptake by the liver and spleen (Woodle and Lasic, 1992; Woodle *et al.*, 1992) and consequently extended plasma circulation times (Blume and Cevc, 1990; Maruyama *et al.*, 1991). The net result is an increased delivery of drug to the neoplasm (Papahadjopoulos *et al.*, 1991). The reduced uptake by the liver and spleen is attributable to a steric hinderance by the polyoxyethylene surface to opsonization processes within the plasma (Lasic *et al.*, 1991).

Tissue/plasma ratios for the various tissues studied are shown in Figure 5.9. The tissue/plasma ratio plot shows a shallow rise for the heart tissue after the administration of niosomes (Figure 5.9a) than the corresponding ratios for the tumour and liver tissue. With doxorubicin solution, no similar distinction can be made between tissues (Figure 5.9b).

The depot nature of Span 60 niosomes is shown both by the persistence of niosome associated DOX at 24 h and also the tissue/plasma ratios. While for DOX solution (Figure 5.9b), equilibrium is reached between plasma levels and tissue levels within

8 h, equilibrium is not reached in the tissues (Figure 5.9a) with DOX niosomes at 24 h. The tissue/plasma ratios for the liver and tumour show a steep rise in the presence of DOX niosomes, while corresponding values for the heart give a less steep rise. The liver and tumour tissue thus offer more efficient drug uptake in the presence of DOX niosomes than heart tissue. While it is known that the liver takes up vesicles by the phagocytic processes of the RES (Hwang, 1987), and some evidence exists of particulate tumour extravasation (Huang, 1992), it is possible that the similar overall uptake kinetics recognized between the liver and tumour tissue, in this work, could be indicative of the uptake of intact DOX Span 60 niosomes. Tumour tissue by virtue of its leaky capillary network (Gerlowski and Jain, 1986), may be able to accumulate DOX niosomes in its extravascular regions. However more evidence is needed before firm conclusions on niosome extravasation can be drawn. Heart tissue, by virtue of its tight endothelial junctions would probably not be a site for niosome extravasation.

With DOX niosomes there was increased drug delivery to the tumour (Figure 5.6) and ultimately increased tumoricidal activity (discussed in this chapter). The more rapid equilibration of the heart tissue with the formulation resulted in an improved AUC tumour to heart ratio (increased from 0.27 to 0.36), while the ratio of peak tissue concentration increased from 0.6 to 1.3. Similar improvements in the heart to tumour drug delivery ratio have been reported for other DOX niosomes (Florence *et al.*, 1990) and DOX phospholipid vesicles (Papahadjopoulos *et al.*, 1991; Gabizon, 1992; Unezaki *et al.*, 1993;).

Data presented above show that the doxorubicin niosomal uptake processes of the liver

Table 5.3: Pharmacokinetic parameters for doxorubicin solution and doxorubicin Span 60 niosomes

DOXORUBICIN FORMULATION	VOLUME OF DISTRIBUTION (mL)	CLEARANCE (mL min^{-1})*
Total doxorubicin niosomes (encapsulated + unencapsulated)	13.6	4.2
niosome associated doxorubicin	16.2	8.1
unencapsulated doxorubicin exited from niosomes	175.5	20.7
doxorubicin solution	66.4	18.2

*for a 30 g mouse

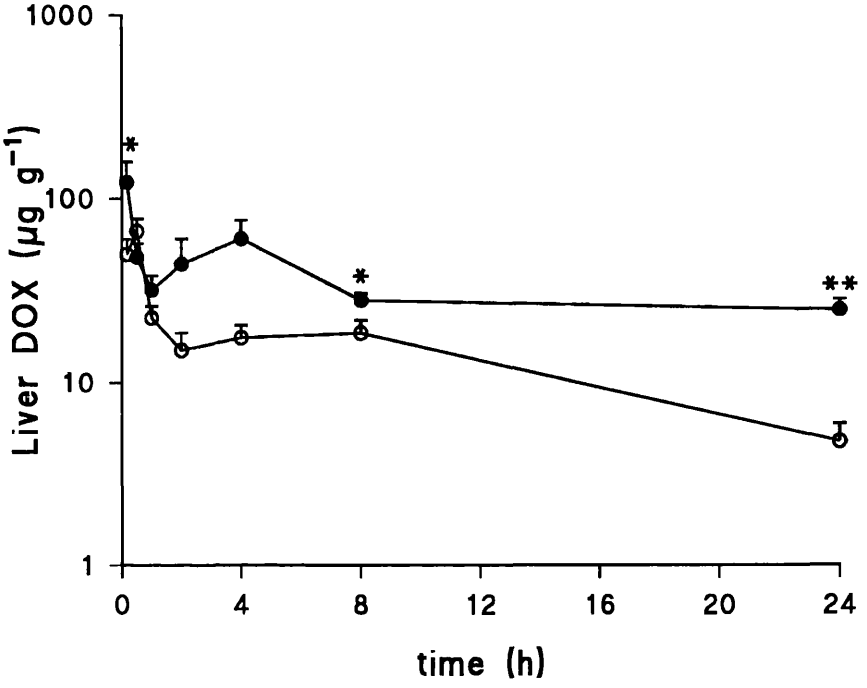

Figure 5.5: Mean liver levels of DOX (± s.e.) after the intravenous injection of DOX Span 60 niosomes to female NMRI tumour bearing mice. ● = 10 mg kg^{-1} DOX Span 60 niosomes, O = 10 mg kg^{-1} DOX solution. * = statistical significance ($p<0.05$), ** = statistical significance ($p<0.01$).

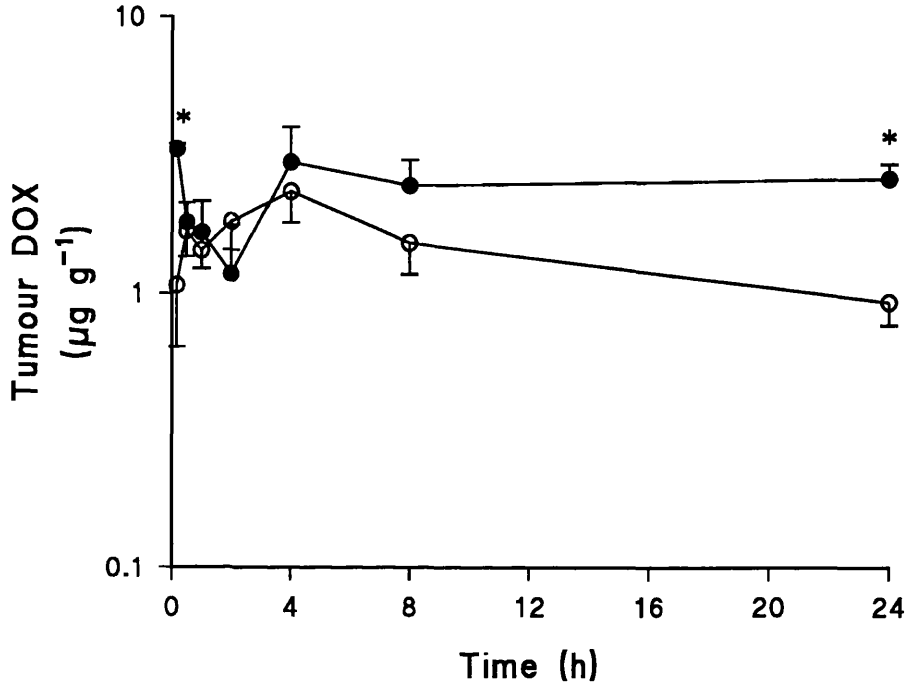

Figure 5.6: Mean tumour DOX levels (± s.e.) after the intravenous injection of DOX Span 60 niosomes to female NMRI tumour bearing mice. Symbols as in Figure 5.5.

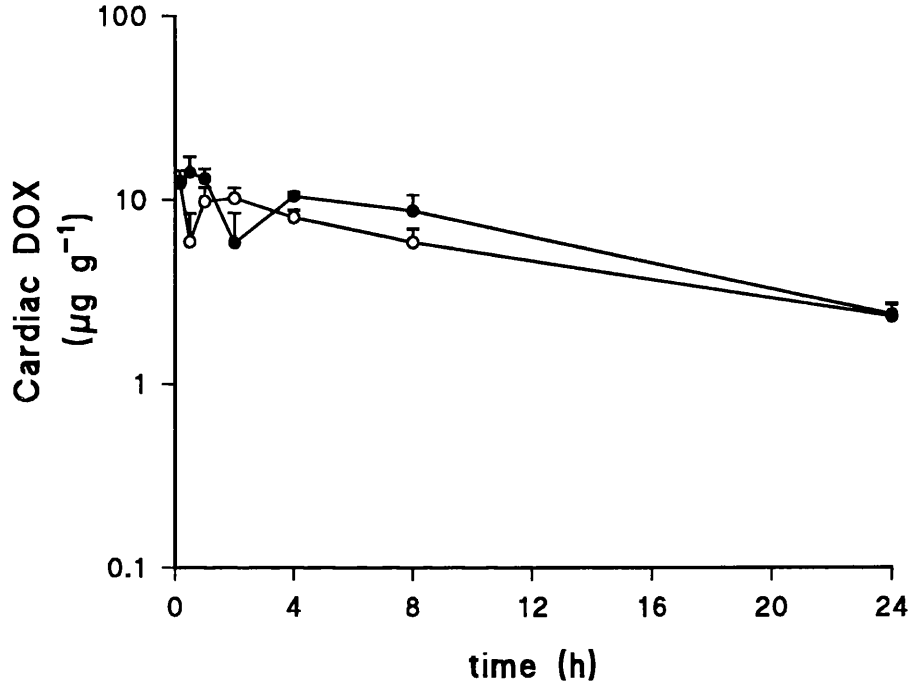

Figure 5.7: Mean cardiac DOX levels (± s.e.) after the intravenous injection of DOX Span 60 niosomes to female NMRI tumour bearing mice. Symbols as in Figure 5.5.

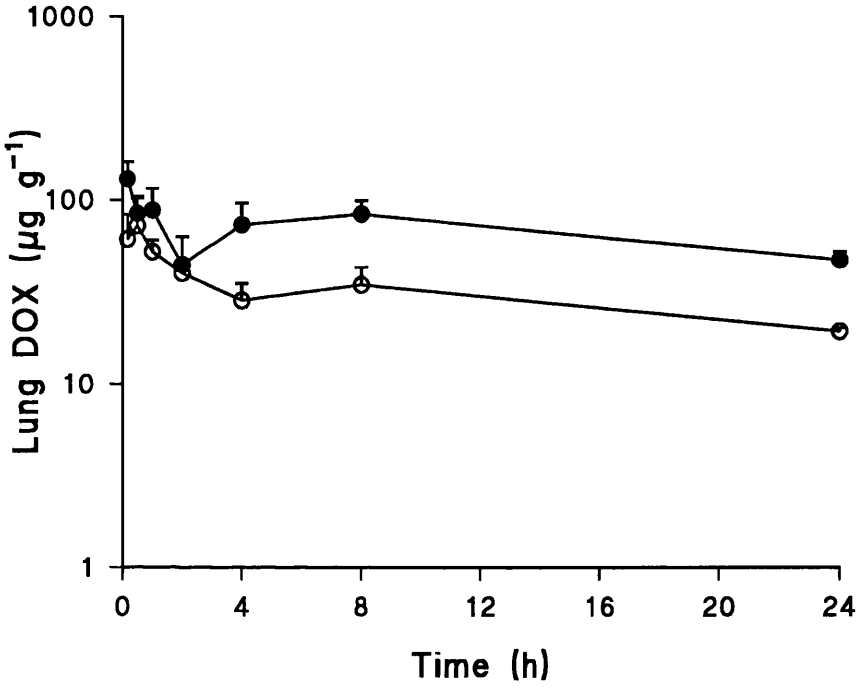

Figure 5.8: Mean lung levels of DOX (± s.e.) after the intravenous injection of DOX Span 60 niosomes to female NMRI tumour bearing mice. Symbols as in Figure 5.5.

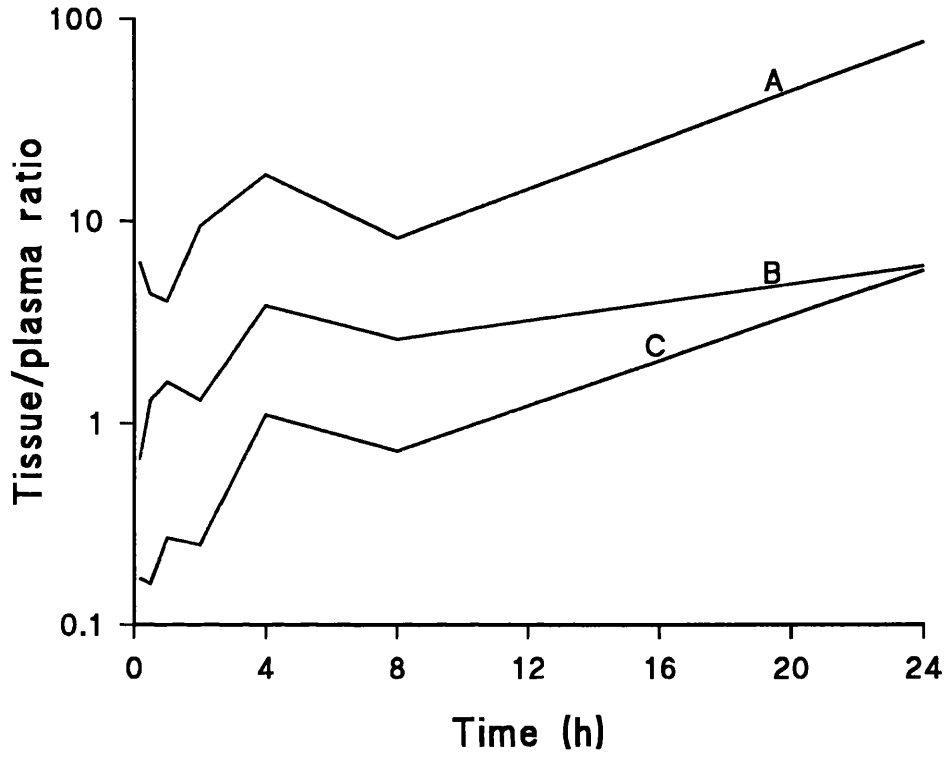

Figure 5.9a: Tissue/plasma ratio - time plots after the intravenous injection of 10 mg kg^{-1} DOX Span 60 niosomes to female NMRI tumour bearing mice. A = liver, B = heart, C = tumour.

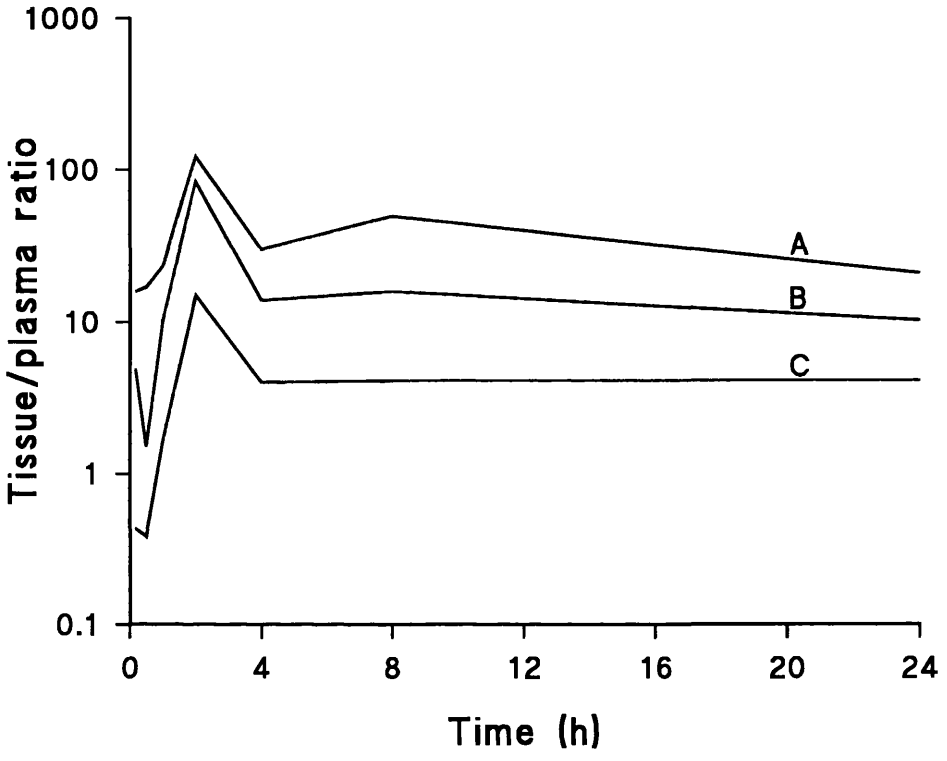

Figure 5.9b: Tissue/plasma ratio - time plots after the intravenous administration of 10 mg kg^{-1} DOX solution. A = liver, B = heart, C = tumour.

are defined by at least two uptake processes and that doxorubicin niosomes exist as a depot in the plasma. The niosomal formulation allows more tumour uptake without a similar increase in drug delivery to the heart.

5.6:4 THE *IN VITRO* RELEASE OF DOXORUBICIN METABOLITES FROM SPAN 60 NIOSOMES IN THE PRESENCE OF PLASMA AND THE ALTERED *IN VIVO* METABOLISM OF DOXORUBICIN WHEN ENCAPSULATED IN SPAN 60 NIOSOMES

Table 5.4 details the essential characteristics of the niosomes used to study the release of DOX metabolites from DOX niosomes in the presence of plasma. Higher percentages of the more lipophilic aglycones DEOXONE, DOXONE and DXOLONE were encapsulated in Span 60 niosomes than the less lipophilic alcohol glycoside metabolite DXOL.

When the availability of DOX metabolites encapsulated in Span 60 niosomes was assessed in the presence of plasma, it was found that the kinetics of the release of DOX metabolites from a mixture of niosomes and plasma proteins was a reflection of the different solubilities of these compounds (Figure 5.10). The more hydrophobic compounds tended to prefer to associate with the niosomes and plasma proteins and were also generally poorly released into the aqueous environment. The reduced alcohol glycoside metabolite DXOL was released faster than the aglycones. Among the aglycones, the alcoholic aglycone DXOLONE was released faster than the keto derivatives DOXONE and DEOXONE. Any drug/ metabolites bound to plasma proteins would be in dynamic equilibrium with the aqueous milieu but would only be released to the aqueous solvent in response to the aqueous solubilities of these compounds. DOX metabolites with poor aqueous solubility released from niosomes

would preferably bind to plasma proteins. Information obtained from this study shows that the more hydrophobic aglycones prefer to associate with the niosomes and plasma proteins. Future studies will focus on the relative partitioning of these compounds between niosomes and plasma proteins.

In the *in vivo,* studies metabolites were detected and quantified in both the plasma niosomal fraction and the released drug fraction (Table 5.4). The AUC's of the various metabolites were higher in the niosomal fraction than in the released drug fraction. The ratio $AUC_{(DXOL)}/AUC_{(DOX)}$ was similar for the niosomal fraction than in the released drug fraction However in the case of the aglycones DOXONE and DEOXONE, the ratios of $AUC_{(DOXONE)}/AUC_{(DOX)}$ and $AUC_{(DEOXONE)}/AUC_{(DOX)}$ were increased three fold in the released compared to the niosomal fraction. This association of metabolites and niosomes could have arisen due to the adsorption of the metabolites, formed outside the vesicles to the vesicle surface or to the degradation of doxorubicin contained within the vesicle bilayer (Figure 2.6).

Liver and lung metabolites from both formulations were also quantified (Table 5.4). In the liver the encapsulation of doxorubicin resulted in higher $AUC_{(metabolite)}$ values for all the metabolites quantified. However when the relevant AUC ratios were calculated the ratio for DOXONE was actually slightly less with the niosome administered animals than with the animals administered DOX solution (Table 5.4).

The lower $AUC_{(aglycone\ metabolite)}/AUC_{(doxorubicin)}$ levels in the niosome fraction, ensures that

Table 5.4: The encapsulation of DOX metabolites in Span 60, cholesterol, Solulan C24 (45: 45: 10) niosomes.

Metabolite	Initial metabolite/lipid molar ratio	% of metabolite actually incorporated into the niosomes
DXOL	0.00037	10.06
DXOLONE	0.0033	29.40
DOXONE	0.016	51.95
DEOXONE	0.0029	52.26

although increased metabolic degradation occurs with the niosome formulation (Table 5.4), a lower proportion of the niosome payload consists of the inactive (Cummings *et al.* 1992b) aglycone metabolite 7-DEOXONE, while the proportion of the cytotoxic metabolite DXOL remains the same for both fractions. This ensures that the long circulating fraction delivers more of the active parent drug and the active metabolite DXOL and less of the inactive 7-DEOXONE to the tissues, principally tumour tissue. Using the lung as a model tissue(Table 5.5)it can be seen that despite the fact that the niosome administered animals had higher DOX tissue levels (AUC = 1632.22 μg.h mL^{-1} after DOX niosomes and 727.58 μg.h mL^{-1} after DOX solution) the level of the inactive aglycone 7-DEOXONE is actually reduced in the animals administered with DOX niosomes (1.37 and 0.76 μg.h mL^{-1} respectively), while the level of the active metabolite DXOL remains proportionally increased for the animals administered with DOX niosomes. Figure 5.11a is a schematic representation of the delivery of the inactive aglycone (7-DEOXONE) to tissues such as the lung. Figure 5.11b, on the other hand is a similar representation of the proportional increase in the level of the active metabolite DXOL to tissues such as the lung.

Despite the fact that the synthesis of 7-DEOXONE is increased in the liver on administration of the vesicular formulation and its formation *in vitro* is accompanied by free radical generation (Bachur *et al.*, 1977), this reaction has been ruled out as the mechanism of DOX cytotoxicity (Cummings *et al.*, 1991) and the synthesis of 7-DEOXONE *in vivo* is considered to be a deactivating transformation.

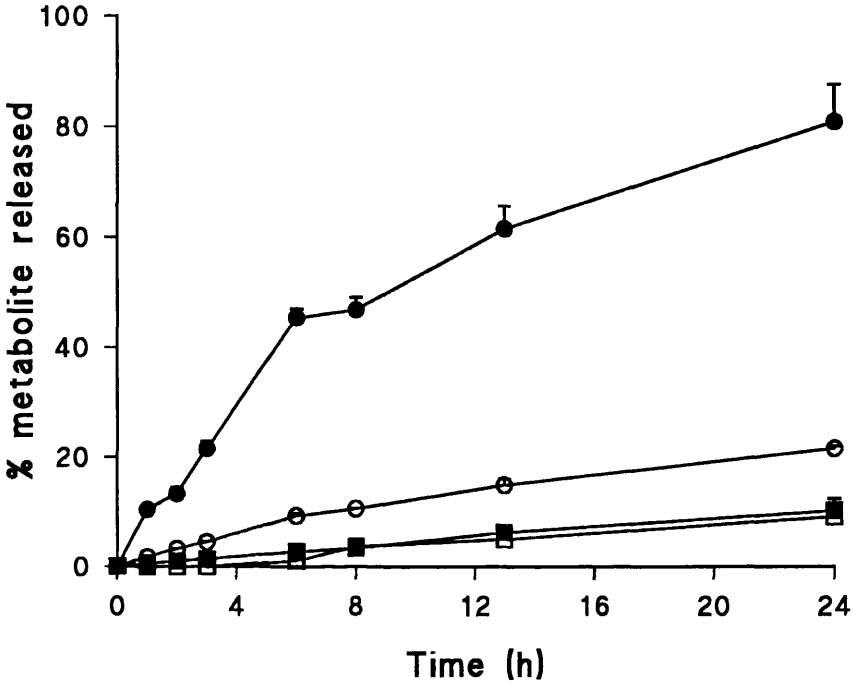

Figure 5.10: The release of DOX metabolites *in vitro* at 36°C from a mixture of Span 60, cholesterol, Solulan C24 (45: 45: 10) niosomes and plasma. ● = DXOL, O = DXOLONE, ■ = DOXONE, □ = DEOXONE.

Table 5.5: AUCs and $AUC_{(metabolite)}/AUC_{(DOX)}$ in the plasma, liver and lung after the administration of doxorubicin Span 60 niosomes

DOXORUBICIN METABOLITE/TISSUE	METABOLITE $AUC^{0.17-24}$ ($AUC_{(metabolite)}$) ($\mu g.h\ mL^{-1}$)	$AUC_{(metabolite)}/AUC_{(DOX)}$
Plasma niosome associated		
DXOL	5.2	0.19
DOXONE	0.32	0.012
7-DEOXONE	0.12	0.0045
Plasma unencapsulated fraction after niosome administration		
DXOL	1.26	0.22
DOXONE	0.23	0.041
7-DEOXONE	0.085	0.015
Liver metabolites with Span 60 niosomes		
DXOL	54.2	0.073
DOXONE	4.0	0.0053
DXOLONE	0.53	0.00071
7-DEOXONE	0.75	0.001
Liver metabolites with DOX solution		
DXOL	12.9	0.037
DOXONE	2.7	0.0078
DXOLONE	0.045	0.00013
7-DEOXONE	0.19	0.00054
Lung metabolites with Span 60 niosomes		
DXOL	80.04	0.049
DOXONE	6.25	0.0038
7-DEOXONE	0.76	0.00046
Lung metabolites with DOX solution		
DXOL	19.97	0.027
DOXONE	2.96	0.0041
7-DEOXONE	1.37	0.0019

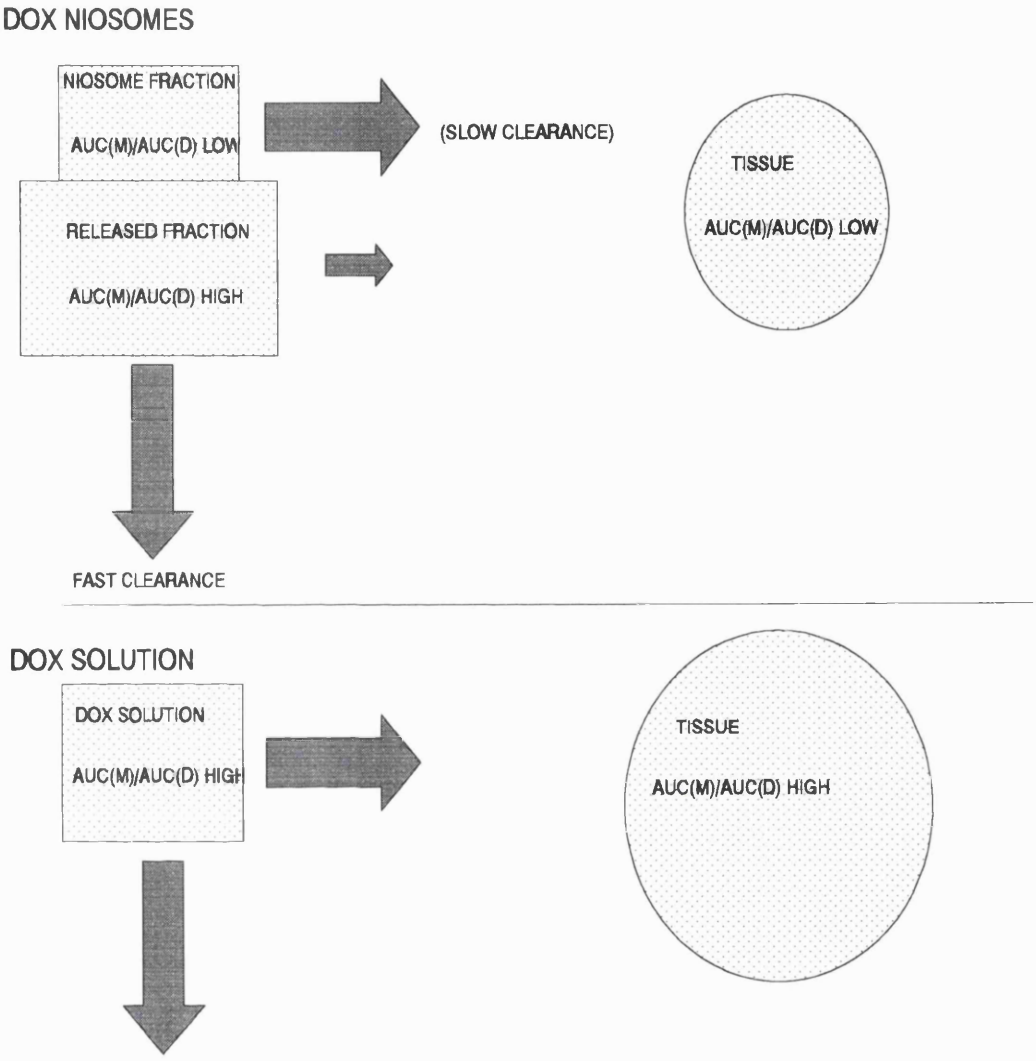

Figure 5.11a: A schematic representation of the delivery of the inactive DOX aglycone metabolite (7-DEOXONE) to tissues such as the lung. A lower proportion of this metabolite in the niosome fraction leads to lower than expected levels of DEOXONE in the lung. AUC(M)/AUC(D) = $AUC_{(METABOLITE)}/AUC_{(DOX)}$

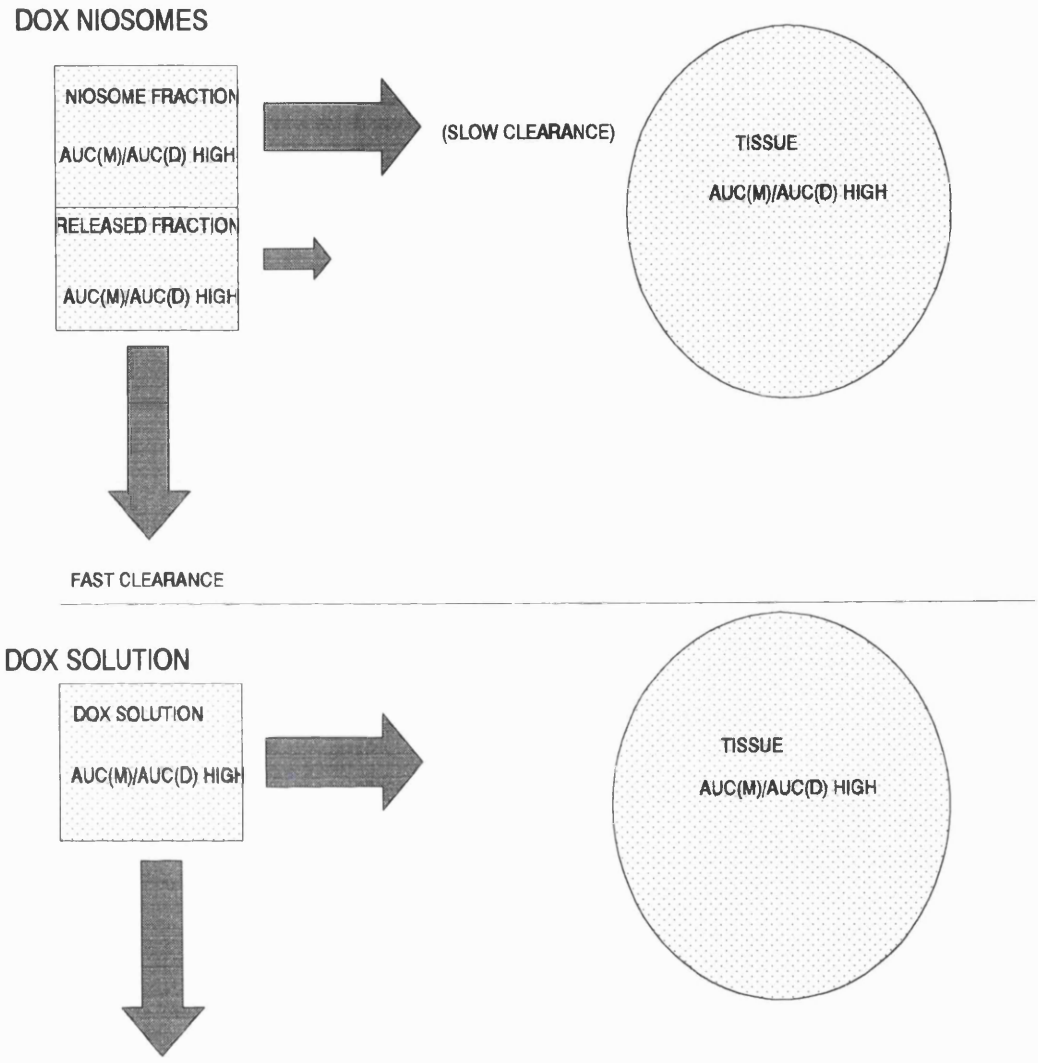

Figure 5.11b: A schematic representation of the level of the active metabolite DXOL in relationship to levels in the long circulating niosome fraction. The level of DXOL in the lung is proportionally high as expected. Abbreviations as in Figure 5.11a.

5.6:5 CONCLUSIONS

We have shown altered biodistribution of DOX on encapsulation in Span 60 niosomes, tissue/plasma DOX ratios rising much more steeply for tumour and liver tissue than they do for heart tissue. This leads to higher drug levels within the tumour and liver tissue with DOX niosomes and an improvement in the tumour to heart drug delivery ratio. Uptake by the liver was defined by a fast followed by a slow phase, the fast phase of which is saturable. The possibility of uptake of intact niosomes by the tumour tissue is envisaged. DOX metabolites were found associated with DOX niosomes *in vivo*, probably due to the adsorption of these compounds to the outside of the bilayer or due to the degradation of the parent molecule within the bilayer.

5.7 THE EVALUATION OF THE TUMORICIDAL ACTIVITY OF DOXORUBICIN NIOSOMES

5.7:1 $C_{16}G_2$ NIOSOMES

DOX niosomes used *in vivo* against the 2 day old MAC 13 tumours had a mean diameter of 105 nm and a DOX/lipid molar ratio of 0.026. Empty niosomes used had a mean diameter of 102 nm. DOX $C_{16}G_2$ niosomes were equiactive* with DOX solution (Figure 5.12). The differences in mean tumour weights from animals bearing the MAC 13 tumour and which had received 10 mg kg^{-1} DOX solution and 10 mg kg^{-1} DOX $C_{16}G_2$ niosomes were not significant using the one way analysis of variance (ANOVA) and later Duncan's multiple range testing ($p > 0.05$).

DOX $C_{16}G_2$ niosomes used against the more established (7 days) MAC 15A tumours had a mean diameter of 100 nm while the empty niosomes used in this experiment

*statistically

had a mean diameter of 96 nm. The mean tumour weight from animals administered DOX $C_{16}G_2$ niosomes at a dose of 3.9 mg kg^{-1} was not significantly different from controls treated with TBS (pH 7.4) or empty niosomes ($p > 0.05$, Figure 5.13). The activity of DOX solution was also not statistically significant at a similar dose. There was however a trend towards increased activity with the use of DOX niosomes against this 7 day old MAC 15A tumour. The failure of this latter experiment to demonstrate a clear cut tumoricidal advantage with DOX niosomes when compared to the drug in solution can be attributed to the low dose employed in this particular case. (Sterile filtration of DOX $C_{16}G_2$ niosomes through 0.22μm filters having reduced the DOX level in the dispersion used in the study).

These niosomes are somewhat smaller than the L'Oreal surfactant niosomes used in earlier studies. In the work of Rogerson and associates (1988) DOX-$C_{16}G_3$ niosomes with a mean diameter of 850 nm successfully increased the tumoricidal activity of the drug in an *in vivo* mouse model bearing a subcutaneously implanted S180 tumour, reducing terminal tumour weight 10 days after dosing (12 days after tumour implantation) from 4.5 g with the drug in solution to 2.0 g with the drug in $C_{16}G_3$ niosomes. On the other hand the use of $C_{16}G_3$ DOX niosomes with a mean diameter of 918 nm resulted in no change in the tumoricidal activity of DOX against a human squamous lung tumour xenograft (WIL) (Kerr *et al.*, 1988). Both studies utilized multilamellar vesicles. A comparison of these results to the results reported herein reveals that the influence of size on the final therapeutic outcome is not necessarily in favour of smaller sizes. These data raise questions about the relationship between tumour extravasation, vesicle size and improved therapeutics with vesicular drug

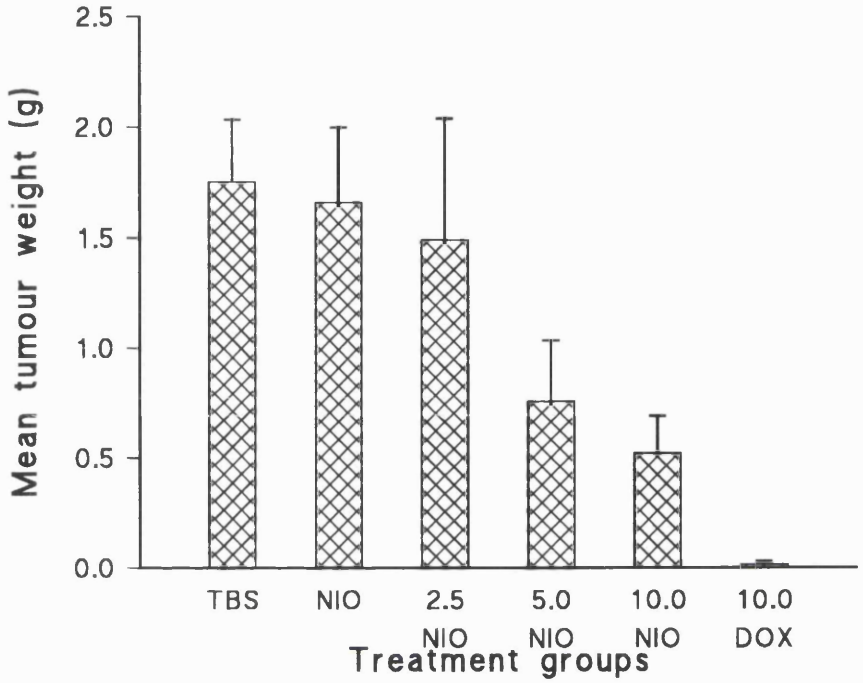

Figure 5.12: The tumoricidal activity of intravenously injected DOX $C_{16}G_2$, cholesterol, Solulan C24 (45: 45: 10) niosomes against a MAC 13 tumour subcutaneously implanted in male NMRI mice. (Expressed as mean tumour weight ± s.e.). TBS = TBS (pH 7.4), NIO = empty niosomes (encapsulating TBS - pH 7.4), 2.5 NIO = 2.5 mg kg^{-1} DOX niosomes, 5.0 NIO = 5.0 mg kg^{-1} DOX niosomes, 10.0 NIO = 10.0 mg kg^{-1} DOX niosomes, 10.0 DOX = 10 mg kg^{-1} DOX solution.

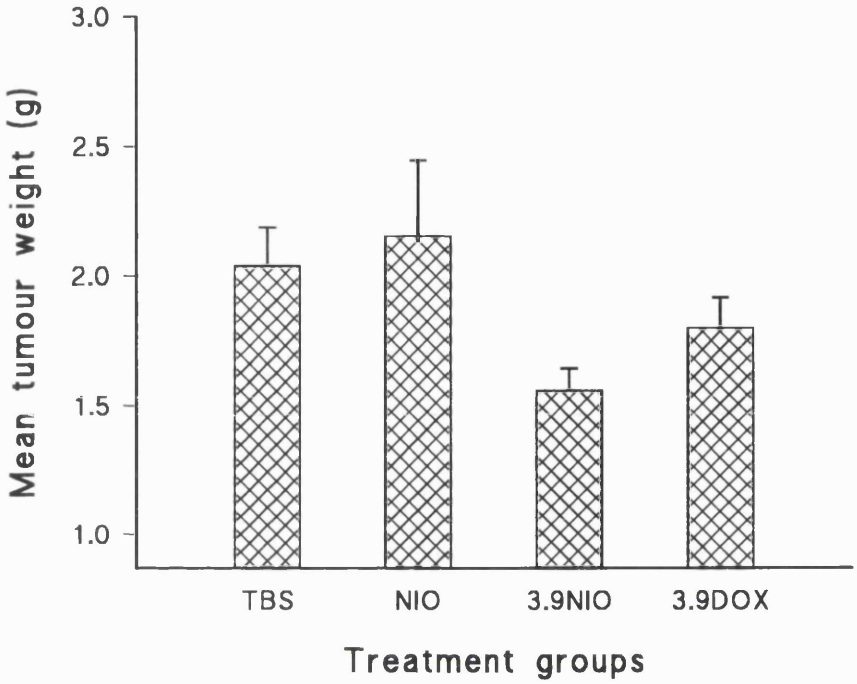

Figure 5.13: The tumoricidal activity of intravenously injected DOX $C_{16}G_2$, cholesterol, Solulan C24 (45: 45: 10) niosomes against a MAC 15A tumour subcutaneously implanted in male NMRI mice. (Expressed as mean tumour weight ± s.e.). TBS = TBS (pH 7.4), NIO = empty niosomes (encapsulating TBS - pH 7.4), 3.9 NIO = 3.9 mg kg^{-1} DOX niosomes, 3.9 DOX = 3.9 mg kg^{-1} DOX solution.

delivery systems. It is believed that the very large size of the $C_{16}G_3$ DOX niosomes used by Rogerson and others (1988) would preclude extravasation. No doubt the inherent sensitivity of the different tumour types to DOX is also a factor worthy of consideration.

Empty niosomes were not active *in vivo* against both the MAC 13 and MAC 15A tumour models.

5.7:2 SPAN 60 NIOSOMES

With Span 60 niosomes two different tumour models were used, (i) a mouse tumour model (MAC 15A) and (ii) a human tumour xenograft grown in immunocompromised mice (PXN/109/TC). Despite the fact that human tumour xenografts do undergo certain changes in kinetics and cell type when transplanted into mice, they do retain some of the host determinants of their response to therapy (Houghton and Houghton, 1987; Steel, 1987). In some situations, they may thus serve as a useful bridge between mouse and man.

Span 60 niosomes used against the MAC 15A tumour had a mean diameter of 171 nm and a DOX/lipid molar ratio of 0.014. Empty Span 60 niosomes had a mean diameter of 132 nm. When these Span 60 niosomes were evaluated against an established (7 day old) MAC 15A tumour they were found to be twice as active as the drug in solution (Figure 5.14) ($p < 0.05$). 5 mg kg^{-1} DOX Span 60 niosomes were equiactive with 10 mg kg^{-1} DOX solution ($p > 0.05$). 10 mg kg^{-1} DOX Span 60 niosomes gave % inhibition values of 49.6%, compared to 26.5% given by 10 mg kg^{-1} DOX solution.

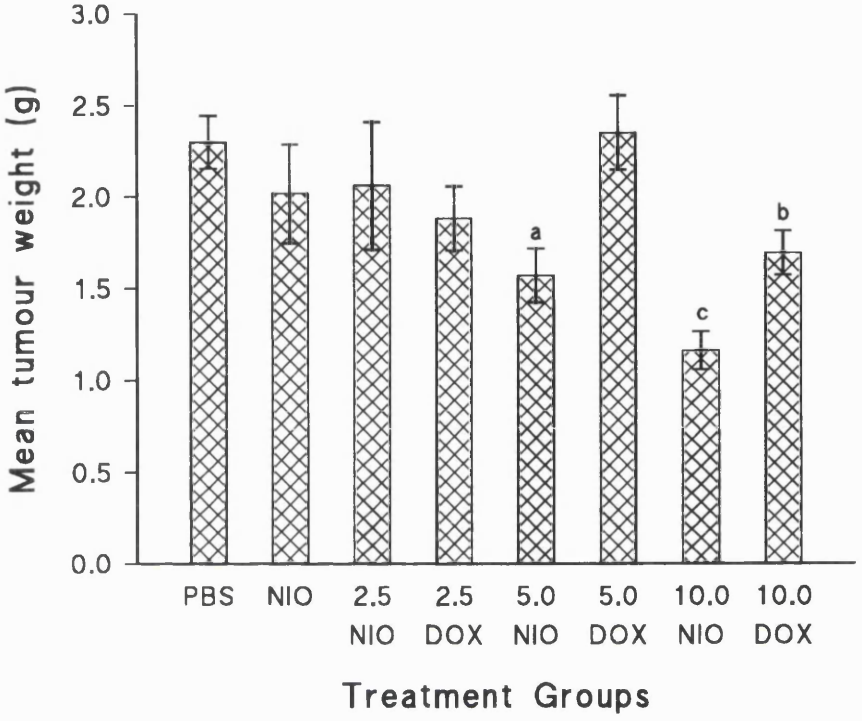

Figure 5.14: The tumoricidal activity of intravenously injected DOX Span 60, cholesterol, Solulan C24 (45: 45: 10) niosomes against a MAC 15A tumour subcutaneously implanted in female NMRI mice. (expressed as mean tumour weight ± s.e.). PBS = PBS (pH 7.4), NIO = empty niosomes (encapsulating PBS - pH 7.4), 5.0 DOX = 5.0 mg kg^{-1} DOX solution, 2.5 NIO, 5.0 NIO, 10.0 NIO & 10.0 DOX are all as is stated in figure 52. The differences between a and b are not statistically significant, while the differences between c and b were statistically significant.

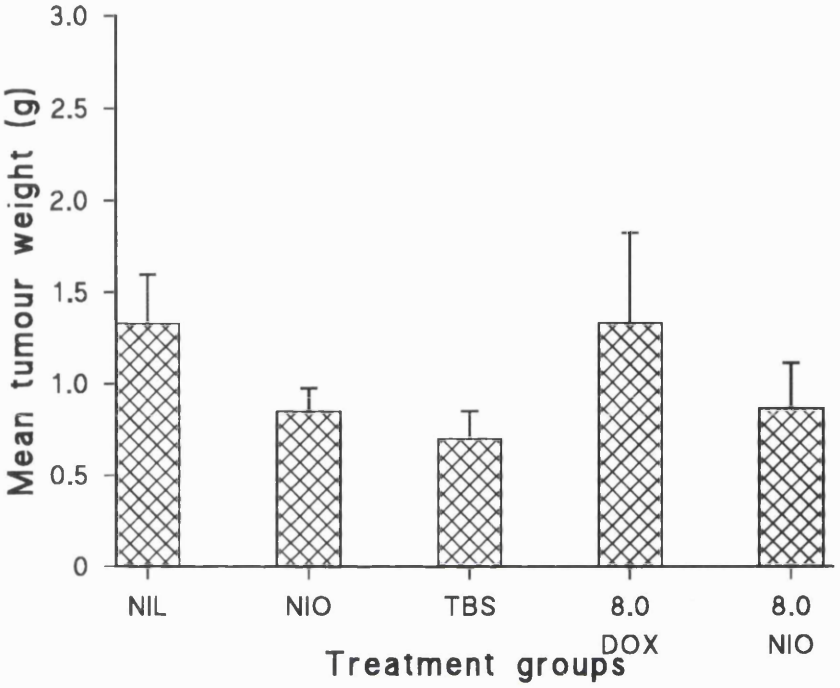

Figure 5.15: The tumoricidal activity of intravenously injected DOX Span 60, cholesterol, Solulan C24 niosomes against a human ovarian cancer xenograft (PXN/109/TC) growing in nude athymic mice. (expressed as mean tumour weight ± s.e.). NIL = no treatment, NIO = empty niosomes (encapsulating TBS - pH 7.4), TBS = TBS (pH 7.4), 8.0 DOX = 8.0 mg kg^{-1} DOX solution, 8.0 NIO = 8.0 mg kg^{-1} DOX in niosomes.

Results on the tumoricidal activity of Span surfactant niosomes are not widely found in the literature,however a study involving sonicated vincristine loaded Span 60 niosomes did indicate an improvement in tumoricidal activity with multiple doses of Span 60 vincristine niosomes (Partharasi *et al.*,1994). The present work however, is the first demonstration of improved tumoricidal activity with DOX Span 60 niosomes.

Niosomes used against the human tumour xenograft PXN/109/TC had a mean diameter of 338 nm and a DOX/lipid molar ratio of 0.012. Empty niosomes had a mean diameter of 151 nm. Data in Figure 5.15 show that the responses of this tumour model to DOX solution and DOX Span 60 niosomes were not significantly different ($p > 0.05$), and indeed treated groups could not be distinguished from the control groups using ANOVA statistics tests. While it is possible that a larger dose of DOX should have been employed, it is speculative to suggest that this was the reason why DOX failed to show any activity against this model tumour. DOX $C_{16}G_3$ niosomes did not increase the activity of DOX in a human tumour xenograft grown in immunocompromised mice (Kerr *et al.*, 1988). The tumour xenograft used in the present study was from the same source as the DOX sensitive CH1 cell line used in the *in vitro* study described in Chapter 3. The outcome of any therapeutic sensitivity assay is influenced by the choice of end point indicator; cell survival studies are, as a rule, a fairly sturdy method of assessment in comparison to studies on tumour growth control (Steel, 1987).

The choice of tumour model must be made in such a way that the appropriate questions are answered by the model (Siemann, 1987). In formulation studies the goal

is to improve the tumoricidal activity of the drug with novel approaches to drug delivery. The fundamental requirement of any tumour model is thus at least an easily demonstrable degree of susceptibility to the free drug, but not to such an extent as to prevent the detection of differences in activity between the various formulations. It is from this perspective that the results with the MAC 15A tumour and $C_{16}G_2$ DOX niosomes (Figure 5.13) or the human ovarian cancer tumour xenograft and the DOX Span surfactant niosomes (Figure 5.15) are viewed. The differences in mean tumour weight between control and treatment groups were not significant in either case ($p > 0.05$), making the assessment of the formulation difficult.

Repeat dosing schedules should be employed for the reasons already advanced in section 5.6.

Model tumours have been used to assess the efficacy of liposomal DOX formulations with varying results, determined not only by intrinsic tumour differences, but also by bilayer characteristics, dosing regimens (multiple dosing versus single doses) and administration routes. Large multilamellar phosphatidylcholine and phosphatidylserine (PS) vesicles evaluated against transplanted metastatic murine lymphomas (J6546) (Gabizon *et al.*, 1982) and a metastatic murine mastocytoma (Balazsovits *et al.*, 1989) showed no improvement over the activity of DOX administered as the free drug in solution, whether repeat (Balazsovits *et al.*, 1989) or single (Gabizon *et al.*, 1982) dosing was employed. Work with single doses of intravenously injected sonicated (65 - 100 nm) DOX hydrogenated phospholipid vesicles showed improved tumoricidal activity in an ascitic form of the murine lymphoma (J6456) (Gabizon, 1992),

expressed as improved survival. Multiple intravenous injections of sonicated DOX phosphatidylserine-phosphatidylcholine liposomes only marginally increased survival times with the metastatic murine lymphoma (J6456) (Gabizon *et al.*, 1982). When multiple dosing and the use of a surface polyoxyethylene compound was employed (Vaage *et al.*, 1992) improved prophylaxis against spontaneous metastasis (with MC19 and MC65 tumours) and increased tumoricidal activity against recently implanted tumours (MC2A, MC2B & MC65) was observed. Similar results with multiple dosing regimens were observed with the use of C-26 colon carcinomas in mice (Huang *et al.*, 1992) and human lung tumour xenografts grown in immunodeficient mice (Williams *et al.*, 1993). The improvement in DOX tumoricidal activity seen with the use of multiple dosed vesicle formulations is a result of the altered pharmacokinetics of DOX on encapsulation (see section 5.6).

Liver metastasis has also been prevented in experiments on rabbits bearing VX2 tumours by the injection of PC DOX liposomes into the portal vein (Ichino *et al.*, 1990). Injections into the hepatic artery increased the tumoricidal activity of DOX dipalmitoylphosphatidylcholine (DPPC) liposomes against W256 liver tumours (Zou *et al.*, 1993).

DOX immunoliposomes, bearing specific surface antibodies, have also been assayed using experimental tumours (Ahmad *et al.*, 1993). Success has been achieved at the bench level although the vertical translation to the clinic may prove somewhat difficult as the clinical tumour of interest may not be adequately characterised with respect to specific tumour antigens.

Intraperitoneal injection of ascites tumour cell lines, followed by the intraperitoneal injection of the novel formulation is a quick method of biological assay of same and the intraperitoneal injection of DOX cardiolipin PC liposomes has been shown to improve the tumoricidal activity of DOX against the P388 ascites tumour (Rahman *et al.*, 1985). The use of the intraperitoneal route and $C_{16}G_2$ DOX niosomes was hampered by the development of an inflammatory response in the lung (Chapter 4).

As already stated, clinical data on the use of DOX niosomes is a logical next step. The feasibility of this move is advanced by the ongoing clinical trials of DOX liposomes (Treat *et al.*, 1989; Rahman *et al.*, 1990; Batist *et al.*, 1991; Currie *et al.*, 1991; Owen *et al.*, 1992; Cowens *et al.*,1993). While it is too early to make any pronouncements on the future widespread clinical use of DOX liposomes as a result of these studies, it must be stated that myelotoxicity is still a very real problem with the use of liposomal DOX formulations in the clinic. Future work with DOX niosomes will be geared towards generating data on this particular aspect of DOX toxicity, using a mouse model, prior to any clinical work.

CHAPTER SIX

CONCLUSIONS AND FUTURE WORK

6.1 CONCLUSIONS

Explorations in any field nearly always result in more questions than the initial exercise sought to answer. This is true of the current study, the objectives of which were to assess the applicability of niosomal drug delivery to the treatment of disease. It was hoped that the therapeutic index would be enlarged. A rigorous challenge is posed by cancer, which still presents a serious threat to the health of us all. Doxorubicin was chosen as the model drug, because it has proved efficacious in the clinic and also because its use is hampered by systemic toxicity. Other minor considerations were the amenability of DOX to precise determination, largely because of the fluorescence of this compound. Niosomes were prepared in various ways and maximal encapsulation was sought. The use of transmembrane proton gradients offered superior encapsulation efficiencies to the use of the more established method of lipid film hydration with a solution of the drug of choice. The need for a small-sized-particle formulation was a factor thought to determine the success or otherwise of the formulation and the small vesicle was aggressively sought. Techniques employed included various mechanical procedures, namely sonication, microfluidization and homogenization. Physicochemical means were also employed and the micelle forming soluble surfactant Solulan C24 was chosen to improve bilayer characteristics in this direction. The discome phase was characterised as a direct but accidental result of this latter manoeuvre.

When the formulations were required to be assayed for biological activity, initially an ascites tumour was to be used, coupled with intraperitoneal injection of the niosome formulation. This led to the characterisation of a lung lesion, that was specific for the

intraperitoneal route of administration of DOX $C_{16}G_2$ niosomes. Empty niosomes did not give rise to this reaction and the exact cause of this reaction is still unknown although we cautiously speculate on the involvement of the heart or a direct action of the formulation of the lung. The clearance of particulate preparations by the lymphatic system is also believed to play a part in this reaction.

The area of multidrug resistance was tentatively explored at the *in vitro* level and marginal improvements with the various niosomal drug delivery systems were observed.

The tumoricidal activity of Span 60 niosomes were the most encouraging results and a doubling of the tumoricidal activity was reported with single intravenous injections of DOX niosomes. The biodistribution studies correlated well with this finding as the delivery of DOX to the tumour tissue was increased by niosomal encapsulation. The niosomes served as a depot within the plasma, increasing to a greater extent the delivery of drug to the tumour than the corresponding delivery to the heart tissue. The therapeutic index as measured by tissue levels was thus widened somewhat. This finding reiterates the role of DOX niosomes in future clinical work.

DOX niosomes from *in vivo* plasma samples were assayed separately from released drug after the administration of DOX niosomes and they were found to persist in the plasma and this is the first report on the longevity of DOX niosomes *in vivo.* Metabolites were found associated with the niosome fraction, although it is not clear whether the drug was degraded while still in the niosome or after the release from

same. This is the first report of such a finding.

The results of this study demonstrate that DOX niosomes are useful for targeting to neoplastic tissue. However, the greatest value of this study is that the *in vivo* disposition of niosomes is now better understood. The surfactants used are cheap, can be stored dry and although in the case of the Span surfactants consist of mixtures of esters and anhydrides, give reproducible results *in vivo* and *in vitro*. Span surfactants are widely used in pharmaceutical formulations and as a food additive and so toxicological concerns are unlikely to hamper future progress.

6.2 FUTURE WORK

In the very near future, the following specific areas will be studied, namely the use of DOX Span 60 niosomes in the clinic. Span surfactant niosomes will be produced and their tolerance assessed in the clinical situation. The issue of myelotoxicity will also be addressed using a mouse model, prior to clinical studies. The modification of niosome surface characteristics needs also to be explored with a view to improving their therapeutic potential.

The full drug carrier potential of discomes should be explored. It is hoped that the discomes will be utilised in medicine. It is proposed that these structures could be used in the field of ophthalmology, precisely because of their large size. However, as their size may be manipulated by the level of Solulan C24 content, it is hoped that smaller sized discomes may be produced. A heterogenous discome/niosome mixture

may be advantageous in the preparation of formulations requiring different release rates of drug at various times of the day.

The issue of multidrug resistance also needs to be studied further. It is hoped that DOX micellar formulations and DOX niosome/free DOX mixtures will be found useful in multidrug resistant cell lines.

REFERENCES

Ahmad, I., Longenecker, M., Samuel, J., Allen, T.M. (1993). Antibody-targeted delivery of doxorubicin entrapped in sterically stabilized liposomes can eradicate lung cancer in mice. Cancer Research, 53: 1484 - 1488.

Allen, T.M., Hansen, C., Martin, F., Redemann, C., Yau-Young, A. (1991). Liposomes containing synthetic lipid derivatives of poly(ethylene glycol) show prolonged circulation half-lives in vivo. Biochimica et Biophysica Acta, 1066: 29 - 36.

Allen, T.M., Hansen, C.B., Guo, L.S.S. (1993). Subcutaneous administration of liposomes: a comparison with intravenous and intraperitoneal routes of injection. Biochimica et Biophysica Acta, 1150: 9 - 16.

Almog, S., Litman, B.J., Wimley, W., Cohen, J., Wachtel, E.J., Barenholz, Y., Ben-Shaul, A., Lichtenberg, D. (1990). States of aggregation and phase transformations in mixtures of phosphatidylcholine and octyl glucoside. Biochemistry, 29: 4582 - 4592.

Arancia, G., Donelli, G. (1991). Cell membranes as targets for anticancer agents. Pharmacological Research, 24: 205 - 217.

Arcamone, F., Franceschi, G., Penco, S. (1969). Adriamycin (14-hydroxydaunomycin), a novel antitumour antibiotic. Tetrahedron Letters, 13: 1007 - 1010.

Areci, R.J. (1993). Clinical significance of P-glycoprotein in multidrug resistance malignancies. Blood, 81: 2215 - 2222.

Assadullahi, T.P., Hidler, R.C., McAuley, A.J. (1991). Liposome formation from synthetic polyhydroxyl lipids. Biochimica et Biophysica Acta, 1083: 271 - 276.

Awasthi, S. Sharma, R., Awasthi, Y.C., Belli, J.A., Frenkel, E.P. (1992). The relationship of doxorubicin binding to membrane lipids with drug resistance. Cancer Letters, 63: 109 - 116.

Azmin, M.N., Florence, A.T., Handjani-Vila, R.M., Stuart, J.F.B., Vanlerberghe, G., Whittaker, J.S. (1985). The effect of non-ionic surfactant vesicle (niosome) entrapment on the absorption and distribution of methotrexate in mice. Journal of Pharmacy and Pharmacology, 37: 237 - 242.

Bachur, N.R., Gordon, S.L., Gee, M.V. (1977). Anthracycline antibiotic augmentation of microsomal electron transport and free radical formation. Molecular Pharmacology, 13: 901 - 910.

Bachur, N.R., Gee, M.V., Friedman, R.D. (1982). Nuclear catalyzed antibiotic free radical formation. Cancer Research, 42: 1078 - 1081.

Balazsovits, J.A.E., Mayer, L.D., Bally, M.B., Cullis, P.R., McDonnel, M., Ginsberg, R.S., Falk, R.E. (1989). Analysis of the effect of liposome encapsulation on the

vesicant properties, acute and cardiac toxicities, and antitumour efficacy of doxorubicin. Cancer Chemotherapy and Pharmacology, 23: 81 - 86.

Baillie, A.J., Florence, A.T., Hume, L.R., Muirhead, G.T., Rogerson, A. (1985). The preparation and properties of niosomes - non-ionic surfactant vesicles. Journal of Pharmacy and Pharmacology, 37: 863 - 868.

Baillie, A.J., Coombs, G.H., Dolan,T.F., Laurie, J. (1986). Non-ionic surfactant vesicles, niosomes, as a delivery system for the anti-leishmanial drug, sodium stibogluconate. Journal of Pharmacy and Pharmacology, 38: 502 - 505.

Bally, M.B., Nayar, R., Masin, D., Cullis, P.R., Mayer, L.D. (1990). Studies on the myelosuppressive activity of doxorubicin entrapped in liposomes. Cancer Chemotherapy and Pharmacology, 27: 13 - 19.

Bar-Shira-Maymon, B., Michowitz, M., Gibli, O., Klein, O., Pinchasov, A., Leibovici, J. (1992). Effect of a membrane-active agent on uptake of adriamycin in Lewis lung carcinoma cells derived from 'primary' and 'metastatic' growths. Chemotherapy, 38: 66 - 73.

Bartoszek, A., Wolf, C.R. (1992). Enhancement of doxorubicin toxicity following activation by NADPH cytochrome P450 reductase. Biochemical Pharmacology, 43: 1449 - 1457.

Batist, G., Mayer, L., Pilkiewicz, F., Wang, T., Skrutkowska, M., Zukiwski, A., Ahlgren, P., Skelton, J., Gruner, P., Leyland-Jones, B. (1991). Liposomal doxorubicin (TLC D99) in experimental and clinical breast cancer is effective and less toxic. Proceedings of the American Association for Cancer Research, 32: 183.

Beck, W.T. (1987). The cell biology of multiple drug resistance. Biochemical Pharmacology, 36: 2879 - 2887.

Belvedere, G., Suarato, A., Geroni, C., Giuliani, F.C., D'Incalci, M. (1989). Comparison of intracellular drug retention, DNA damage and cytotoxicity of derivatives of doxorubicin and daunorubicin in a human colon carcinoma cell line (LoVo). Biochemical Pharmacology, 38: 3713 - 3721.

Benchekroun, M.N., Pourquier, P., Schott, B., Robert, J. (1993). Doxorubicin-induced lipid peroxidation and glutathione peroxidase activity in tumour cell lines selected for resistance to doxorubicin. European Journal of Biochemistry, 211: 141 - 146.

Bertani, T., Rocchi, G., Sacchi, G., Mecca, G., Remuzzi, G. (1986). Adriamycin-induced glomerulosclerosis in the rat. American Journal of Kidney Diseases, VII: 12 - 19.

Blume, G., Cevc, G. (1990). Liposomes for sustained drug release in vivo. Biochimica et Biophysica Acta, 1029: 91 - 97.

Boiocchi, M., Toffoli, G. (1992). Mechanism of multidrug resistance in human tumour cell lines and complete reversion of cellular resistance. European Journal of Cancer, 28A: 1099 - 1105.

Boucek, R.J., Olson, R.D., Brenner, D.E., Ogunbunmi, E.M., Inui, M., Fleischer, S. (1987). The major metabolite of doxorubicin is a potent inhibitor of membrane-associated ion pumps. The Journal of Biological Chemistry, 262: 15851 - 15856.

Bouma, J., Beijnen, J.H., Bult, A., Underberg, W.J.M. (1986). Anthracycline antitumour agents. Pharmaceutisch Weekblad Scientific Edition, 8: 109 - 133.

Bourhis, J., Riou, G., Bénard, J. (1990). *Expression de la P-glycoprotéine 170 (GP 170) et résistance à la chimiothérapie des cancers humains.* Bulletin of Cancer, 77: 957 - 965.

Brandl, M.M., Bachmann, D., Drechsler, M., Bauer, K.H. (1993). Liposome preparation using high-pressure homogenizers. In Liposome Technology Volume I, (2nd edition), Gregoriadis, G. (ed). CRC press, London, pp49 - 65.

Bruno, N.A., Slate, D.L. (1990). Effect of exposure to calcium entry blockers on doxorubicin accumulation and cytotoxicity in multidrug-resistant cells. Journal of the National Cancer Institute, 82: 419 - 424.

Burke, T.G. Tritton, T.R. (1985). Location and dynamics of anthracyclines bound

to unilamellar phosphatidylcholine vesicles. Biochemistry, 24: 5972 - 5980.

Cable, C. (1990). An examination of the effect of surface modifications on the physicochemical and biological properties of non-ionic surfactant vesicles. PhD Thesis, University of Strathclyde, Glasgow.

Cable, C., Florence, A.T. (1988). Mixed poly(glycerol)-poly(oxyethylene) ether niosomes. Journal of Pharmacy and Pharmacology, 40: 30P.

Calabersi, P., Chabner, B.A. (1990). Antineoplastic agents. In Goodman and Gilman's Pharmacological Basis of Therapeutics (8th edition), Goodman, Gilman, A., Rall, T.W., Nies, S.A., Taylor, P. (eds), Pergamon Press, New York, pp1209 - 1263.

Carter, K.C., Baillie, A.J., Alexander, J., Dolan, T.F. (1988). The therapeutic effect of sodium stibogluconate in BALB/c mice infected with *Leishmania donovani* is organ-dependent. Journal of Pharmacy and Pharmacology, 40: 370 - 373.

Cevc, G. (1993). Lipid properties as a basis for membrane modelling and rational liposome design. In Liposome Technology Volume I, Gregoriadis, G. (ed), CRC Press, London, pp1 - 36.

Chan-Lam, D., Copplestone, J.A., Prentice, A., Price, R., Johnson, S., Phillips, M. (1992). Idarubicin cardiotoxicity in acute myeloid leukaemia. Lancet, 340: 185 -186.

Chandraprakash, K.S., Udupa, N., Umadevi, P., Pillai, G.K. (1990). Pharmacokinetic evaluation of surfactant vesicle-entrapped methotrexate in tumour bearing mice. International Journal of Pharmaceutics, 61: R1 - R3.

Cittadini, A., Fazio, S., D'Ascia, C., Basso, A., Bazzicalupo, L., Picardi, G., Saccà. L. (1991). Subclinical cardiotoxicity by doxorubicin: a pulsed Doppler echocardiographic study. European Heart Journal, 12: 1000 - 1005.

Clough, G. (1991). Relationship between microvascular permeability and ultrastructure. Progress in Biophysics and Molecular Biology, 55: 47 - 69.

Codde, J.P., Lumsden, A.J., Napoli, S., Burton, M.A., Gray, B.N. (1993). A comparative study of the anticancer efficacy of doxorubicin carrying microspheres and liposomes using a rat liver tumour model. Anticancer Research, 13: 539 - 544.

Cohen, E. (1975). The permeability of liposomes to non-electrolytes. Journal of Membrane Biology, 20: 205 - 234.

Combs, A.B., Acosta, D., Ramos, K. (1985). Effects of doxorubicin and verapamil on calcium uptake in primary cultures of rat myocardial cells. Biochemical Pharmacology, 34: 1115 - 1116.

Cowens, J.W., Creaven, P.J., Greco, W.R., Brenner, D.E., Tung, Y., Ostro, M., Ginsberg, R., Petrelli, N. (1993). Initial clinical (phase I) trial of TLC D-99

(doxorubicin encapsulated in liposomes). Cancer Research, 53: 2796 - 2802.

Cullis, P.R., Hope, M.J., Bally, M.B., Madden, T.M., Mayer, L.D., Janoff, A.S. (1987). Liposomes as pharmaceuticals. In Liposomes from Biophysics to Therapeutics, Ostro, M.J. (ed), Marcell Dekker, Inc., New York, pp39 - 72.

Cummings, J., Stuart, J.F.B., Calman, K.C. (1984). Determination of adriamycin, adriamycinol and their 7-deoxyaglycones in human serum by high-performance liquid chromatography. Journal of Chromatography, 311: 125 - 133.

Cummings, J., McArdle, C.S. (1986). Studies on the *in vivo* disposition of adriamycin in human tumours which exhibit different responses to the drug. British Journal of Cancer, 53: 835 - 838.

Cummings, J., Wilmott, N., More, I., Kerr, D.J., Morrison, J.G., Kaye, S.B. (1987). Comparative cardiotoxicity and antitumour activity of doxorubicin (adriamycin) and 4'-deoxydoxorubicin and the relationship to *in vivo* disposition and metabolism in the target tissue. Biochemical Pharmacology, 36: 1521 - 1526.

Cummings, J., Anderson, L., Willmott, N., Smyth, J.F. (1991). The molecular pharmacology of doxorubicin *in vivo*. European Journal of Cancer, 27: 532 - 535.

Cummings, J., Allan, L., Willmott, N., Riley, R., Workman., P., Smyth, J.F. (1992a). The enzymology of doxorubicin quinone reduction in tumour tissue. Biochemical

Pharmacology, 44: 2175 - 2183.

Cummings, J., Willmott, N., Hoey, B.M., Marley, E.S., Smyth, J.F. (1992b). The consequences of doxorubicin quinone reduction *in vivo* in tumour tissue. Biochemical Pharmacology, 44: 2165 - 2174.

Curran, F.C., Luce, J.K. (1989). Ocular adverse reactions associated with adriamycin (doxorubicin). American Journal of Ophthalmology, 108: 709 - 711.

Currie, V.E., Muindi, J., Young, C.W. (1991). A phase I comparative pharmacological study of standard and liposome-encapsulated doxorubicin (Dox and Lipodox). Proceedings of the American Association for Cancer Research, 32: 201.

Cuvier, C., Roblot-Treupel, L., Millot, J.M., Lizard, G., Chevillard, S., Manfait, M., Couvreur, P., Poupon, M.F. (1992). Doxorubicin-loaded nanospheres bypass tumour cell multidrug resistance. Biochemical Pharmacology, 44: 509 - 517.

Danhauser-Riedl, S., Hausmann, E., Schick, H-D., Bender, R., Dietzfelbinger, H., Rastetter, J., Hanauske, A-R. (1993). Phase I clinical and pharmacokinetic trial of dextran conjugated doxorubicin (AD-70, DOX-OXD). Investigational New Drugs, 11: 187 - 195.

Darnell, J., Lodish, H., Baltimore, D. (1990). Molecular and cell biology (2nd edition), WH Freeman and Co., New York.

Davies, K.J.A., Doroshow, J.H., Hochstein, P. (1983). Mitochondrail NADH dehydrogenase-catalyzed oxygen radical production by adriamycin, and the relative inactivity of 5-iminodaunorubicin. FEBS letters, 153: 227 - 230.

Demichelli, R., Bonciarelli, G., Jirillo, A., Foroni, R., Petrosino, L., Targa, L., Garusi, G. (1985). Pharmacologic data and technical feasibility of intraperitoneal doxorubicin administration. Tumori, 71: 63 - 68.

Denekamp, J. (1992). The choice of experimental tumour models in cancer research: the key to ultimate success or failure. NMR in Biomedicine, 5: 234 - 237.

Dodd, D.A., Atkinson, J.B., Olson, R.D., Buck, S., Cusack, B.J., Fleischer, S. , Boucek, R.J. Jr. (1993). Doxorubicin cardiomyopathy is associated with a decrease in calcium release channel of the sarcoplasmic reticulum in a chronic rabbit model. Journal of Clinical Investigation, 91: 1697 - 1705.

Dordal, M.S., Winter, J.N., Atkinson, A.J. Jr. (1992). Kinetic analysis of P-glycoprotein-mediated doxorubicin efflux. Journal of Pharmacology and Experimental Therapeutics, 263: 762 -766.

Doroshow, J. (1983). Effect of anthracycline antibiotics on oxygen radical formation. Cancer Research, 43: 460 - 472.

Doroshow, J. (1991). Doxorubicin-induced cardiac toxicity. New England Journal of

Medicine, 324: 843 - 844.

Doyle, L.A. (1993). Mechanisms of drug resistance in human lung cancer cells. Seminars in Oncology, 20: 326 - 337.

Dupou-Cézanne, L., Sautereau, A-M., Tocanne, J. (1989). Localization of adriamycin in model and natural membranes. European Journal of Biochemistry, 181: 695 - 702.

Druckmann, S., Gabizon, A., Barenholz, Y. (1989). Separation of liposome-associated doxorubicin in human plasma: implications for pharmacokinetic studies. Biochimica et Biophysica Acta, 980: 381 - 384.

Echegoyen, L.E., Hernandez, J.C., Kaifer, A.E., Gokel, G.W., Echegoyen, L. (1988). Aggregation of steroidal lariat ethers: the first example of non-ionic liposomes (niosomes) formed from neutral crown ether compounds. Journal of the Chemistry Society and Chemical Communications, 12: 836 - 837.

Eliot, H., Gianni, L., Myers, C. (1984). Oxidative destruction of DNA by the adriamycin-iron complex. Biochemistry, 23: 928 - 936.

Florence, A.T. (1993). Non-ionic surfactant vesicles: preparation and characterization. In Liposome Technology Volume I (2nd edition), Gregoriadis, G. (ed), CRC Press, London, pp157 - 176.

Florence, A.T., Baillie, A.J. (1989). Non-ionic surfactant vesicles - alternatives to liposomes in drug delivery. In Novel Drug Delivery and its Therapeutic Application, Prescott, L.F., Nimmo, W.S. (eds), John Wiley and Sons Ltd, New York, pp281 - 296.

Florence, A.T., Cable, C., Cassidy, J., Kaye, S.B. (1990). Non-ionic surfactant vesicles as carriers of doxorubicin. In Targeting of Drugs, Gregoriadis, G., Allison, A.C., Poste, G. (eds). Plenum Press, New York, pp117 - 126.

Fu, L.X., Waagstein, F., Hjalmarson, Å. (1990). A new insight into adriamycin-induced cardiotoxicity. International Journal of Cardiology, 29: 15 - 20.

Frezard, F., Garnier-Suillerot, A. (1991). DNA-containing liposomes as a model for the study of cell membrane permeation by anthracycline derivatives. Biochemistry, 30: 5038 - 5043.

Gabizon, A.A. (1992). Selective tumour localization and improved therapeutic index of anthracyclines encapsulated in long-circulating liposomes. Cancer Research, 52: 891 -896.

Gabizon, A., Dagan, A., Goren, D., Barenholz, Y., Fuks, Z. (1982). Liposomes as *in vivo* carriers of adriamycin: reduced cardiac uptake and preserved antitumour activity in mice. Cancer Research, 42: 4734 - 4739.

Gabizon, A., Shiota, R., Papahadjopoulos, D. (1989). Pharmacokinetics and tissue

distribution of doxorubicin encapsulated in stable liposomes with long circulation times. Journal of the National Cancer Institute, 81: 1484 - 1488.

Gabizon, A.A., Barenholz, Y., Bialer, M. (1993). Prolongation of the circulation time of doxorubicin encapsulated in liposomes containing a polyethylene glycol-derivatized phospholipid: pharmacokinetic studies in rodents and dogs. Pharmaceutical Research, 10: 703 - 708.

Gabizon, A., Catane, R., Uziely, B., Kaufmann, B., Safra, T., Cohen, R., Martin, F., Huang, A., Barenholz, Y. (1994). Prolonged circulation time and enhanced accumulation in malignant exudates of doxorubicin encapsulated in polyethylene-glycol coated liposomes. Cancer Research, 54: 987 - 992.

Gebicki, J.M., Hicks, M. (1976). Preparation and properties of vesicles enclosed by fatty acid membranes. Chemistry and Physics of lipids, 16: 142 - 160.

Gennis, R.B. (1989). Biomembranes. Springer-Verlag, New York.

Gerlowski, L.E., Jain, R.K. (1986). Microvascular permeability of normal and neoplastic tissue. Microvascular Research, 31: 288 - 305.

Gibaldi, M. (1991). Biopharmaceutics and clinical pharmacokinetics (4th edition). Lea and Febiger, Philadelphia.

Goodman, J., Hochstein, P. (1977). Generation of free radicals and lipid peroxidation by redox cycling of adriamycin and daunomycin. Biochemical and Biophysical Research Communications, 77: 797 - 803.

Goorin, A.M., Chavenet, A.R., Perez-Atyade, A.R., Cruz, J., McKone, R., Lipschultz, S.E. (1990). Initial congestive heart failure, six to ten years after doxorubicin chemotherapy for childhood cancer. Journal of Pediatrics, 116: 144 - 147.

Gould-Fogerite, S., Mannino, R.J. (1993). Preparation of large unilamellar liposomes with high entrapment yield by rotary dialysis or agarose plug diffusion. In Liposome Technology Volume I (2nd edition), Gregoriadis, G. (ed), CRC Press, London, pp67 - 80.

Gregoriadis, G., Ryman, B.E. (1972). Fate of protein-containing liposomes injected into rats. European Journal of Biochemistry, 24: 485 - 491.

Gregoriadis, G., da Silva, H., Florence, A.T. (1990). A procedure for the efficient entrapment of drugs in dehydration-rehydration liposomes (DRV's). International Journal of Pharmaceutics, 65: 235 - 242.

Guo, L.S.S., Fielding, R.M., Lasic, D.D., Hamilton, R.L., Mufson, D. (1991). Novel antifungal drug delivery: stable amphotericin B-cholesteryl sulfate discs. International Journal of Pharmaceutics, 75: 45 - 54.

Gupta, P.K. (1990). Drug targeting in cancer chemotherapy: A clinical perspective. Journal of Pharmaceutical Sciences, 79: 949 - 962.

Gupta, P.K., Hung, C.T. (1989). Effect of carrier dose on the multiple tissue disposition of doxorubicin hydrochloride administered via magnetic albumin microspheres in rats. Journal of Pharmaceutical Sciences, 78: 745 - 748.

Gupta, P.K., Hung, C.T., Rao, N.S. (1989). Ultrastructural disposition of adriamycin-associated magnetic albumin microspheres in rats. Journal of Pharmaceutical Sciences, 78: 290 - 294.

Gutteridge, J.M.C. (1982). The role of superoxide and hydroxyl radicals in phospholipid peroxidation catalyzed by iron salts. FEBS letters, 150: 454 - 458.

Gutteridge, J.M.C., Toeg, D. (1982). Adriamycin-dependent damage to deoxyribose: a reaction involving iron, hydroxyl and semiquinone free radicals. FEBS letters, 149: 228 - 232.

Gutiérrez, P.L., Gee, M.V., Bachur, N.R. (1983). Kinetics of anthracycline antibiotic free radical formation and reductive glycosidase activity. Archives of Biochemistry and Biophysics, 223: 68 - 75.

Guyton, A.C. (1981). Textbook of medical physiology (6th edition), W.B. Saunders Co., Philadelphia.

Handjani-Vila, R.M., Ribier, A., Rondot, B., Vanlerberghe, G. (1979). Dispersions of lamellar phases of on-ionic lipids in cosmetic products. International Journal of Cosmetic Science, 1: 303 - 314.

Handjani-Vila, R.M (1990). Non-ionic vesicles as drug delivery systems. Minutes of the 5th International Pharmaceutical Technology Symposium, Ankara, 213 - 227.

Haran, G., Cohen, R., Bar, L.K., Barenholz, Y. (1993). Transmembrane ammonium sulfate gradients in liposomes produce efficient and stable entrapment of amphipathic weak bases. Biochimica et Biophysica Acta, 1151: 201 - 215.

Harashima, H., Ohshima, S., Midori, Y., Yachi, K., Kikuchi, H., Kiwada, H. (1992). Kinetic analysis of tissue distribution of doxorubicin incorporated in liposomes in rats: I. Biopharmaceutics and Drug Disposition, 13: 155 - 170.

Harashima, H., Midori, Y., Ohshima, SY., Yachi, K., Kikuchi, H., Kiwada, H. (1993). Kinetic analysis of tissue distribution of doxorubicin incorporated in liposomes in rats: (II). Biopharmaceutics and Drug Disposition, 14: 595 - 608.

Hargreaves, W., Deamer, D.W. (1978). Liposomes from ionic single chain amphiphiles. Journal of the American Chemical Society, 17: 3759 - 3768.

Harrigan, P.R., Wong,K.F., Redelmeier, T.E., Wheeler, J.J., Cullis, P.R. (1993). Accumulation of doxorubicin and other lipophilic amines into large unilamellar

vesicles in response to transmembrane pH gradients. Biochimica et Biophysica Acta, 1149: 329 - 338.

Hengge, U.R., Brockmeyer, N.H., Baumann, M., Reimann, G., Goos, M. (1993). Liposomal doxorubicin in AIDS-related Kaposi's sarcoma. Lancet, 342: 497.

Herman, E.H., Rahman, A., Ferrans, V.J., Vick, J.A., Schein, P.S. (1983). Prevention of chronic doxorubicin cardiotoxicity in beagles by liposomal encapsulation. Cancer Research, 43: 5427 - 5432.

Hershko, C., Link, G., Tzahor, M., Kaltwasser, J.P., Athias, P., Grynberg, A., Pinson, A. (1993). Anthracycline toxicity is potentiated by iron and inhibited by deferoxamine: studies in rat heart cells in culture. Journal of Laboratory and Clinical Medicine, 122: 245 - 251.

Hirano, K., Hunt, C.A., Strubbe, A., MacGregor, R.D. (1985). Lymphatic transport of liposome-encapsulated drugs following intraperitoneal administration - effect of lipid composition. Pharmaceutical Research, 2: 271 - 278.

Hofland, H.E.J., Bouwstra, J.A., Verhoef, J.C., Buckton, G., Chowdry, B.Z., Ponec, M., Junginger, H.E. (1992). Safety aspects of non-ionic surfactant vesicles: a toxicity study related to the physicochemical characteristics of non-ionic surfactants. Journal of Pharmacy and Pharmacology, 44: 287 - 294.

Houghton, J.A., Houghton, P.J. (1987). The suitability and use of human tumour xenografts. In Rodent Tumour Models in Experimental Cancer Chemotherapy, Kallman, R.F. (ed), Pergamon Press, New York, pp199 - 204.

Huang, S.K., Lee, K-D., Hong, K., Friend, D.S., Papahadjopoulos, D. (1992). Microscopic localization of sterically stabilized liposomes in colon carcinoma-bearing mice. Cancer Research, 52: 5135 - 5143.

Hwang, K.J. (1987). Liposome pharmacokinetics. In Liposomes from Biophysics to Therapeutics, Ostro, M.J. (ed). Marcel Dekker Inc, New York, pp109 - 156.

Hunter, C.A., Dolan, T.F., Coombs, G.H., Baillie, A.J. (1988). Vesicular systems (niosomes and liposomes) for delivery of sodium stibogluconate in experimental murine visceral leishmaniasis. Journal of Pharmacy and Pharmacology, 40: 161 - 165.

Ichino, T., Yotsuyanagi, T., Mizuno, I., Akamo, Y., Yamamoto, T., Saito, T., Kurahashi, S., Tanimoto, N., Yura, J. (1990). Antitumour effect of liposome-entrapped adriamycin administered via the portal vein. Japanese Journal of Cancer Research, 81: 1052 - 1056.

Israelachvili, J.N. (1985). Intermolecular and surface forces. Academic Press, Sydney.

Israelachvili, J.N. (1992). Intermolecular and surface forces. Academic Press, New York.

Ito, H., Miller, S.C., Billingham, M.E., Akimoto, H., Torti, S.V., Wade, R., Gahlmann, R., Lyons, G., Kedes, L., Torti, F.M. (1990). Doxorubicin selectively inhibits muscle gene expression in cardiac muscle cells *in vivo* and *in vitro*. Proceedings of the National Academy of Science, 87: 4275 - 4279.

Jackson, M.L., Schmidt, C.F., Lichtenberg, D., Litman, B.J., Albert, A.D. (1982). Solubilization of phosphatidylcholine bilayers by octyl glucoside. Biochemistry, 21: 4576 - 4582.

Jain, R.K. (1990). Vascular and interstitial barriers to delivery of therapeutic agents in tumours. Cancer and Metastasis Reviews, 9: 253 - 266.

Jones, A.P., Crawford, S.M. (1989). Anthracycline-induced toxicity affecting palmar and plantar skin. British Journal of Cancer, 59: 814.

de Jong, J., Schoofs, P.R., Snabilié, A.M., Bast, A., van der Vijgh, J.F. (1993). The role of biotransformation in anthracycline-induced cardiotoxicity in mice. Journal of Pharmacology and Experimental Therapeutics, 266: 1312 - 1320.

Juliano, R.L. (1991). A new perspective for drug delivery research. In Targeted Drug Delivery, Juliano, R.L. (ed). Springer Verlag, New York, pp1 - 10.

Katagari, Y., Mabuchi, K., Itakura, T., Naora, K., Iwamoto, K., Nozu, Y., Hirai, S., Ikeda, N., Kawai, T. (1989). Adriamycin-lipiodol suspension for i.a. chemotherapy of hepatocellular carcinoma. Cancer Chemotherapy and Pharmacology, 23: 238 - 242.

Kato, S., Ideguchi, H., Muta, K., Nishimura, J., Nawata, H. (1991). Absence of correlation between cytotoxicity and drug transport by P-glycoprotein in clinical leukemic cells. European Journal of Hematology, 47: 146 - 151.

Kato, Y., Watanabe, K., Hosokawa, T., Hayakawa, E., Ito, K. (1993). Modification of liposomes by addition of HCO60. I. Targeting of liposomes to liver by the addition of HCO60 to liposomes. Biology and Pharmacy Bulletin, 16: 960 - 964.

Kattan,J., Droz, J-P., Couvreur, P., Marino, J-P., Boutan-Laroze, A., Rougier, P., Brault, P., Vranckx, H., Grognet, J-M., Morge, X., Sancho-Garnier, H. (1992). Phase I clinical trial and pharmacokinetic evaluation of doxorubicin carried by polyisohexylcyanoacrylate nanoparticles. Investigational New Drugs, 10: 191 - 199.

Keizer, H.G., Schuurhuis, G.J., Broxterman, H.J., Lankelma, J., Schoonen, W.G.E.J., van Rijn, J., Pinedo, H.M., Joenje, H. (1989). Correlation of multidrug resistance with decreased drug accumulation, altered subcellular drug distribution, and increased P-glycoprotein expression in cultured SW-1573 human lung tumour cells. Cancer Research, 49: 2988 - 2993.

Keizer, H.G., Pinedo, H.M., Schuurhuis, G.J., Joenje, H. (1990). Doxorubicin

(adriamycin): a critical review of free radical-dependent mechanisms of cytotoxicity. Pharmacology and Therapeutics, 47: 219 - 231.

Kemps, J.M.A., Crommelin, D.J.A. (1988). Chemische stabiliteit van fosfolipiden in farmaceutische preparaten. Pharmaceutisch Weekblad, 123: 355 - 363.

Kerr, D.J., Rogerson, A., Morrison, G.J., Florence, A.T., Kaye, S.B. (1988). Antitumour activity and pharmacokinetics of niosome encapsulated adriamycin in monolayer, spheroid and xenograft. British Journal of Cancer, 58: 432 - 436.

Kim, J-G., Kim, J-D. (1991). Vesicle to micelle transitions of egg phosphatidylcholine liposomes induced by nonionic surfactants, poly(oxyethylene) cetyl ethers. Journal of Biochemistry, 110: 436 - 442.

Kirby, C., Clarke, J., Gregoriadis, G. (1980). Effect of the cholesterol content of small unilamellar liposomes on their stability *in vivo* and *in vitro*. Biochemical Journal, 186: 591 - 598.

Kirby, C., Gregoriadis, G. (1983). The effect of lipid composition of small unilamellar liposomes containing melphalan and vincristine on drug clearance after injection into mice. Biochemical Pharmacology, 32; 609 - 615.

Kiwada, H., Nimura, H., Fujisaki, Y., Yamada, S., Kato, Y. (1985a). Application of synthetic alkyl glycoside vesicles as drug carriers. I. Preparation and physical

properties. Chemical and Pharmaceutical Bulletin, 33; 753 - 759.

Kiwada, H., Nimura, H., Kato, Y. (1985b). Tissue distribution and pharmacokinetic evaluation of the targeting efficiency of synthetic alkyl glycoside vesicles. Chemical and Pharmaceutical Bulletin, 33: 2475 - 2482.

Kiwada, H., Nakajima, I., Matsuura, H, Tsuji, M., Kato, Y. (1988). Application of synthetic alkylglycoside vesicles as drug carriers. III. Plasma components affecting stability of the vesicles. Chemical and Pharmaceutical Bulletin, 36: 1841 - 1846.

Klibanov, A.L., Maruyama, K., Torchilin, V., Huang, L. (1990). Amphipathic polyethyleneglycols effectively prolong the circulation time of liposomes. FEBS Letters, 268: 235 - 237.

Konohana, A. (1992). Blue-gray pigmentation in a patient receiving doxorubicin. Journal of Dermatology, 19: 250 - 252.

Kresta, A., Shek, P.N., Odumeru, J., Bohnen, J.M.A. (1993). Distribution of free and liposomal-encapsulated cefoxitin in experimental intra-abdominal sepsis in rats. Journal of Pharmacy and Pharmacology, 45; 779 - 783.

Kumar, L., Kochupillai, V. (1990). Doxorubicin induced hyperpigmentation. New Zealand Medical Journal, 103: 165.

Kume, Y., Maeda, F., Harashima, H., Kiwada, H. (1991). Saturable, non-Michaelis-Menten uptake of liposomes by the reticuloendothelial system. Journal of Pharmacy and Pharmacology, 43: 162 - 166.

Lahtinen, R. Kuikka, J., Nousiainen, T., Uusitupa, M., Länsimies, E. (1991). Cardiotoxicity of epirubicin and doxorubicin: a double-blind randomized study. European Journal of Haematology, 46: 301 - 305.

de Lange, J.H.M., Schipper, N.W., Schuurhuis, G.J., ten Kate, T.K., van Heijningen, Th.H.M., Pinedo, H.M., Lankelma, J., Baak, J.P.A. (1992). Quantification by laser scan microscopy of intracellular doxorubicin distribution. Cytometry, 13: 571 - 576.

Lasic, D.D., Martin, F.J., Gabizon, A., Huang, S.K., Papahadjopoulos, D. (1991). Sterically stabilized liposomes: a hypothesis on the molecular origin of the extended circulation times. Biochimica et Biophysica Acta, 1070: 187 - 192.

Lasic, D. (1992). Liposomes. American Scientist, 80: 20 - 31.

Lee, F.Y., Sciandra, J., Siemann, D.W. (1989). A study of the mechanism of adriamycin resistance *in vivo*. Biochemical Pharmacology, 38: 3697 - 3705.

Lesieur, S., Grabielle-Madelmont, C., Paternostre, M-T., Moreau, J-M., Handjani-Vila, R-M., Ollivon, M. (1990). Action of octylglucoside on non-ionic monoalkyl amphiphile-cholesterol vesicles: study of the solubilization mechanism. Chemistry and

Physics of Lipids, 56: 109 - 121.

Levy, D., Gulik, A., Seigneuret, M., Rigaud, J-L. (1990). Phospholipid vesicle solubilization and reconstitution by detergents. Symmetrical analysis of the two processes using octaethylene glycol mon-*n*-dodecyl ether. Biochemistry, 29: 9480 - 9488.

Leyland-Jones, B. (1993). Targeted drug delivery. Seminars in Oncology, 20: 12 - 17.

Lin, S-Y., Wu, W-H., Lui, W-Y. (1992). *In vitro* release, pharmacokinetic and tissue distribution studies of doxorubicin hydrochloride (adriamycin HCl) encapsulated in lipiodolized w/o emulsions and w/o/w multiple emulsions. Pharmazie. 47: 439 - 443.

Lipowsky, R. (1991). The conformation of membranes. Nature, 349: 475 - 481.

Lowry, O.H., Rosebrough, N.J., Farr, A.L., Randall, R.J. (1951). Protein measurement with Folin phenol reagent. Journal of Biological Chemistry, 193: 265 - 275.

Loveless, H., Arena, E., Felsted, R.L., Bachur, N.R. (1978). Comparative mammalian metabolism of adriamycin and daunorubicin. Cancer Research, 38: 593 - 598.

Magnusson, J.O., Bergdahl, B., Bogentoft, C., Gustafsson, S., Jonsson, U.E. (1984). Increased metabolism to dihydrodigoxin after intake of a microencapsulated

formulation of digoxin. European Journal of Clinical Pharmacology, 27: 197 - 202.

Maincent, P., Thouvenot, P., Amicabile, C., Hoffman, M., Kreuter, J., Couvreur, P., Devissaguet, J.P. (1992). Lymphatic targeting of polymeric nanoparticles after intraperitoneal administration in rats. Pharmaceutical Research, 9: 1534 - 1539.

Martin, D.S., Balis, M.E., Fisher, B., Frei, E., Freireich, E.J., Heppner, G.H., Holland, J.F., Houghton, J.A., Houghton, P., Johnson, R.K., Mittelman, A., Rustum, Y., Sawyer, R.C., Schmid, F,.A., Stolfi, R.L., Young, C.W. (1986). Role of murine tumour models in cancer treatment research. Cancer Research, 46: 2189 - 2192.

Martí, A., Armengol, X., Estelrich, J., Hernández-Borrell, J. (1992). Encapsulation of doxorubicin in neutral liposomes by passive methods: evidence of drug-lipid interaction at neutral pH. Journal of Microencapsulation, 9: 191 - 200.

Martini, F. (1992). Fundamentals of Anatomy and Physiology (2nd edition). Prentice Halls, New Jersey.

Maruyama, K., Unezaki, S., Takahashi, N., Iwatsuru, M. (1993). Enhanced delivery of doxorubicin to tumour by long circulating thermosensitive liposomes and local hyperthermia. Biochimica et Biophysica Acta, 1149: 209 - 216.

Mayer, L.D., Bally, M.B., Hope, M.J., Cullis, P.R. (1985). Uptake of antineoplastic agents into large unilamellar vesicles in response to a membrane potential. Biochimica

et Biophysica Acta, 816: 294 - 302.

Mayhew, E., Lazo, R., Vail, W.J., King, J., Green, A.M. (1984). Characterization of liposomes prepared using a microemulsifier. Biochimica et Biophysica Acta, 775: 169 - 174.

Mayhew, E., Cimino, M., Klemperer, J., Lazo, R., Wiernikowski, J., Arbuck, S. (1990). Free and liposomal doxorubicin treatment of intraperitoneal colon 26 tumour: therapeutic and pharmacological studies. Selective Cancer Therapeutics, 6: 193 - 209.

Menger, F. (1993). Chemical collectivism. Chemistry in Britain, March - April 1993: 300 - 302.

Mickisch, G., Rahman, A., Pastan, I., Gottesman, M.M. (1992). Increased effectiveness of liposome-encapsulated doxorubicin in multidrug-resistant-transgenic mice compared to free doxorubicin. Journal of the National Cancer Institute, 84: 804 805.

Minderman, H., Linssen, P., Wessels, J., Haanen, C. (1993). Cell cycle uptake, retention and toxicity of idarubicin , daunorubicin and doxorubicin. Anticancer Research, 13: 1161 - 1166.

Montero, M.T., Martí, A., Hernàndez-Borrel, J. (1993). The active trapping of doxorubicin in liposomes by pH gradient: photon correlation spectroscopy and

fluorimetric study. International Journal of Pharmaceutics, 96: 157 - 165.

Mori, A., Klibanov, A.L., Torchilin, V.P., Huang, L. (1991). Influence of the steric barrier activity of amphipathic poly(ethyleneglycol) and ganglioside GM_1 on the circulation time of liposomes and on the target binding of immunoliposomes *in vivo*. FEBS letters, 284: 263 - 266.

Moser, P., Marchant-Arvier, M., Labrude, P., Handjani-Vila, R-M., Vigneron, C. (1989). *Niosomes d'hémoglobine I. Préparation, propriétés physicochemiques et oxyphoriques, stabilité.* Pharmaceutica Acta Helvetiae, 64; 192 - 202.

Moser, P., Marchant-Arvier, M., Labrude, P., Vigneron, C. (1990). *Niosomes d'hémoglobine II. Interactions in vitro avec les protéines plasmatiques et les phagocytes.* Pharmaceutica Acta Helvetiae, 65: 82 - 92.

Mross,K., Mayer, U., Hamm, K., Burk, K., Hossfeld, D.K. (1990). Pharmacokinetics and metabolism of iodo-doxorubicin and doxorubicin in humans. European Journal of Clinical Pharmacology, 39: 507 - 513.

Muindi, J., Sinha, B.K., Gianni, L., Myers, C. (1985). Thiol-dependent DNA damage produced by anthracycline-iron complexes. Molecular Pharmacology, 27; 356 - 365.

Mushlin, P.S., Cusack, B.J., Boucek, R.J., Andrejuk, T., Li, X., Olson, R.D. (1993). Time-related increases in cardiac concentrations of doxorubicinol could interact with

doxorubicin to depress myocardial contractile function. British Journal of Pharmacology, 110: 975 - 982.

Mustonen, P., Kinnunen, P.K.J. (1993). On the reversal by deoxyribonucleic acid of the binding of adriamycin to cardiolipin-containing liposomes. Journal of Biological Chemistry, 268: 1074 - 1080.

Myers, C.E., McGuire, W.P., Liss, R.H., Ifrim, I., Grotzinger, K., Young, R.C. (1977). Adriamycin; the role of lipid peroxidation in cardiac toxicity and tumour response. Science, 197: 165 - 167.

Nair, S., Singh, S.V., Samy, T.S.A., Krishnan, A. (1990). Anthracycline resistance in murine tumour leukemic P388 cells. Biochemical Pharmacology, 39: 723 - 728.

Neri, B., Cini-Neri, G., Bandinelli, M., Pacini, P., Bartalucci, S., Ciapini, A. (1989). Doxorubicin and epirubicin cardiotoxicity: experimental and clinical aspects. International Journal of Clinical Pharmacology, Therapy and Toxicology, 27: 217 - 221.

Neumann, R., Ringsdorf, H. (1986). Peptide liposomes from amphiphilic amino acids. Journal of the American Chemical Society, 108: 487 - 490.

Nugent, L.J., Jain, R.K. (1984). Extravascular diffusion in normal and neoplastic tissue. Cancer Research, 44: 238 - 244.

Ohta, S., Igarashi, S., Honda, A., Sato, S., Hanai, N. (1993). Cytotoxicity of adriamycin - containing immunoliposomes targeted with anti-ganglioside monoclonal antibodies. Anticancer Research, 13: 331 - 336.

Okahata, Y., Tanamachi, S., Nagai, M., Kunitake, T. (1981). Synthetic bilayer membranes prepared from dialkyl amphiphiles with non-ionic and zwitterionic head groups. Journal of Colloid and Interfacial Science, 82: 401 - 417.

Olin, T., Saldeen, T. (1964). The lymphatic pathways from the peritoneal cavity: a lymphangiographic study in the rat. Cancer Research, 24: 1700 - 1711.

Olson, R.D., Mushlin, P.S., Brenner, D.E., Fleischer, S., Cusack, B.J., Chang, B.K., Boucek, R.J. Jr. (1988). Doxorubicin cardiotoxicity may be caused by its metabolite, doxorubicinol. Proceedings of the National Academy of Science, 85; 3585 - 3589.

Olson, R.D., Mushlin, P.S. (1990). Doxorubicin cardiotoxicity; analysis of prevailing hypotheses. FASEB Journal, 4; 3076 - 3086.

Oudard, S., Thierry, A., Jorgensen, T.J., Rahman, A. (1991). Sensitization of multidrug-resistant colon cancer cells to doxorubicin encapsulated in liposomes. Cancer Chemotherapy and Pharmacology, 28; 259 - 265.

Owen, R.R., Sells, R.A., Gilmore, I.T., New, R.R.C., Stringer, R.E. (1992). A phase I clinical evaluation of liposome entrapped doxorubicin (Lip-Dox) in patients with

primary and metastatic hepatic malignancy. Anti-Cancer Drugs, 3: 101 - 107.

Oya, M., Shimada, T., Nakamura, M., Uchida, Y. (1993). Functional morphology of the lymphatic system in the monkey diaphragm, 56: 37 - 47.

Özer, A.Y., Hincal, A.A., Bouwstra, J.A. (1991). A novel drug delivery system: non-ionic surfactant vesicles. European Journal of Pharmacy and Biopharmaceutics, 37: 75 - 79.

Papahadjopuolos, D., Gabizon, A. (1990). Liposomes designed to avoid the reticuloendothelial system. In Horizons in Membrane Biotechnology, Wiley-Liss, Inc., New York, pp85 - 93.

Papahadjopoulos, D., Allen, T.M., Gabizon, A., Mayhew, E., Matthay, K., Huang, S.K., Lee, K-D., Woodle, M.C., Lasic, D.D., Redemann, C., Martin, F.J. (1991). Sterically stabilized liposomes: improvements in pharmacokinetics and antitumour therapeutic efficacy. Proceedings of the National Academy of Science, 88; 11460 - 11464.

Parr, M.J., Bally, M., Cullis, P.R. (1993). The presence of G_{M1} in liposomes with entrapped doxorubicin does not prevent RES blockade. Biochimica et Biophysica Acta, 1168: 249 - 252.

Parthasarathi, G., Udupa, N., Umadevi, P., Pillai, G.K. (1994). Niosome encapsulation

vincristine sulfate: improved anticancer activity with reduced toxicity in mice. Journal of Drug Targeting, (in press).

Paternostre, M-T., Roux, M., Rigaud, J-L. (1988). Mechanism of membrane protein insertion into liposomes during reconstitution procedures involving the use of detergents. 1. Solubilization of large unilamellar liposomes (prepared by reverse-phase evaporation) by triton X-100, octyl glucoside, and sodium cholate. Biochemistry, 27: 2668 - 2677.

Peterson, H-I., Appelgren, K.L. (1973). Experimental studies on the uptake and retention of labelled proteins in a rat tumour. European Journal of Cancer, 9: 543 - 547.

Phillies, G.D.J. (1990). Quasielastic light scattering. Analytical Chemistry, 62; 1049 - 1057.

Philppott, J.R., Liautard, J.P. (1993). A mild method for the preparation of very large unilamellar liposomes. In Liposome Technology Volume I (2nd edition), Gregoriadis, G. (ed), CRC Press, London, pp82 - 110.

Piscitelli, S.C., Rodvold, K.A., Rushing, D.A., Tewksbury, D.A. (1993). Pharmacokinetics and pharmacodynamics of doxorubicin in patients with small cell lung cancer. Clinical Pharmacology and Therapeutics, 53; 555 - 561.

Powis, G. (1987). Metabolism and reactions of quinoid anticancer agents. Pharmacological therapeutics, 35: 57 - 162.

Praet, M., Defrise-Quertain, F., Ruysschaert, J.M. (1993). Comparison of adriamycin and derivatives uptake into large unilamellar lipid vesicles in response to a membrane potential. Biochimica et Biophysica Acta, 1148: 342 - 350.

Preiss, R., Sohr, R., Kittelmann, B., Müller, E., Haase, D. (1989). Investigations on the dose-dependent pharmacokinetics of adriamycin and its metabolites. International Journal of Clinical Pharmacology, Therapy and Toxicology, 27: 156 -164.

Priebe, W., Van, N.T., Burke, T.G., Perez-Soler, R. (1993). Removal of the basic centre from doxorubicin partially overcomes multidrug resistance and decreases cardiotoxicity. Anti-cancer Drugs, 4: 37 - 48.

Rahman, A., White, G., More, N., Schein, P.S. (1985). Pharmacological, toxicological, and therapeutic evaluation in mice of doxorubicin entrapped in cardiolipin liposomes. Cancer Research, 45: 796 - 803.

Rahman, A., Treat, J., Roh, J-K., Potkul, L.A., Alvord, W.G., Forst, D., Wooley, P.V. (1990). A phase I clinical trial and pharmacokinetic evaluation of liposome-encapsulated doxorubicin. Journal of Clinical Oncology, 8: 1093 - 1100.

Rahman, A., Husain, S.R., Siddiqui, J., Verma, M., Agresti, M., Center, M., Safa,

A.R., Glazer, R.I. (1992). Liposome-mediated modulation of multidrug resistance in human HL-60 leukemia cells. Journal of the National Cancer Institute, 84: 1909 - 1915.

Ralston, E., Blumenthal, R., Weinstein, J.N., Sharrow, S.O., Henkart, P. (1980). Lysophosphatidylcholine in liposomal membranes. Biochimica et Biophysica Acta, 597: 543 - 551.

Ramanchandran, C., Yuan, Z.K., Huang, X.L., Krishan, A. (1993). Doxorubicin resistance in human melanoma cells: MDR-1 and glutathione S-transferase π gene expression. Biochemical Pharmacology, 45: 743 - 751.

Riordan, J.R., Ling, V. (1979). Purification of P-glycoprotein from plasma membrane vesicles of chinese hamster ovary cell mutants with reduced colchicine permeability. Journal of Biological Chemistry, 254: 12701 - 12705.

Riordan, J.R., Deuchars, K., Kartner, N., Alon, N., Trent, J., Ling, V. (1985). Amplification of P-glycoprotein genes in multidrug resistant mammalian cell lines. Nature, 316: 817 - 819.

Roepe, P.D. (1992). Analysis of the steady-state and initial rate of doxorubicin efflux from a species of multidrug-resistant cells expressing different levels of P-glycoprotein. Biochemistry, 31; 12555 - 12564.

Rogerson, A., Cummings, J., Florence, A.T. (1987). Adriamycin-loaded niosomes: drug entrapment, stability and release. Journal of Microencapsulation, 4: 321 - 328.

Rogerson, A., Cummings, J., Willmott, N., Florence, A.T. (1988). The distribution of doxorubicin in mice following administration in niosomes. Journal of Pharmacy and Pharmacology, 40; 337 - 342.

Rogerson, A., Baillie, A.J., Florence, A.T. (1989). Some properties of non-ionic surfactant vesicles and their component mono and dialkyl non-ionic polyglycerol surfactants. In Surfactants in Solution, volume 8, Mittal, K. (ed), Plenum Press, New York, pp321 - 332.

Sada, E., Katoh, S., Terashima, M., Kawahara, H., Katoh, M. (1990). Effects of surface charges and cholesterol content on amino acid permeabilities of small unilamellar vesicles. Journal of Pharmaceutical Sciences, 79: 232 - 235.

Sadasivan, R., Morgan, R., Fabian, C., Stephens, R. (1991). Reversal of multidrug resistance in HL-60 cells by verapamil and liposome-encapsulated doxorubicin. Cancer Letters, 57: 165 - 171.

Schenk, P., Nuhn, P., Fichtner, I., Arndt, D. (1990). Studies on sucrose-palmitate-stearate-containing vesicles encapsulating the cytostatic drug methylglyoxal-bis-guanyl-hydrazone. Pharmazie, 45: 747 - 749.

Schott, B., Londos-Gagliardi, D., Ries, C., Huet, S., Robert, J. (1993). Pharmacological and molecular characterization of intrinsic and acquired doxorubicin resistance in murine tumour cell lines. Journal of Cancer Research and Clinical Oncology, 119: 527 - 532.

Schurtenberger, P., Hauser, H. (1993). Size characterization of liposomes. In Liposome Technology Volume I, (2nd edition), Gregoriadis, G. (ed). CRC press, London, pp253 - 270.

Schuurhuis, G.J., Broxterman, H.J., de Lange, J.H.M., Pinedo, H.M., van Heijningen, T.H.M., Kuiper, C.M., Scheffer, G.L., Scheper, R.J., van Kalken, C.K.K., Baak, J.P.A., Lankelma, J. (1991). Early multidrug resistance, defined by changes in intracellular doxorubicin distribution, independent of P-glycoprotein. British Journal of Cancer, 64: 857 - 861.

Senior, J., Delgado, C., Fisher, D., Tilcock, C., Gregoriadis, G. (1991). Influence of surface hydrophilicity of liposomes on their interaction with plasma protein and clearance from the circulation: studies with poly(ethylene glycol)-coated vesicles. Biochimica et Biophysica Acta, 1062: 77 - 82.

Seras, M., Handjani-Vila, R-M., Ollivon, M., Lesieur, S. (1992). Kinetic aspects of the solubilization of non-ionic monoalkyl amphiphile-cholesterol vesicles by octylglucoside. Chemistry and Physics of Lipids, 63: 1- 14.

Siemann, D. (1987). Satisfactory and unsatisfactory tumour models: factors influencing the choice of a tumour model for experimental evaluation. In Rodent Tumour Models in Experimental Cancer Chemotherapy, Kallman, R.F. (ed), Pergamon Press, New York, pp12 - 15.

Sinha, B.K., Gregory, J.L. (1981). Role of one-electron and two-electron reduction products of adriamycin and daunomycin in deoxyribonucleic acid binding. Biochemical Pharmacology, 30: 2626 - 2629.

Skehan, P., Storeng, R., Scudiero, D., Monks, A., McMahon, J., Vistica, D., Warren, J.T., Bokesh, H., Kenney, S., Boyd, M.R. (1990). New colorimetric assay for anticancer-drug screening. Journal of the National Cancer Institute, 82: 1107 - 1113.

Skladanowski, A., Konopa, J. (1993). Adriamycin and daunomycin induce programmed cell death (apoptosis) in tumour cells. Biochemical Pharmacology, 46: 375 - 382.

Small, D.M., Penkett, S.A., Chapman, D. (1969). Studies on simple and mixed bile salt micelles by nuclear magnetic resonance spectroscopy. Biochimica et Biophysica Acta, 176: 178 - 179.

Sognier, M., Zhang, Y., Eberle, R.L., Belli, J.A. (1992). Characterization of adriamycin-resistant and radiation-sensitive chinese hamster cell lines. Biochemical Pharmacology, 44: 1859 - 1868.

Sokolove, P. (1991). Oxidation of mitochondrial pyridine nucleotides by aglycone derivatives of adriamycin. Archives of Biochemistry and Biophysics, 284: 292 - 297.

Sokolove, P.M., Shinaberry, R.G. (1988). Na^+-independent release of Ca^{2+} from rat heart mitochondria. Biochemical Pharmacology, 37: 803 - 812.

Solary, E., Bidan, J-M., Calvo, F., Chauffert, B., Calliot, D., Mugneret, F., Gauville, C., Tsuruo, T., Carli, P-M., Guy, H. (1991). P-glycoprotein expression and *in vitro* reversion of doxorubicin resistance by verapamil in clinical specimens from acute leukaemia and myeloma. Leukemia, 5: 592 - 597.

Speth, P.A.J., van Hoesel, Q.G.C.M., Haanen, C. (1988). Clinical pharmacokinetics of doxorubicin. Clinical Pharmacokinetics, 15: 15 - 31.

Steel, G.G. (1987). How well do xenografts maintain the therapeutic response characteristics of the source tumour in the donor patient? In Rodent Tumour Models in Experimental Cancer Chemotherapy, Kallman, R.F. (ed), Pergamon Press, New York, pp205 - 208.

Steinherz, L., Steinherz, P. (1991). Delayed cardiac toxicity from anthracycline therapy. Pediatrician, 18: 49 - 52.

Storm, G., Steerenberg, P.A., Emmen, F., van Borssum Waalkes, M., Crommelin, D.J.A. (1988). Release of doxorubicin from peritoneal macrophages exposed *in vivo*

to doxorubicin-containing liposomes. Biochimica et Biophysica Acta, 965: 136 - 145.

Takanashi, S., Bachur, N.R. (1976). Adriamycin metabolism in man. Drug Metabolism and Disposition, 4: 79 - 87.

Tanaka, M., Fukuda, H., Horiuchi, T. (1990). Properties of the aqueous vesicle dispersion formed with poly(oxyethylene)hydrogenated castor oil. Journal of Applied Organic Chemistry and Synthesis, 67: 55 - 60.

Tasset, C., Goethals, F., Préat, V., Roland, M. (1990). Effect of polyoxyethylene glycol (24) cholesterol on the solubility, toxicity and activity of amphotericin B. International Journal of Pharmaceutics, 58: 41 - 48.

Tewey, K.M., Rowe, T.C., Yang, L., Halligan, B.D., Liu, L.F. (1984). Adriamycin-induced DNA damage mediated by mammalian DNA topoisomerase II. Science, 226: 466 - 468.

Thierry, A.R., Jorgensen, T.J., Forst, D., Belli, J.A., Dritschilo, A., Rahman, A. (1989). Modulation of multidrug resistance in chinese hamster cells by liposome-encapsulated doxorubicin. Cancer Communications, 1: 311 - 316.

Thierry, A.R., Dritschilo, A., Rahman, A. (1992). Effect of liposomes on P-glycoprotein function in multidrug resistant cells. Biochemical and Biophysical Research Communications, 187: 1098 - 1105.

Thierry, A.R., Vigé, D., Coughlin, S.S., Belli, J.A., Dritschillo, A., Rahman, A. (1993). Modulation of doxorubicin resistance in multidrug-resistant cells by liposomes. FASEB Journal, 7: 572 - 579.

Thies, R.L., Cowens, D.W., Cullis, P.R., Bally, M.B., Mayer, L.D. (1990). Method for rapid separation of liposome-associated doxorubicin from free doxorubicin in plasma. Analytical Biochemistry, 188: 65 - 71.

Titulaer, H.A.C., Eling W.M.C., Crommelin, D.J.A., Peters, P.A.M., Zuidema, J. (1990). The parenteral controlled release of liposome encapsulated chloroquine in mice. Journal of Pharmacy and Pharmacology, 42: 529 - 532.

Treat, J. (1989). Liposome encapsulated doxorubicin preliminary results of phase I and phase II trials. In Liposomes in the Therapy of Infectious Diseases and Cancer, Lopez-Berenstein, G., Fidler, I.J. (eds), Alan R. Liss, New York, pp353 - 365.

Tritton, T.R., Yee, G. (1982). The anticancer agent adriamycin can be actively cytotoxic without entering cells. Science, 217: 248 - 250.

Tsilibary, E.C., Wissig, S.L. (1983). Lymphatic absorption from the peritoneal cavity: regulation of patency of mesothelial stomata. Microvascular Research, 25: 22 - 39.

Udupa, N., Chandraprakash, K.S., Umadevi, P., Pillai, G.K. (1993). Formulation and evaluation of methotrexate niosomes. Drug Development and Industrial Pharmacy,

19: 1331 - 1342.

Unezaki, S., Maruyama, K., Ishida, O., Takahashi, N., Iwatsuru, M. (1993). Enhanced tumour targeting of doxorubicin by ganglioside GM1-bearing long-circulating liposomes. Journal of Drug Targeting, 1: 287 - 292.

Usansky, J.I., Liebert, M., Wedemeyer, G., Grossmann, H.B., Wagner, J.G. (1991). The uptake and efflux of doxorubicin by a sensitive human bladder cancer cell line and its doxorubicin-resistant subline. Selective Cancer Therapeutics, 7: 139 - 150.

Vaage, J., Mayhew, E., Lasic, D., Martin, F. (1992). Therapy of primary and metastatic mouse mammary carcinomas with doxorubicin encapsulated in long circulating liposomes. International Journal of Cancer, 51: 942 - 948.

Vanlerberghe, G., Handjani-Vila, R-M., Berthelot, C., Sebag, H. (1972). *Synthèse et activité de surface comparée d'une série de nouveaux dérivéś non ioniques.* Proceedings of the 6th International Congress on Surface Active Agents, 1972, Carl Hanser, München (1973), pp139 - 155.

Vanlerberghe, G., Handjani-Vila, R-M., Ribier, A. (1978). *Les "niosomes" une nouvelle famille de vésicules à base d'amphiphiles non ioniques.* Colloques Nationaux du C.N.R.S., No. 938, pp303 - 311.

Vemuri, S., Yu, C-D., Wangsatorntanakun, V., Roosdorp, N. (1990). Large scale

production of liposomes by a microfluidizer. Drug Development and Industrial Pharmacy, 16: 2243 - 2256.

Volm, M., Mattern, J. (1993). Detection of multiple resistance mechanisms in untreated human lung cancer. Onkologie, 16: 189 - 194.

Walter, A., Vinson, P.K., Kaplun, A., Talmon, Y. (1991). Intermediate structures in the cholate-phosphatidylcholine vesicle-micelle transition. Biophysical Journal, 60: 1315 - 1325.

Wang, A.,H.-J., Ughetto, G., Quigley, G.J., Rich, A. (1987). Interactions between an anthracycline antibiotic and DNA: molecular structure of daunomycin complexed to d(CpGpTpApCpG) at 1.2-Å resolution. Biochemistry, 26: 1152 - 1163.

Washington, C., Davis, S.S. (1988). The production of parenteral feeding emulsions by microfluidizer. International Journal of Pharmaceutics, 44: 169 - 176.

Weinstein, J.N., Yoshikami, S., Henkart, P., Blumenthal, R., Hagins, W.A. (1977). Liposome-cell interaction: transfer and intracellular release of a trapped fluorescent marker. Science, 195: 489 - 491.

Williams, S., Alosco, T.R., Mayhew, E., Lasic, D.D., Martin, F.J., Bankert, R.B. (1993). Arrest of human lung tumour xenograft growth in severe combined immunodeficient mice using doxorubicin encapsulated in sterically stabilized

liposomes. Cancer Research, 53: 3964 - 3967.

Willmott, N., Kamel, H.M.H., Cummings, J., Stuart, J.F.B., Florence, A.T. (1984). Adriamycin-loaded albumin microspheres: lung entrapment and fate in the rat. In Microspheres and Drug Therapy. Pharmaceutical, Immunological and Medical Aspects. Davis, S.S., Illum, L., McVie, J.G., Tomlinson, E. (eds), Elsevier Science Publishers, London, pp205 - 215.

Willmott, N., Cummings, J. (1987). Increased anti-tumour effect of adriamycin-loaded albumin microspheres is associated with anaerobic bioreduction of drug in tumour tissue. Biochemical Pharmacology, 36: 521 - 526.

de Wolf, F.A. (1991). Binding of doxorubicin to cardiolipin as compared to other anionic phospholipids - an evaluation of electrostatic effects. Bioscience Reports, 11: 275 - 284.

de Wolf, F.A., Maliepaard, M., van Dorsten, F., Berghuis, I., Nicolay, K., de Kruijff, B. (1991a). Comparable interaction of doxorubicin with various acidic phospholipids results in changes of lipid order and dynamics. Biochimica et Biophysica Acta, 1096: 67 - 79.

de Wolf, F.A., Demel, R.A., Bets, D., van Kats, C., de Kruijff, B. (1991b). Characterization of the interaction of doxorubicin with (poly)phosphoinositides in model systems. FEBS Letters, 288: 237 - 240.

de Wolf, F.A., Staffhorst, R.W.H.M., Smits, H-P., Onwezen, M.F., de Kruijff, B. (1993). Role of anionic phospholipids in the interaction of doxorubicin and plasma membrane vesicles: drug binding and structural consequences in bacterial systems. Biochemistry, 32: 6688 - 6695.

Woodcock, D.M., Linsenmeyer, M.E., Chojnowski, G., Kriegler, A.B., Nink, V., Webster, L.K., Sawyer, W.H. (1992). Reversal of multidrug resistance by surfactants. British Journal of Cancer, 66: 62 - 68.

Woodle, M.C., Lasic, D.D. (1992). Sterically stabilized liposomes. Biochimica et Biophysica Acta, 1113: 171 - 199.

Woodle, M.C., Matthay, K.K., Newman, M.S., Hidayat, J.E., Collins, L.R., Redemann, C., Martin, F.J., Papahadjopoulos, D. (1992). Versatility in lipid compositions showing prolonged circulation with sterically stabilized liposomes. Biochimica et Biophysica Acta, 1105: 193 - 200.

Yanagawa, H., Ogawa, Y., Furuta, H., Tsuno, K. (1989). Spontaneous formation of superhelical strands. Journal of the American Chemical Society, 111: 4567 - 4570.

Yeung, T.K., Hopewell, J.W., Simmonds, R.H., Seymour, L.W., Duncan, R., Bellini, O., Grandi, M., Spreafico, F., Strohalm, J., Ulbrich, K. (1991). Reduced cardiotoxicity of doxorubicin given in the form of N-(2-hydroxypropyl)methacrylamide conjugates: an experimental study in the rat. Cancer Chemotherapy and Pharmacology, 29: 105 -

111.

Yokoyama, M., Miyauchi, M., Yamada, N., Okano, T., Sakurai, Y., Kataoka, K., Inoue, S. (1990). Characterization and anticancer activity of the micelle-forming polymeric anticancer drug adriamycin-conjugated poly(ethylene glycol)-poly(aspartic acid) block copolymer. Cancer Research, 50: 1693 - 1700.

Yoshioka, T., Florence, A.T. (1994). Vesicle (niosome)-in-water-in-oil (v/w/o) emulsions: an *in vitro* study. International Journal of Pharmaceutics (in press).

Yoshioka, T., Sternberg, B., Florence, A.T. (1994). Preparation and properties of vesicles (niosomes) of sorbitan monoesters (Span 20, 40, 60 and 80) and a sorbitan triester (Span 85). International Journal of Pharmaceutics, 105: 1- 6.

Yourtee, D.M., Elkins, L.L., Nalvarte, E.L., Smith, R.E. (1992). Amplification of doxorubicin mutagenicity by cupric iron. Toxicology and Applied Pharmacology, 116: 57 - 65.

Zhang, Y., Sweet, K.M., Sognier, M.A., Belli, J.A. (1992). An enhanced ability for transforming adriamycin into a noncytotoxic form in a multdrug-resistant cell line (LZ-8). Biochemical Pharmacology, 44: 1869 - 1877.

Zou, Y., Horikoshi, I., Kasagi, T., Gu, X., Perez-Solar, R. (1993). Organ distribution and antitumour activity of free and liposomal doxorubicin injected into the hepatic

artery. Cancer Chemotherapy and Pharmacology, 31: 313 - 318.

PUBLICATIONS

Copies of publications generated by this study appear on the following pages. In addition to these are the following:

1. Uchegbu, I.F., Turton, J.A., Double J.A., Florence, A.T. (1994). Drug distribution and a pulmonary adverse effect of intraperitoneally-administered doxorubicin niosomes in male AKR mice. Biopharmaceutics and Drug Disposition (in press).

2. Uchegbu, I.F., Turton, J.A., Double, J.A., Florence, A.T. (1994). The distribution and metabolism of doxorubicin sorbitan monostearate (Span 60) niosomes in mice. (Submitted to British Journal of Cancer).

Journal of Pharmacy and Pharmacology, 44(S): (1992).

1052

DISCOMES: DISC-SHAPED VESICLES FROM A NON-IONIC SURFACTANT

I. Uchegbu, J Bouwstra[1], A.T. Florence, Centre for Drug Delivery Research, School of Pharmacy, University of London, London, U.K. and [1]Centre for Bio-Pharmaceutical Sciences, University of Leiden, The Netherlands

Addition of surfactants to vesicular dispersions can lead to solubilization of the vesicles and their subsequent translation into mixed micellar systems (Kim & Kim 1991). We have found that discoid structures, as seen under the light microscope, exist under certain conditions of the phase diagram of non-ionic surfactant vesicles (NSVs) prepared from a hexadecyl diglycerol ether, cholesterol and dicetylphosphate (DCP) (69:29:2) by hand-shaking and sonication followed by incubation with a soluble cholesteryl polyether. The NSV dispersions were incubated at 74°C for 1h with various proportions of Solulan C24, a poly [24] oxyethylene cholesteryl ether. Turbidity measurements were made at 350nm. "Break points" were identified in the turbidity vs surfactant concentration plots.

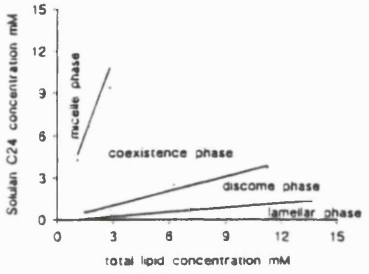

Fig. 1 Vesicle to micelle transition phase diagram Surfactant IV: cholesterol: DCP (69:39:2).

These points of sharp differences in turbidity are indicative of a change in phase of the dispersion. Based on these "break points", a partial phase diagram was constructed (Fig.1). Four phases can be identified : a lamellar phase, a micellar phase, an uncharacterized coexistence phase and a novel phase we have called the discome phase. Dispersions in the discome phase consisted of large "discomes" (30-60μm mean volume diameter). Lipids in the proportions found in the discome phase (i.e. surfactant, cholesterol, Solulan C24, DCP 49:19.5:29.5:2), when sonicated produced discomes. Formation of these discomes was accompanied by a slow increase in particle size of the dispersion which was almost clear immediately after sonication but slowly became more turbid and eventually showed the presence of a sediment.

Discomes entrap water soluble solutes. When lipid films were hydrated with 8mM of the aqueous volume marker 5(6)-carboxyfluorescein (CF) aqueous entrapment values of 1.209 ± 0.97 L mol^{-1} lipid representing 3.603 ± 2.916% entrapment were obtained. The release of CF was measured over a 24 hour period at room temperature and the discomes were found to retain 50% of their entrapped solute.

Kim, J., Kim, J. (1991) J Biochem 110: 436-442

AN INVESTIGATION INTO THE EFFECT OF DRUG INCLUSION ON THE DIELECTRIC RESPONSE, SURFACE TENSION AND DROPLET SIZE DISTRIBUTION OF SELF-EMULSIFYING SYSTEMS

D.Q.M.Craig[1], H.S.R.Lievens[2], K.G.Pitt[2], D.E.Storey[2]
[1]Centre for Material Sciences, School of Pharmacy, University of London, 29-39 Brunswick Square, London WC1N 1AX [2]Merck Sharp and Dohme Research Laboratories, Hoddesdon, Herts EN11 9BU

Self-emulsifying drug delivery systems (SEDDS) have been defined as mixtures of oil and surfactant which emulsify in water under conditions of gentle agitation (Pouton 1985). These systems may be used as drug delivery vehicles by incorporating poorly water-soluble drugs in the oil-surfactant mixture which may then be taken orally. In the present study, the effect of the inclusion of a poorly water soluble CCK_B receptor antagonist (L-365,260) on the behaviour of the oil/surfactant mixtures and the formed emulsions is reported. Two SEDDS vehicles were prepared containing Labrafil M2125 CS (Gattefosse, France) (56% or 62% v/v), Tween 80 (ICI Chemicals, Macclesfield) (30% v/v), propylene glycol (K. and K. Greef Ltd., Croydon) (3% v/v), distilled water (5% v/v) and 0% or 6% drug. The vehicles were analysed using a dielectric spectrometer (Dielectric Instrumentation Ltd., Herts) over a frequency range of 10^4 to 10^{-2}Hz. This technique involves the measurement of the response of a sample to an applied electric field and expresses that response in terms of the capacitance (storage component) and dielectric loss (loss component). Further details of this technique have been given elsewhere (Craig et al 1990). Surface tension measurements were performed using a DuNouy apparatus (Central Scientific Company, Chicago). Emulsions were prepared by adding 0.5ml of the vehicle to 200mls deionised water. Droplet size analysis was performed using a Malvern Mastersizer (Malvern Instruments Ltd, Malvern).

The results from the dielectric study are shown in Fig.1. The presence of the drug caused a decrease in both the capacitance and loss, suggesting an interaction between the drug and one or more charge carrying components of the vehicle. The surface tension decreased from 39.63mNm^{-1} (+/-0.36) to 37.86mNm^{-1} (+/-0.47) on addition of 6% w/v drug. The droplet size data is shown in Fig.2. The data shows that changing the formulation results in a bimodal distribution being seen for the system containing no drug while the emulsion containing 6% w/v drug showed a single distribution peak over the size range studied. The study therefore indicates that there is an interaction between the drug and the Labrafil vehicle and that the change in formulation on addition of the drug leads to a decrease in the surface tension, which may be expected to result in a decrease in vehicle/water interfacial energy and hence an increase in droplet surface area. The study therefore demonstrates that dielectric spectroscopy and surface tension measurements may detect changes in the vehicle properties on altering the formulation and that these changes may affect the size distribution of SEDDS emulsions.

Fig.1: Dielectric response of SEDDS vehicles

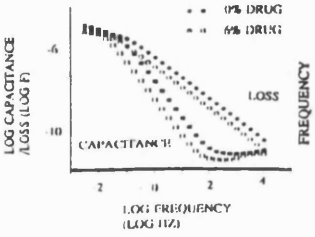

Fig.2: Droplet size distribution of formed emulsions

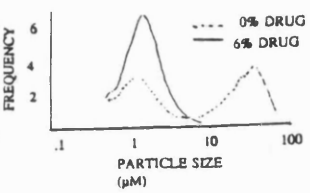

Craig, D.Q.M. et al (1990) Pharm.Tech.Int. 2:61-64
Pouton, C.W. (1985) Int.J.Pharm. 27:335-348

Reprinted from The Journal of Physical Chemistry, 1992, 96.

Large Disk-Shaped Structures (Discomes) in Nonionic Surfactant Vesicle to Micelle Transitions

Ijeoma F. Uchegbu, Joke A. Bouwstra,† and Alexander T. Florence*

Centre for Drug Delivery Research, School of Pharmacy, 29/39 Brunswick Square, University of London, London WC1N 1AX, U.K., and Center for Bio-Pharmaceutical Sciences, University of Leiden, Leiden, The Netherlands *(Received: July 20, 1992; In Final Form: September 23, 1992)*

Addition of surfactants to vesicular dispersions can lead to solubilization of the vesicles and their subsequent translation into mixed micellar systems (Kim and Kim, 1991). We have found that large discoid structures exist under certain conditions of the phase diagram of nonionic surfactant vesicles prepared from a hexadecyl diglycerol ether ($C_{16}G_2$), cholesterol, and dicetyl phosphate (DCP) in the molar ratio 69:29:2 by mechanical shaking and sonication followed by incubation with a soluble polyoxyethylene cholesteryl ether, Solulan C24, at 74 °C. Turbidity measurements were made at 350 nm. Break points were identified in the turbidity vs Solulan C24 concentration plots, where sharp differences in the turbidity of the dispersion occur, and are indicative of a change in phase. A partial phase diagram was constructed for the system in which four phases can be identified: a lamellar phase, a micellar phase, an uncharacterized phase, and a novel phase we have called the "discome" phase. Dispersions in the discome phase comprised large discomes (volume distribution mean diameter 12–60 μm). Lipids in the proportions found in the discome phase (i.e., $C_{16}G_2$:cholesterol:Solulan C24:DCP 49:19.5:29:2), when sonicated, produced discomes, formation of which was accompanied by a slow increase in particle size of the dispersion immediately after sonication. Discomes entrap water soluble solutes. When lipid films are hydrated with 8 mM 5(6)-carboxyfluorescein (CF), aqueous entrapment values of 1.209 ± 0.97 L/mol lipid were recorded. The release of CF over a 24-h period at room temperature was measured. Discomes were found to retain 50% of the entrapped CF. The drug delivery potential of these discomes in the field of ophthalmology is highlighted.

Introduction

The addition of critical amounts of soluble surface-active molecules to vesicular dispersions of phospholipids leads to the breakdown or solubilization of the vesicles and the formation of a mixed micellar phase. Such vesicle to micelle transitions, of sonicated egg yolk phosphatidylcholine liposomes, have been achieved by the addition of non-ionic surfactants of the polyoxyethylene cetyl ether class.[1] In this system a region occurs where lamellar and mixed micelles coexist. In studies of the vesicle–micelle transition in cholate–phosphatidylcholine systems, Walter et al.[2] identified structures intermediate between vesicles and micelles. On increasing the bile salt concentration, more multilamellar vesicles were detected, but, in addition, "open" vesicles, large (twenty to several hundred nanometers in diameter) bilayer sheets, and long (150–300 nm) flexible cylindrical vesicles were seen.[2] Earlier studies[3] of the phase behavior of phosphatidylcholine in cholate–water systems led to the hypothesis of an intermediate discoidal mixed micelle. Walter et al.,[2] in their work, discovered very large vesicles (>1 μm) coexisting with vesicles in the 30–80-nm size range.

In previous studies,[4-9] we have used nonionic surfactants of low aqueous solubility as analogues of phospholipids. Nonionic surfactant vesicles (NSVs or niosomes) are similar in many respects to liposomes, being prepared in the same way and, under a variety of conditions, forming unilamellar or multilamellar structures which entrap lipid soluble or water soluble solutes.[10] In this study the nonionic surfactant used is $C_{16}G_2$ (Figure 1a), an alkyl diglycerol ether from which vesicles are formed. Dicetyl phosphate (DCP), an ionic surfactant, was incorporated into the bilayer at a level of 5% (molar), to prevent aggregation of the vesicles. Solubilization of the vesicle bilayer was studied using the soluble surfactant Solulan C24, a poly(24)oxyethylene cholesteryl ether (Figure 1b). Here we report the presence of large disk-shaped structures as a distinguishable phase in the vesicle to micelle transition phase diagram of this system. Vesicle to micelle transitions of sonicated vesicles prepared from $C_{16}G_2$ have been studied using the detergent octylglucoside,[11] but structures similar to the ones identified in the present study were not reported in the $C_{16}G_2$-octylglucoside study. Disk-shaped structures were observed, however, when the preparation of NSVs was attempted using $C_{16}G_2$, cholesterol, and Solulan C24.[12,13]

Materials

The nonionic surfactants used to form the vesicles, hexadecyl diglycerol ether ($C_{16}G_2$ (Figure 1a) kindly donated by L'Oreal, France, and Solulan C24 (Figure 1b) obtained from D. F. Anstead Ltd. were both used as received. Cholesterol and 5(6)-carboxyfluorescein (CF) were obtained from Sigma Chemical Corp., and dicetyl phosphate (DCP) was obtained from Fluka Chemika, Germany. All organic solvents were obtained from BDH, U.K.

Methods

Preparation of Nonionic Surfactant Vesicles. Total lipid (1.5 mM) in the following molar proportions, $C_{16}G_2$:DCP:cholesterol 69:2:29, was dissolved in 30 mL of chloroform in a 250-mL round-bottomed flask. The organic solvent was removed under reduced pressure at a temperature of 55 °C on a Heidolph rotary evaporator. The resulting lipid film was dried under a steady stream of nitrogen for 20 min to ensure complete removal of the organic solvent. It was then hydrated with 100 mL of water by shaking on a flask shaker, over a water bath at a temperature of 55 °C. The resulting multilamellar nonionic surfactant vesicles were sonicated using an MSE PG100 150-W probe sonicator with the power set at 20% of its maximum output. Sonication was performed in 3 × 4 min bursts at an initial temperature of 55–60 °C with a 30-s cooling period in between each burst. The dispersion was then left to cool.

Solubilization of Vesicles Using Solulan C24. The dispersion obtained from the above procedure with a total lipid concentration of 15 mM was diluted to produce dispersions containing total lipid concentrations of 1.5, 3.0, and 7.5 mM. These dispersions were incubated with various proportions of 15 mM Solulan C24 in a shaking water bath at a temperature of 74 °C for 1 h. Once the mixtures had cooled to room temperature, their absorbance was measured on a Shimadzu multipurpose recording spectrophotometer with the wavelength set at 350 nm.

Size Growth Study. Lipid aggregates were prepared by hydrating 300 μmol total lipid in the proportions $C_{16}G_2$:cholesterol:Solulan C24:DCP 49:19.5:2 with 10 mL of 65 μmol CF in phosphate buffered saline (PBS) (NaCl 140 mM, Na_2HPO_4 0.18 mM, $NaH_2PO_4 \cdot 2H_2O$ 3.2 nM, KCl 2.7 mM) pH 7.4. This was followed by probe sonication in 10 × 1 min bursts with the in-

* Address correspondence to this author.
† University of Leiden.

0022-3654/92/2096-10548$03.00/0

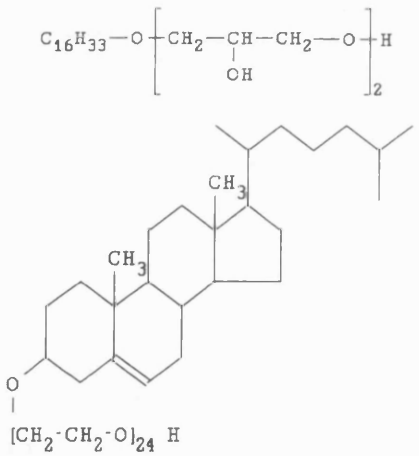

Figure 1. (a, top) $C_{16}G_2$. (b, bottom) Solulan C24.

strument set at 20% of its maximum output and with a 30-s cooling period between each burst. The hydration and initial sonication temperature was 55–60 °C. Once the dispersion had cooled to room temperature, samples were carefully withdrawn and sized on a Malvern Series 2600 droplet and particle sizer (M4.4) using PBS (pH 7.4) as the diluent.

In Vitro Release of CF from Discomes. Preparation of Discomes. A 500-μmol sample of total lipid in the proportions $C_{16}G_2$:cholesterol:Solulan C24:DCP 49:19.5:29.5:2 was hydrated and probe sonicated in 10 × 1 min bursts with the instrument set at 20% of its maximum output and with a 30-s cooling period in between bursts, either with 8 mM CF in PBS (pH 7.4) or with PBS (pH 7.4) alone. The latter dispersion shall be referred to as empty discomes. The dispersions were left to stand at room temperature for at least 18 h, and the discomes containing CF were subsequently dialyzed in 15 cm of dialysis tubing (Visking 20/32), clipped 1 cm from each end with dialysis clips, for 80 h against 800 mL of PBS (pH 7.4) at a temperature of 4 °C. Dialysis was carried out in the dark. The dialysis medium was changed 6 times, and the removal of CF not encapsulated by the lipid aggregates was assumed to be complete when the fluorescence in the dialysis medium had reached a limiting value. Fluorescence was measured (Perkin Elmer LS-3 fluorescence spectrometer) at an excitation wavelength of 486 nm and emission wavelength of 514 nm. Fluorescence photomicrographs of these discomes were recorded (Nikon Microphot FXA equipped with a fluorescent light source).

Assay of Discomes for CF and Calculation of the Entrapment Volume of Discomes. To 1 mL of the dispersion obtained from the dialysis procedure described above was added 1 mL of 2-propanol to disrupt the discomes. The resulting solution was diluted to 25 mL with PBS (pH 7.4) and the fluorescence measured as described previously. Standard solutions were prepared by diluting known quantities of CF with PBS (μH 7.4) while ensuring each final dilution of 25 mL in volume contained 1 mL of 2-propanol. Entrapment volumes were calculated as liters of hydrating solution per mole of total lipid used initially. It was assumed that the aqueous solution entrapped by the lipid aggregates was at the same concentration as the solution used to hydrate the lipids initially and also that there was no loss of lipid during the procedures.

Measurement of CF Release Rates. Into 10-cm lengths of dialysis tubing, clipped 1 cm from each end, was placed either of the following: CF loaded discomes or empty discomes + CF or CF solution. Each of the samples was present in triplicate and contained the same concentration of CF. The former two groups also contained as far as possible the same lipid levels. These dialysis tubes were placed in 250-mL stoppered conical flasks containing 100 mL of PBS pH 7.4. The conical flasks were placed in a shaking water bath at 25 °C. At regular time intervals, 4-mL aliquots were withdrawn from the solution external to the dialysis tubing and their fluorescence measured. These 4-mL aliquots were replaced once their fluorescence had been determined, to ensure the volume of the PBS external to the dialysis tubing remained constant.

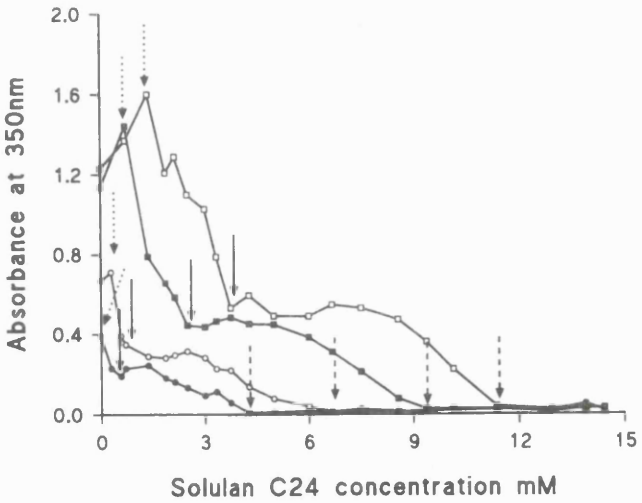

Figure 2. Turbidity measurements on $C_{16}G_2$:cholesterol:DCP 69:39:2 NSVs incubated with Solulan C24 at 74 °C for 1 h: (●) NSV total lipid concentration 1.5 mM; (○) NSV total lipid concentration 3.0 mM; (■) NSV total lipid concentration 7.5 mM; (□) NSV total lipid concentration 15 mM. Arrows indicate points of distinct change in the nature of the dispersion. Dotted arrows indicate the start and hatched arrows indicate the end of the micellization process. The solid arrows indicate similar troughs in all four plots.

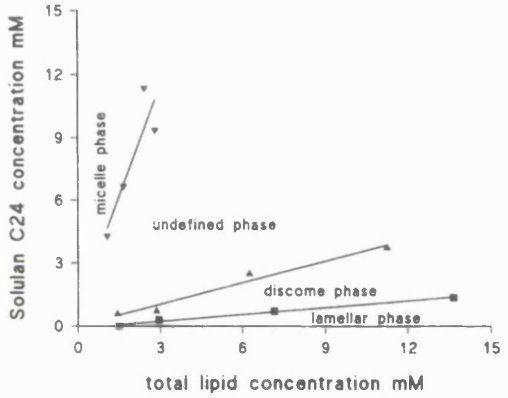

Figure 3. Vesicle to micelle transition phase diagram for $C_{16}G_2$, cholesterol, DCP NSVs solubilized with Solulan C24.

Turbidity Measurements on Discomes and Conventional NSVs Produced from $C_{16}G_2$, Cholesterol, Solulan C24, as a Function of Temperature. Three different lipid mixtures, present as films that were prepared by the evaporation of suitable chloroform solutions under vacuum were hydrated with water (150 μmol of lipid: 10 mL of water). They were then probe sonicated in 10 × 1 min bursts with the sonicator set at 20% of its maximum power output and with 30 s between each burst for cooling. $C_{16}G_2$, cholesterol, and Solulan C24 in the following proportions were used 50:40:10, 50:30:20, and 50:20:30. Microscopic examination of the dispersions after sonication revealed discomes in the 20 and 30% Solulan C24 preparations. Turbidity measurements were carried out on all three samples on a Sigma ZWSII spectrophotometer at temperatures of 30 and 37 °C at 350 nm.

Results

Turbidity Measurements. Turbidity measurements of the vesicle dispersions (Figure 2) expressed as a function of the Solulan C24 concentration gave plots that are similar in shape and can be largely characterized by three break points as indicated by the arrows. These break points indicate a distinct change in the nature of the dispersion. Turbidity titrations of vesicles with soluble surfactants are used to characterize the solubilization of vesicle bilayers by such soluble surfactants by way of turbidity vs surfactant concentration plots.[1,2,11,14-18] Plots of Solulan C24 con-

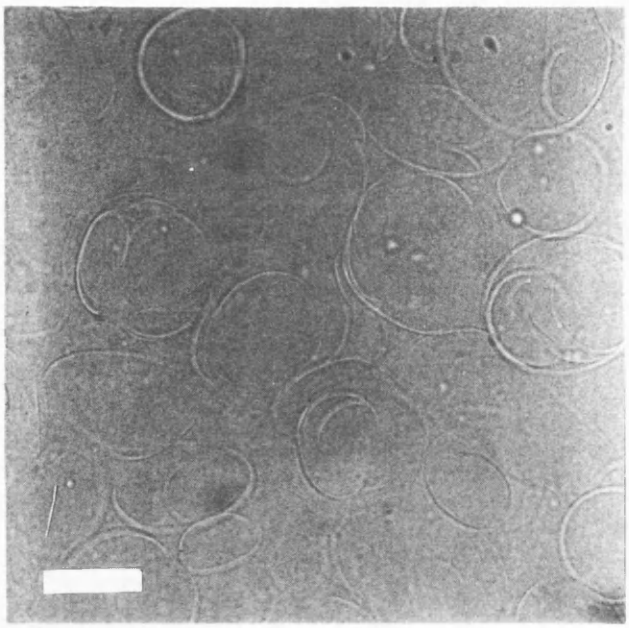

Figure 4. Photomicrograph X800 magnification of discomes (bar = 25 μm) produced by incubating $C_{16}G_2$:cholesterol:DCP 69:39:2 NSVs with Solulan C24 in the proportions total lipid in NSVs:Solulan C24 12.86:2.14.

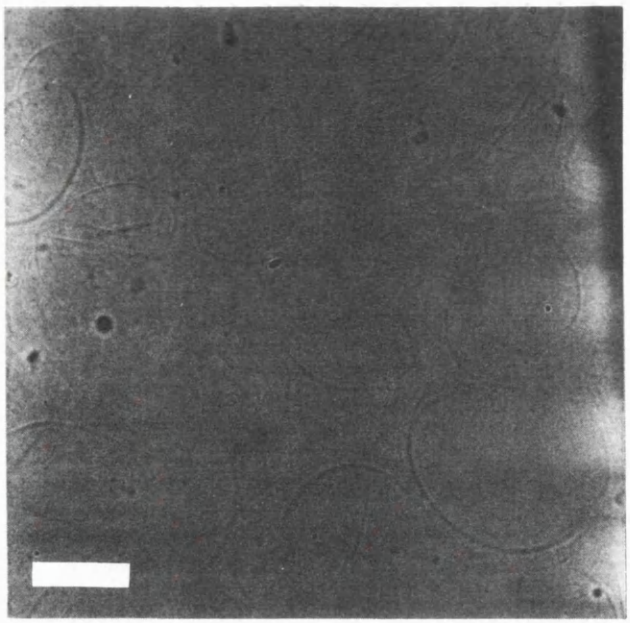

Figure 5. Photomicrograph X800 magnification of discomes (bar = 25 μm) produced by incubating $C_{16}G_2$:cholesterol:DCP 69:39:2 NSVs in the proportions total lipid in NSVs:Solulan C24 10.71:4.29.

centration vs total lipid concentration at these identified break points yield straight-line plots (Figure 3) that effectively describe the partial phase diagram of the system. A novel phase was identified which we have called the discome phase. This phase consisted of large disk-shaped structures (11-60 μm volume mean diameter) (Figures 4 and 5). Discomes of different sizes can be seen. Larger discomes were formed with higher Solulan C24 levels and vice versa.

The equations that describe the straight-line plots in Figure 3 are

micelle/undefined phase:

$$y = 3.540x + 0.848 \quad (r = 0.89) \qquad (1)$$

undefined/discome phase:

$$y = 0.343x + 0.015 \quad (r = 0.98) \qquad (2)$$

lamellar/discome phase: $y = 0.108x - 0.089$ $(r = 0.99)$ (3)

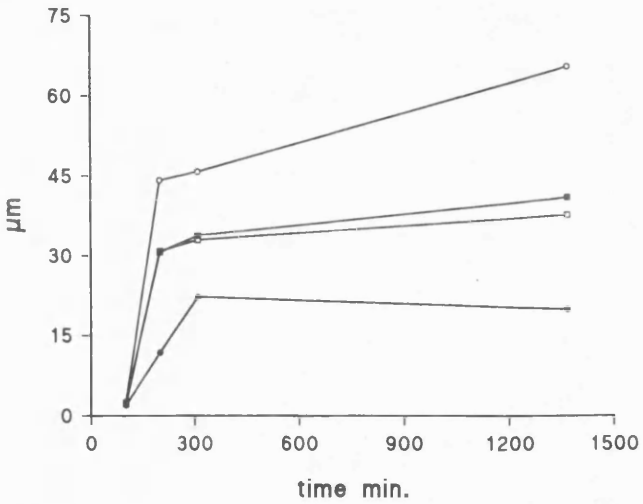

Figure 6. Growth of nonionic surfactant vesicles produced by hydration and sonication of $C_{16}G_2$:cholesterol:Solulan C24:DCP 49:19.5:29.5:2 with time. Size distribution data expressed as (■) volume distribution mean diameter, and % undersize (% undersize, refers to a specified diameter below which the indicated percentage of the particle population fall); (○) 90% undersize; (□) 50% undersize; (●) 10% undersize.

Size Growth. A rapid increase in size is experienced by the nonionic surfactant particles over a short period of time (Figure 6). The nonionic surfactant aggregates were prepared by hydrating $C_{16}G_2$, cholesterol, Solulan C24, and DCP (49:19.5:29.5:2) with 8 mM CF, followed by sonication. Most of the growth takes place in the first 5 h after sonication with little change thereafter. This increase in size is accompanied by an easily distinguishable change in the turbidity of the dispersion, with the discomes eventually forming a loose sediment in what was previously an almost clear dispersion.

Encapsulation Efficiency. The aqueous entrapment efficiency of discomes when encapsulating CF showed considerable batch-to-batch variation. A mean value (n = 3) of 1.2009 ± 0.97 L of hydrating solution per mole of lipid used was obtained. This represents a percentage entrapment of about 3.603 ± 2.916%. Discomes loaded with CF could be visualized under the light microscope using a fluorescent light source (Figures 7a,b). They were largely similar in structure of the discomes obtained by Solulan C24 solubilization of the $C_{16}G_2$ nonionic surfactant vesicles (Figures 4 and 5). The different methods of preparation of the discomes, viz., Solulan C24 vesicle solubilization (Figures 4 and 5) and the hydration of a lipid film (Figures 7 and 8) did not appear to affect the discome structure. Discomes encapsulating water (Figures 4 and 5) and discomes encapsulating a buffered CF solution (Figures 7 and 8), were also similar in structure.

In Vitro Release. The discomes retain about 50% of their aqueous volume marker over a 24-h period at room temperature (Figure 8). A mixture of empty discomes and CF that had been incubated with CF at room temperature for 1 h showed a virtually identical release profile with a CF solution of similar concentration. This is evidence that CF is not adsorbed on the surface of the discomes to any significant degree.

Prolonged Dialysis at Room Temperature. An apparently oligolamellar nonionic surfactant aggregate was produced after dialysis of a dispersion of CF loaded discomes at room temperature for 80 h (Figure 9). Entrapment of CF is still evident in this particle as indicated by the fluorescence exhibited.

Turbidity of the Discome Dispersion as a Function of Temperature. Turbidity data of three nonionic surfactant vesicle dispersions containing 10, 20, and 30% Solulan C24, respectively, and taken at 30 and 37 °C are shown in Figure 10. The 20 and 30% Solulan C24 nonionic surfactant vesicle dispersions when viewed under the light microscope were seen to contain discomes. The 30% Solulan C24 dispersion showed a marked loss of turbidity when the temperature was raised from 30 to 37 °C, an indication of the instability of the dispersion at the higher temperature, although discomes could still be seen under the light microscope

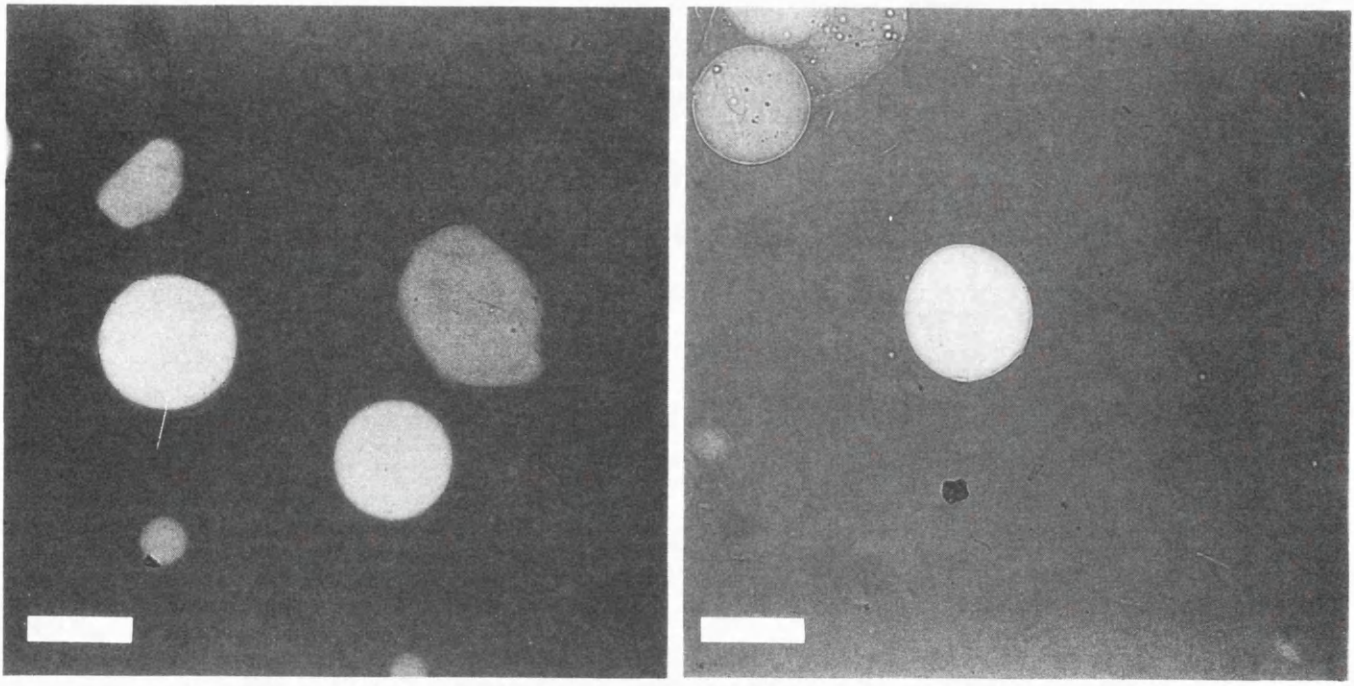

Figure 7. (a, left; b, right) Photomicrograph X200 magnification of CF loaded discomes (bar = 100 μm) produced by hydration and sonication of $C_{16}G_2$:cholesterol:Solulan C24:DCP 49:19.5:29.5:2 with CF.

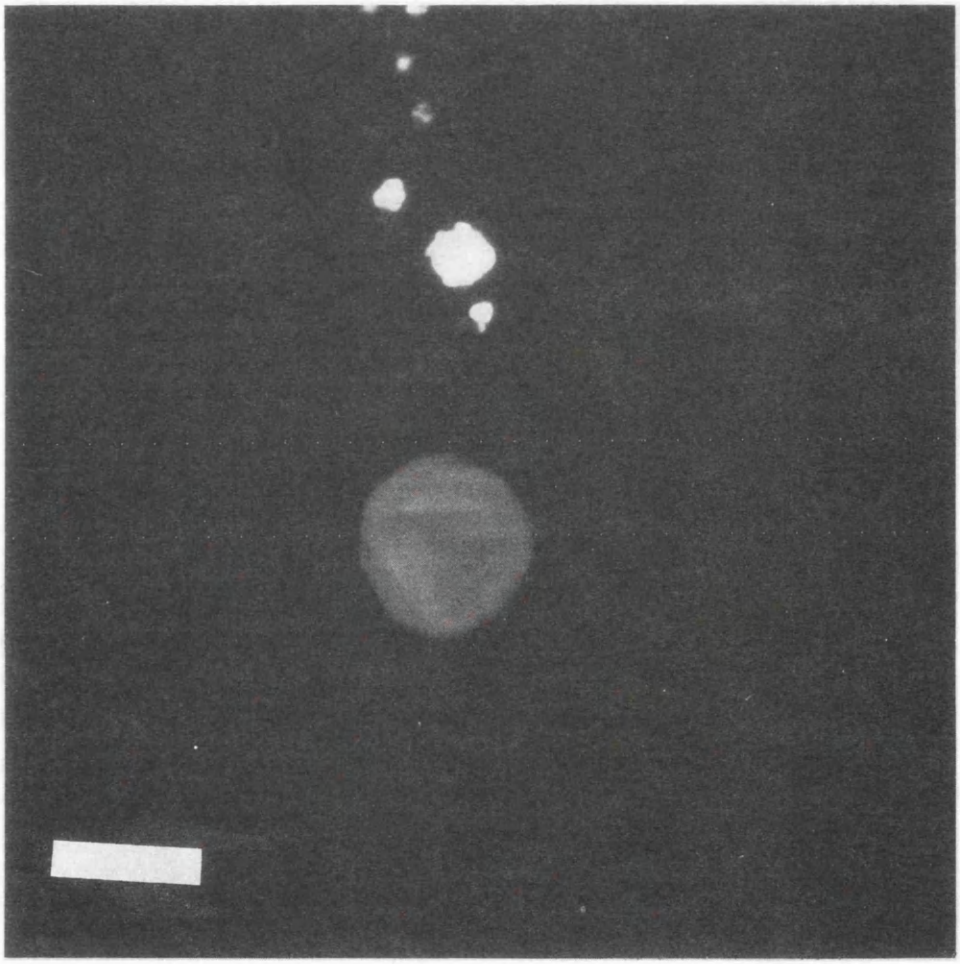

Figure 8. Photomicrograph X200 magnification of CF loaded discomes (bar = 100 μm) produced by hydration and sonication of $C_{16}G_2$:cholesterol:Solulan C24:DCP 49:19.5:29.5:2 and following dialysis at room temperature for 80 h.

when smears were taken from a dispersion at 40 °C.

Discussion

The structures identified in the present study are unique by virtue of their large size. Size measurements of 12–60-μm volume distribution mean diameter have been recorded. The large sizes of the aggregates is unexpected in a sonicated lipid dispersion. Discomes are also unique because they possess asymmetric structures within their population. They are formed when Solulan C24, $C_{16}G_2$, cholesterol, and DCP are hydrated in the following

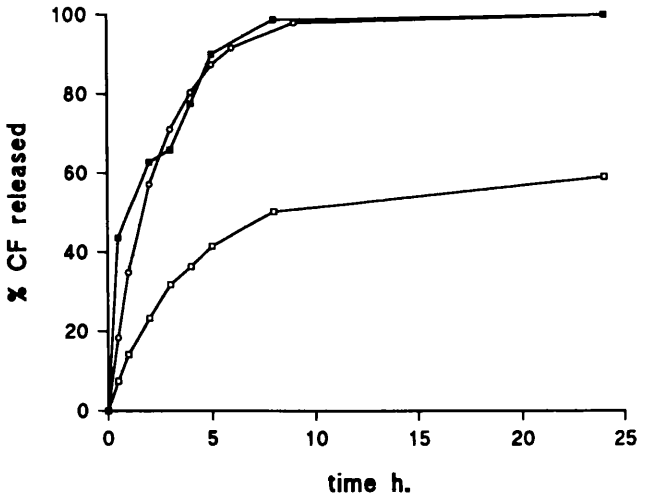

Figure 9. In vitro release of CF from discomes at room temperature: (□) 65 μmol CF in discomes; (■) 65 μmol CF solution; (○) 65 μmol CF + empty discomes.

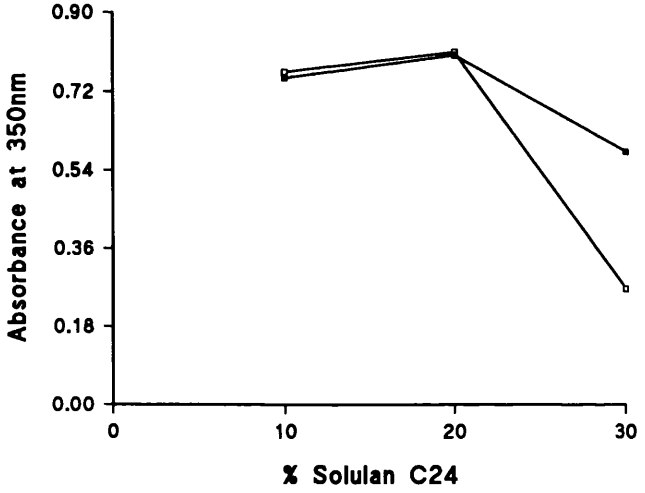

Figure 10. Turbidity measurements on nonionic surfactant vesicles and discomes, containing varying proportions of Solulan C24, at 30 and 37 °C: (■) 30 °C; (□) 37 °C.

proportions 29.5:49:19.5:2 and the resulting dispersion sonicated. They form slowly from the original smaller aggregates in the sonicated dispersion. We have made a preliminary report of their presence in dispersions containing Solulan C24[12,13] but here present a more detailed study of their characteristics.

The size of the discomes is, to some extent, dependent on the Solulan C24 concentration in the system. Discomes produced when $C_{16}G_2$, cholesterol, DCP NSVs (69:39:2) were incubated with Solulan C24 in the ratio total lipid:Solulan C24 12.86:2.14 (Figure 4), show smaller structures than the discomes produced when NSVs were incubated with Solulan C24 in the ratio of total lipid:Solulan C24 10.71:4.29 (Figure 5). Volume distribution mean diameters of both dispersions of 17.75 and 53 μm, respectively, were recorded. The turbidity of the dispersions, however, decreases with increasing Solulan C24 concentration. This decrease in turbidity with increase in size is explained by the accompanying decrease in the number of the particles formed leading to a lower light scattering. The increase in size of the discomes that accompanies the increase in the level of Solulan C24 in the system is due to the fact that Solulan C24 is a much larger molecule (molecular weight = 1443) with a greater surface area than the other molecules in the system ($C_{16}G_2$ molecular weight 390; cholesterol molecular weight 386.7); the inclusion of Solulan C24 in the lipid membrane would thus give rise to larger structures due to the inherent large bulk of the Solulan C24 molecule. Solulan C24 is also a relatively hydrophilic molecule. It contains 24 oxyethylene units and would thus be well hydrated. The added bulk created by the associated water molecules would lead to an increase in the hydrophilic head group cross-sectional area and in turn to an increase in volume of the nonionic surfactant aggregates produced in these systems of increasing Solulan C24 content. The molecules of hydration when also incorporated into the discome membrane in increasing quantity would be expected to yield structures with decreasing light density. The equations describing the straight lines in the partial phase diagram can be used to describe quantitatively the solubilization process in the fashion of Levy et al.[16]

$$[D_T] = R_{eff}[L] + [D_W]$$

where [L] and $[D_T]$ are the total lipid ($C_{16}G_2$, cholesterol, and DCP) and Solulan C24 concentration, respectively, $[D_W]$ is the Solulan C24 concentration in the continuous phase, and R_{eff} is the effective Solulan C24:lipid ratio at which the phase transitions occur. The transition from lamellar to discome phase occurs at an effective Solulan C24:lipid ratio of 0.108 or alternatively at a Solulan C24 mole fraction of 0.1 within the lipid aggregates. The transition from discome to the undefined phase occurs at an effective Solulan C24:lipid ratio of 0.343 or a Solulan C24 mole fraction of 0.25 within the lipid aggregates. The transition from the undefined phase to the micellar phase occurs at a Solulan C24:lipid ratio of 3.540 or a Solulan C24 mole fraction of 0.78 within the lipid aggregates. It follows, therefore, that the formation of discomes is only favored if the mole fraction of Solulan C24 in the lipid aggregates lies between approximately 0.1 and 0.25. A Solulan C24 level within the lipid aggregates above a mole fraction of 0.25 does not yield discomes; once the Solulan C24 mole fraction within the lipid aggregates reaches 0.78 the formation of mixed micelles is favored and an isotropic liquid is obtained. Size measurements on the mixed micellar dispersion gave a z-average mean hydrodynamic diameter of 3.9 nm (Malvern automeasure 4700V4).

A $C_{16}G_2$:cholesterol molar ratio of 7:3 favors the formation of discomes. Increasing the cholesterol level in the vesicular dispersion above this, prior to challenge with Solulan C24, suppresses the production of discomes. We have found that in order to prevent the formation of discomes and produce conventional vesicular dispersions which nevertheless incorporate Solulan C24 in the bilayer, a molar ratio of $C_{16}G2$:cholesterol of 1:1 is optimal. The role of cholesterol in preventing the insertion of octylglucoside into the bilayer of $C_{16}G_2$ vesicles during the micellization of these vesicles has been reported.[11] It is clear that the low mole fraction of cholesterol in the vesicular dispersion prior to their challenge with Solulan C24 facilitates the production of discomes by making the vesicular bilayer more permeable to the Solulan C24 molecules. The solubilization of nonionic surfactant vesicles by Solulan C24 can be said to proceed in the following manner. As the Solulan C24 concentration in the system increases, it partitions progressively between the continuous phase and the bilayer until a critical level is reached in the vesicular bilayer phase and the vesicular phase gives rise to the discome phase. The partitioning of Solulan C24 within the discome membrane and continuous phase proceeds until eventually the level of Solulan C24 in the discomes leads to their breakdown to give other aggregates. Finally solubilization is complete with the production of mixed micelles.

Discomes are different from the bilayer sheets reported in the transition from vesicle to micelles in the phosphatidylcholine–sodium cholate system reported by Walter et al.[2] They are also different from the discoid micelles found in phosphatidylcholine–octylglucoside vesicle to micelle transitions.[16] Discomes are much larger than both of these structures and, in addition, they appear in the main to be oval in shape. They are also able to encapsulate an aqueous volume and retain 50% of the encapsulated material over a 24-h period at room temperature. The empty discomes incubated with CF for 1 h immediately prior to the in vitro release measurement did not show that CF is in any way associated with the surface of the discomes, leading to the conclusion that any CF found to be associated with the discomes must be encapsulated and not adsorbed on the surface of the discome membrane.

While the separation of the entrapped solute from the unen-

trapped solute by dialysis of these discomes at 4 °C did not appear to change their morphology (Figure 7a,b), dialysis at room temperature for prolonged periods does affect the morphology of the discomes (Figure 9). In the latter figure, an oligolamellar lipid aggregate is formed with the retention of the entrapped CF. It seems that the discome structure collapses to produce conventional multilamellar vesicles as a result of the loss of Solulan C24 from the lipid aggregates through prolonged dialysis at room temperature, a process not significant at 4 °C. The removal of detergent from mixed micelles by dialysis results in the production of unilamellar vesicles[11,14] and a similar process of detergent depletion seems to be operating here. It is conceivable that the discomes are formed from a lipid bilayer although the exact nature of the discome membrane requires further investigation. The solubilization of liposomes by various detergents namely octylglucoside,[14,17] octaethylene glycol mono-*n*-dodecyl ether,[16] and polyoxyethylene cetyl ethers[5] at room temperature produced transition phase diagrams consisting of essentially three phases, the lamellar phase, the micellar phase, and a region where lamellae and micelles are coexistent. The region of transition of vesicles to spherical micelles in the PC-cholate system has been described as consisting of "open" vesicles and bilayer sheets from which develop cylindrical micelles.[2] Solubilization of $C_{16}G_2$, cholesterol-rich vesicles using the detergent octylglycoside has been described as consisting of essentially three stages, namely, a lamellar phase, a micellar phase, and a phase in which octylglycoside penetrates the vesicle membrane, i.e., attains a level of saturation, albeit nonhomogeneous distribution within the membrane and is then distributed throughout the membrane, and micellization results. In the present study, the micellization of nonionic surfactant vesicles studied at elevated temperatures by multiple sample preparation as opposed to the titrimetric methods used elsewhere[2,5,17] produced a novel phase consisting of large stable discomes in addition to the lamellar phase, micellar phase, and the third phase which marks the transition of discomes to micelles.

Discomes are stable for up to 6 months when stored at 4 °C. However, the discome dispersion exhibits a decrease in turbidity when heated to 37 °C, indicative of instability at this temperature.

The fact that discomes are capable of aqueous entrapment augurs well for their use as drug delivery vesicles in the field of ophthalmology, for instance, where their large size and minimal opacity will be advantageous. However, the apparent instability of discome dispersions at 37 °C is a finding that requires further study. The asymmetry observed in some of the discomes seems to suggest that the discome membrane is in some way heterogeneous at a molecular level. This could explain the nonuniform curvature of the discome membrane. A heterogeneous distribution of detergent molecules during the vesicle to micelle transition of $C_{16}G_2$ vesicles facilitated by the detergent octylglucoside has been postulated previously.[11]

Acknowledgment. I.F.U. gratefully acknowledges the financial support of L'Oreal France Ltd.

References and Notes

(1) Kim, J.; Kim, J. *Biochemistry* **1991**, *110*, 436–442.
(2) Walter, A.; Vinson, P. K.; Kaplun, A.; Talmon, Y. *Biophys. J.* **1991**, *60*, 1315–1325.
(3) Small, D.; Penkett, P. A.; Chapman, D. *Biochim. Biophys. Acta* **1969**, *176*, 178–189.
(4) Baillie, A. J.; Florence, A. T.; Hume, L. Muirhead, G. T.; Rogerson, A. *J. Pharm. Pharmacol.* **1985**, *37*, 863–868.
(5) Rogerson, A.; Baillie, A. J.; Florence, A. T. In *Surfactants in Solution*; Mittal, K. L., Ed.; Plenum Press: New York, 1989; Vol. 8, pp 321–332.
(6) Florence, A. T.; Cable, C.; Cassidy, J.; Kaye, S. B. In *Targeting of Drugs: Optimization Strategies*; Gregoriadis, G., Allison, A. C.; Poste, G., Eds.; Plenum Press: New York, 1990; pp 117–125.
(7) Rogerson, A.; Cummings, J.; Wilmott, N.; Florence, A. T. *J. Pharm. Pharmacol.* **1988**, *40*, 337–342.
(8) Kerr, D. J.; Rogerson, A.; Morrison, G. J.; Florence, A. T.; Kaye, S. B. *Br. J. Cancer* **1988**, *58*, 432–436.
(9) Rogerson, A.; Cummings, J.; Florence, A. T. *J. Microencapsulation* **1987**, *4*, 321–328.
(10) Florence, A. T.; Baillie, A. J. In *Novel Drug Delivery and its Therapeutic Application*; Prescott, L. F., Nimmo, W. S., Eds.; John Wiley and Sons Ltd.: New York, 1989; pp 281–296.
(11) Lesieur, S.; Grabielle-Madelmont, C.; Paternoste, M.; Moreau, J.; Handjani-Vila, R.; Ollivon, M. *Chem. Phys. Lipids* **1990**, *56*, 109–121.
(12) Cable, C.; Florence, A. T. *J. Pharm. Pharmacol.* **1988**, *40*, 30P.
(13) Cable, C. *Ph.D. Thesis*, University of Strathclyde, Glasgow, 1990.
(14) Almog, S.; Litman, B. J.; Wimley, W.; Cohen, J.; Wachtel, E. J.; Barenholz, Y.; Ben-Shaul, A.; Lichtenberg, D. *Biochemistry* **1990**, *29*, 4582–4592.
(15) Paternoste, M.; Roux, M.; Rigaud, J. *Biochemistry* **1988**, *27*, 2668–2677.
(16) Levy, D.: Gulik, A.; Seigneuret, M.; Rigaud, J. *Biochemistry* **1990**, *29*, 9480–9488.
(17) Jackson, M. L.; Schmidt, C. F.; Lichtenberg, D.; Litman, B. J.; Albert, A. D. *Biochemistry* **1982**, *21*, 4276–4582.
(18) Miguel, M.; Eidelman, O.; Ollivon, M.; Walter, A. *Biochemistry* **1989**, *28*, 8921–8928.

8th LIPOSOME WORKSHOP, OBERJOCH, GERMANY. 2ND-8TH APRIL 1993.

PHYSICAL AND BIOLOGICAL CHARACTERISATION OF NON-IONIC SURFACTANT VESICLES (NIOSOMES).

Ijeoma Uchegbu[1], John Double[2], Lloyd Kelland[3], John Turton[4], Alexander T. Florence[1].

1. Centre for Drug Delivery Reseach, School of Pharmacy, 29-39 Brunswick Square, London WC1N 1AX.

2. Clinical Oncology Unit, University of Bradford, Bradford, West Yorkshire, BD7 1DP.

3. The Institute of Cancer Research: Royal Cancer Hospital, Drug Developement Section, Drug Evaluation Team, Block E, 15 Cotswold Road, Belmont, Sutton, Surrey SM2 5NG.

4. Toxicology Department, School of Pharmacy, 29-39 Brunswick Square, London WC1N 1AX.

Non-ionic surfactants are synthetic amphiphiles capable of forming vesicles in a manner analogous to liposomes[1].

The delivery of cytotoxic agents to neoplastic tissue is a complex problem due to the heterogenous nature of the tumour vasculature and the barrier offered to drug transport by the high interstitial pressure within the tumour. Encapsulation of anti-cancer drugs within non-ionic surfactant vesicles (NSVs), by offering protection against various endogenous degradative processes and also by affording an increased mean residence time within the plasma compartment may enhance the delivery of cytotoxic agents to tumour tissue.

Non-ionic surfactant vesicles, were prepared from $C_{16}G_2$ (a C16-triglycerol surfactant),

---

[1]Florence A.T. and Baillie A.J. Non-ionic surfactant vesicles - alternatives to liposomes in drug delivery? In. *Novel Drug Delivery and Its Therapeutic Application.* L.F. Prescott and W. S. Nimmo (eds). John Wiley and Sons (1989), pp281-295.

cholesterol and Solulan C24. Solulan C24, a cholesteryl polyoxyethylene ether was incorporated into the NSV membrane to enable a steric barrier operate against the phagocytic processes of the reticuloendothelial system and to reduce the mean vesicular size. However, as the levels of Solulan C24 within the non-ionic surfactant vesicle membrane were increased, the classical vesicular structure was transformed to give discomes[2]. The level of Solulan C24 within the vesicles was, as a result of this finding, limited to 10% molar.

Non-ionic surfactant vesicles, encapsulating doxorubicin were prepared from $C_{16}G_2$, cholesterol and Solulan C24 (45:45:10) and administered intraperitoneally. The treatment groups within the experiment consisted of the following: a) 2.5mg/kg doxorubicin NSVs, b) 5.0mg/kg doxorubicin NSVs, c) 10mg/kg doxorubicin NSVs, d) 10mg/kg doxorubicin solution. An inflammatory response manifesting in the lung was observed when NSVs were administered by this route, but was not observed in a subsequent study in which doxorubicin NSVs were administered intravenously.

$C_{16}G_2$ NSVs encapsulating doxorubicin were evaluated *in-vivo* against 2 day old MAC 13 tumours grown in male NMRI mice, at three different dose levels: a) 2.5mg/kg doxorubicin NSVs, b) 5.0mg/kg doxorubicin NSVs and c) 10mg/kg doxorubicin NSVs. Control groups were set up consisting of: a) 10mg/kg doxorubicin solution, b) tris buffered saline (TBS) and c) empty NSVs. Results showed a demonstrable effect at the 2 higher dose levels, with the 10mg/kg doxorubicin NSVs and 10mg/kg doxorubicin solution showing similar activity (Fig. 1).

A similar challenge with the same type of NSVs, but at a lower dose level, and against a more established tumour - MAC 15A - although appearing to give a slight biological

---

[2] Uchegbu I.F., Bouwestra, J.A. and Florence, A.T. Large disk-shaped structures (discomes) in non-ionic surfactant vesicle to micelle transitions. *J. Phys. Chem.* 96: 10548-10553.

response, showed activity that was statistically indistinguishable from the controls.

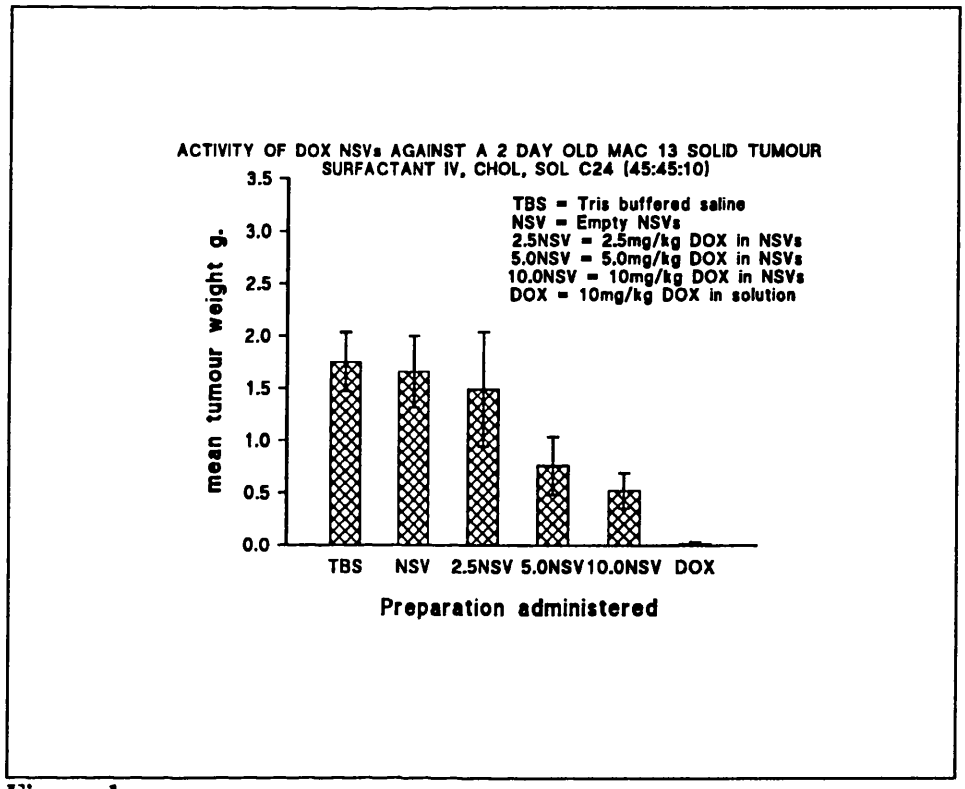

Figure 1

It was found that some of the Span surfactants demonstrated superior encapsulation efficiencies over $C_{16}G_2$. Also it was thought that by using Span surfactants in our studies progression from the bench to the clinic may be expedited. Non-ionic surfactant vesicles were prepared from Span 60 and evaluated *in-vivo* against an established MAC 15A tumour at three dose levels: a) 2.5mg/kg doxorubicin NSVs, b) 5.0mg/kg doxorubicin NSVs and

c) 10mg/kg doxorubicin NSVs. Control groups were set up consisting of: a) 10mg/kg doxorubicin solution, b) empty NSVs c) no treatment. A clear response was observed when treated and control animals were compared (Fig. 2). Comparable activity was observed between animals treated with 5mg/kg doxorubicin NSVs and 10mg/kg doxorubicin solution.

Various NSVs were tested *in-vitro*, against a human ovarian cancer cell line showing resistance to doxorubicin. A slight improvement in activity was observed with the NSV preparations when compared to the drug in solution (Fig. 3). In summary $C_{16}G_2$ NSVs and

Span 60 NSVs have been evaluated against various tumour systems and resistant cell line *in-vitro*. $C_{16}G_2$ NSVs showed activity that was comparable to an equivalent dose of doxorubicin solution, while Span 60 NSVs showed improved activity over doxorubicin solution. *In-vitro* the activity of various NSVs was marginally superior to doxorubicin solution.

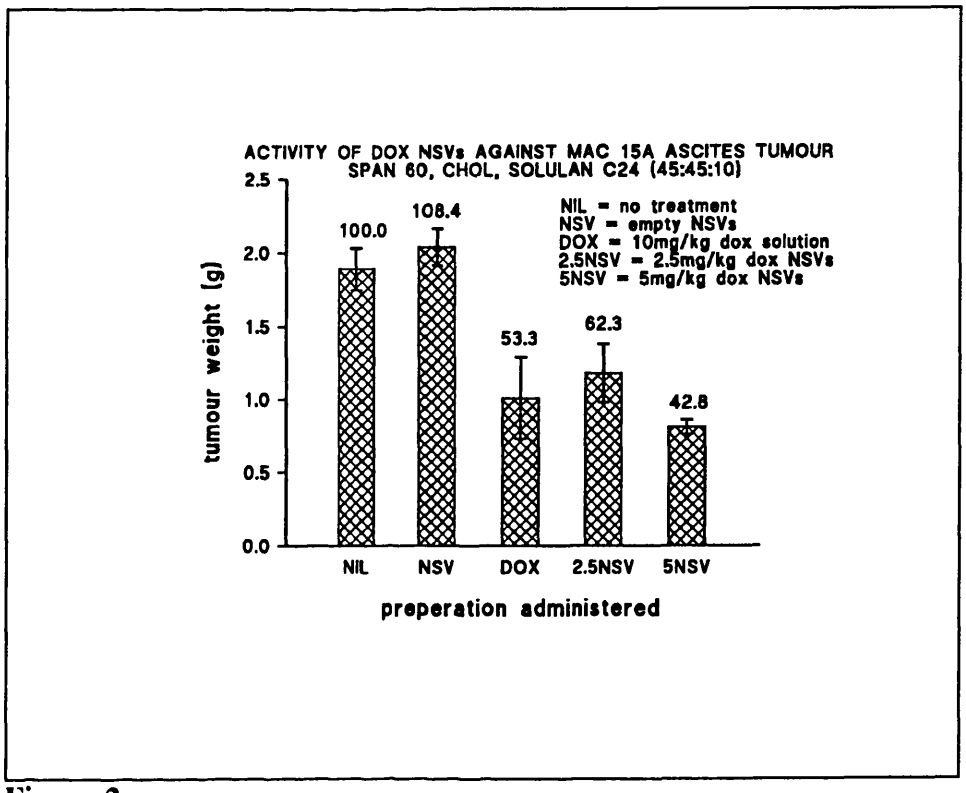

Figure 2

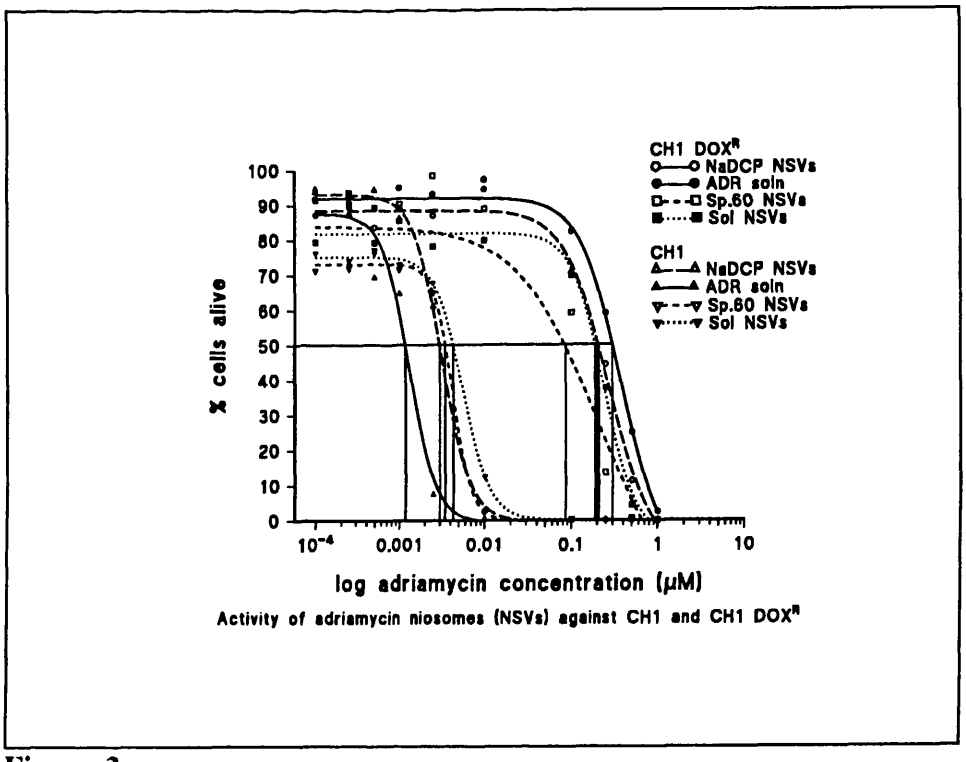

Figure 3

NIOSOMAL DOXORUBICIN IN TUMOUR BEARING MICE

Ijeoma Uchegbu, John A. Double*, John A. Turton, Alexander T. Florence

Centre for Drug Delivery and Department of Toxicology, School of Pharmacy, University of London, London. *Clinical Oncology Unit, Bradford University, Bradford.

The encapsulation of doxorubicin in niosomes has been shown to improve the tumoricidal activity of this cytostatic[1,2].
Doxorubicin niosomes prepared from sorbitan monostearate (Span 60), cholesterol, Solulan C24 (45:45:10) were administered to female NMRI mice bearing a 9 day old MAC 15A subcutaneously implanted tumour. In mice administered doxorubicin niosomes, plasma doxorubicin associated with the niosomes was separately quantified from doxorubicin that had exited from the niosomes. The latter being present either in the free form or bound to plasma proteins. At least 90% of the plasma doxorubicin was associated with the niosomes 4h after dosing, falling to 50% after 24h. The clearance of doxorubicin that had escaped from the niosomes was about 10 fold greater than the clearance of doxorubicin still associated with the niosomes - 176.5mL min^{-1} and 16.2mL min^{-1} respectively. The area under the plasma level-time curve (for the 24h study period) increased 6 fold when doxorubicin niosomes were administered, compared to when the drug was administered in solution (66.0 μg.h mL^{-1} and 10.3μg.h mL^{-1}). The area under the tumour level-time curve was increased by over 50% by the administration of the drug encapsulated in niosomes compared to the drug administered in solution (58.6μg.h mL^{-1} and 34.3μg.h mL^{-1}) respectively. Drug levels in the heart were statistically indistinguishable, regardless of the formulation administered.
Modest tumour targeting was achieved by increasing the tumour to heart ratio from 0.27 to 0.36 by the encapsulation of doxorubicin in Span 60 niosomes.
Doxorubicin metabolites were found associated with the niosomes in the plasma, namely doxorubicinol and the aglycones doxorubicinone, doxorubicinolone and 7-deoxydoxorubicinone, showing signs of intravesicular metabolic activity. We believe this finding to be due to the fact that doxorubicin was present in the vesicle bilayer and was thus accessible to the degradative enzymes. Although the AUC's of all metabolites were indeed generally higher in the niosome associated fraction, than those found in the fraction of drug that had diffussed from the niosomes, the $AUC_{(metabolite)}/AUC_{(doxorubicin)}$ was lower for the encapsulated fraction, with the exception of doxorubicinol where values were similar.
Levels of liver metabolites, were found to be higher in the animals administered niosomes. $AUC_{(metabolite)}/AUC_{(doxorubicin)}$ values were also higher in this group (except doxorubicinone which gave lower values).
Span 60 niosomes have been shown to double the tumoricidal activity of doxorubicin in male NMRI mice bearing a 5 day old MAC 15A tumour[3].

1. A Rogerson, J. Cummings, N. Wilmott, A.T. Florence, J. Pharm. Pharmacol. 40:337-342 (1988).
2. D.J. Kerr, A. Rogerson, G.T. Morrison, A.T. Florence, S.B. Kaye, Br. J. Cancer, 58: 432-436 (1988)
3. I.F. Uchegbu, J.A. Turton, J.A. Double, A.T. Florence, J. Pharm. Pharmacol. (in press).

Journal of Pharmacy and Pharmacology, 45(S2): (1993)

1112

THE ACTIVITY OF DOXORUBICIN NIOSOMES AGAINST A RESISTANT HUMAN OVARIAN CANCER CELL LINE

I.F. Uchegbu, L.R. Kelland[1], J.A. Turton, A.T. Florence, School of Pharmacy, University of London, London WC1N 1AX. 1. The Institute of Cancer Research, Sutton, Surrey SM2 5NG.

Various doxorubicin (DOX) particulate delivery systems have been found to circumvent acquired multi-drug resistance in tumour cells, both in vitro and in vivo (Sadavisan et al 1991 and Cuvier et al 1992). Doxorubicin loaded niosomes were evaluated in-vitro against a human ovarian cancer cell line, made resistant to Doxorubicin by repeated in-vitro exposure to the agent. Niosomes were prepared by hydrating thin lipid films of a) $C_{16}G_2$ (a C16-diglycerol ether), cholesterol and Solulan C24 (a polyoxyethylene-cholesteryl ether) (45:45:10); b) Span 60, cholesterol and Solulan C24 (45:45:10) with 1 mg ml^{-1} doxorubicin solution in Tris buffered saline (TBS) and c) $C_{16}G_2$, cholesterol and sodium dicetyl phosphate (47.5:47.5:5) with 0.29 mg ml^{-1} doxorubicin in TBS, all at 60-70°C. The characteristics of the resulting niosomes are as shown in Table 1.

Table 1: Properties of doxorubicin sonicated niosomes.

niosome composition	mean size (nm)	encapsulation efficiency mmol DOX mol $lipid^{-1}$
$C_{16}G_2$, NaDCP (NaDCP)	520	2.84
$C_{16}G_2$, SolulanC24 (Sol)	154	3.17
Span 60, SolulanC24 (Sp6)	161	10.45

Incubation of these niosomes at various dose levels, with a sensitive (CH1) and a resistant (CH1 DOX^R) cell line, produced the survival curves shown in Fig. 1. Although the niosomes showed marginally improved activity over doxorubicin solution, against the resistant cell line CH1 DOX^R, essentially there was cross resistance, with the niosomes showing reduced activity against the parent line (CH1).

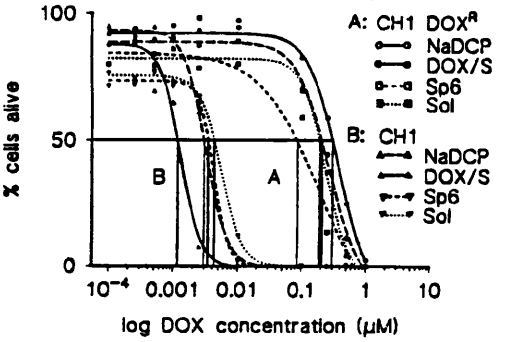

Fig. 1: Activity of doxorubicin niosomes against CH1 and CH1 DOX^R with doxorubicin solution (DOX/S) as control.

The evaluation of Span 60 niosomes in vivo against CH1 xenografts revealed a similar profile of anti-cancer activity to that observed in vitro. It is concluded that although doxorubicin niosomes are slightly more active in vitro against a model ovarian cancer cell line, with acquired resistance, they are unable to reverse the resistance to an appreciable extent.

Cuvier, C. et al (1992) Biochem. Pharmacol. 44: 509-517
Sadavisan, R. et al (1991) Cancer Lett. 57: 165-171

HEPATIC MICROSOMAL METABOLISM OF DIAZEPAM AND ITS INHIBITION BY OMEPRAZOLE

K.Zomorodi, J.B.Houston, Department of Pharmacy, University of Manchester, Manchester M13 9PL, UK

Omeprazole is a substituted benzimidazole which binds avidly to cytochromes P450 *in vitro* and is implicated as an inhibitor of hepatic oxidative metabolism. Hence there is a theoretical basis for drug interactions when omeprazole is prescribed with other drugs. One particular interaction which has attracted much attention due to its pronounced severity and the possible selectivity of the inhibition effect involves omeprazole and diazepam (Andersson 1991). We have investigated the metabolism of diazepam to three metabolites - 3-hydroxy- (3H), 4'-hydroxy- (4H) and nordiazepam (N) - *in vitro* and assessed the inhibitory action of omeprazole on each pathway.

Standard methodology was used to prepare hepatic microsomes from male Sprague Dawley rats. Phenobarbitone (PB-80mg kg^{-1}) and dexamethasone (DEX-100mg kg^{-1}) were injected intraperitoneally once daily for 3 days to induce P450 2B and 3A families and hence produce customized microsomes. Microsomes from untreated (UT) rats were also used in which the major P450 families are 2C and 2D. Microsomal incubations were carried out with a NADPH regenerating system under conditions which were linear with respect to time and protein concentration. In the inhibition experiments omeprazole was added 10 min prior to diazepam. HPLC was used to assay all metabolites and parent drug simultaneously following a solvent extraction according to the methods of Reilly et al 1990.

Comparison of the rates of disappearance of diazepam and the rates of production for the three metabolites confirmed that no other primary pathways occurred in any of the three microsomal preparations. In UT microsomes the three pathways were of approximately equal importance as judged by the Vmax/Km ratios (16-18 μL min^{-1} (mg microsomal protein)$^{-1}$). However the Km values indicated greater affinity for the production of N. K_I values were in the 100 μM range, equal to or greater than the Km values in these microsomes (Km/K_I ratio 0.1-1.1). In PB microsomes only N and 3H pathways are of importance, both occurring at approximately three times the rate of UT with Km values similar to UT. For 3H production the omeprazole K_I was much lower than the diazepam Km (Km/K_I ratio 3.6) and for N production the opposite effect occurred (ratio 0.3). In DEX microsomes 3H production dominated diazepam metabolism with a Vmax/Km ratio 14-fold greater than UT due to 5-fold increase in Vmax and a reduction in Km of one third. The K_I in the later system was 35 μM, approximately half the value of the Km. 4-hydroxylation is of minor importance in the customized microsomes (1-3% of diazepam metabolism) and this balance of metabolic pathways equates with human microsomes.

Overall these data indicate that 3-hydroxylation of diazepam is the major site of inhibition by omeprazole. In all three microsomal preparations the K_I is lower than the Km (Km/K_I ratio 1.1-3.6). N production is less prone to omeprazole inhibition; K_I exceeds Km in all three systems (ratio 0.1-0.9). This selectivity in the inhibitory action of omeprazole towards different cytochromes P450 is consistent with our earlier investigations with a variety of substrates (Zomorodi & Houston, 1992).

Andersson, T. (1991) Clin. Pharmacokin. 21, 195-212
Reilly, P.E.B. et al (1990) Mol. Pharmacol. 37 767-774
Zomorodi, K., Houston, J.B. (1992) Br.J.Clin.Pharmacol. 24 167P

Journal of Pharmacy and Pharmacology, 45(S2): (1993).

1140

DEVELOPMENT OF A MICROPARTICULATE DRUG DELIVERY SYSTEM FOR USE IN HORMONE REPLACEMENT THERAPY

J. S. Malhi, I. S. Jumnoodoo, S. K. Malhi, Department of Pharmacy, University of Brighton, Moulsecoomb, Brighton BN2 4GJ, UK

Hormone replacement therapy (HRT) is indicated for the alleviation of perimenopausal symptoms which arise as a result of oestrogen deficiency. Whilst oestrogen administration is effective in controlling these symptoms, unopposed oestrogen therapy is associated with a number of unpleasant side-effects which include endometrial hyperplasia. The risk of hyperplasia is reduced by concurrent systemic administration of a progestogen, however, this frequently results in abnormal plasma lipid profiles. This problem may be overcome if it were possible to deliver the progestogen directly to the endometrium without it entering the systemic circulation. One such method is currently available, the levonorgestrel-releasing intrauterine device (Levonova), however, this device is physically too large for easy insertion through the constricted perimenopausal cervix. There is a paucity of data concerning the diameter of the postmenopausal cervix, however, the diameter of the cervix varies from 3 mm at ovulation to 1 mm postmenstrually (Elstein 1974). Reynolds et al (1992) described a much smaller device (0.5 mm in diam.) which readily traverses the cervix, nonetheless, this device also requires the patient to attend an outpatient clinic and this may limit its use. The ability of small inanimate india ink particles to migrate into the uterus following vaginal inoculation has been reported by Egli & Newton (1961) thus indicating that small particles may be passively transported through the cervix as a consequence of uterine myometrial activity and/or by cervical kinocilia which line the cervical epithelia. Thus drug-loaded microparticles placed in the proximity of the cervical os may similarly be transported into the uterus and this may provide a favourable means of targeted drug delivery to the uterus. The aims of the present study were to develop progestogen-containing microcapsules (MCs) for potential use in HRT.
Norethisterone acetate (NA) containing MCs were prepared by complex coacervation using the following method: 50 mg NA were dissolved in 2.5mL arachis oil and this mixture was then dispersed in a 2% gelatin solution at 41°C. To this an equal volume of 2% acacia solution were added and the oil kept in suspension by continuous stirring. The pH of the mixture was adjusted to 4.1 by the addition of 0.5 M HCl to initiate coacervation which was confirmed by viewing aliquots of the mixture under a light microscope. The mixture was then continuously stirred for a further 20 min whilst the temperature was reduced to 4°C by means of an iced water bath. The walls of the MCs thus formed were hardened by the addition of 25% glutaraldehyde and the mixture stirred for a further 60 min. The coacervate was then washed with cold reverse osmosis water and the MCs allowed to settle. The supernatant was decanted and the MCs freeze-dried. The particle size of the MCs was determined by laser light scattering (LLS) using a Malvern Mastersizer and by image analysis (IA) using SEM. The release of NA into chloroform/PBS at pH 7.36 (1:4) was determined using a modified USP basket and assayed by glc using testosterone as an internal standard.
Up to 84% of NA could be encapsulated into MCs with a volume mean diameter of 53.54μm as determined by LLS and 22.22μm as determined by SEM. This demonstrates a potential difficulty when sizing particles using LLS since the technique cannot distinguish between single particles and aggregates whereas IA does not suffer from this drawback (Malhi et al 1990). The particles are sufficiently small to easily traverse the cervix. The rate of NA release from the MCs was approximately 0.3mg per minute over a period of 180 minutes at the end of which the MCs were depleted of NA. This is in excess of the amounts required in HRT, however, the release rate may easily be controlled by use of a controlled-release membrane or by reducing the concentration of drug in the MCs thus it is suggested that this may be a useful drug delivery system for use in HRT.

Egli, G. & Newton, M. (1961) Fertil. Steril. 12: 151-155
Elstein, M. (1974) Clin. Obstet. Gynecol. 1: 345-368
Malhi, S. K. et al (1990) Presented at the Symposium on Surface and Colloid Chemistry, Nottingham.
Reynolds, J. P. et al (1992) J. Pharm. Pharmacol. 44 (Suppl): 83

THE BIODISTRIBUTION AND TUMORICIDAL ACTIVITY OF DOXORUBICIN-LOADED NIOSOMES

I. F. Uchegbu, J.A. Turton, J.A. Double[1], A.T. Florence. School of Pharmacy, University of London, London WC1N 1AX. 1. Clinical Oncology Unit, University of Bradford, Bradford, West Yorkshire, BD7 1DP.

Span surfactants and glycerol alkyl ethers have been studied as the basis for niosomal anti-cancer drug delivery. Doxorubicin loaded $C_{16}G_2$ (a C16-diglycerol ether)-stearylamine niosomes when administered intravenously (IV) have been shown to retard the clearance of doxorubicin from the plasma (Florence et al 1990). We have studied the biodistribution following intraperitoneal (IP) administration to male AKR mice (Fig. 1), and tumoricidal activity against a 2 day old MAC 13 tumour of sonicated doxorubicin

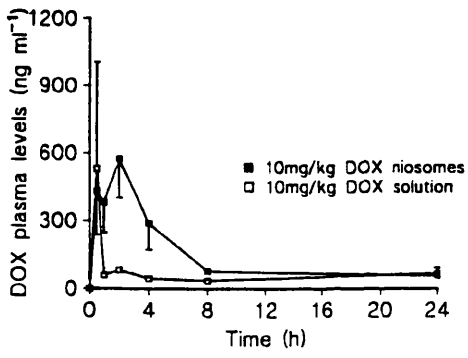

Fig. 1: Doxorubicin plasma levels following IP injection

$C_{16}G_2$ niosomes. These niosomes at a dose level of 2.5 mg kg^{-1}, 5.0 mgkg^{-1} and 10 mg kg^{-1} of doxorubicin administered IV showed a statistically significant anti-tumour effect in animals treated with 5 mg kg^{-1} and 10 mg kg^{-1} doxorubicin niosomes. $C_{16}G_2$ niosomes were equiactive with doxorubicin solution.
Vesicles prepared from the Span surfactants, which are mono- esters

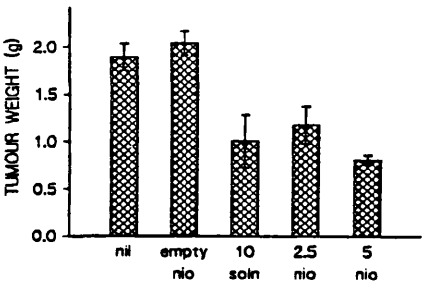

Fig. 2: Activity of doxorubicin Span 60 niosomes (nio) against a MAC 15A tumour.

and anhydrides of sorbitol (Yoshioka et al 1992), were loaded with doxorubicin and entrapment efficiency and size studied. Doxorubicin loaded Span 60 niosomes were evaluated in vivo against a MAC 15A tumour in male NMRI mice(Fig. 2). Span 60 niosomes were twice as active as doxorubicin solution.

Florence, A.T. et al (1990), Targeting of Drugs. Gregoriadis, G., Allison, A.C., Poste, G. (eds). Plenum Press, New York. pp117-125.
Yoshioka, T. et al (1992) J. Pharm. Pharmacol. 44: 1044.

9th LIPOSOME WORKSHOP, OBERJOCH, GERMANY. 13th-18th MARCH 1994

NIOSOMAL DOXORUBICIN IN TUMOUR BEARING MICE

Ijeoma Uchegbu, John A. Double*, John A. Turton, Alexander T. Florence

Centre for Drug Delivery and Department of Toxicology, School of Pharmacy, University of London, London. *Clinical Oncology Unit, Bradford University, Bradford.

The encapsulation of doxorubicin in niosomes has been shown to improve the tumoricidal activity of this cytostatic[1,2].

Doxorubicin niosomes prepared from sorbitan monostearate (Span 60), cholesterol, Solulan C24 (45:45:10) were administered to female NMRI mice bearing a 9 day old MAC 15A subcutaneously implanted tumour. In mice administered doxorubicin niosomes, plasma doxorubicin associated with the niosomes was separately quantified from doxorubicin that had exited from the niosomes. The latter being present either in the free form or bound to plasma proteins. At least 90% of the plasma doxorubicin was associated with the niosomes 4h after dosing, falling to 50% after 24h. The clearance of doxorubicin that had escaped from the niosomes was about 10 fold greater than the clearance of doxorubicin still associated with the niosomes - 176.5mL min^{-1} and 16.2mL min^{-1} respectively. The area under the plasma level-time curve (for the 24h study period) increased 6 fold when doxorubicin niosomes were administered, compared to when the drug was administered in solution (66.0 µg.h mL^{-1} and 10.3µg.h $mL^{-1)}$. The area under the tumour level-time curve was increased by over 50% by the administration of the drug encapsulated in niosomes compared to the drug administered in solution (58.6µg.h mL^{-1} and 34.3µg.h mL^{-1}) respectively. Drug levels in the heart were statistically indistinguishable, regardless of the formulation administered. Modest tumour targeting was achieved by increasing the tumour to heart ratio from 0.27 to 0.36 by the encapsulation of doxorubicin in Span 60 niosomes.

Doxorubicin metabolites were found associated with the niosomes in the plasma, namely doxorubicinol and the aglycones doxorubicinone, doxorubicinolone and 7-deoxydoxorubicinone. We believe this to be due to either the absorption of these compounds to the vesicle surface, once formed outside the vesicles or to be due to intravesicular metabolic activity as doxorubicin was present in the vesicle bilayer and was thus accessible to the degradative enzymes. Although the AUC's of all metabolites were indeed generally higher in the niosome associated fraction, than those found in the fraction of drug that had diffused from the niosomes, the $AUC_{(metabolite)}/AUC_{(doxorubicin)}$ was lower for the encapsulated fraction, with the exception of doxorubicinol where values were similar.

Levels of liver metabolites, were found to be higher in the animals administered niosomes. $AUC_{(metabolite)}/AUC_{(doxorubicin)}$ values were also higher in this group (except doxorubicinone which gave lower values).

Span 60 niosomes have been shown to double the tumoricidal activity of doxorubicin in male NMRI mice bearing a 5 day old MAC 15A tumour[3].

1. A Rogerson, J. Cummings, N. Wilmott, A.T. Florence, J. Pharm. Pharmacol. 40:337-342 (1988).
2. D.J. Kerr, A. Rogerson, G.T. Morrison, A.T. Florence, S.B. Kaye, Br. J. Cancer, 58: 432-436 (1988)

3. I.F. Uchegbu, J.A. Turton, J.A. Double, A.T. Florence, J. Pharm. Pharmacol, 45: 1140 (1993).

THE DELIVERY OF DOXORUBICIN TO TUMOUR TISSUE IN A MOUSE MODEL, WITHIN NIOSOMES. 21A

Ijeoma F. Uchegbu, John A. Double, John A. Turton and Alexander T. Florence.

Conventional methods of drug delivery to diseased tissue are inefficient and imprecise. The optimization of delivery requires that the tissue of interest be guaranteed an exclusive pharmacodynamic interaction with the drug. Doxorubicin is a potent antineoplastic agent (Calaberesi and Chabner 1990) and the use of this agent in cancer chemotherapy adequately exemplifies the need for drug targeting. Doxorubicin chemotherapy is associated with a number of dose limiting adverse effects, the most debilitating of which are cardiotoxicity and myelosupression (Speth et al 1988). The encapsulation of doxorubicin in niosomes has improved the tumoricidal activity of the drug over the solution in the mouse tumour model (Rogerson et al 1988, Uchegbu et al 1993a). We have studied the biodistribution of a doxorubicin loaded niosome drug delivery system in an effort to assess the degree of targeting associated with this system. Span 60, cholesterol and Solulan C24 (45: 45: 10) were used to prepare niosomes and the niosome biodistribution studied in female NMRI tumour bearing (MAC 15A) mice. The area under the plasma level time curve was increased 6 fold by encapsulation of the drug in niosomes. Quantification of doxorubicin in plasma was performed on the niosome associated and unencapsulated drug using a gel filtration procedure (Fig. 1)(Uchegbu et al 1993b). The area under the tissue level time curve was increased in all tissues, including the tumour tissue. The depot nature of niosomal doxorubicin within the vascular space was confirmed by a) the presence of at least 90% of the drug within the vascular space still associated with niosomes 4h after dosing and b) the difference in the shape of the tissue to plasma ratio plots(Figs 2&3). The tumour, heart ratio (% of dose at peak drug levels) was increased from 0.6 to 1.3 with doxorubicin niosomes. In conclusion doxorubicin niosomes offer a drug delivery advantage over the drug in solution.

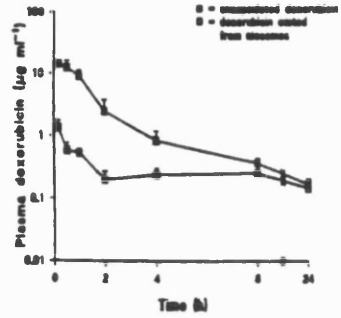

Figure 1: Plasma levels of free and encapsulated doxorubicin

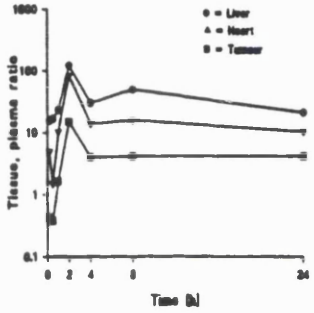

Figure 2: Tissue/ plasma ratio of doxorubicin (solution) to be compared with data in Fig. 3.

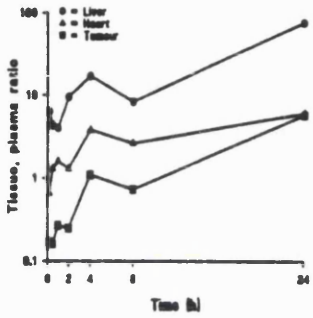

Figure 3: Tissue/ plasma ratio of doxorubicin (niosomes).

IJEOMA F. UCHEGBU

21B

ACADEMIC BACKGROUND

Right from my earliest days in undergraduate pharmacy school, I have always wanted a career in research. In my third year I was awarded the university prize for the best student in the B.Pharm part II examination. I graduated with a second class upper division honours degree and did my internship year (pre-registration) as a civilian with the Nigerian Army medical corps. Soon after this I went on to do a masters degree in pharmaceutical chemistry, studying the biodegradation of chloroquine, particularly its N-oxidation products.

I came to the Centre for Drug Delivery Research at the School of Pharmacy, Brunswick Square in 1991 seeking to make the shift from pharmaceutical chemistry to drug delivery. Straight away, I started working on a novel drug delivery system and our findings were published in the Journal of Physical Chemistry in 1992. That same year I presented a paper on certain aspects of our work at the British Pharmaceutical Conference (BPC) scientific session in Birmingham. This year (1993) I submitted 2 abstracts to the BPC science session in Reading and presented some of our results at an oral and at a poster session. Earlier on in the year I attended an international liposome workshop in Oberjoch, Germany and participated by giving an oral presentation on certain aspects of niosomal drug delivery. I have recently submitted for review an abstract for an international liposome meeting to be held in London next month. Currently I am preparing three manuscripts on various aspects of niosomal drug delivery and writing up my thesis.

RESEARCH INTERESTS

I am particularly interested in the development of novel drug delivery systems. The physical chemistry of these systems and their behaviour in the biological environment will form the main part of my work in the near future.

DOXORUBICIN METABOLISM IN SPAN 60 NIOSOMAL SYSTEMS

I.F. Uchegbu, J.A. Double, J.A. Turton, A.T. Florence

School of Pharmacy, Brunswick Square, London, WC1N 1AX.

INTRODUCTION

The use of drug delivery systems to circumvent the dose limiting cardiomyopathy and myelosupression[1] of doxorubicin (DOX) has involved liposomes[2] and polymeric particles[3]. Niosomes, vesicles formed from non-ionic surfactants in a manner analogous to liposomes[4] have been employed in mice in attempts to improve the therapeutic index of DOX[5-6]. While most studies with delivery systems focus on altered pharmacokinetics, usually increased plasma levels, scant attention has been paid to the potential for an altered metabolic profile. However DOX niosomes and DOX albumin microspheres are associated with either increased or decreased levels of the inactive metabolite 7-deoxydoxorubicinone (DEOXONE), respectively[3,5].

METHODS

The biodistribution and metabolite formation of 235nm DOX sorbitan monostearate (Span 60) niosomes (10mg kg^{-1}) was studied in female NMRI tumour bearing mice after IV injection. Plasma samples were fractionated over a Sepharose 2B column and niosome associated and unencapsulated DOX (free and plasma protein bound) separately quantified. DOX and DOX metabolites were assayed in tissue samples by an HPLC method[7].

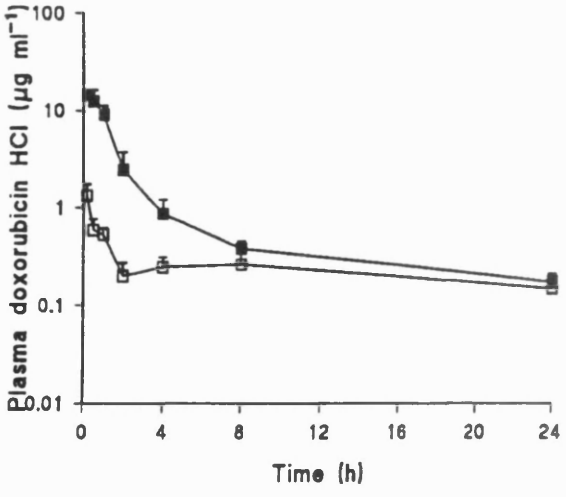

Figure 1: Plasma levels of DOX after the administration of doxorubicin Span 60 (10mg kg^{-1}) niosomes to female NMRI tumour bearing mice; ■ = encapsulated DOX, □ = unencapsulated DOX.

RESULTS AND DISCUSSION

90% of plasma DOX was found to be associated with the niosomes in vivo at 4h (Fig. 1), falling to 50% after 24h. This shows that DOX niosomes are relatively stable in vivo. The clearance of DOX that had escaped from the niosomes was 10 fold greater than the clearance of niosome associated drug (176.5mL h^{-1} and 16.2mL h^{-1} respectively) and the area under the plasma level time curve (AUC) was increased 6 fold by niosomal encapsulation (66.0μg.h mL^{-1} versus 10.3μg.h mL^{-1}). Modest tumour targeting was achieved by increasing the AUC tumour to heart ratio from 0.27 to 0.36. DOX metabolites, namely doxorubicinol (DXOL), the aglycones doxorubicinone (DXONE), doxorubicinolone (DXOLONE) and 7-deoxydoxorubicinone (DEOXONE) were found associated with the niosomes in the plasma. This is attributed to the adsorption of these metabolites to the vesicles once formed outside the vesicle or to the degradation of DOX while still resident within the bilayer. The AUC's of all metabolites found in the niosome fraction were indeed generally higher than those found in the fraction of plasma drug that had diffused from the niosomes. The $AUC_{(metabolite)}$ to $AUC_{(DOX)}$ ratios were however lower for the plasma niosome fraction with the exception of DXOL (similar values) (Table 1). Overall metabolic activity and $AUC_{(metabolite)}/AUC_{(DOX)}$ ratios were higher in the liver (the main organ of metabolic activity) of animals administered niosomes with the exception of DXONE (Table 1). The inactive aglycone metabolite levels in the lung were diminished or unchanged by the niosome formulation, despite the greater delivery of parent drug to this tissue with the niosomal system (Table 1). This can be

Proceedings of the 21st International Symposium on Controlled Release of Bioactive Materials (in press).

attributed to the fact that the long circulating plasma niosome fraction was associated with a

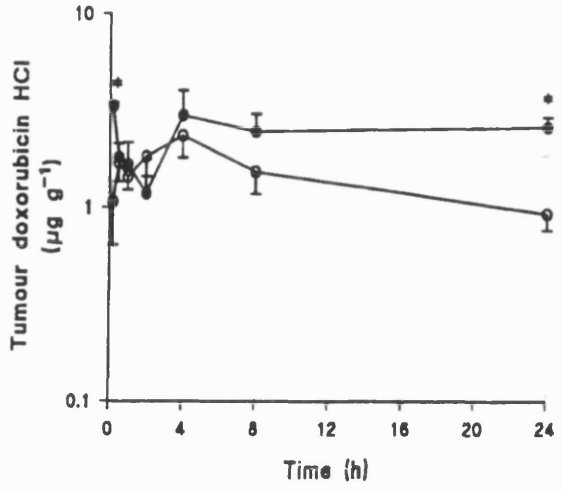

Figure 2: DOX tumour levels after the administration of DOX Span 60 niosomes (10mg kg^{-1}) to female NMRI tumour bearing mice; ● = DOX niosomes, ○ = DOX solution.

Table 1: AUCs and $AUC_{(metabolite)}/AUC_{(DOX)}$ in the plasma,liver and lung after the administration of DOX Span 60 niosomes.

DOX metabolite and tissue	Metabolite AUC µg.h $mL^{-1}(g^{-1})$	$AUC_{(metabolite)}/AUC_{(DOX)}$
Plasma niosome associated		
DXOL	5.2	0.19
DXONE	0.32	0.012
DEOXONE	0.12	0.0045
Plasma unencapsulated fraction after DOX niosomes		
DXOL	1.26	0.22
DXONE	0.23	0.041
DEOXONE	0.085	0.015
Liver metabolites after DOX niosomes		
DXOL	54.2	0.073
DXONE	4.0	0.0053
DXOLONE	0.53	0.00071
DEOXONE	0.75	0.001
Liver metabolites after DOX solution		
DXOL	12.9	0.037
DXONE	2.7	0.0078
DXOLONE	0.045	0.00013
DEOXONE	0.19	0.00054
Lung metabolites after DOX niosomes		
DXOL	80.04	0.049
DXONE	6.25	0.0038
DEOXONE	0.76	0.00046
Lung metabolites after DOX solution		
DXOL	19.97	0.027
DXONE	2.96	0.0041
DEOXONE	1.37	0.0019

relatively smaller proportion of the aglycone metabolites. Conversely, the level of the cytotoxic metabolite DXOL was increased in the lung of animals administered the niosome formulation.

CONCLUSIONS

Niosomes were found associated with DOX metabolites in the plasma. All DOX metabolites in the liver were increased with Span 60 niosomes. DOX delivery to the lung was increased with Span 60 niosomes, but the level of the inactive aglycones in the lung were either reduced (DEOXONE) or unchanged (DXONE); while the level of the cytotoxic metabolite DXOL was increased. This unexpected lung metabolite profile is attributed to the fact that the long circulating plasma niosomes are associated with a smaller proportion of the inactive aglycones than the unencapsulated plasma fraction.

REFERENCES

1. Calaberesi, P. and Chabner, B.A., Goodman and Gilman's The Pharmacological Basis of Therapeutics, Goodman Gilman, A., Rall, T.W., Nies, S.A., (eds), Pergamon Press, New York, 1990, pp1209-1263.
2. Gabizon, A., Cancer Res. **52,** 891-896 (1992).
3. Cummings, J., Willmott, N., Marley, E., Smyth, J., Biochem. Pharmacol. **41,** 1849-1854 (1991).
4. Florence, A.T. and Baillie, A.J., Novel Drug Delivery and its Therapeutic Applications, Prescott, L.F., Nimmo, W.S. (eds), Wiley, Chichester, 1989, pp281-295.
5. Rogerson, A., Cummings, J., Willmott, N., Florence, A.T., J. Pharm. Pharmacol., **40,** 337-342 (1988).
6. Uchegbu, I.F., Double, J.A., Turton, J.A., Florence, A.T., J. Pharm. Pharmacol., (in press).
7. Cummings, J., Stuart, J.F.B., Calman, K., J. Chromatography, **311,** 125-133 (1984).

ACKNOWLEDGEMENTS

I.F.U. gratefully acknowledges the financial support of L'Oreal France.